THE GEOTECTONIC EVOLUTION OF THE KAZAURE SCHIST BELT IN THE PRECAMBRIAN BASEMENT OF NW NIGERIA

BY

DANBATTA, UMAR ADAMU

THE GEOTECTONIC EVOLUTION OF THE KAZAURE SCHIST BELT IN THE PRECAMBRIAN BASEMENT OF NW NIGERIA

BY

DANBATTA, UMAR ADAMU
(PH.D/SCI./2800/91-92)

A DISSERTATION SUBMITTED TO THE POSTGRADUATE SCHOOL, AHMADU BELLO UNIVERSITY, IN PARTIAL FULFILLMENOF THE REQUIREMENTS FOR THE AWARD OF THE DEGREE OF DOCTOR OF PHILOSOPHY (Ph.D.)

DEPARTMENT OF GEOLOGY,
FACULTY OF SCIENCE,
AHMADU BELLO UNIVERSITY ZARIA.

OCTOBER, 1999

DECLARATION

This is to certify that this thesis titled **"THE GEOTECTONIC EVOLUTION OF THE KAZAURE SCHIST BELT IN THE PRECAMBRIAN BASEMENT OF NW NIGERIA"** by U.A. Danbatta, is the result of an original investigation. Information derived from all other published or unpublished works referred to in this thesis have been acknowledged in the text. This work, or part of it, has not been submitted in any form for any other Diploma or Degree.

Signed..... Candidate

U. A. DANBATTA

CERTIFICATION

This thesis entitled **"THE GEOTECTONIC EVOLUTION OF THE KAZAURE SCHIST BELT IN THE PRECAMBRIAN BASEMENT OF NW NIGERIA"** by U.A. Danbatta, meets the regulations governing the award of the degree of Doctor of Philosophy of Ahmadu Bello University and is approved for its contribution to scientific knowledge and literary presentation.

Professor E.C. IKE
Chairman Supervisory Committee.

9/2/2000
DATE

Professor A.C. AJIBADE
Member Supervisory Committee.

17/2/2000
DATE

Professor K. Schoeneich
Postgraduate Co-ordinator
Department of Geology.

9.02.2000
DATE

Dr. I. Garba
Head of Department of
Geology.

17/2/2000
DATE

Professor S.B. OJO
Dean, Postgraduate School,
A.B.U. Zaria.

18/05/00
DATE

DEDICATION

This research work is dedicated to my Late Father **Alhaji ADAMU NAMURA** (SARKIN NOMA DA KWANGILA) and **Professor MICHAEL WOAKES**, a former staff of the Department of Geology, Ahmadu Bello University, Zaria.

ACKNOWLEDGEMENTS

The fieldwork, most of the petrographic studies and thesis preparation were done from or in the Department of Geology, Ahmadu Bello University (A.B.U.) Zaria. The field work was supported by the Department of Geology and a research grant from the Ahmadu Bello University (A.B.U.) Zaria. I am grateful to the A.B.U. Authorities.

The laboratory analyses were done at McGill University Montreal Canada, under Nigerian Indigenous Building Materials Project, funded by Canadian International Development Agency (CIDA). They were done under the direction and guidance of Prof. AhmedAli Tariq. The samples and other relevant data have been deposited with Prof. R. Doig, Department of Earth and Planetary Sciences, McGill University, who is interested in undertaking U-Pb age determinations on the said samples. The moral and financial support for the trip to Canada and laboratory analyses are gratefully acknowledged.

I am deeply indebted and grateful to members of my supervisory committee, Professors E.C. Ike and A.C. Ajibade who provided the constructive criticism and encouragement required for its successful completion. Professor Ike, the Dean of Faculty of Science, a former Head of Department, and Co-ordinator of the CIDA funded Nigerian Indigenous Building Materials Project, served as a Chairman of my supervisory committee and an early mentor. He provided tremendous help for my trip to Canada as

a special doctoral student and transport needs for the fieldwork, and I am grateful to him.

An equally invaluable contribution has been made by Professor A.C. Ajibade, who together with Professors M.A. Rahaman and Michael Woakes, introduced me to the Geology of NW Nigeria and provided the environment in which my interest in the schist belts could grow. I am very grateful to all of them. Professor Charles Ajibade suffered with me through the development of my M.Sc. thesis, and now this thesis. His numerous corrections and encouragements has helped made this work what it is.

Worthy of mention are Dr. Ibrahim Garba (Ag. Head, Geology Department, A.B.U. Zaria), Dr. A.E.O. Ogezi, Prof. K. Shoeneich, and Prof. S.I. Abaa who have tremendously assisted me. Their numerous valuable suggestions, additions, and corrections, have also helped to improve the standard of the thesis. I am very grateful for that.

Dr. Joseph Omada (former Ag. Head, Geology Department, A.B.U Zaria) showed some interest, and I am grateful for that. I must also express my appreciation for other fellow staff members in the department, who have contributed to this study. People such as Uncle (Dr.) Ikpokonte, Mr. Bala, Mr. Alagbe, Mal. Hamza, and Mr. Majime, have also greatly assisted in one way or the other. I also greatly appreciate the mutual understanding and co-operation of the Departmental technicians

(Mr. Onyeamachi, Mr. Edegbo, Late. Alh. Abu, Mr. Lamia) and draughtsman (Mr. Duro) who provided support at various stages of the project, and also my brother, Alh. Sani of Afribank.

The Author had the opportunity of discussing geological aspects of the area in the field and office with five former B.Sc. students of the Department of Geology, A.B.U. Zaria. These include: Ms. M. Ajidahun; Messrs. S.B. Danpullo; M.L. Garba; A. Ibrahim, and A. Odoma, who all made brief and helpful visits to the project site in the field. Their maps, samples, some structural measurements and descriptions have helped the present study.

I am especially indebted to Professors Ronald Doig and AhmedAli Tariq of the McGill University, who aided in making geochronometric and geochemical analyses. Segments of the thesis have been reviewed by some Staff and Postgraduate students of the Department of Earth and Planetary Sciences, McGill University. These include: Professor Andrew Hynes and his then Ph.D. student, Mr. D.E. Lee; Professor Bob Martin and his then Ph.D. student, Emmanuel Sakoma; Dr. D. H. Smith, George Mclain and others too numerous to be mentioned by names. Their suggestions and corrections have aided and improved the framework of this investigation.

Finally, I am grateful to my wife (Halima) who provided moral support and assistance in the type processing of the thesis.

ABSTRACT

In this study, a systematic qeoloqical investigation of the Kazaure Schist Belt (KZSB) and its adjacent areas in the basement of northwestern Niqeria have led to the interpretation of its qeotectonic evolution, and the production of a qeoloqical map on a scale of 1:100,000. The KZSB consists predominantly of quartzites, politic rocks, and metaconqlomerates. Minor rocks include metavolcanics, metasandstones and ferruqinous quartzites.

The Belt as a whole is enclosed by miqmatite-qneiss basement and I-type Older Granites. The miqmatite-qneiss basement comprises of miqmatite, biotite qneiss and Older Metasediments and underlies the Younqer Metasediments. However the qranites are considered to be intrusive into the metasediments. The Kalanqai Fault System (Truswell and Cope, 1963) of Birnin Gwari-Malumfashi Schist Belts is shown to extend into the KZSB and even beyond. It has produced fault breccia and mvlbnitic rocks which have now been studied in detail.

The rocks in the area have been subjected to at least two intense phases of ductile deformation (Dj and D_2), which conform to a pattern of recumbent N-S trendinq Fl folds locally refolded to NNE-SSW trendinq upriqht F_2 folds and affected by qranite intrusion and heteroqeneous strain related to faultinq. The deformation events were accompanied by two

phases of progressive reqional metamorphism followed bv a static metamorphic phase. The first phase of reqional metamorphism attained amphibolite facies (Mj), whilst the second phase was of qreenschist facies (M2).

The qranitic rocks in the KZSB have limited ranqe in SiO_2 (69.76-72.03%), have hiqh alkali contents, low CaO and MqO values and a Shand index of < 2. In the metasediments the values of potash are hiqher than those of soda, contents of alumina are hiqh, MqO is in excess of CaO, while there is relative liqht R.E.E. enrichment relative to heavy R.E.E depletion in the schists. Geochemical characterisation indicates the Kazaure qranitoids to be I-type qenerated in a syn-collisional settinq and the metasediments oriqinated from post-Archaen qreywacke-type sediments.

Five samples of a syntectonic coarse-qrained porphvritic qranite define a 4-point, whole-rock Rb-Sr. errorchron correspondinq to an aqe of 592 +14 Ma with an initial ratio of 0.7097 + 0.0004. This is distinctly a Pan-African aqe and is taken as the crystallization aqe of the qranite. The aqe of D_1 and D_2 deformations and metamorphisms in the Kazaure Belt is therefore shown to be Pan-African. However the Younqer Granite rocks of the Daura Iqneous Complex rocks were emplaced much later durinq the Mesozoic era (Jacobson et al.. 1964).

These with other supportive qeological data from adiacent schist belts have allowed the erection of a model of evolution for the KZSB. The KZSB evolved throuqh ensialic processes on the miqmatite-gneiss basement with the protoliths forminq the metasediments deposited in a predominantly shelf or deltaic environment to allow deposition of coarse clastic sediments. This model has specifically been linked to basinal marqin development related to the compressional reqimes of the Pan-African subduction at the West African craton marqin. The Kazaure basin developed as a result of dominq, extension and continental riftinq due to back-arc spreadinq related to the Pan-African subduction.

TABLE OF CONTENTS

TITLE	PAGE
Title Page	i
Declaration	ii
Certification	iii
Dedication	iv
Acknowledgements	v
Abstract	viii
Table of Contents	xi
List of Tables	xix
List of Maps	xxi
List of Figures	xxii
List of Plates	xxv

CHAPTER ONE: INTRODUCTION

1.1 THE PRECAMBRIAN ROCKS OF NW NIGERIA: THE KAZAURE SCHIST BELT....1

1.2 LOCATION AND ACCESSIBILITY....3

1.3 RELIEF AND DRAINAGE....3

1.4 CLIMATE AND VEGETATION....7

1.5 PREVIOUS WORK....8

1.6 PRESENT STUDY....11

1.6.1 Aims and Objectives....11

1.6.2 Methodology for field mapping....11

1.6.3 Methodology for geochemical analyses...13

TITLE PAGE

CHAPTER TWO: REGIONAL GEOLOGY

2.1 INTRODUCTION.....15

2.2 THE NIGERIAN BASEMENT COMPLEX.....16

2.2.1 Characteristics of the Migmatites and gneisses.....18

2.2.2 Characteristics of the Schist belts.....19

2.2.3 Characteristics of the Older Granites.....25

2.2.4 Characteristics of the Volcanics.....27

2.3 IMPRINTS OF OROGENIC EVENTS IN THE NIGERIAN BASEMENT.....27

2.3.1 Eburnean and Older orogenic events.....27

2.3.2 The Kibaran orogenic event.....29

2.3.3 The Pan-African orogenic event.....31

2.4 AGE OF THE SCHIST BELTS.....35

2.5 PREVIOUS MODELS OF EVOLUTION OF THE SCHIST BELTS.....39

2.5.1 Schist Belts Evolution through ensialic processes.....39

2.5.2 Schist Belts Evolution through ensimatic processes.....41

2.5.3 Schist Belts Evolution through both ensialic and ensimatic processes.....44

2.6 NATURE OF THE DAMAGARAN, ADRAR DES IFORAS AND HOGGAR REGIONS.....45

CHAPTER THREE: LITHOLOGY AND FIELD RELATIONS IN THE STUDY AREA

3.1 INTRODUCTION.....48

3.2 MIGMATITE-GNEISS COMPLEX.....50

TITLE PAGE

3.2.1 Lithology, Distribution and Field relationships.....50

3.2.2 Biotite Gneiss.....51

3.2.3 Migmatite.....53

3.2.4 Older metasediments.....53

3.3 YOUNGER METASEDIMENTS AND METAVOLCANICS.....55

3.2.1 Lithology, Distribution and Field relationships.....55

3.3.2 Quartzite.....56

3.3.3 Metapelites.....58

3.3.4 Metaconglomerate.....61

3.3.5 Metasandstone.....61

3.3.6 Metavolcanics.....62

3.3.7 Ferruginous quartzite (FQZ).....63

3.4 FAULT ROCKS.....65

3.4.1 Field Characteristics of the Fault rocks.....65

3.5 GRANITE.....68

3.5.1 Lithology, Distribution and Field relationships.....68

3.5.2 Medium-grained Granite.....69

3.5.3 Granodiorite.....69

3.5.4 Porphyritic Granite.....69

3.5.5 Hornblende Granite.....70

3.5.6 Aplite and Pegmatite.....72

TITLE PAGE

3.6 THE DAURA YOUNGER GRANITE COMPLEX.....73

3.6.1 Lithology, Distribution and Field relationships.....73

3.6.2 Rhyolites.....74

3.5.3 Quartz Syenite.....76

3.5.4 Biotite granite.....76

3.7 SEDIMENTARY FORMATIONS.....77

3.8 SUPERFICIAL DEPOSITS.....78

CHAPTER FOUR: PETROGRAPHY

4.1 INTRODUCTION.....81

4.2 MIGMATITE-GNEISS COMPLEX.....81

4.2.1 Biotite gneiss.....81

4.2.2 Migmatite.....83

4.3 YOUNGER METASEDIMENTS AND METAVOLCANICS.....87

4.3.1 Quartzite.....87

4.3.2 Metapelites.....90

4.3.3 Metaconglomerate.....92

4.3.4 Metavolcanic rocks.....92

4.3.5 Ferruginous quartzite (FQZ).....94

4.4 FAULT ROCKS.....95

4.6.1 Microscopic Description.....95

4.5 GRANITE.....98

4.5.1 Megascopic Description.....99

4.5.2 Microscopic Description.....101

TITLE PAGE

4.6 THE DAURA YOUNGER GRANITE COMPLEX.....106

4.6.1 Megascopic Description.....106

4.6.2 Microscopic Description.....108

CHAPTER FIVE: STRUCTURAL GEOLOGY

5.1 INTRODUCTION.....110

5.2 METHOD OF ACCUMULATION AND ANALYSIS OF STRUCTURAL DATA.....111

5.3 DESCRIPTION OF MEGASCOPIC STRUCTURES.....115

5.3.1 Introduction.....115

5.3.2 Major Folds.....116

5.3.3 Lineaments/Fractures.....119

5.4 DESCRIPTION OF MESOSCOPIC STRUCTURES.....124

5.4.1 Introduction.....124

5.4.2 Mesostructures in the basement gneisses and migmatites.....125

5.4.3 Mesostructures in the Younger metasediments.....130

5.4.4 Joints.....147

5.5 DESCRIPTION OF MICROSCOPIC STRUCTURES.....149

5.6 SUPERIMPOSITION OF STRUCTURES.....150

5.7 CLASSIFICATION OF THE MAJOR STRUCTURES.....151

5.7.1 Major D_1 Structures.....152

5.7.2 Major D_2 Structures.....152

5.8 STRAIN ANALYSIS (Kinematic Indicator).....153

TITLE PAGE

5.9 STRUCTURAL SYNTHESIS.....156

5.9.1 Ductile Structures.....156

5.9.2 Brittle Structures.....162

5.9.3 Summary of Structural events.....164

CHAPTER SIX: GEOCHEMISTRY AND GEOCHRONOLOGY

6.1 INTRODUCTION.....168

6.2 GEOCHEMISTRY OF METASEDIMENTS.....169

6.2.1 Major Elements.....169

6.2.2 Trace Elements.....172

6.3 GEOCHEMISTRY OF METAVOLCANICS.....181

6.4 GEOCHEMISTRY OF THE GRANITES.....184

6.4.1 Major Elements.....184

6.4.2 Trace Elements.....195

6.5 GEOCHRONOLOGY OF KAZAURE GRANITE.....198

6.5.1 Analytical methods.....198

6.5.2 Isotope Results and Computations.....200

6.5.3 Interpretations.....204

6.6 AGE OF THE KAZAURE SCHIST BELT.....206

CHAPTER SEVEN: DEFORMATION HISTORY AND METAMORPHISM

7.1 INTRODUCTION.....208

7.2 MINERAL PARAGENESIS.....209

7.2.1 Gneisses and Migmatites.....209

7.2.2 Metasediments.....211

TITLE PAGE

7.3 METAMORPHIC GRADE.....212

7.4 RELATIONSHIP OF METAMORPHISM TO DEFORMATION....215

7.4.1 First metamorphic event (M_1).....215

7.4.2 Second metamorphic event (M_2).....215

7.4.3 The retrograde metamorphism (X).....216

7.4.4 Summary of metamorphic events.....218

CHAPTER EIGHT: *GEOTECTONIC EVOLUTION OF THE* KAZAURE SCHIST BELT

8.1 INTRODUCTION.....220

8.2 ORIGIN OF THE KAZAURE ROCKS.....220

8.2.1 Origin of the the migmatite-gneiss Basement.....222

8.2.2 The origin and palaeo-environment of deposition of the Younger Metasediments and metavolcanics.....224

8.2.3 Origin and Tectonic environment of Older Granite Emplacement.....228

8.3 CORRELATION WITH OTHER NW NIGERIA SCHIST BELTS.....228

8.3.1 Comparison of the Younger Metasediments..229

8.3.2 Comparison of the ductile structures.....230

8.3.3 Comparison of brittle structures.....223

8.4 CORRELATION WITH DAMAGARAN, HOGGAR AND ADRAR DE FORAS REGIONS.....238

8.5 MODEL FOR THE EVOLUTION OF THE KAZAURE SCHIST BELT IN THE CONTEXT OF NW NIGERIA.....239

8.5.1 Preamble.....239

8.5.2 Origin of the Kazaure Palaeo-basin.....240

TITLE PAGE

8.5.3 Compression of the Kazaure Palaeo-basin.....243

8.5.4 Late tectonic effects.....244

8.5.5 Timing of the Extensional and Compressional Regimes.....245

8.5.6 Remarks on the Evolution of the whole NW Nigeria Schist Belts.....248

8.6 CONCLUSION.....253

8.7 RECOMMENDATIONS FOR FUTURE WORK.....256

REFERENCES.....257

APPENDIX A.....279

APPENDIX B.....284

LIST OF TABLES

TABLE PAGE

4.1 Modal Composition of Biotite gneiss.....84

4.2 Modal Analyses of Sheared gneisses from the Kazaure area.....97

6.1 Chemical (weight percent) and trace element (part per million) composition of the Mica Schist from the Kazaure schist belt area.....170

6.2 Chemical (weight percent) and trace element (part per million) composition of the Quartzites from the Kazaure schist belt area.....171

6.3 Chemical composition (weight percent) of Garnet from the BIF at Kazaure.....176

6.4 Rare earth element (REE) contents in mica schists from the Kazaure belt.....178

6.5 Chemical composition (weight percent) of the metavolcanic rocks.....182

6.6 Major chemical (weight percent) and normative composition of the porphyritic Granite.....186

6.7 Major chemical (weight percent) and normative composition of the medium grained granite.....187

6.8 Major chemical (weight percent) and normative composition of the hornblende granite and granodiorite 188

6.9 Trace element chemical composition (part per million) of the porphyritic Granite.....196

6.10 Trace element chemical composition (part per million) of the fine to medium grained Granite....196

6.11 Trace element chemical composition (part per million) of the hornblende granite and granodiorite.....197

6.12 Geochronometric Samples' Description, Locality and Co-ordinates.....200

6.13 Rb-Sr analytical data of Whole-rock Determinations from Granites in the Kazaure Schist Belt region.....200

TABLE PAGE

7.1 Mineral Paragenesis in the rocks of Kazaure Schist Belt.....210

8.1 The chronological order of events in Kazaure region and its adjacent areas.....221

8.2 Deformation history established for the schist belts in NW Nigeria.....232

LIST OF MAPS

MAP		PAGE
1.	Geological map of Kazaure Schist Belt and and adjacent ares at 1:100,000 scale.....	*Back pocket*
2.	Geological map of parts Of Kazaure and Malumfashi Belts at 1:100,000 scale.....	*Back pocket*

LIST OF FIGURES

FIGURE PAGE

1.1 Simplified geological map of Nigeria showing the distribution of the Schist belts and the location of the study area.....2

1.2 Outline geological map of parts of NW Nigeria showing the basement complex, sedimentary basins and location of the study area.....4

1.3 Map showing drainage pattern and location of major rivers in the study area.....6

2.1 Interpretation of the Anka, Maru, and Wonaka belts according to Wright (1979).....43

2.2 Interpretation of the Anka and Maru belts according to Holt (1982).....45

2.3 Map showing the Pan-African mobile belt and the suggested correlation between Central Hoggar and Western Nigeria.....46

3.1 Geological map of Kazaure and its adjacent areas (simplified from Maps 1 and 2) 49

4.1 Q.A.P Diagram showing the modal composition of the biotite gneiss, sheared gneiss and aplite vein.....85

5.1 An interpretation of satellite image of Central Nigeria ($7^0$40'N) Kazaure and the surrounding areas.....112

5.2 Map showing location of Major Structures in the Kazaure region and its surroundings.....113

5.3 Kazaure area: Structures and Lithologies.....114

5.4 Lower hemisphere equal area projection of poles to foliation of Kazaure major antiform and minor F_2 fold axes.....117

5.5 Rose Diagram of Lineaments/Fractures more than 2 km long in the mapped area.....122

5.6 Lower hemisphere equal area projection of poles to foliations and lineations in migmatite-gneiss area.....128

FIGURE PAGE

5.7 Lower hemisphere equal area projection of lineations and poles to foliation in the Kazaure area.....131

5.8 Lower hemisphere equal area projection of lineations and poles to foliation in other metasedimentary areas.....142

5.9 Rose Diagram for the strikes of joints measured in the study area 148

5.10 Sketch of an ellipsoidal structure of deformed pelitic clasts exposing XZ surface.....155

5.11 Sketch diagrams drawn from the field and thin-sections showing fabric relations in quartz-muscovite-schist at Kazaure.....157

5.12 Schematic block diagrams showing the major style of folding: (a) N-S Recumbent F_1 phase of folding (b) NNE-SSW Upright F_2 phase of folding.....159

5.13 Lower hemisphere equal area projection of poles to linear minor structures and regional fold axes.....161

5.14 Lower hemisphere equal area projection of compiled planar structures.....163

6.1 The field of the Kazaure metasediments in an ACF triangular diagram after Miyashiro (1973).....174

6.2 TiO_2 versus SiO_2 discrimination diagram (after Tarney, 1977).....175

6.3 Chondrite normalized REE distribution patterns in four Kazaure mica schist samples.....179

6.4 SiO_2-K_2O diagram of Kazaure metavolcanics (After Taylor, 1969).....183

6.5 AFM diagram showing compositional variation of the granitic and metavolcanics rocks.....185

6.6 The field of the Kazaure granitoid in a CIPW Normative Q-Ab-Or triangular diagram.....190

FIGURE PAGE

6.7 Chemical classfication of Kazaure plutonic rocks based on alkali contents (after Harpum, 1963).....191

6.8 An A/CNK (Shand Index) diagram showing the Peralkaline nature of the granitoids.....192

6.9 An ACF diagram showing the I-type character of the Kazaure granitoids.....194

6.10 Rb-SiO_2 discrimination diagram used for the tectonic classification of granitic rocks.....199

6.11 Rb-Sr isochron diagram for the whole rock samples from the Kazaure Belt Older Granites.....203

8.1 Cross-sections through the project area. Lines of cross-sections are as in Maps 1 and 2.....223

8.2 Major fracture and lineament trends in the Nigerian Basement Complex.....234

8.3 Development of a greenstone type margin basin by back-arc extension (Modified from Tarney et al., 1976).....241

8.4 Diagrams showing hypothetical evolution of the Kazaure Schist Belt.....242

8.5 Schematic section across the West African craton margin showing the effects of the Pan-African event in the basement of Western Nigeria.....246

8.6 Diagrams showing hypothetical evolution of Anka, Maru, Wonaka and Kazaure schis belts. The line of section is along latitude $12^0 30'$N.....249

8.7 Diagrams showing hypothetical evolution of Zuru, Kushaka, Birnin and Malumfashi belts. The line of section is along latitude $11^0 5'$ N.....250

(Maps 1 and 2 are at the back pocket).

LIST OF PLATES

PLATE **PAGE**

3.1 Photograph of biotite gneiss east of Yashi (UD202). Note the isoclinal upright fold outlined by foliation trends.....52

3.2 Photograph of a migmatite showing a mesocratic (dark) palaeosome and a leucocratic (light coloured) neosome. Note complex and ptygmatitic fold structures.....52

3.3 Photograph of feldspathic quartzite (Q) within highly weathered biotite gneiss (G). Note the subordinate amounts of kaolinised clay (C).....54

3.4 Photograph of a massive quartzite ridge (Q) showing its characteristic outcropping nature on top of the ridge. Location: Wawanrafi (UD40)....57

3.5 Photograph of quartzite (Q) in fault-contact with a conglomerate ridge (C) which runs on the western limit of Kazaure town around Dutsin Baraden.....57

3.6 Photograph of pyhllite outcropping in the core of F_2 synform along River Tuwari behind Local Education Offices Kazaure (UD27). Note the S_2 crenulation cleavage locally refoliating S_1 and the grovvy shapes (G) parallel to an L_2 Lineation..60

3.7 Photograph of metavolcanic outcrop (MV) intercalated with schists (SC) at Makoda. The pits were dug by excavators who use the rock in dam construction. Note the isoclinal upright F_2 fold of schistosity in the schists at the lower right hand corner.....63

3.8 Photograph of Ferruginous quartzites outcrop (FQ) on top of a ridge, Matanfada (UD812). Note its occurrence as floats (F) just below the ridge.....63

3.9 Photograph of a fault breccia (FB) trending NNE -SSW and dipping steeply W, bent in some places. Note the closely spaced fracture cleavage.....66

PLATE PAGE

3.10 Photograph of the coarse porphyritic granite at Dutsen Dan Bakoshi (UD238). Note the characteristic outcrop pattern composed of boulders that have formed due to jointing.....71

3.11 Photograph of rhyolites (R) locally covered by superficial deposits. Note the bouldery outcropping nature of the rhyolite.....75

3.12 Photograph of quartz syenite intrusion at Rogogo (UD498). Note the outcropping nature of the syenite which is almost completely covered by superficial deposits.....75

4.1 Photomicrograph of schistose quartzite showing pre-existing foliation kinked folded by later deformation (Sample UD65).....89

4.2 Photomicrograph of cataclastic texture in a quarztitic fault breccia. Note the recyrstallized quartz porphyroclasts (Q).....96

4.3 Photomicrograph of cataclastic texture showing strained and broken grains of quartz (Q) and plagioclase (P) in a thin section of the sheared gneiss (UD228).....96

4.4 Photomicrograph of fine-medium grained granite showing sericitized large grains of quartz (Q), plagioclase (P) and earlier formed biotite (B) extensively retrogressed to chlorite (C).....102

5.1 Photograph of migmatite-gneiss exhibiting weak N-S oriented gneissic banding.....127

PLATE PAGE

5.2 Photograph of fine-medium grained granite intruding mica schist in the Kazaure area (UD59). Note re-orientation of pre-existing N-S structures into an ENE trend and the characteristic joint pattern.....134

5.3 N-S oriented mesoscopic folds in micaceous quartzites, largely obliterated by later deformations. Note the contorted and domal form of the small interference structure due to the NNE-SSW refolding effect.....134

5.4 Photograph of tight to isoclinal NNE- trending non-cylindrical fold in a quartz schist. Note the foliation trending parallel to the axial trend of the fold as outlined, and also the lineation (L).....136

5.5 Photograph of quartz biotite schist showing intersection between the N-S/NNE- striking foliations.....140

7.1 Photomicrograph of quartz mica schist showing S_1 schistosity parallel to the recrystallised quartz vein (Q) formed during M_1 metamorphism defined by fine-grained biotite, muscovite, chlorite and larger quartz grains.....211

7.2 Photomicrograph of S_2 cleavage in metapelites marked by the preferred growth (arrow) of quartz (Q) and mica (M), which is altered to chlorite (C) in some places. Note the K-feldspar (F) replacing the muscovite. This preferred orientations formed during the M_2 Metamorphism.....211

7.3 Photomicrograph of a biotite gneiss showing M_2 metamorphic fabric which is contemporaneous with the D_2 ductile deformation event that rotated porphyroblasts and affected S_1 schistosity.....215

7.4 Photomicrograph of mica schist showing trains of biotite crystals (arrow) which formed during the major period of biotite porpyroblasts (B) growth.....215

CHAPTER ONE:

GENERAL INTRODUCTION

1.1 THE PRECAMBRIAN ROCKS OF NW NIGERIA

The Precambrian rocks of Nigeria are best exposed in northwestern Nigeria, hence this area is considered important for understanding the geology of the Nigerian Basement Complex (Ajibade et al., 1987a). The area has been intensively studied by various workers over several years (Truswell and Cope, 1963; Fargher, 1965; McCurry, 1973; 1976; Grant, 1978; Ajibade, 1980; Egbuniwe, 1982; Holt, 1982; Danbatta, 1991).

The Kazaure Schist Belt (KZSB) is one of the many schist belts of northwestern Nigeria, and lies in the northeastern margin of the zone (Fig 1.1).

The KZSB and the northern parts of Malumfashi Schist Belt have not been studied in great detail. As a result, data about the succession of rocks and their structural relationships in the area are very scanty. In this work, attention is focused on understanding the geology of the Kazaure area as an additional contribution towards a better understanding of the schist belts and the relationship between these belts and the orogenic events in the Nigerian Basement Complex.

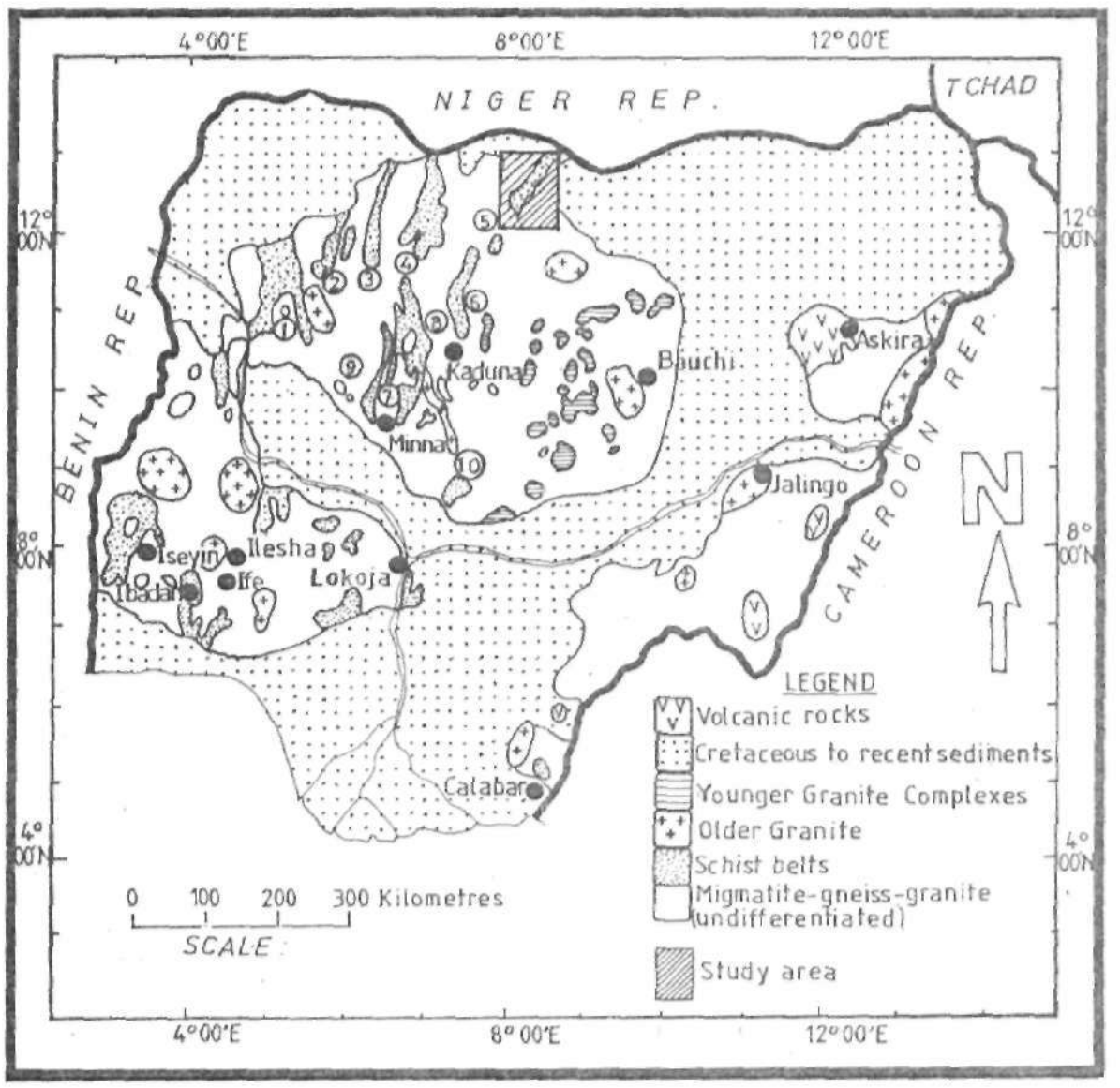


Fig. 1.1. Simplified geological map of Nigeria showing the distribution of the schist belts and the location of the study area. (1) Zuru, (2) Anka, (3) Maru, (4) Wonaka, (5) Kazaure, (6) Malumfashi, (7) Birnin-Gwari, (8) Kushaka, (9) Ushama, (10) Toto.
(Modified after Ajibade et.al. 1987[a]).

1.2 LOCATION AND ACCESSIBILITY

The study area is part of the Upper Proterozoic-Lower Palaeozoic terrane of NW Nigeria, and lies within latitudes 12^0 N and 13^0 N and longitude $7^0$50' E and $8^0$40' E (Figs. 1.1 and 1.2). Geographically the area cuts across Katsina, Jigawa and Kano States of Nigeria, covering a total area of 90 X 110 km^2.

The area is accessible via the Kano-Danbatta-Kazaure-Daura road which crosses the area from South to North; the Kano-Bichi-Yashi road and the Kazaure-Roni-Ingawa road (Maps 1 and 2). There are also numerous other motorable roads, which include the Kazaure-Birkin road, Daura-Rogogo road, the Roni-Achilafia road and the Achilafia-Yan Kwashi Road. There is also a network of footpaths throughout the area, thus making it very accessible by both foot and vehicles.

1.3 RELIEF AND DRAINAGE

The study area consists of a series of discontinuous ridges (of metasediments) and inselbergs (of gneisses and granites), which give it a slightly rugged landscape. The highest point in the region is the Dutsen Dan Bakoshi Peak (114 m above the plain) at the extreme southwestern portion of the area. Other prominent peaks include that of Bayan Dutse Peak (106 m above the plain) near Kazaure town, and the peak at Waire Hill which sharply rises to 92 m above the plain.

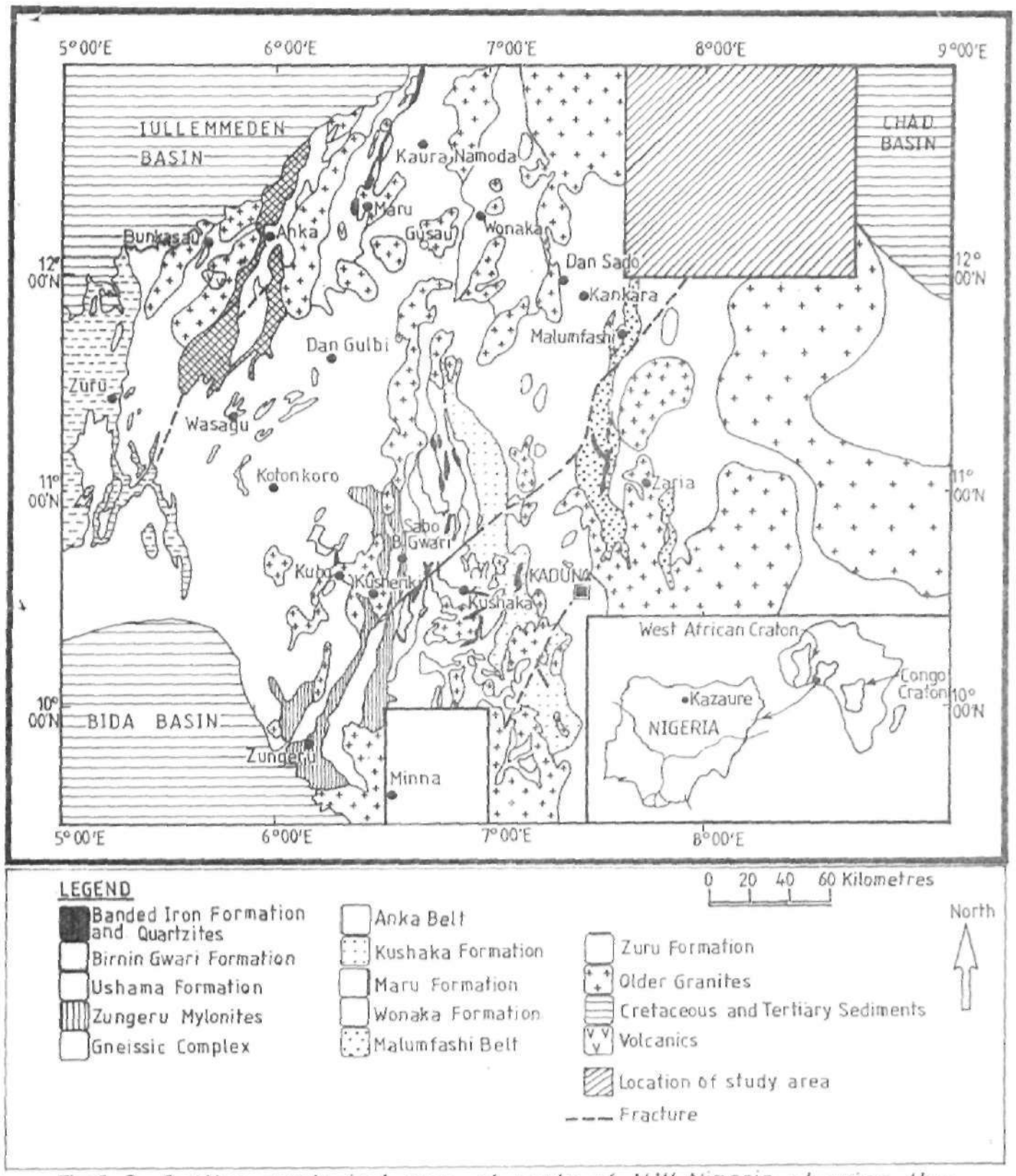


Fig.1.2. Outline geological map of parts of N.W. Nigeria showing the basement complex, sedimentary basins and location of the study area. Inset is showing the regional geological setting of Nigeria within the African shield (Modified from Ajibade, 1980).

The lowest point in the project area is located at the central area in the Gari River Valley, with a gradual decrease in slope towards the southeast. The area forms part of the "Northern Nigeria Plains" (Burke and Durotoye, 1970), and consists of smaller "undulating" plains like the Kazaure, Tangwai, Katsina and Gari (Abubakar, 1988).

The geology in the area controls and influences the pattern of the drainage. The area is drained by nine main rivers: the Tuwari, Gari, Tagwai, Hausani, Karaduwa, Watari, Tomas, Kiye and Sabke rivers, mainly with a dendritic drainage pattern (Fig. 1.2). The Tuwari River flows northeastwards through a rugged terrain and turn southeasterly near Kazaure town. River Gari flows northeastwards across regional strike to its junction with the Tagwai River, from where it changes course to a more easterly flow direction similar to that of River Kiye. It is the longest river in the area.

River Tagwai is joined by River Dakwau and the two together with River Sabke and River Karaduwa, have a general northward flow direction. However, Rivers Hausani and Jakara flow in a general north-eastward direction, with the later heavily polluted by industrial wastes. Rivers Watari and Tomas have a general southeasterly flow direction, though the later has changed course around Kunya area, where it bends and flow northeastward. There is a major agricultural project in the

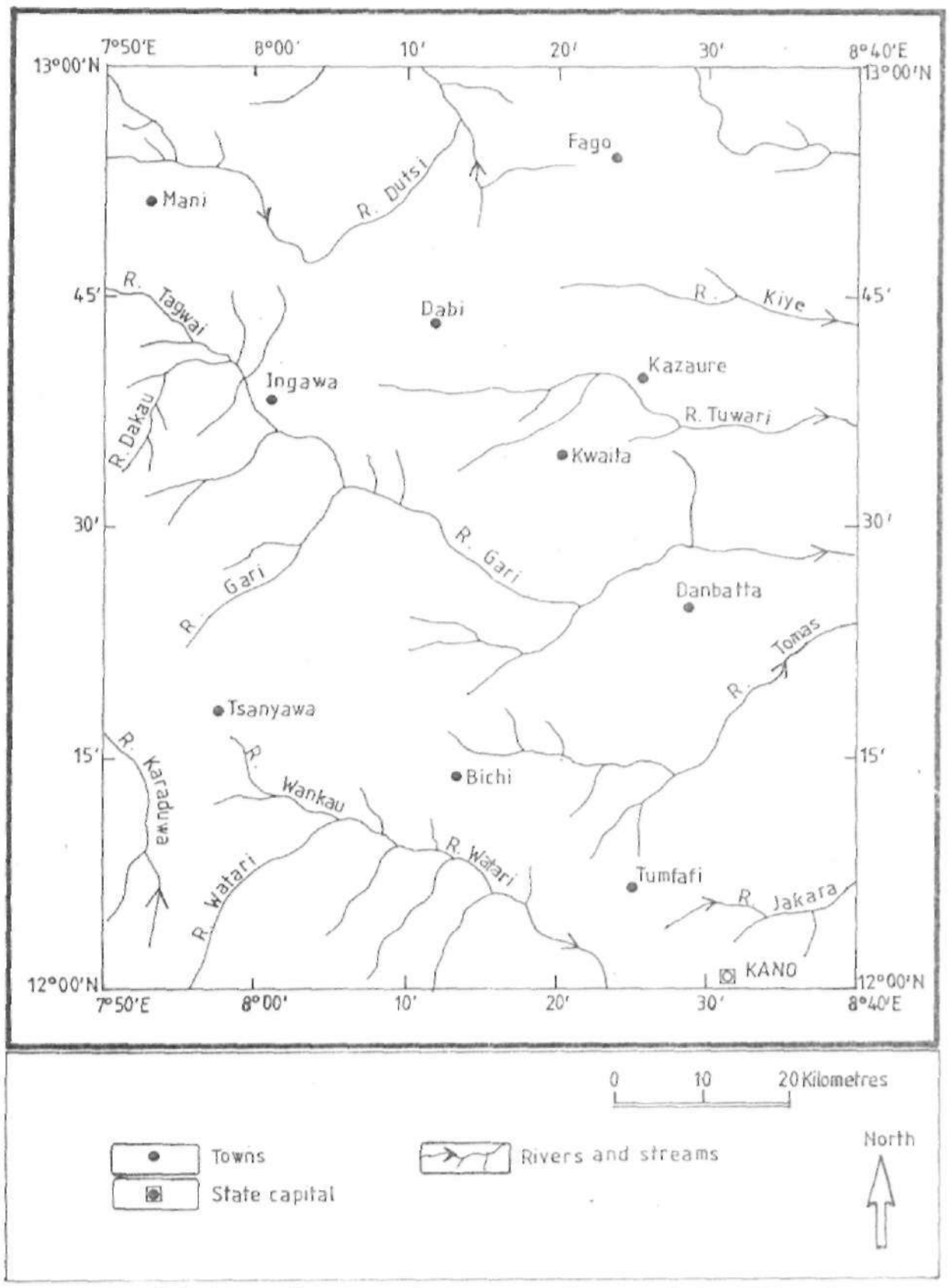


Fig. 1. 3. Map showing drainage pattern and location of major rivers in the study area .

area, with supply of food and water for human and animal consumption available throughout the year. This is due to the numerous dams located in the area among which are: Kazaure dam, Gari dam, Minjibir dam and Tomas dam.

1.4 CLIMATE AND VEGETATION

The map area lies within the Sudan tropical climate zone of Nigeria and is characterised by two main seasons, rainy and dry seasons which is typical of northern Nigeria. The rainy season which is warm and wet commences from May to September, while the dry season from October to April, respectively.

The study area receives an average annual rainfall of about 1200 mm in the south to 650 mm in the north (Jarret, 1976). The dry season has low humidity and is marked by Harmattan wind from Sahara. The temperature condition is dependant on the prevailing season. However, it is generally high throughout the year and can markedly alternate between the day time and night, especially in March.

There is a thick soil cover, supporting thorn-bush vegetation. Both cultivated and uncultivated vegetation are found in the map area. The uncultivated vegetation cover is typical of Sudan Savannah with scattered treess mostly shrubs with only a few tall trees like thorn Acacia, baobab, and grasses. It is denser along river channels due to the presence of moisture which allows the vegetation to flourish.

Settlements in this area are dense with many villages moderately populated by Hausa and Fulani. The Hausas are mostly farmers and traders, while the Fulanis are farmers and cattle rearers. The cultivated vegetation mainly consists of crops like maize, millet, guinea corn, ground-nut, beans and cotton.

The vegetation cover has been tremendously reduced due to deforestation through bush burning and fire-wood collection. As such numerous afforestation projects like shelter belts have been established in the area to help check the menace of erosion.

1.5 PREVIOUS WORK

The Kazaure Schist Belt is a narrow belt (1-3 km wide) of metasediments which trends northeastwards from south of Bichi to east of Daura for about 85 km along strike. Some workers have carried out reconnaissance geologic mapping of parts of the Kazaure belt in the sixties (e.g Morton, 1967). Turner and Webb (1974) and Aderotoye (1977) were also among the earlier workers who gave account of the geology of the Kazaure belt. Turner and Webb (1974) were the first to identify some of the main lithological units of the area while mapping the Daura Younger Granites. They identified quartz schists, metaconglomerates and quartzites (most of which were brecciated and filled with black magnetite).

Aderotoye (1977) described the distribution and field relationships of the Kazaure rocks. He mapped some NE-trending discontinuous ridges of intensely folded quartzites, metaconglomerates and schists, intruded by Older Granites. He also recognised the silica sand deposit in the area and established a classification scheme for the sand based on their colour and grain sizes.

Previous work on Sheet 57 (Bichi) and Sheet 58 (Kunya) has been largely restricted to reconnaissance lithologic mapping by the Geological Survey of Nigeria (GSN) [Mbonu, 1974). There are unpublished and published reports describing Older Granite occurrences on these Sheets. According to the published map of Nigeria by the Geological Survey of Nigeria (GSN) [Dessauvagie, 1974], the rocks in the area mapped belong to the Nigerian Basement Complex. Macleod (1966) described the Kaolin deposits which lie close to Bichi.

The area to the immediate southwest of the study area forms the northernmost portion of the Malumfashi belt not studied before (Figs. 1.1 and 1.2), although the southern portion had been studied by McCurry (1970; 1971; 1973; 1976). She mapped the southern portion of the Malumfashi Belt and documented the occurrence of younger metasediments, basement gneisses and migmatites, and Older Granite intrusions.

According to McCurry's observations, at least two major tectonic episodes have affected both the reactivated basement complex and the younger supracrustal rocks in this area. She distinguished an early phase of deformation (D_E) and a later phase (D_L), both of which resulted in intense isoclinal folding. Her earlier structures (D_E) have a general ENE trend, while the latter ones (D_L) are dominantly N-S oriented, and have obliterated or transposed the earlier foliations.

Verheijein and Ajakaiye (1977) have correlated a distinct negative gravity anomaly to the metasediments in the Kazaure area. Turner (1983) also briefly described the Kazaure Belt and concluded that it has a simple structural style and is free from central granite intrusion. He also suggested the possible similarities of the Kazaure rocks to those of Malumfashi Belt.

Ajidahun (1996); Danpullo (1996) Garba (1996); Ibrahim (1996) and Odoma (1996) have studied the geology of parts of the Kazaure Belt. They noted the occurrence of quartzites, mica schists, and some structures. Some parts of the area are unconformably overlain to the north by Cretaceous sediments of the Iullummedin Basin, and to the northeast by Tertiary sediments of the Chad Basin.

1.6 PRESENT STUDY

1.6.1 Aim and Objectives

The aim of this study is to carry out a comprehensive geological, structural and geochronological study of the Kazaure Schist Belt (KZSB) with the objective of proposing a geotectonic model of the evolution of the Belt. Specifically the work is designed to:

(i) Study the lithology and field relationships of the component rock units of the Kazaure Schist Belt and surrounding area.

(ii) Study the nature of deformation(s) and metamorphism in the study area.

(iii) Provide geochemical data on whole rock compositions of the rock units in the study area, leading to a Rb-Sr isotope geochronology of some of the granitic rocks.

(iv) Propose a model for the geotectonic evolution of the Kazaure Schist Belt.

1.6.2 Methodology for field mapping

The main problem in the Kazaure area is the lack of good and continuous outcrops due to intense tropical weathering. Therefore, the geologic field mapping in this study was carried out using air-photo interpretation and ground traverses provided by roads and footpaths, as well as river and stream courses. Topographic maps on a scale of 1:50,000 and air photographs on a scale of 1:40,000 (covering the whole

469074

project area) provided topographic details for the exercise. ERTS Band 5 (Landsat imagery) was also used, especially as an additional aid in interpreting major structures.

The field and photogeological data were then transferred to Sheets 35 (Kazaure), 57 (Bichi), and parts of 36 (Baure) and 58 (Kunya), 56 (Musawa), and 34 (Kastina), all on a scale of 1:100,000 (Maps 1 and 2). This was to portray in full the broad structures and lithological units of the Kazaure Schist Belt and surrounding areas. The geological features from these maps were finally transferred to another reduced scale map (Fig. 3.1), in order to have a quick regional overview of the geology of the whole area.

Field work was started in December 1991 and samples of the different rocks were collected for geochemical and geochronological analyses (Maps 1 and 2). Further visits were made to the area in July, 1996 and August, 1998. The field data were supplemented by microscopic examination of thin sections of the rocks collected. Modal compositions of most of the investigated rocks were established by visual estimation.

During the mapping exercise, emphasis was laid on the number and types of outcrops, surface structures and fracture analysis. A portion of the most accessible area with relatively good exposures and structures found around Kazaure

was specifically mapped on a scale of 1:12,500 in order to locate and study minor structures in detail. In addition, by utilizing the experience gained in the structural mapping above, the large scale structural analysis was extended to other selected small areas in the central and southwestern portions of the project area where the rocks outcrop as migmatite-gneiss and metasedimentary units.

1.6.2 Methodology for geochemical analyses

The whole-rock geochemical analyses of thirty five (35) representative granite, quartzite, mica schist and metavolcanic samples were carried out in the Department of Earth and Planetary Sciences, McGill University, using a Phillips PW2400 X-ray Florescence Spectrometer.

The X-ray fluorescence (XRF) analyses were carried out following the procedure of Bertin (1975). The analysis involves the determination of elemental concentrations by comparing absorbance of whole-rock samples (ignited fused beads) and those of artificial standards. The studied Rare Earth Elements (REE) were determined using Inductively Coupled Plasma torch combined with a mass spectrometric techniques (ICP-MS techniques). Details of the operating conditions and

accuracy of the R.E.E. analysis are given in Walsh et al. (1981) and Watkins (1989).

All the laboratory Rb-Sr work was carried out at the Department of Geology, Universite' de Quebec', Montreal' Canada, following the method described by Pankhurst and O'nions (1973). The Rb/Sr ratios were determined using X-ray fluorescence spectrometry. Sr concentrations and compositions measurements were done by Dr. N. Norman following the method outlined by Potts (1987). The Sr was separated using standard ion-exchange techniques and analysed using mass spectrometric techniques.

The analytical techniques used are based on X-ray fluorescence, ICP-MS and mass spectrometry methods, respectively. However, electron microprobe was used for the chemical analysis of some garnets. Details of the chemical and analytical procedures are described in Appendix A. Notes describing the fundamentals of the Rb-Sr dating method and the details of experimental uncertainties are given in Appendix B.

CHAPTER TWO:

REGIONAL GEOLOGY

2.1 INTRODUCTION

The Nigerian Precambrian Basement Complex forms part of a huge African platform of crystalline rocks which are partially masked by flat lying cover of sedimentary rocks of many ages. The African continent resulted from a series of progressive cratonisation of ancient rock remnants during at least five major orogenies (Read and Watson, 1975). These are the Liberian (3000 ± 200 Ma), Shamvian (2500 ± 200 Ma), Eburnean (2000 ± 200 Ma), Kibaran (1100 ± 200 Ma) and Pan-African (650 ± 200 Ma), respectively (Ekwueme, 1993). According to Clifford (1970), three African cratons: the West African, Congo and Kalahari cratons, were carved out at the end of these orogenies.

Nigeria lies within the vast Pan-African (650 ± 200 Ma) mobile belt (Kennedy, 1964; Wright, et al., 1985) which separates the West African and Congo cratons (Fig. 1.2). Lithostratigraphic, structural and geochronological investigations on the Precambrian rocks of Nigeria have revealed imprints of the five major orogenies that have affected the evolution of Africa (Section 2.3).

The previous geochronological investigations undertaken on the basement rocks of Nigeria are first reviewed, and these include those of Grant (1970; 1978), Oversby (1975), Hubbard (1975), Ogezi (1977), Mullum (1978), Ajibade (1980), Holt (1982), Rahaman et al. (1983), Ekwueme et al. (1987) and Ekwueme (1990a; 1990b; 1992), among others. This review will hopefully provide a framework for the conceptual interpretation of a Rb-Sr isotopic age now available from the KZSB area (Section 5.5).

2.2 THE NIGERIAN BASEMENT COMPLEX

The Nigerian Basement Complex rocks outcrop over about 60% of the total surface area of the country, in four broad segments. These are the northwestern Nigeria, southwestern Nigeria, northeastern Nigeria, and southeastern Nigeria (Mambilla Plateau and Oban Massif) segments. Intruding and truncating the Nigerian basement are a number of Younger Granite Complexes of Mesozoic age (Falconer, 1911; Jacobson et al., 1964). Deposited on the crystalline rocks are Cretaceous and younger sedimentary rocks along the Benue and Niger valleys, the delta region, the Iullemmeden basin and the Chad basin (Figs. 1.1 and 1.2).

The Nigerian Basement Complex within the Pan-African terrain has four broad lithological units viz:-

a) A polycyclic basement of migmatites and gneisses together

with relics of ancient metasediments (the "Older Metasediments" with calcareous schists, marbles and sillimanite and/or kyanite bearing quartzites). This is generally of amphibolite facies grade of metamorphism and is believed to have had multiple metamorphic episodes (Grant, 1970; 1971; Wright, 1971 and Oversby, 1975).

b) Younger low to medium grade metasediments and metavolcanics which form distinct NNE-SSW trending belts within the migmatite-gneiss complex. The metasediments are believed to be supracrustal cover sequences to the migmatite-gneiss complex (Rahaman, 1976a; Grant, 1978).

c) Syntectonic to late tectonic Older Granite suite which intruded both the migmatite-gneiss basement and the metasediments. The Older Granite suite includes porphyritic biotite granites, granodiorites, diorites, gabbros, charnockites and syenites (Russ, 1957; McCurry, 1976 and Fitches et al., 1985). The most predominant are the granodiorites.

d) Unmetamorphosed alkaline, calc-alkaline volcanic and hypabbysal rocks which overlie or intrude the basement migmatite-gneisses, schist belts and granitic rocks associated with the Lower Palaeozoic uplift following the Pan-African orogeny (Farghar, 1961; McCurry, 1976).

The first published account of research on the migmatite-gneiss complex of NW Nigeria was by Dunstan (1908), who mapped

quartzites, quartz schists, amphibolites and gneisses around Zungeru. However, Falconer (1911) was the first to describe the geology and geography of the whole of northern Nigeria. Russ (1957) also investigated parts of Niger, Zaria and Sokoto Provinces all in northwestern Nigeria, with reference to gold exploration. These and other workers have described the geology in various parts of the migmatite-gneiss complex of northwestern Nigeria (Figs. 1.1 and 2.1).

2.2.1 Characteristic of the Migmatites and gneisses.

The gneisses of the Nigerian basement normally have a variable lithology, including augen-gneiss, sheared gneisses and mylonites (McCurry, 1973; Ekwueme and Onyeagocha, 1982; Danbatta, 1986). Associated with these are relics of ancient metasediments (commonly feldspathic quartzites) which were correlated with the Birrimian metasediments of Ghana by McCurry (1976).

Most authors agree with the view that the rocks are largely of sedimentary origin (paragneiss) with associated minor igneous rocks which have been variably altered by metamorphic and magmatic processes. There are different types of migmatised (e.g banded gneiss) and unmigmatised gneisses, which form the host into which the intrusive granitoids were emplaced.

Ajibade et al., (1987a; 1987b) have also shown that there are at least two generations of migmatitic-gneiss of widely differing ages within the Nigerian Basement Complex. In line with this suggestion, they report that most parts of Minna which were mapped as migmatite-gneiss complex, contain large volumes of weakly to strongly foliated granites which they demonstrated to be intrusive into schists. The two types of migmatites are the early migmatites (high grade migmatites) and the Pan-African migmatites (injection-type migmatites).

According to Ajibade (1982), the early migmatites can be distinguished from the Pan-African migmatites in that the latter are typically banded and complexly folded with several generations of axial planar foliations and stromatic, agmatitic and nebulitic structures (Mehnert, 1968; 1971). The Pan-African migmatites on the other hand, were formed mostly as a result of magmatic intrusions that altered pre-Pan African granitic bodies (e.g Ekwueme, 1992; Annor and Coker, 1994) and the low grade schists during the emplacement of the early phases of the Older Granites.

2.2.2 Characteristics of the Schist belts

The schist belts in Nigeria are best developed in the northwest in zone about 300 km wide. The first obvious characteristic of the schist belts is the ubiquitous presence of low to medium-grade metasedimentary and metavolcanic rocks

and their NNE-SSW trends. The schist belts occur predominantly as series of synformal troughs and strike ridges, intercalated with relics of migmatites and gneisses or intruded granites which separate and/or lie within them. Each of the schist belt is separated from adjacent ones by these migmatites, gneisses or granites.

Wright and McCurry (1970), Hubbard (1975) and Klemm et al., (1984) compared the outcrop pattern of the schist belts to that of the Archaean greenstone belts. Of critical importance in comparing the two belts is their bulk composition. The schist belts have predominantly clastic sediments with minor volcanic rocks. This differentiates them from the Greenstone belts elsewhere (e.g. Ekwueme and Attoh, 1997) which predominantly consist of volcanic rocks. They however, have the following features in common: synclinal structure, size, low metamorphic grade, occurrence of banded iron formation and gold mineralisation, and the presence of volcanic and clastic rocks (Turner, 1983).

All the schist belts are predominantly composed of metamorphosed pelitic to semi-pelitic rocks (e.g. Ekwueme, 1995a), but each belt differs in the amount of such lithologies as conglomerates, greywackes, quartzites, calcareous rocks and volcanic rocks. The rocks in the schist

belts are usually micaceous schists, phyllites, amphibolites, quartzites and ferruginous quartzites, as well as acid and intermediate volcanic and plutonic rocks interbedded with the metasedimentary rocks.

The acid and mafic-ultramafic volcanic rocks are generally represented by rhyolites, dacites, basalts and microtonalites. Geochemical data indicate that the amphibolites in the schist belts are largely tholeiitic in nature and of ocean floor and island arc affinities (McCurry and Wright, 1977). Ogezi (1977, 1981) has interpreted some of the ultramafic rocks as depleted dunites and harzburgites.

Oyawoye (1964) and McCurry (1976) suggested that the occurrence of the schist belts is restricted to West of longitude 8^0 E. However, Ajibade (1976) drew attention to the quartz schists and metaconglomerates reported by Turner and Webb (1974) around the Daura Younger Granites east of longitude $8^0$30'E. In addition, Ekwueme and Onyeagocha (1986) and Ekwueme (1987a; 1990a; 1990b) have for the first time mapped and documented the occurrence of metasedimentary rocks of the Uwet area, southeastern Nigeria which also occur east of longitude $8^0$30'E.

Turner (1983) and Ajibade et al., (1987) identified and classified ten main schist belts in the northwestern and

northcentral parts of Nigeria (Fig. 2.1, above). The ten schist belts include the Birnin Gwari, Kushaka, Wonaka, Zuru, Anka, Maru, Ushama, Malumfashi (or Karau Karau) and Kazaure Belts. Of these the following have been studied in detail: Malumfashi (McCurry, 1973), Kushaka (Truswell and Cope, 1963; Grant, 1978), Ushama (Ajibade, 1980), Birnin Gwari (Truswell and Cope, 1963; Ajibade, 1980), Anka (Fargher, 1961; Holt, 1982), Maru (Egbuniwe, 1982), Toto (Ajibade et al., 1987) and Zuru (McCurry, 1976; Danbatta, 1991). Not much is known about the remaining two schist belts, Kazaure and Wonaka.

The first attempt at a systematic structural investigation in parts of NW Nigeria was made by McCurry (1970; 1971; 1976). In these works, McCurry observed that two phases of intense isoclinal deformation have affected both the reactivated crystalline Basement Complex and the Younger Metasediments (Section 1.5).

Since McCurry's work, more research work has been carried out on various aspects of the geology of north-western Nigeria. Grant (1978) described the structures in the Kushaka and Birnin Gwari Schist belts, where he identified four phases of deformation in the Kushaka Schist Formation.

Ajibade (1980) worked in the Zungeru region where he described

a complex structural sequence from parts of the Birnin Gwari Schist and Ushama Schist Formations. He identified four deformation episodes that have affected the rocks in these areas, and later defined the Zungeru Mylonites. The Zungeru Mylonites are cataclastic rocks derived from the adjacent migmatites and gneisses (Ajibade et al., 1979). The Zungeru Mylonites are considered to have formed during the initial folding (D_1) of the Birnin Gwari Schist Formation. However, Annor and Coker, (1994) were only able to document the occurrence of two main deformation events affecting both the gneissic complex and schists in the Birnin Gwari-Kushaka area not investigated by Ajibade (1980).

Egbuniwe (1982) investigated the Maru Belt area and was able to document four deformation episodes. According to him, D_1 produced flat-lying folds and fabrics with N-S hinges at about 1068 Ma (Kibaran times), D_2 produced steep N-S trending axial planes and structures, while D_3 and D_4 are localised in nature. Egbuniwe (1982) also compared rocks in the Maru Belt with similar sequences (Formations) in Anka, Birnin Gwari and Ushama Belts. According to him the Maru Belt is a lateral equivalent of the Anka, both of which are probably the northward extension of the Birnin Gwari Formation and Kushaka Formation. However, the Birnin Gwari Formation which is a quiet water deposit containing conglomerates, metapelites etc, is stratigraphically more related to the Anka Belt.

Holt (1982) worked in the Anka Belt area where he described a single Pan-African deformation episode (D_1) that has affected the rocks of the area at about 760 Ma. He described upright, shallow plunging and non-cylindrical F_1 folds which occur trending NNE with shallow plunge values. According to Holt (1982) other localised deformations are due to granitic intrusions and heteregeneous strain related to faulting. He also mapped the occurrence of two major fracture systems, the earlier one trending N-S and the later NE-SW.

Turner (1983), following the work of Grant (1978) and others, investigated and classified all of the schist belts into either Kibaran or Pan-African age. His Kibaran belts show complex structural style, while his Pan-African ones have straight structural style. In addition, Danbatta (1991) noted three deformation episodes, (D_1, D_2 and D_3), as affecting the rocks in the southeastern portion of the Zuru belt. The Mainamaji Area of Bauchi State has also been mapped for the first time by Egbuniwe (1994). He was able to document the occurrence of two deformation episodes, D_1 and D_2, which have affected the quartzites and cataclastic rocks in the area.

Schist belt occurrences in the southwestern Nigeria region include those of Ife-Ilesha, Egbe-Isanlu, Kabba-Lokoja-Igarra

and Iseyin-Oyan belts (Turner, 1983; Ajibade et al., 1987; Elueze, 1988). Some of these southwestern Nigeria belts have higher metamorphic grade and are regarded as lateral equivalents of the Birrimian supracrustal. In the case of the Ife-Ilesha belt, it was interpreted as an Archaen greenstone belt by Hubbard (1968) and Klemm et al. (1984). Occurrences of schists have also been reported on the Oban massif (Ekwueme, 1985; Ekwueme and Onyeagocha, 1986), Kafanchan-Kwoi-Kachia area and Jalingo-Yola-Gongola axis (Rahaman, 1988a).

There are many similarities in age, lithologies and evolution among the northwestern Nigeria schist belts. However correlation with schist belts from southwestern Nigeria is less clear as the southwestern region is very poorly exposed and schist belts are not well defined (Rahaman, 1973; 1976a; 1976b; 1988a and 1988b).

2.2.3 Characteristics of the Older Granites

The intrusive granitoids of northwestern Nigeria were first named Older Granites by Falconer (1911), to distinguish them from the tin-bearing "Younger Granites" of Jurassic age which occur in Central Nigeria. The Older Granites occur as distinct plutons of limited petrographic types (Ekwueme and Onyeagocha, 1985b; Rahaman, 1988b). Examples of these include the Zaria Granite Batholith (Ike, 1988) and the Maiinchi Granite Batholith (Egbuniwe, 1982) which are oriented in a general N-S direction.

The Older Granites in Nigeria include a wide range of rocks varying in composition from tonalite through granodiorite to granite, syenite and charnockitic rocks (Hubbard, 1968). Other members of the Older Granite suite include diorites and gabbros. However, the suite is dominated by granites and granodiorites. The textures of these granites vary from porphyritic to fine and coarse grained and the granites are massive to strongly foliated in nature. Fitches et al., (1985) have earlier argued that the foliation in the granites is as a result of post emplacement deformation.

The geochemistry of the Older Granites of Nigeria has been studied (e.g Ogezi, 1977; Ajibade, 1980; Egbuniwe, 1982; and Rahaman, 1988b). The Older Granites in northwestern Nigeria have a calc-alkaline I-type characteristics, resembling those generated at very deep crustal levels or in the upper mantle during subduction and collision processes (e.g Fitches et al., 1985).

Rahaman (1988a) has timed the emplacement of the Older Granites during the Pan-African orogeny, and interpreted them as high level intrusions, emplaced by stoping and diapiric processes. In addition, McCurry and Wright (1971) have earlier classified the granitic rocks into syn-to late-tectonic varieties. The syntectonic granitic rocks are foliated with

gradational contacts and xenolithic inclusions, while the late-tectonic variety are said to be weakly foliated, and highly fractured. The dark fine-grained granite was considered to be the earliest phase of the Older Granite plutonic cycle (McCurry, 1976). This occurs as xenoliths and small dyke-like bodies within the other types of Older Granite bodies.

2.2.4 Characteristics of the volcanic rocks

These early Palaeozoic volcanics vary in composition from acid to basic and ultrabasic and are mainly dacites and rhyolites (Utke, 1987). K-Ar dating on these rocks reveals a 500 Ma age which narrowly post-dates the main Pan-African deformation (McCurry and Wright, 1977).

2.3 IMPRINTS OF OROGENIC EVENTS IN THE NIGERIAN BASEMENT

2.3.1 Eburnean and Older orogenic events

The Eburnean orogeny (2,000 $\pm$ 200 Ma) which is regarded as the last major orogenic event to have affected the West African Craton on a regional scale, has its suture at Sassandra (Wright, 1985). It is considered to have resulted from a continent-continent collision along an eastward dipping Benioff zone, which is now marked by the occurrence of a thick mylonite zone.

Grant (1970) was among the first to demonstrate the occurrence of granitic rocks of Eburnean age in southern Nigeria. He

obtained Rb/Sr whole-rock age of 2282 ± 73 Ma for a pink granite gneiss which is emplaced into banded gneisses and quartzites around Ibadan. However, Oversby (1975) obtained a Pb-Pb Archaean age of 2750 Ma when he dated the banded gneisses which were cut by dolerite dykes in the Ojo Quarry near Ibadan.

Hurley (1966) had also obtained indications of Eburnean and older ages from migmatites in northwestern Nigeria, such as the Rb-Sr whole-rock isochron age of 2235 ± 30 Ma on the Kaduna migmatites in the Muslim cemetery. McCurry (1976) has also correlated the migmatite-gneiss complex with the Liberian or Dahomeyan (2,800 Ma).

However, Ogezi (1977), in elaborating on the occurrence of Eburnean and older ages in northwestern Nigeria, obtained Rb-Sr data on the migmatites and gneisses from various parts of the region. He for example obtained scattered ages of between 3,100 and 2,400 Ma reference lines on the Kaduna (Kabala/ Badarawa) and Mallam Tanko migmatites, as well as ages between 3,100 and 600 Ma reference lines on the Malumfashi migmatites, respectively. These Eburnean (Birrimian) ages are more of basement reactivation and deformation ages than those of granite emplacement ages.

Although the Eburnean event was accompanied by widespread granitic activity and greenschist facies metamorphism, there is no confirmed evidence for the occurrence of Eburnean sediments in Nigeria. It is however, one of the most widespread dated event in the Nigerian basement (Ekwueme, 1990c; Ekwueme and Kroner, 1994).

2.3.2 The Kibaran orogenic event

There are widespread evidence for an intense Kibaran event which is confined to the mobile belt east of the West African craton. It is characterised by distinct E-W to NW- trending fold structures accompanied by amphibolite facies of metamorphism grading to granulite (Baer, 1981). Some workers have mapped the Oti/Volta lineament as the boundary between the Kibaran and Eburnean domains (Kroner, 1981; 1983).

Evidence for a possible Kibaran event in the northwestern Nigeria basement was first reported by Grant et al., (1972) who provided two single-sample whole-rock ages of 1275 ± 75 and 1120 ± 70 Ma for banded gneiss from the Kusheriki region. He also obtained Rb-Sr single whole rock age of 1315 ± 75 Ma on a migmatite sample just West of Kaduna, and a similar age of 1159 ± 70 on another migmatite sample 200 km West of Kaduna (Grant et al., 1972).

KASHIM IB...

Ogezi (1977) has also reported a possible Kibaran age of 1065 ± 65 Ma on the Sokoto River migmatite. He however observed that the age might be a mixed age considering the data are a two point isochron. Ogezi (1977) also obtained a 3-point Rb/Sr errorchron age of 1158 ± 30 m.y with an initial $^{Sr}87/^{Sr}86$ ratio of 0.7117 on the Gusau migmatites. According to him this Kibaran Gusau migmatites "remained a closed system with respect to Rb and Sr, and were not affected by the Pan-African deformational/metamorphic event".

Snelling (1964), and Egbuniwe (1982) have dated the Kanoma discordant body as Kibaran (765 Ma). Along the same line Ekwueme (1987b; 1988), Ekwueme and Caen-Vachette (1992) and Ekwueme et al., (1987) have documented evidence for the existence of Kibaran event in the basement rocks of southeastern Nigeria. The interpretation of the age of the northwestern Nigeria schist belts is mainly based on the Kibaran isotopic age obtained from phyllites of the Maru Belt (Ogezi, 1977; Holt et al., 1978), and the documented Kibaran isotopic overprinting of basement gneisses in several parts of the region (Grant et al., 1972).

Although the above radiometric ages reflect the Kibaran event in Nigeria, the concept of Kibaran event in Nigeria is one of the most controversial. However, according to Ajibade et al., (1987a), there is no major Kibaran event in the country. This

is probably because no major granitic intrusions of that age are found in Nigeria.

2.3.3 The Pan-African orogenic event

Majority of age determinations are Pan-African and were mainly obtained from members of the Older Granite Suite of northern and northcentral Nigeria. The precise nature and significance of the Pan-African event is a subject of differing interpretations. The common view today is that the Pan-African event is related to plate tectonic activities involving the collision of the Birrimian plate (comprising the present West African craton) and the Dahomean plate (comprising the present day Nigerian-Benin shield) [Burke and Dewey, 1972; Grant, 1979; Turner, 1983].

These processes involve crustal thinning and ensimatic mechanisms that led to ocean opening, subduction and continental collision-type orogeneses in response to the closure of the Buem ocean at the eastern margin of the West African craton along an east-dipping plane (Burke and Dewey, 1972; Black et al., 1979; Caby et al., 1981). According to Burke and Dewey (1972), the early stage of the Pan-African event started with the opening and closing of the Buem ocean in Late Proterozoic (Neoproterozoic) times.

The closure is along an east-dipping plane, and this reactivated Dahomea, while Birrimea remained stable (Burke and Dewey, 1972). This led to the development of a complete orogenic cycle during the Pan-African in West Africa (Grant, 1968; 1969; McCurry, 1971; 1978). Fitches (1970) and Grant (1970; 1971), on the other hand interpreted the Pan-African as a thermo-tectonic event in parts of Nigeria and adjacent countries.

The first published radiometric age determinations from the Nigerian basement by Truswell and Cope (1963), Snelling (1964), and Jacobson et al. (1964), are K-Ar and Rb-Sr data on fine grained micas and whole-rock from the Older Granite Suite. These ages lie in the range 450-550 Ma, and are thought to mark the final stages of the Pan-African event.

Ogezi (1977) described Rb-Sr isochron ages on the Maiinchi granodiorite (Maru Belt) and Zaria granite (Fig 2.2), respectively. From the Zaria Granite, Ogezi (1977) obtained a whole -rock, Rb-Sr, 3-point errorchron corresponding to an age of 794 $\pm$ 73 Ma. with a low initial ratio of 0.7044, but relatively high error ($\pm$ 0.0053). He considers this errorchron age as the age of intrusion of the granite. The Zaria granite is a typical syn-tectonic batholith (McCurry, 1973) and is therefore the oldest dated member of the Pan-African granite cycle in Nigeria.

The Maiinchi Granodiorite yields an eleven point Rb-Sr, isochron age of 679 ± 65 Ma. with an initial ratio of 0.7074 ± 0.0008 which defines the age of intrusion of a granodioritic magma probably generated by the partial fusion of older crustal components (Ogezi, 1977).

Apart from these results, the Pan-African is also recognised in the gneisses and migmatites of Malumfashi area, where eight gneiss samples define an imprecise whole rock errorchron age of 610 Ma, with an initial ratio of 0.7107 ± 0.0021 (Ogezi, 1977). He interpreted this age as the metamorphic age of the gneisses and migmatites, during which there was an open system in the Rb-Sr physico-chemical environment of pre-existing basement rocks.

Van Breemen et al., (1977) obtained Rb-Sr isochron age of 692 ± 161 Ma and a U-Pb Zircon age of 605 ± 10 Ma on the Panyam granite. They also obtained a Rb-Sr age of 663 ± 164 Ma from Bauchi charnockitic rocks, and concluded that the peak period of Older Granite emplacement in north-central Nigeria took place about 610 Ma ago. Snelling, (1964) reported a K-Ar age of 780 ± 40 Ma from a hornblende granite which occur 6.5 km away from Kano. Tougarinov et al., (1968), also reported a U-Pb age of 680 ± ? Ma on K-feldspar from Rukuba Older Granite.

In the Kusheriki area to the southwest of the KZSB, Jacobson et al., (1964) have reported Rb-Sr single whole rock age of 549 ± 14 Ma for a porphyritic granite. Similarly, Van Breeman et al., (1977) have obtained ages of 605 ± 10 m.y. (U-Pb on zircons) and 609 ± 23 m.y. (Rb-Sr, 5-point isochron) respectively, on foliated granites from the Panyam and Bauchi areas.

Broadly similar analytical results were obtained by Ajibade (1980) for the Minna Granite Batholith. He obtained an errorchron age of 505 ± 12 Ma on biotite from the Minna granodiorite. Ogezi (1977) has also obtained a Rb-Sr age of 565 ± 46 Ma on a gneissic granite from Saibodji, Gusau. All these are consistent with previous correlations among the Older Granite complexes in northwestern Nigeria.

On the basis of available data, van Breemen et al., (1977) and Ajibade et al., (1987) reported that most Rb-Sr isotopic measurements on the Older Granites from northwestern Nigeria give initial $^{87}Sr/^{86}Sr$ ratios of 0.7065 to 0.7125. These initial ratios are above the Upper mantle value of 0.701 (600 Ma ago), and provide an opportunity to discuss the source rocks. The workers hence interpreted them as suggesting heavy contamination (by older crustal rocks) of magmas originally produced by the partial fusion of upper mantle rocks. A second

alternative is that the Pan-African granite melts were generated by partial melting of lower older crustal rocks (high initial ratio).

Dada (1995) reviewed all the published radiometric ages and drew attention to the fact that they do not correspond to any specific crustal event. He also suggests the significant involvement of older Archaean crustal components during the formation of the Late Proterozoic crust in the Nigerian basement.

2.4 AGE OF THE SCHIST BELTS

The age relationship among the schist belts of Nigeria is largely unresolved, as various ages have been assigned to them. On the basis of available isotopic data, the schist belts of Nigeria are also assumed to be of two types: the ancient metasediments (mainly found in southwestern Nigeria) and the low grade schists (the Younger metasediments), mainly found in northwestern Nigeria).

Russ (1957) and Oyawoye (1964) were the first to assign Archaean (Palaeoproterozoic) age to the schist belts, while Hubbard (1975) was the first to assign the Ile-Ife belt to Kibaran event (1100 Ma) and the Ibadan belt to Eburnean event (2,000 Ma). However, Oyawoye (1972) and Olade and Elueze

(1979) considered the schist belts to be middle Proterozoic, while Burke and Dewey (1972) considered the schist belts to be involved in Eburnean (2,000 Ma) and Pan-African events.

All the radiometric age interpretations reported from the schist belts of northwestern Nigeria are significantly different. These could be assigned to three schools of thought on the age of schist belts, apart from the minority view of Truswell and Cope (1963) who proposed that the whole basement experienced a single Gwarian (Pan-African episode) of deposition, deformation and metamorphism. These schools are represented by:

a). Ogezi (1977) and Ajibade (1980) who placed the main deformation and metamorphism of the sediments in the Kibaran (1,100 Ma), with a further reactivation accompanied by widespread granitic intrusion in the Pan-African (550 Ma).

b). McCurry (1973, 1976) who proposed that all of the low-grade schist belts were originally equivalent to the Katangan (800 - 1000 Ma) metasedimentary cover of Central Africa and became down-folded into the reactivated basement of gneisses and migmatites during the Pan-African.

c). Grant (1978) and Turner (1983) who concluded on structural grounds that the belts are probably of different ages, and belong to at least two major

deformational cycles, the Kibaran (1100 ± 150 Ma) and Pan-African (600 ± 150 Ma).

One of the radiometric data for the schist belts was reported by Ogezi (1977) who obtained an 11-point Rb-Sr isochron age of 1064 ± 64 Ma from Maru phyllites. This age was confirmed by Ajibade (1980) who re-analyzed the same samples from the Maru belt. This is the first and only data suggesting a Kibaran metamorphic age for these schist belts, and many models on the evolution of the schist belts have been based on it (section 2.5).

McCurry's (1973; 1978) proposal was based on K-Ar mica and whole rock data which varied from 600-450 Ma, as determined from a range of samples of metasediments and volcanics by Harper et al., (1973). She interpreted all the geologic relations in the Malumfashi belt, as well as in other northwestern Nigeria schist belts, as Pan-African in age.

Ogezi (1977) has also obtained a 4-point Rb-Sr whole rock which gave an errorchron age of 496 ± 50 Ma on the metasandstones of Sado area. In addition, several other workers have obtained Pan-African ages from the schist belts. These include Ajibade (1980) who obtained a Pan-African Rb-Sr isochron age of 566 ± 17 Ma on phyllites from the Birnin Gwari Schist Formation. He however interpreted the Birnin Gwari belt as having Kibaran and Pan-African ages.

Holt (1982) has also demonstrated the existence of Pan-African age in the Anka schist belt by obtaining a Rb-Sr age of 762 Ma on tonalites which are intercalated with phyllites and volcano-clastics in the belt. Wright (1979) had earlier interpreted the Anka Belt volcanics as of probable Kibaran age, as they were affected by Pan-African deformation.
On the basis of available information, Ajibade et al. (1987a) concluded that the schist belts of northwestern Nigeria are all of the same age and that they were deformed and metamorphosed for the first time during the Pan-African event.

More recent studies (Annor, 1995; Olabaniyi, 1997; and Annor et al., 1998) have assigned pre-Neoproterozoic age to some of the belts. These workers used established chronostratigraphic markers (where they occur), as reliable clues in constraining the age of the Nigerian schist belts. One of this is Algoma Banded Iron Formations (BIF'S) which are known to be exclusively restricted to the Archaean and Palaeoproterozoic (James, 1992; Klein and Beukes, 1993). Their occurrence in an area was therefore used to model the earliest age of deformation and metamorphism in the belts.

In the Egbe-Isanlu area, Komatiitic peridotite and Algoma-type BIF were used as chronostratigraphic markers by Olabaniyi (1997), to constrain the age of the metasediments in the area to a Paleoproterozoic age. The Algoma-type BIF which has been

reported from Maru, Malumfashi, Birnin Gwari, Kushaka, Muro and Igarra-Kabba-Lokoja schists, was also used as a chronostratigraphic marker. According to this hypothesis, D_1 deformation and metamorphism in Nigerian schist belts with documented occurrence of Algoma BIF'S is pre-Neoproterozoic.

2.5 PREVIOUS MODELS OF EVOLUTION OF THE SCHIST BELTS

All the models of evolution of the schist belts of Nigeria formulated over the years could be classified under three main headings:

(a) Those in favour of the evolution of the schist belts through ensialic processes (e.g McCurry, 1971).

(b) Those in favour of the evolution of the schist belt through ensimatic processes (e.g Ajibade and Wright, 1989). Other examples here include Ogezi, (1977) and Bafor, (1982) who suggest the formation of rift zones where sufficient extension led to the production of small ocean basin.

(c) Those in favour of the evolution of the schist belts through both ensialic and ensimatic processes (e.g Holt, 1982).

2.5.1 Schist Belts Evolution through ensialic processes

According to some workers, the schist belts were once a widespread supracrustal cover rocks deposited in a single basin on the migmatite-gneiss basement and intruded by Older

Granites (Russ, 1957; Oyawoye, 1964; 1972; McCurry, 1971; 1976; Ajibade, 1971; 1976; Grant, 1968; 1978).

McCurry (1971; 1976), Burke and Dewey (1972) and Vaniman (1976), among others, have specifically proposed the schist belts to have evolved through ensialic processes on the basement. Vaniman (1976) proposed the existence of a major Nigerian sedimentary trough to be responsible for the deposition of the schist belts. He interpreted the trough as a back-arc basin developed during the Pan-African collision of Dahomea with Birrimea basements. In southwestern Nigeria, the model of Olade and Elueze (1979) also invoked a marginal basin model to explain the evolution of the Pan-African schist belts.

Chukwu-Ike (1978) identified major marginal faults associated with the schist belts in northwestern Nigeria. He argued that the schist belts are fault bounded ensialic troughs. Turner (1983) however considered the Anka belt with the Maru, Birnin Gwari, Wonaka, Malumfashi and Kazaure Belts (80 km east, 100 km southeast, 100 km east, 120 km southeast and 140 km east of Anka, respectively), as forming in one back-arc basin. The Maru, Kushaka and Zuru belts were also considered by him to have formed another basin, with the Zuru quartzites representing basin margin deposits.

Fitches et al. (1985) considered that lateral changes in volcanism and facies within a complex volcano-sedimentary basin is responsible for the differences in lithology between the belts. Similarly, Udoh (1987) considered the Zuru and Kushaka belts as ensialic sedimentary trough deposits.

While working in the Anka area, Holt (1982) observed that the Anka metavolcanics have chemical characteristics of both island arcs and continental environments. He concluded that the schist belts were deposited in a retro-arc basin related to the subduction processes along the margin of the West African craton. This conforms with Ajibade et al. (1987a) argument that the evolution of the schist belts is probably related to graben-like structures formed during the Pan-African event, about 600 Ma ago. This view point was further discussed by Olabaniyi (1997), who interpreted the formation of the Egbe-Isanlu basin as a result of plume-induced continental rift. He however ascribed his D_1 and D_2 events to the Eburnean and Pan-African events, respectively.

2.5.2 Schist Belts Evolution through ensimatic processes

McCurry and Wright (1977), Wright and Ogezi (1977), Holt et al. (1978), Utke (1987) and Rahaman et al. (1988), among others, considered the schist belts to be products of ensimatic processes. Turner (1983) and Utke (1987) suggested that the schist belts represent additional microcontinents

separated from a pre-existing one. There are also geochemical evidence that suggest the schist belts evolved as small oceans (Bafor, 1982, 1988; Shibayan, 1990). This is presumed to account for the possible existence of a palaeosuture in the northwestern Nigerian basement (Ajibade and Wright, 1989). These workers have suggested that the Nigerian basement may represent an aggregation or "mosaic" of island arcs, inter arc sedimentary basins and continental fragments.

2.5.3 Schist Belts Evolution through both ensialic and ensimatic processes

Wright (1979) has proposed a model for the evolution of some of the NW Nigeria schist belts, in which he suggested the closure of small oceans between a series of microcontinents. According to him the Maikwonga-Sado mafic/ultramafic rocks are remnants of a Kibaran (1100 Ma) palaeosuture involving collision between micro-continents (Fig. 2.1).

The mafic and ultramafic units preserved in the Sado fault zone (Anka Belt area, Ogezi, 1977; Holt, 1980) and Anka fault system (Zuru Belt area, McCurry and Wright, 1977; Ajibade and Wright, 1989; Danbatta, 1991), have ensimatic affinities. Schist belts without such features were considered ensialic basins. Danbatta (1991) supported this interpretation and considered the southwestern portion of the Zuru belt to represent back-arc basin deposits, with the present lineaments

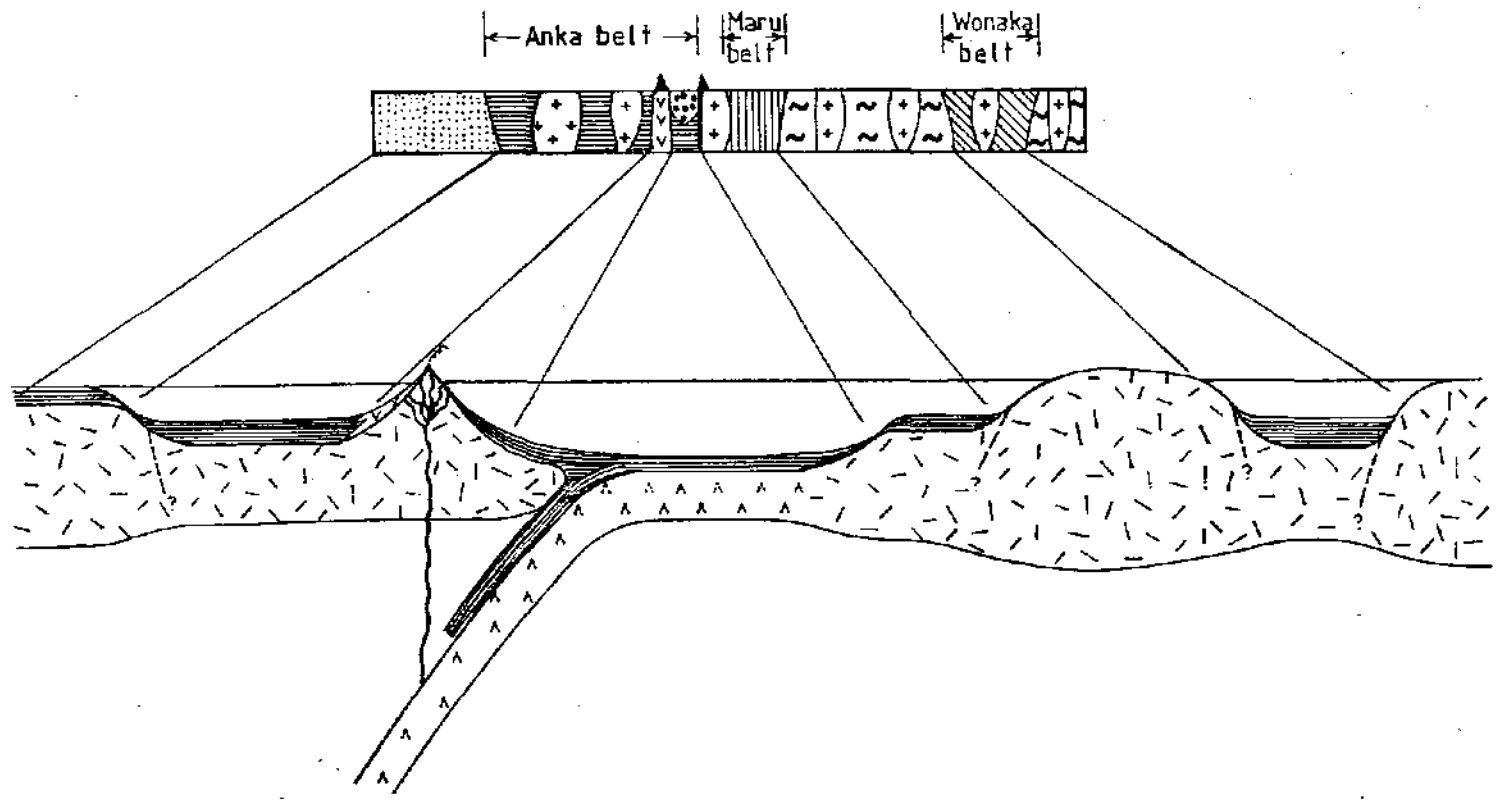


Fig. 2.1. Interpretation of the Anka, Maru and Wonaka belts (Wright, 1979).

in the Zuru area (KFS) marking a possible palaeosuture e.g Wright and Ajibade (1989). The Anka (Fig. 2.2) and Zuru belts are considered to be a pair of belts that evolved through ensimatic processes. The evolution of all the northwestern Nigeria schist belts is now considered in one geotectonic model, as proposed in chapter 8 below.

2.6 NATURE OF THE DAMAGARAN, ADRAR DES IFORAS AND HOGGAR REGIONS

The geologic framework of the Pan-African mobile belt to the north of the Nigerian basement (i.e Damagaran, Adrar des Iforas and Hoggar regions), were also briefly reviewed as part of the geotectonic setting of the study area (Fig. 2.3). The Damagaran region of Southern Niger mostly consists of metasediments with quartzites more predominate (Turner and Webb, 1974; Black, 1980). The evolution of the Adrar Des Iforas - Hoggar region involved the collision about 600 Ma between the passive continental margin of the West African craton and the active continuity margin (Pharussian belt) of the Tuareg shield

French geologists have established the complex nature of the geology of the Adrar Des Iforas - Hoggar region (Bertrand and Caby, 1978). The region is divided into three zones (Fig. 2.3):

a. a marginal zone containing ophiolitic assemblages e.g the Timitrine in Western Adrar Des Iforas of Mali (Black et

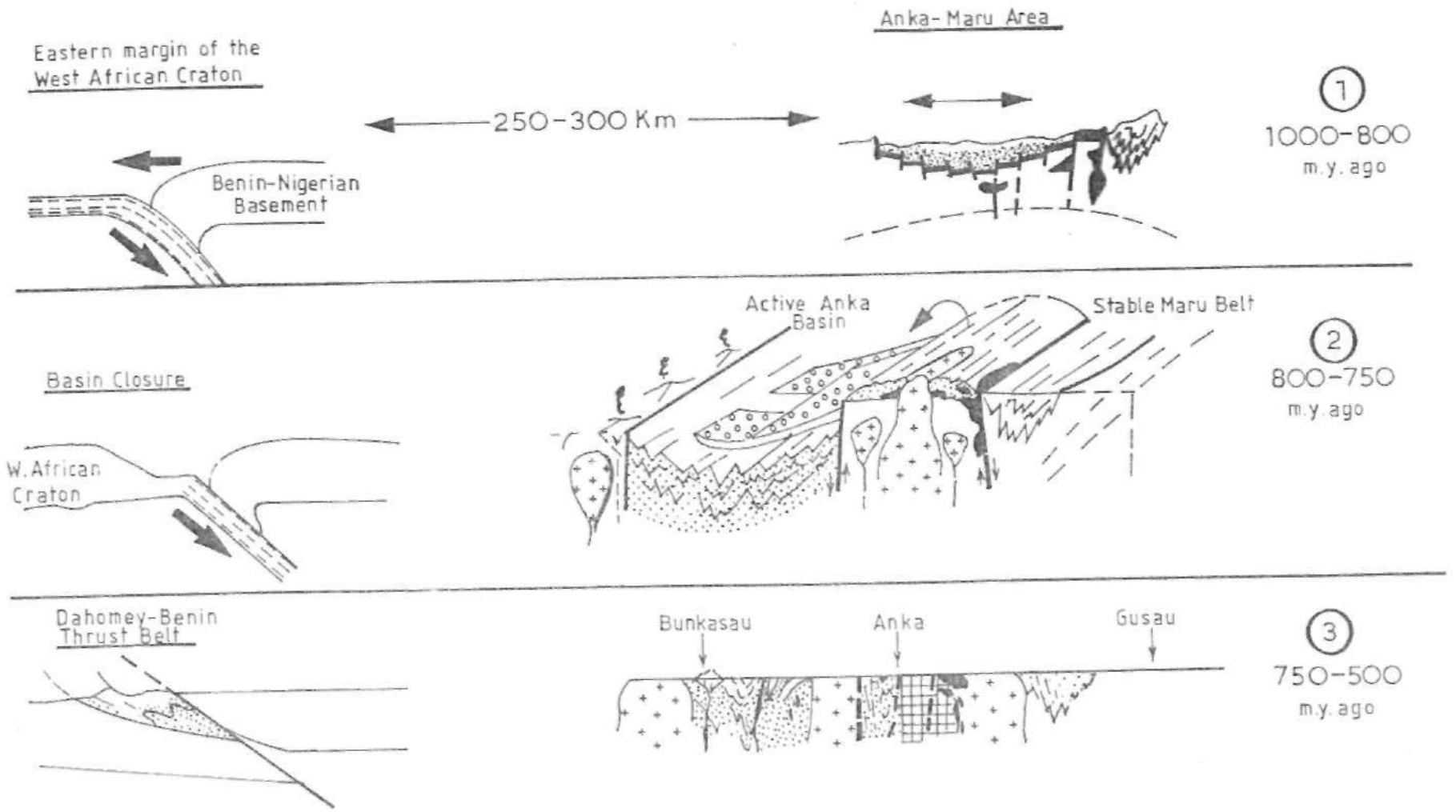


Fig.2.2. Interpretation of the Anka and Maru belts according to Holt (1982).

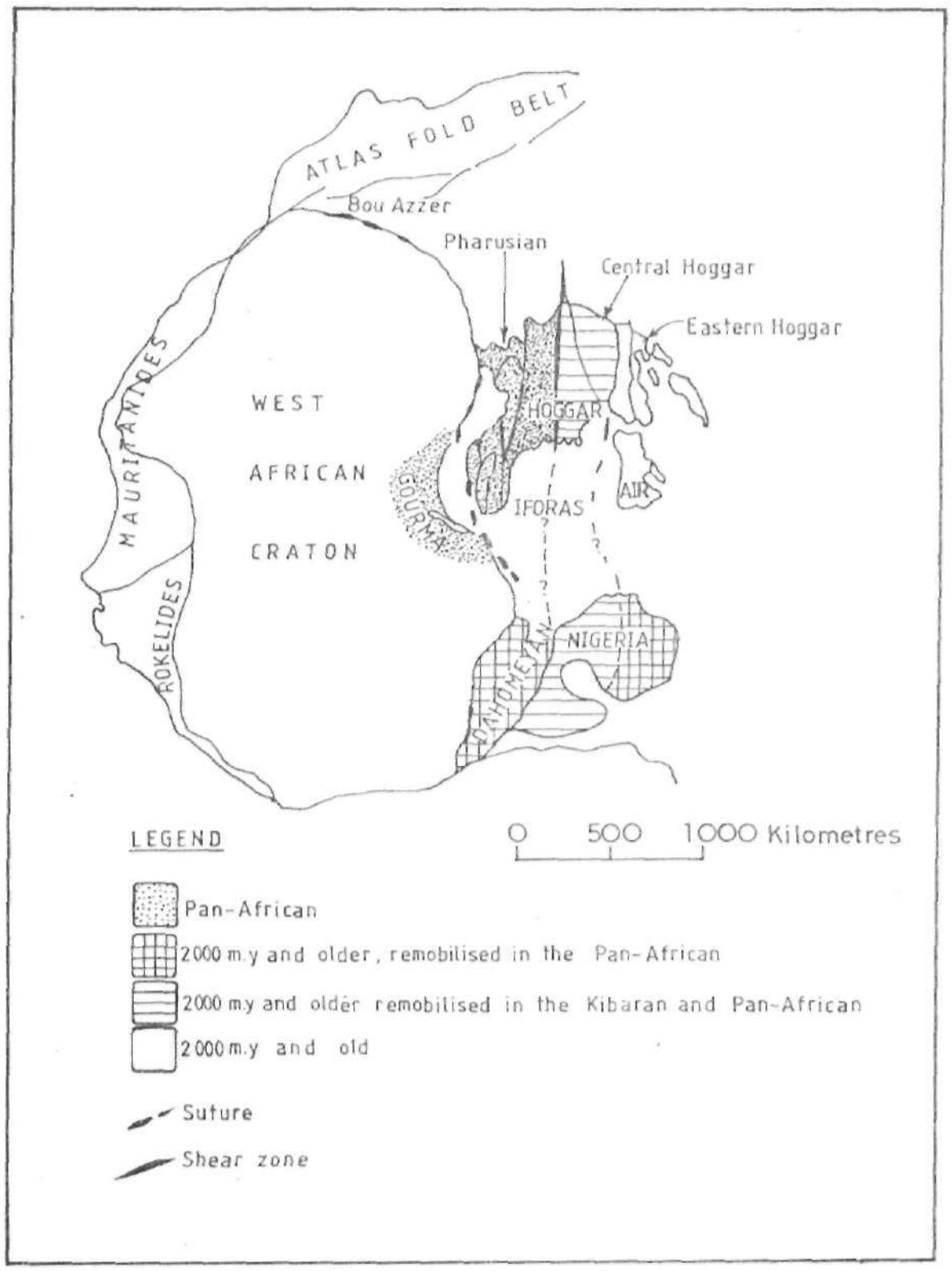


Fig.2.3. Map showing the Pan-African mobile belt and the suggested correlation between Central Hoggar and Western Nigeria (*modified from* Bertrand and Caby, 1978; Black et al., 1979).

al., 1979), which borders the West African craton in suture zones. Parts of the Pharusian belt represent a palaeo-rift system bordering the craton margin in Western Hoggar (Bertrand and Caby, 1978). Further east, the Pharusian belt contains island arc and Andean type assemblages.

b. a central zone comprising Eastern Adrar Des Iforas (Mali) and the Central Hoggar (Algeria). It consists of Eburnean and Kibaran gneisses and granites that have been affected by the later Pan-African event.

c. a stable cratonic area of platform sediments unaffected by the Pan-African event. It forms the East Saharan craton in Eastern Hoggar, which is subdivided into three units by mylonite belts. Two of these basement units are separated by the Tiririne Formation. This formation is a late narrow Pan-African metasedimentary and metavolcanic unit that evolved through ensialic processes (Black et al., 1979).

CHAPTER THREE:

LITHOLOGY AND FIELD RELATIONS IN THE STUDY AREA

3.1 INTRODUCTION

The rocks in the map area comprise the following main units:- migmatite-gneiss basement complex, younger metasediments and metavolcanics, granites, Younger Granite igneous rocks, fault rocks and sedimentary rocks (Fig. 3.1). The southeastern, the central and the northeastern parts of the map area are underlain by the granites with laterites capping some of them. The Daura Igneous Complex rocks and the Gundumi and Chad Sedimentary Formations, occur mainly in the northeastern and northwestern marginal parts of the project area (Maps 1 and 2).

The younger metasediments in the map area occur in two major belts which constitute component units of the schist belts of central and southwestern Nigeria. One of this belt, the Kazaure Belt, is more than 85 km long and extends northeastward towards the Nigeria-Niger border where it is overlain by sediments. The other belt is 45 km long and is located in the southwest of the map area where it trends southwards joining another metasedimentary belt, the Malumfashi Belt.

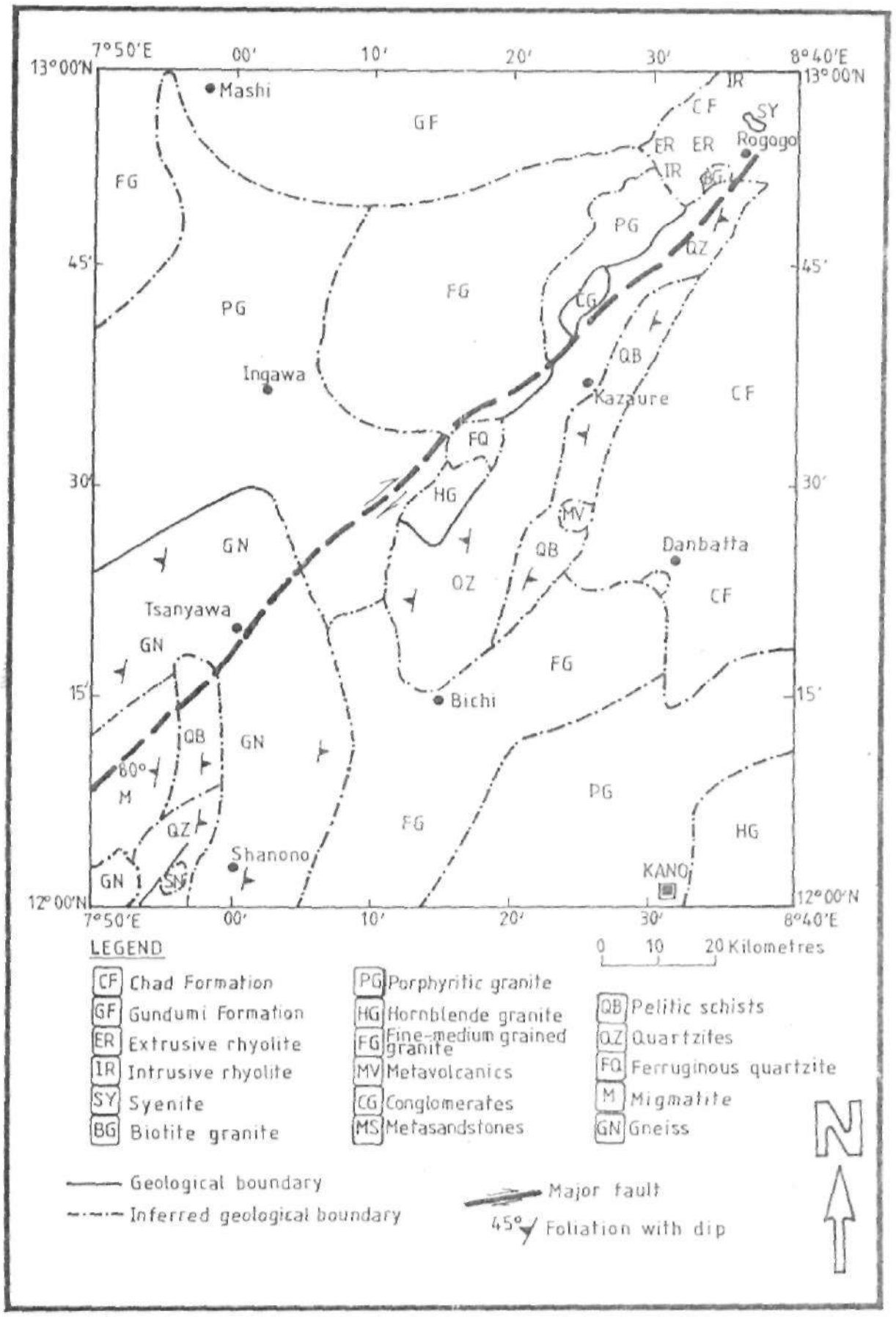


Fig. 3.1. Geological map of Kazaure and adjacent areas. (Simplified from Maps 1 and 2).

gneiss is exposed (Plate 3.1), while in others it is migmatite. However there is gradation between these two rock units with gneiss showing diffuse zones of concordant migmatization and pegmatization, and the migmatite showing lit-par-lit injections (Plate 3.2).

3.2.2 Biotite gneiss

The biotite gneiss occurs as low lying ridges along river valleys. It also occurs associated with migmatites and whalebacks in the southwestern portion of the area (Plate 3.1). This relationship is more frequently observed in the northern side of the Bichi-Tsanyawa-Yashi road where the migmatites and gneisses have a gradational contact. In addition, there is also a gradational boundary between the biotite gneiss and quartz schists especially at Tsaure (UD201), the extreme southwestern portion of Map 2.

It is worth noting that apart from the basement outcrops in the southwest, the only other basement outcrop is a very small exposure of a highly weathered low-lying biotite gneiss ridge which occurs just southwest of Danbatta. This heavily jointed gneiss outcrop forms a basement inlier surrounded by the Chad Formation sands and clays (Map 1).



Plate 3.1 Photograph of biotite gneiss east of Yashi (UD202). Note the isoclinal upright fold outlined by foliation trends. The biro is perpendicular to the fold axial trace. S_2 foliation trends NNE as a gneissic layering.



Plate 3.2 Photograph of a migmatite showing a mesocratic (dark) palaeosome and a leucocratic (light coloured) neosome. Note complex and ptygmatitic fold structures. Location: Kekaji.

3.2.3 Migmatite

The migmatite mainly occurs as low lying ridges and whalebacks in the southwestern portion of the study area (Plates 3.2). It is limited in occurrence but more concentrated in Kekaji (UD204), Farin ruwa (UD205) and Goron Dutse town (UD206) [Map 2]. In these places the mgmatite occurs as small low-lying hills and along stream channels.

3.2.4 Older Metasediments

Occurrences of Older Metasediments are most commonly observed as scattered and highly weathered relics feldspathic schists outcrops along the Kano-Bichi road. Field relationships reveal this type of older schists as low-lying outcrops in the peneplain of the area, especially after Mil Tara town (UD207).

Other Older Metasediments include feldspathic quartzites which outcrop as boulders interbedded with N-S striking and elongated gneissic bodies, with the biotite gneiss badly weathered and transformed to laterites in most places. It occurs as large boulders in laterite quarries along the Danbatta - Kazaure road. In some other places e.g at Tsaure (UD201), the feldspathic quartzite outcrops are found occurring as large (5 X 15 m) bodies within a highly weathered hill (Plate 3.3).

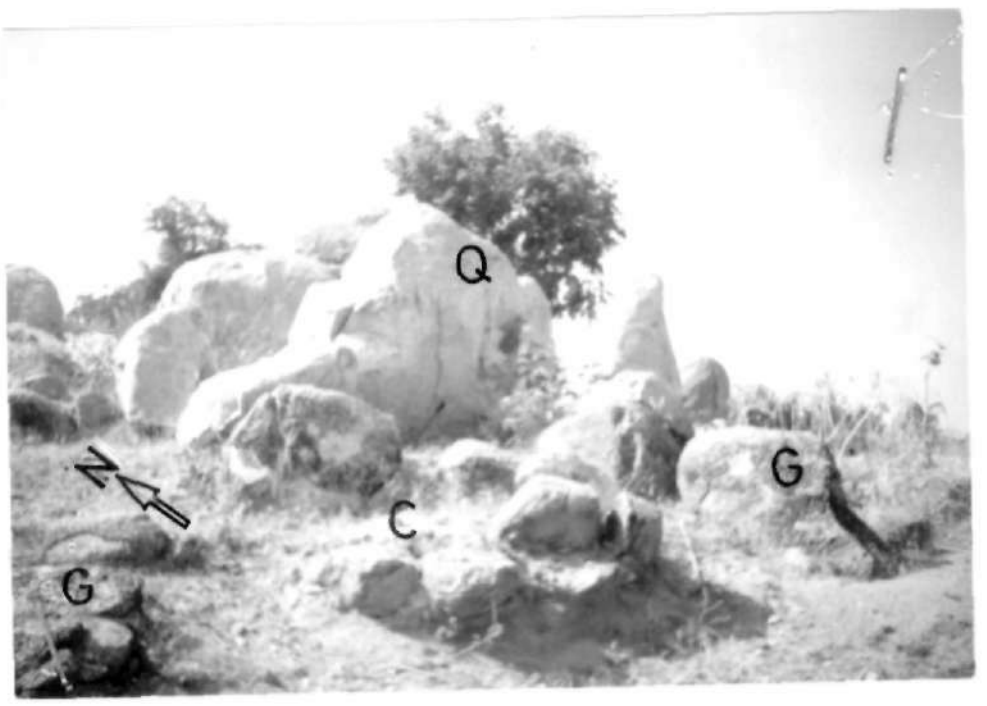


Plate 3.3 Photograph of feldspathic quartzite (Q) within highly weathered biotite gneiss (G). Note the subordinate amounts of kaolinised clay (C). Location: Tsaure (UD201).

Much of the migmatite-gneisses separating the metasediments are regarded as basement to the metasediments. This is further supported by the presence of already deformed boulders of migmatitic gneisses in the conglomerate. The presence of schist boulders in the conglomerate has prooved the existence of older schist material predating the Younger Metasediments.

3.3 YOUNGER METASEDIMENTS AND METAVOLCANICS

3.3.1 Lithology, Distribution and Field relationships

The occurrence of metasediments in the study area appears to be extensive, although exposures are generally very poor. Exposures of the metasediments occur mostly along river valleys and on top of a number of ridges that trend NNE to NE and rising abruptly above the general ground level of the area. As earlier mentioned, the ridges occur in two main belts defining the Kazaure Schist Belt and part of the Malumfashi Schist Belt.

The Kazaure Schist Belt is defined from north to south by the main ridges and/or hills at: Fitare and Sabaru, Bayan Dutsin, Panda, Baraden, Wawarrafi (UD40), Dutsin Kodawa (UD27) Dutsin Kwaita (UD25), Dutsin Wajila (UD26) all of which are located on Map 1. On Map 2 the Kazaure belt is marked by elongated hills at Waire (UD65) and Kuskurmi (UD62), while the main ridges outlining the Malumfashi metasediments are mainly the ones at Dutsen Dan Bakoshi (UD228). The well marked Kazaure belt ridges form a 100-450 m wide and 1-2 km long

discontinuous band (in some cases about 1.5 km apart) which run from Maibara in the north (Map 1) through Kuka to Chiromawa in the south (Map 2), for at least 85 km along strike.

The Younger Metasediments in the Kazaure-Malumfashi area consist of at least six distinct lithologies of metasedimentary and metavolcanic rocks. These are: quartzites, metapelites, metaconglomerates, metasandstones, metavolcanics and ferruginous quartzites (Maps 1 and 2). The quartzites and the metapelites are the most extensive rock types among the Younger Metasediments, with the metapelites the least exposed. Only a small proportion of the metasediments (10 percent) is formed by the metaconglomerates, metasandstones and metavolcanics.

3.3.2 Quartzites

The quartzite shows textural gradation from a massive variety (Plate 3.4) through a schistose one to quartz schist, with the quartz schist containing bodies of phyllites. The schistose quartzites are also seen associated with the metapelites in several places. The massive quartzite outcrop on top of the NNE- trending ridges from Maibara through Kazaure and Waire Hill to just west of Bichi, adjacent to few hundred metres of metapelites intercalated with thin layers of fine quartzite. However, the quartzite (Plate 3.5) is in fault-contact with the subvertical bed of conglomerate which runs on the western



Plate 3.4. Photograph of a massive quartzite ridge (Q) showing its characteristic outcropping nature on top of the ridge. Location: Wawanrafi (UD40).



Plate 3.5. Photograph of quartzite (Q) in fault-contact with a conglomerate ridge (C) which runs on the western limit of Kazaure town around Dutsin Baraden.

limit of Kazaure town. There is a sharp contact between these two lithologies in this place. The quartzitic rocks are cut by quartz veins in several exposures, some of which seem to be geometrically related to small folds.

3.3.3 Metapelites

The metapelites underlie a number of ridges which define at least two belts adjacent to the quartzites. One of these occurs in the east where the low-lying ridges occur at Kazaure (UD59), in and around Kwadage (UD18), Gora (UD35) and west of Saye (UD60). The other belt occur to the west at a locality west of Tsanyawa (UD233) and at other localities at Dutsen Dan Bakoshi (UD228) and Farin Ruwa (UD232).

There are three textural types of the metapelites which are mapped as quartz-biotite schists, biotite-muscovite schists and phyllites. The quartz biotite schist is the most abundant, and a continuous gradation between the different rock types has been observed in several places. The pelites are generally soft and weathered except where they are indurated by later silicification. In the field the quartz-biotite schist is generally distinguished from the biotite-muscovite schists by their coarser grain size). The different textural varieties of the metapelites appear to be randomly distributed throughout the area.

The strongly foliated varieties of the metapelites occur mainly as weathered outcrops, especially along River Tuwari (UD27) where the river cuts across the strike of the KSB at Kazaure (Plate 3.6). This also occurs along River Karaduwa in and around Dan Bakoshi town. The intimate relationship between the metapelitic rocks makes it difficult to separately represent all of them on the maps (Fig. 3.1 and Maps 1 and 2). However, the phyllites which occur as a small lens along the Kalangai lineament (UD28), is distinguished from the quartz-biotite schist from air-photo interpretation.

The biotite-muscovite schist was found associated with the phyllites in most outcrops and the transition is always gradual, as earlier described. The phyllites are also associated with weakly developed slates in few localities, such as along River Tuwari, just behind the Offices of Kazaure Local Government Education Authority. Occurrences of phyllites have also been observed at Dutsen Dan Bakoshi at the extreme southwest of the map.

The quartz mica schists often contain discrete injections of granite and pegmatite inclusions, often along cleavage planes. These granite and pegmatites inclusions in the metasediments have been mapped in some places, while in other places they give the rock a banded migmatitic appearance. The pelitic schist at the schist-granite boundaries, contains about 19% tourmaline.



Plate 3.6 Photograph of pyhllite outcropping in the core of F_2 synform along River Tuwari behind Local Education Offices Kazaure (UD27). Note the S_2 crenulation cleavage locally refoliating S_1 and the grovvy shapes (G) parallel to an L_2 Lineation.

3.3.4 Metaconglomerates

Five kilometres north of Kazaure town, conglomerates are exposed close to Bayan Dutse Village. These contain the best exposure of this rock (Plate 3.5). They attain a thickness approaching 250 m, with the contact zone consisting of a polymict breccia. Also, in the NE, conglomerates are exposed in the Kiye river (UD437). The metaconglomerates are closely associated with the metapelites, with the matrix materials consisting of quartzites and metapelites. Widespread weathering has made it difficult to distinguish the metaconglomerates from the rest of the metasediments.

3.3.5 Metasandstones

In the SW of the study area, slightly metamorphosed brownish sandstones occur interbedded with quartzites, phyllites, weathered schists, conglomerates and purple clays at Dutsen Dan Bakoshi. The metasandstones have a very low metamorphic grade and are only found at Dutsen Dan Bakoshi (UD228) which is located within the northernmost portion of the Malumfashi belt. As such they display some fine sedimentary structures like cross-bedding and ripple marks, while the conglomerate pebbles are mainly deformed.

The conglomerate pebbles and cobbles have ellipsoidal shapes with the longest axes lying in the regional schistosity. The pelitic pebbles are mainly quartz biotite schists, while the quartzitic pebbles include tourmaline bearing quartzite.

3.3.6 Metavolcanics

Some metavolcanic rocks occur intercalated with the metasediments and are confined to Makoda, at the central part of the project area. The volcanic units are poorly exposed and mainly occur as sills or flows intercalated with the metasediments (Plate 3.7). The same occurrence was also documented to the west of Makoda at Ganji (along the Danbatta-Kuka road, Map 2). The volcanic outcrops are deformed and metamorphosed, and of very limited extent. A special interest was paid to the contact relationships between them and the metasedimentary rocks. However, their contact relationships with the surrounding metasediments is not known, as no "in situ" outcrop exposing the contact has been found. As such, the pattern of their distribution was not worked out in detail.

3.3.7 Ferruginous quartzites (FQZ)

A poorly exposed ferruginous quartzite occurs in the vicinity of Kunchi, southwest of the area (Map 1). Exposures of it occur around Sodawa (UD77) and 2km east of Matanfada (UD81) near highly laterised ridges (Plate 3.8). The ferruginous quartzite (FQZ) outcrop as 1-5 m thick discontinuous sheets typically occurring in a N-S trending lateritised ridges. The lateritised ridges which consist of unbanded pisolithic

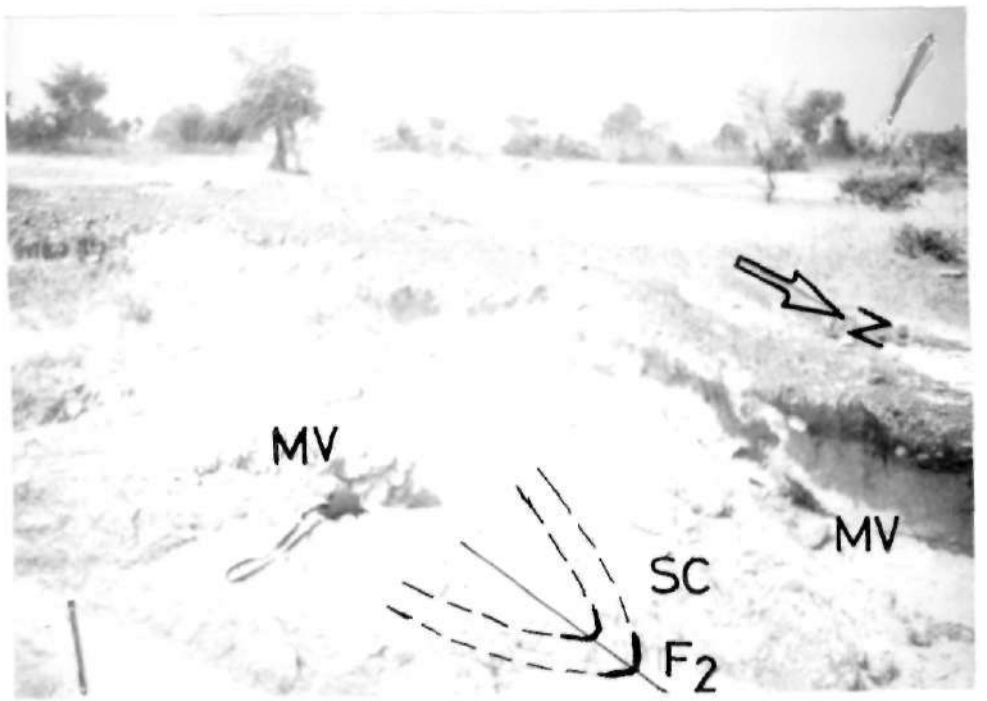


Plate 3.7 Photograph of metavolcanic outcrop (MV) intercalated with schists (SC) at Makoda. The pits were dug by excavators who use the rock in dam construction. Note the isoclinal upright F_2 fold of schistosity in the schists at the lower right hand corner.



Plate 3.8 Photograph of Ferruginous quartzites outcrop (FQ) on top of a ridge, Matanfada (UD812). Note its occurrence as floats (F) just below the laterised ridge.

ironstones, are not described. Only those with the quartz-bearing bands are described in the present study.

The exposed width of the ferruginous quartzites on the ridges is about 15-50 m, and the strike length of the ridges is in the order of 1-2.5 km. To the south, the ferruginous quartzite is limited by outcrops of the hornblende granite around Kunchi (UD139), while towards the north erosion has removed the continuation of the horizon.

The FQZ is fractured and broken up into boulders and pebbles on top of the ridges, and occurs as floats on the surrounding plains. However, at Kazaure town (by the Sand quarry along Roni road, UD 234), the FQZ occurs as a poorly outcropping dense rock intercalated with mica schist in a farmland.

The size of the FQZ in the Kazaure belt area is not impressive, but its existence is not unexpected, since iron-formations are found in some of the northern schist belts (Adekoya, 1993). A detailed investigation of this Kazaure iron deposit occurrence was earlier planned by the Nigerian Steel Council (NSC), but was abandoned after analysis revealed it is gritty and of low grade.

3.4 FAULT ROCKS

3.4.1 Field Characteristics of the Fault rocks

The rocks of the map area are transversed by a major dextral transcurrent fault zone, the Kalangai Fault System (KFS) and a number of other shear zones, which are localised zones bearing imprints of intensive ductile and brittle deformations. This is shown on a regional scale as well as at outcrop scales (Plate 3.9). The position of the KFS in the map area is defined by a topographic elevation extending northeast along the southern part of the area (Fig. 3.1).

The KFS has affected the rocks in the area through dynamic metamorphism. It is marked by a series of disconnected ridges of brecciated and silicified country rocks composed of fault breccia, sheared gneiss, cataclastic quartzite and mylonitized schists. Some samples of the sheared gneiss were taken for modal analyses. The KFS contains numerous steeply dipping, closely spaced planes that strike north-northeast and northeast. This defines a zone parallel to the host foliations, which is up to 50 - 100 m wide and up to 400m long at Dankari (Dakwat Lake Area).

In the Amaryawa area (Map 1), the KFS is subvertical with planes trending 040^0 and dipping about 38^0E (in the basement complex rocks) to almost N-S (in the metasediments). At



Plate 3.9 Photograph of a fault breccia (FB) trending NNE-SSW and dipping steeply W, bent in some places. Note the closely spaced fracture cleavage. Location: Kwaita (UD247).

Gwirta, there is an occurrence of porphyritic rhyolites which are brecciated and ferruginised with abundant quartz-haematite veining in the east (Map 1). Near Gwirta are also narrow brecciated ridges of quartzite that show minor haematite veining, and pegmatite infilling along most of them. The quartz-haematite veining is considered to have resulted from brittle deformation due to cataclasis movements, and is independent of any high temperature metamorphism.

There is also a sheared quartzite in the KFS, which has defined a breccia zone at Fitare. This zone is characterised by large angular fragments of quartzite (pink) cemented by white secondary quartz. At Dankari and NE of Sabaru (Map 1) brecciation of the quartzite and infiltration by haematite must have taken place. The fault breccia in these two areas are also commonly marked by the occurrence of some boudinage structures.

Outcrops of mylonitized schists occur 2 km along the Kazaure-Panda road, few metres north of the road (UD22), while the metaconglomerate is foliated near the shear zone. Other mylonitized schists occur as north-south trending ridges at the northeastern and southeastern parts of the area (Maps 1 and 2). They occur as highly sheared, foliated and fine to medium grained well-lineated rocks with distinctive pinkish to yellow colour. The westernmost quartzite in this area has not been affected and was distinguished by its lack of shearing.

3.5 GRANITE

3.5.1 Lithology, Distribution and Field relationships

A major part of the study area is underlain by grey to pink coloured granitoids, which occur as inselbergs and low lying whalebacks. The granitoids occur as massive fractured plutons with irregular shapes, roughly occupying two belts in the NW and SW parts of the map area. The granites sharply intrude the metasediments and migmatite-gneiss unit, with the sharp contacts suggesting their younger age. There is a close mutual relationship between the granites and the gneisses. No changes have been observed at their contacts, although gneisses with older metasediments are frequently preserved as xenolithic bands in the granites.

The granite can be subdivided into the following categories:

(a) Aplite and pegmatite.

(b) Porphyritic hornblende granite.

(c) Porphyritic granite.

(d) Medium-grained granodiorite.

(e) Medium-grained granite.

These different varieties of granite have a very poorly developed foliation and their chemical analyses and geochronology are shown and discussed in Chapter 5 of this thesis.

3.5.2 Medium-grained granite

The medium-grained variety outcrops at Unqwan Tudu (UD152), Dansure (UD63), Roni (UD409), Korevel (UD417) and along the tributaries of River Sabke [UD592] (Map 1). It forms mainly stocks of various sizes, some of which are heavily jointed. The granitic units appear to have a regular pattern of occurrence with the fine to medium-grained variety intruding the porphyritic granite.

3.5.3 Granodiorite

Granodiorite occurs as small intrusions at Wakai (UD222), around Ingawa (UD225), southeast of Ladan (UD220) and along the tributaries of River Gari (UD223) in the south of Map 1. It also underlies the extreme northwestern portion of the project area where it outcrops along the stream channels in and around Dan Ashitari (UD224), and south of Takurdawa and northwest of Dan Ashitari (UD227). The granodioritic outcrops are well exposed and their pale whitish surface appears to be more resistant to weathering. They are net-veined by fine to medium-grained granite, in some places.

3.5.4 Porphyritic granite

The porphyritic granite is exposed at Dansure (UD39), Achilafia (UD138), east of Sada (UD111), and in and around Ladan where it is quarried for construction purposes (Map 1). Other occurrences of this rock unit underlie all the other granitic exposures, especially in the southwest of Map 1, the

central and eastern portions of Map 2 e.g at Lambu Hill (UD240), located at the extreme southern boundry. In addition there are exposures of porphyritic granite at the Dutsen Dan Bakoshi (Plate 3.10). Both the granite and the pegmatitic veins in this hill are sporadically overlain by the schists, quartzites and metasandstones.

The porphyritic granite has a sharp contact with the surrounding rocks and contains xenoliths of the fine-medium grained granite, and is believed to be the youngest rock in the area. However, contacts between the two main types of granite are gradational. Other minor phase of the granite include a highly weathered diorite south of Goron Dutse (near Kano, UD238). The coarse-grained porphyritic granite is the most abundant granite type in the area.

3.5.5 Hornblende granite

A minor hornblende variety of the porphyritic granite exists, with the hornblende granite forming a lens in the porphyritic granite. It is exposed along a stream channel just outside Kunchi and along River Gari (Maps 1 and 2). Other exposures of the hornblende granite occur in the extreme southeast of the project area where it defines prominent hills at Sambgona (UD520, UD522) and east of Kano (UD530), respectively.

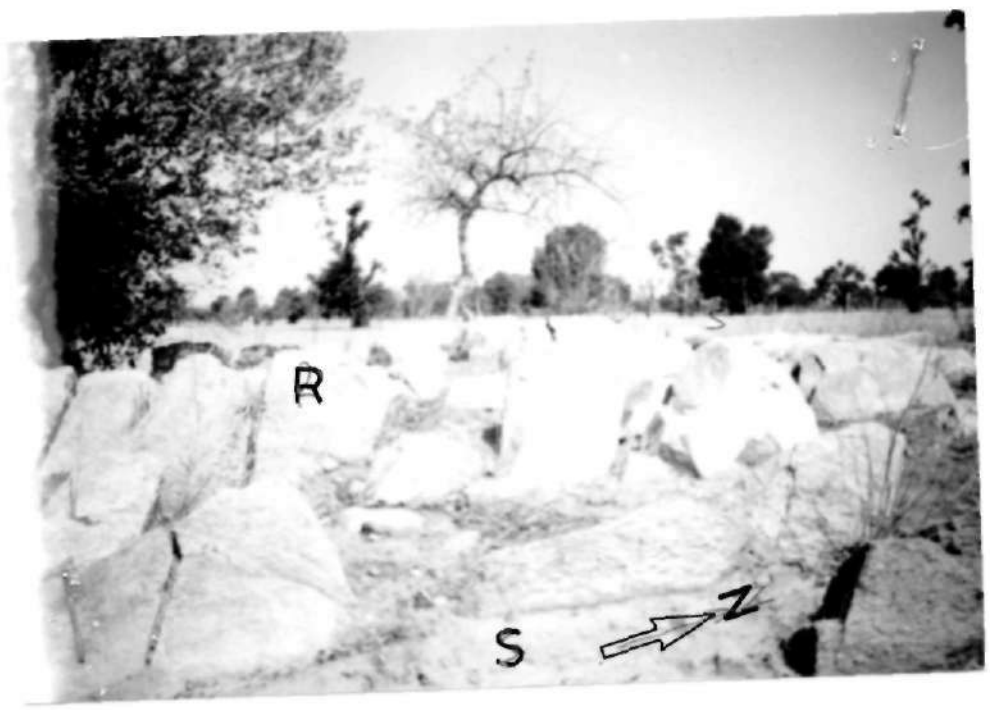


Plate 3.10. Photograph of the coarse porphyritic granite at Dutsen Dan Bakoshi (UD238). Note the characteristic outcrop pattern composed of boulders that have formed due to jointing.

KASHIM IBRAHIM

The hornblende granite also outcrops as a hill and resistant bands in almost N-S striking low-lying ridges, at Sambgona, still SW of Kano. It also outcrops in whalebacks and ridges, especially along the Kano-Yada Kunya road (UD518) and Kano-Gezawa road (UD519).

3.5.6 Aplite and Pegmatite

3.5.6.1 Aplite

Aplite occurs as minor irregular dykes and veins in the granites, and sometimes the schist. The margins of the veins and dykes are coarser in grainsize and more feldspathic in mineralogy, than the interiors. They generally vary in thickness from 10 to 60 cm and can be traced for several metres.

3.5.6.2 Pegmatite

Numerous and sparsely distributed pegmatites occur as veins, dykes and irregular intrusive bodies in the granites and gneisses, and sometimes in the schists. In the schist they often penetrate along foliation planes, but in most places they were seen obliquely crosscutting the schist as veins and dykes.

The pegmatites north of Tsanyawa extend for about 20 metres in a general N-S to NNE-SSW direction. They are of striking interest because they are situated near a major fault and

contain black tourmaline. Other pegmatites include the ones at Kunchi and Dutsin Dan Bakoshi. The Kunchi pegmatites extend for about 20-60 metres in length along the river bank of River Gari, with some trending about NE-SW. They show zoning of minerals, with quartz crystals at the center and orthoclase feldspars at the sides.

3.5.6.3 Quartz veins

Quartz veins are widely distributed and occur in dimensions from a few centimetres to 50 cm across. They are found in almost all the rock types, but are more common in the granites. Other quartz veins are minor and probably occupy fractures related to the regional joint pattern of the area.

These types are found intercalated with the metasediments where they formed quartz boudins (e.g at Kazaure, behind the Petrol station located on the west side on your way to Daura). They are not always concordant with the foliation of the metasediments. Sometimes they are found strongly folded, boudinaged and elongated in a general NNE-SSW direction.

3.6 THE DAURA YOUNGER GRANITE COMPLEX

3.6.1 Lithology, Distribution and Field relationships

The Daura igneous complex contains rhyolite, and intruding within and below the rhyolites are syenites and biotite granites. These rocks are not well exposed, and they occur as

boulders which are resistant to erosion (Plates 3.11 and 3.12). The contact between the granite suite and the adjoining basement rocks is discordant, with textural variation from the contact to the granite. This was mainly observed at Rogogo. Near the biotite granite occurrence in this vicinity, are boulders of Older Granite with numerous leucocratic veins.

3.6.2 Rhyolites

In the area around Gwirta and Rogogo, two different types of rhyolites exist in the Daura granite complex. They are earlier intrusive and later extrusive rhyolitic rocks, distinguished from each other by their textures and occurrence. In the field, the rocks occur northwest and southwest of Rogogo, as light coloured and glassy rhyolite, with minor agglomerates (Plate 3.11). The rhyolites are locally covered by Cretaceous sandstones and conglomerates, and this concealed the actual contact between the volcanic rocks and the basement.

South and southwest of Rogogo altered rhyolite lavas are interbedded with tuffs and agglomerates and in some places with comenditic ignimbrites. South of the area are massive altered rhyolites sometimes autobrecciated. Within this volcanic area, intrusions of rhyolite dykes also occur.



Plate 3.11. Photograph of rhyolites (R) locally covered by superficial deposits. Note the bouldery outcropping nature of the rhyolite. Location: Southwest of Rogogo (UD500).



Plate 3.12 Photograph of quartz syenite intrusion at Rogogo (UD498). Note the outcrooping nature of the syenite which is almost completely covered by superficial deposits especially at the right hand corner of the picture.



Plate 3.11. Photograph of rhyolites (R) locally covered by superficial deposits. Note the bouldery outcropping nature of the rhyolite. Location: Southwest of Rogogo (UD500).



Plate 3.12 Photograph of quartz syenite intrusion at Rogogo (UD498). Note the outcrooping nature of the syenite which is almost completely covered by superficial deposits especially at the right hand corner of the picture.

3.6.3 Quartz syenite

In the southeast of the Rogogo area, there is also an occurrence of quartz syenite intrusion, which has chilled margins along its eastern and southern edges. The syenites at the contact zones posses fine-grained varieties which are discordant with the country rock (Plate 3.12) and in contact with volcanic agglomerates. These suggest an intrusive mode of emplacement for the syenite.

3.6.4 Biotite granite

An unfoliated biotite granite occurs as an isolated hill about 9 km southeast of Rogogo. It consits of both medium and coarse grained varieties in transitional contact relationship. The coarse grained biotite granite occurs in the lower slopes to the NW of the hill and is pale grey in colour, with abundant mesoperthitic feldspar grains and brown biotite. It occurs in subordinate amount when compared with the medium-grained variety.

The top of the hill predominantly consists of the medium-grained biotite granite which is the dominant rock type. The porphyritic microgranite occurs near the contact with the basement, SW of Rogogo. A variety of the microgranite occurs as a small dyke like body of light brown (reddened) microgranite in the same locality.

3.7 SEDIMENTARY FORMATIONS

The northern part of the map area forms the southern fringes of the Gundumi and Chad Formations. Details of the major parts of these Formations which lie outside the study area can be found in Barber (1965) and Kogbe (1977). The main sedimentary rocks in the Gundumi formation are Cretaceous sandstones and conglomerates, while Pliocene to Pleistocene sands and clays formed the argillaceous Chad Formation of lacustrine origin.

The Chad formation is uncomformably overlying the basement, with sediments still accumulating in the lake. The sandstone unconformably overlies the basement, and two varieties of the sandstone were identified based on mineralogy, texture and general appearance. They include: a ferruginous sandstone which is coarse grained, and a feldspathic sandstone which is fine to medium. The ferruginous variety is generally dark brown and rusty, consisting of poorly sorted quartz (40% of the rock), badly weathered feldspars (30% of the rock), iron oxides (15% of the rock) and some rare mica flakes (2% of the rock).

The fine to medium variety is a well sorted whitish grey rock, consisting of sub-angular to sub-rounded pebbles and boulders of quartz, feldspars, muscovite and iron oxide. Cementing materials include very fine-grained quartz, chlorite, green

biotite, epidote and carbonates. The feldspathic sandstone is less ferruginous and forms the basal sandstone layer in the area, with the feldspars intensely weathered into friable clays. Stratification in the sandstone is rarely observed. However, an angular feldspathic sandstone containing pegmatitic materials in its matrix was observed. This occurs as 100 m thick sequence of feldspathic sandstone beds (arkoses) interbedded with the ferruginous sandstone.

3.8 SUPERFICIAL DEPOSITS

The superficial deposits include laterites and alluvium deposits, formed as a result of weathering of the different lithologies in the map area. Indurated laterites occur as low lying hills and ridges which form a hard cover, and are very common occurrences in and around the map area.

River deposits in the area include pale coloured sand occurring in the better developed drainage channels and alluvium in poorly developed drainages. The alluvium contains varying amounts of sand, silt and clay. Half of the area mapped is covered by red sandy soils which support the thick thorn vegetation. Most of the laterites and alluvium are exploited for economic purposes like construction of roads, buildings and bridges.

In the southeastern portion of Sheet 35, there is a silica sand deposit in and around Bare Bari village, near the water logged and swampy areas. The silica sand deposit occurs in two horizons of 2-3 m and about 6 m thicknesses, both west and east of the Kazaure-Danbatta-Kano road. The top part, which forms the thinner horizon is reddish brown and contains silt and clay. In the bottom and thicker horizon, the sands are white in colour. This could be due to the leaching away of the brownish colouring films of iron oxides during transportation or the top sand horizon may have been stained. This silica deposit has been investigated by the Kano State Government for the purpose of establishing a glass manufacturing industry.

Other superficial deposit occurrences of economic importance are the impure kaolin clay deposits at Kunchi, Tsanyawa, Dawakin Tofa, and Minjibir (Maps 1 and 2), which are intensely leached of K and have a composition close to $Al_2O_3.2SO_2.2H_2O$. They have some impurities (upto 45%) and these include quartz (as sandy soil mixture), alkalis, titania, iron oxides, calcium, magnesium and organic matter from different sources. The Tsanyawa kaolin clay occurs near Bichi and was originally discovered and reported by the Geological Survey of Nigeria (MacLeod, 1966). It occurs within weathered granite gneiss in two localities located 2 and 12 km southeast of Tsanyawa, both associated with weathered pegmatites.

In the first locality, the kaolin is exposed as a N-S trending body with an average width of 8m and a length of 200m, while the second deposit is exposed in pits and quarries which cover a very wide area of about about 15,000 m^2. The thickness of this kaolin deposit is not known, but it is estimated to be about 20m from handdung wells located in the area. The Dawakin Tofa and Minjibir kaolin deposits are purer than the Tsanyawa deposit and are fine-grained, porous and residual in nature. The kaolin deposits in the area probably formed as a result of kaolinazation over pegmatites (Grim, 1968).

CHAPTER FOUR:

PETROGRAPHY

4.1 INTRODUCTION

The detailed description of textural relationships and optical properties of the different mineral phases in the different rock types encountered in the field are given in this chapter. The petrographic studies involve both the megascopic and microscopic study of the mapped rocks. The microscopic study entails the preparation and description of thin sections of some selected rock samples collected from the field. This sets the scene for the detailed analysis of microstructures and the overall objective of deducing the metamorphic grade of the rocks.

4.2 MIGMATITE-GNEISS COMPLEX

4.2.1 Granite Gneiss

4.2.2.1 Megascopic Description

The granite gneiss consists of unfoliated granitic rocks which locally give the biotite gneiss a migmatitic aspect (Plate 3.1). It is a distinctive medium-to-coarse-grained porphyroblastic rock with well-developed foliation.The foliation is defined by the segregation of quartz-feldspar and biotite-rich trails which surround porphyroblasts of feldspar up to 4 cm X 2 cm long. It is a light grey leucocratic rock,

with the ferromagnesian minerals (e.g biotite) tending to concentrate into parallel alignment of darker bands (Plate 3.1). The granite gneiss is also characterised by the occurrence of xenolithic inclusions of Older Metasediments e.g feldspathic quartzites (Plate 3.3) and schists. These mainly contain quartz with subordinate amounts of kaolinised plagioclase, microcline grains, haematite, and muscovite, as accessory minerals.

Other types of gneiss exist and they include biotite gneiss, grey hornblende bearing biotite gneiss and garnet biotite gneiss. These gneisses have coarse grained texture and occur as massive outcrops exhibiting slight foliation. The biotite-hornblende grey gneiss is composed of quartz, plagioclase, biotite, and hornblende, with some little microcline. The garnet biotite gneiss (Fig. 3.1 and Map 1) consists of small deep red garnets, quartz, feldspars and mica which are visible in the gneiss.

4.2.2.2 Microscopic Description

Modal analyses revealed that more than 94% of the biotite gneiss rock consists of K-feldspar, plagioclase and quartz, in that order of abundance. Biotite, muscovite and accessories constitute the remaining 6% (Table 4.1, Fig. 4.1). The K-feldspar is a microcline and it forms subhedral grains about

3 mm long and 1 mm wide. The microcline exhibits carlsbad twinning and some of the crystals are partly surrounded by sodic plagioclase.

The plagioclase is dominantly oligoclase (An_{28}) as determined using Michael-levy method (e.g Ekwueme, 1994a), with some colourless grains exhibiting albite twinning. Where it is in contact with microcline it is replaced by a myrmekite. Biotite, which is the dominant mafic mineral, is present in amounts ranging from 2-6%. It forms well aligned tabular flakes.

Muscovite grains are partly altered to a fine-grained highly birefringent mineral (clays). It occurs as a pale green to colourless flake, sometimes locally intergrown with biotite. The accessory minerals in the gneiss include zircon, apatite, rutile and opaque minerals. The rock plots in the granitic field on a QAP diagram of Streickeisen (1976). [Table 4.1 and Fig. 4.1].

4.2.2 Migmatite

4.2.2.1 Megascopic Description

Migmatite is a medium to coarse grained rock that is distinctively banded and intricately associated with the granite gneiss. It is greyish to pinkish in colour and

Table 4.1- Modal of Granite gneiss.

Rock Type	Granite Gneiss						
Sample No.	UD190	UD194	UD195	UD200	UD201	UD202	UD208
Quartz	37	26	28	27	29	25	24
Plagioclase	18	31	33	37	32	30	41
Potassic feldspar	39	40	34	27	38	33	33
Biotite	4	3	4	6	1	7	1
Muscovite	-	-	0.5	1.5	-	2	-
Opaque minerals	2	-	0.5	1.5	-	3	1

Location of Samples (Map 2):

UD190: An outcrop in a laterite pit, NW of Tsanyawa.

UD194: West of Tafahiya.

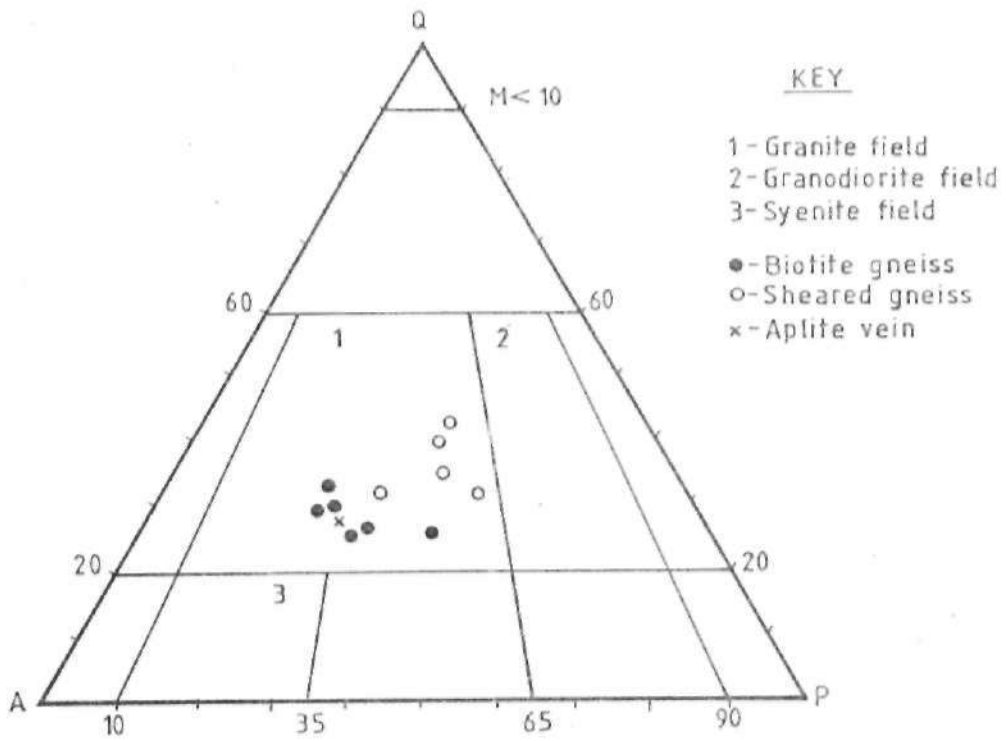
UD195: About 2 km W of Gogori along River Watari.

UD200: Slightly weathered ridge from within 3 km radius of Danbatta, to the SW.

UD201: Low-lying N-S trending ridge, occurring 1 km east of Tsaure.

UD202: An outcrop west of Yashi village.

UD208: A weathered outcrop near Shanono.



Q - Quartz, A - Alkali feldspar (Microcline, Orthoclase, Albite)
P - Plagioclase, M - Mafic minerals (Micas, Amphiboles, Opaques e.t.c.)

Fig. 4.1. O.A.P. diagram showing the modal composition of the biotite gneiss, sheared gneiss and aplite vein.

consists of stromatic, nebulitic and agmatitic structures (Fig. 3.1) [Mehnert, 1968; 1971]. The migmatitic banding is regular in form and consists of two components - a palaeosome and a neosome.

The palaeosome consists of a medium to coarse grained gneissic fabric which contains K-feldspar (44%), quartz (30%), biotite (10%) and plagioclase (15%). The constituent minerals are distributed into darker laminae. The neosome consists of a light grey, medium grained to more diffused-textured fabric with aplitic features. It consists of equigranular quartz, plagioclase, microcline in about equal proportion and subordinate amounts of biotite and muscovite.

Two main types of migmatites are distinguished in the area. These are medium-grained stromatic migmatite and a coarser-grained nebulitic variety, with an agmatitic variety occurring locally in very small amounts. The stromatic migmatite forms a complex pattern defined by a neosome that consists of veins and dykes of pegmatitic materials quartz and feldspars.

The nebulitic migmatite shows no complex fold and flow structures. It is defined by a simple alternation of a light leucosome band rich in quartz feldspathic minerals and a dark melanosome band mainly composed of mafic minerals (Plate 3.2). These bands are generally thin, discontinuous and mostly weak in nature.

4.2.1.2 Microscopic Description

Under the microscope, the quartz grains in the granite gneiss component of the migmatite form fairly large subhedral aggregates with wavy extinction due to strain. However, there are also smaller grains of the quartz that occur together with similar grains of microcline and microcline perthite, forming myrmekitic intergrowths.

Plagioclase consists mainly of oligoclase (An_{26}) that occurs as fine-medium grained subhedral crystals. Most of the plagioclase in the studied samples are altered to sericite and muscovite. The biotite occurs as very minute brownish flakes parallel to the banding in the rock, while K-feldspar is a microcline which mainly forms tabular crystal grains. Accessories include muscovite, opaque oxides, apatite and zircon.

4.3 YOUNGER METASEDIMENTS AND METAVOLCANICS

4.3.1 Quartzite

4.3.1.1 Megascopic Description

The quartzite occurs as a granular, massive to fissile rock with three different varieties distinguished based on textural and compositional relationships. These include a whitish massive variety which is poor in micaceous minerals (Plate 3.4), a brownish variety and a grey to yellowish fine to medium-grained schistose variety which is micaceous. The

quartzite essentially consists of quartz, with some minor impurities of muscovite and haematite.

The schistosity in the impure micaceous quartzites is defined by biotite and larger muscovite flakes, with some reddish brown iron oxides along the schistosity plane. A boudinaged fine-grained whitish quartzite with irregular cleavage planes, was also observed at Kwaita (Map 1). In addition, occasional fragments of tourmaline-bearing quartzite fragments (tourmalinites) were picked up along River Tuwari at Kazaure.

The tourmaline constitutes about 25% of the rock by volume and occur as radially arranged needles. The thicknesses of the tourmaline quartzite clasts range from <1 cm to about 80 cm and their lengths from 100 cm to 500 cm. The tourmaline crystals locally occur as green to yellowish aggregates, and lack colour zoning.

4.3.1.2 Microscopic Description

In thin section the quartzites show quartz with interlocking granular texture constitutes about 90% of the rock, while feldspars, micas and opaque minerals constitute the remaining 10%, sometimes growing around the quartz grains (Plate 4.1). Zircon and rutile needles are the accessory minerals in the rock. The feldspars (especially plagioclase) are sometimes kaolinised while the micas are mainly muscovite. The fissile quartzite contains more muscovite than the other varieties,

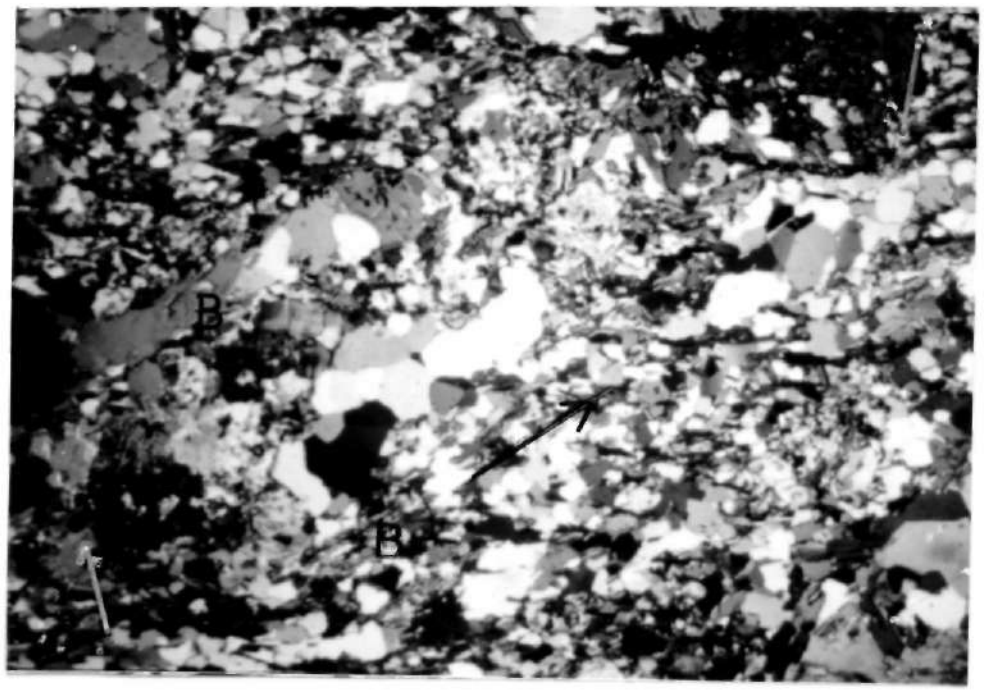


Plate 4.1: Photomicrograph of schistose quartzite showing pre-existing foliation kinked folded by later deformation (Sample UD65). The foliation is mainly defined by the lenticular biotite flakes (B). Cross-polars, Magnification = X22.

hence the name muscovite quartzite for this more micaceous quartzite.

4.3.2 Metapelites

4.3.2.1 Megascopic Description

There are three textural types of the metapelites which are mapped as quartz-biotite schists, biotite-muscovite schists and phyllites.

a). Quartz-biotite schists

The quartz biotite schist is typically a fine grained greyish to brown rock, with approximately equal proportions of quartz, biotite and feldspar. The quartz biotite schist is massive with rather weak schistosity, defined by a preferential alignment of phyllosilicate minerals in the matrix around quartz porphyroblasts. The phyllosilicates (biotite, + muscovite, + chlorite) in the quartz biotite schist defined a weak domainal schistosity.

b). Biotite-muscovite (Mica) Schist

Despite its poor exposure, the biotite-muscovite schist is the second most abundant pelite in the area, and is sometimes referred to as the mica schist. In hand specimens, it is commonly brown to light greyish in colour, and fine to medium grained in texture.

c). Phyllites

The phyllites and mica schists are generally biotite-rich with the mica having an approximate modal proportion of greater or equal to 40% in the rock. The schistosity is defined by a very strong preferential alignment of phyllosilicate minerals and by the absence of minerals larger than fine-grained quartz (Plates 3.6 and 3.7). These platy and prismatic minerals are aligned to form a weak compositional banding.

4.3.2.2 Microscopic Description

In thin sections of quartz-biotite schists, the schistosity is defined by a QF-(quartz rich) and M- (mica rich) domains. It occurs as porphyroblast and in the groundmass. Plagioclase occurs with many of the grains occurring untwinned, while biotite occurs as brown flakes arranged axial planar to the minor folds. Muscovite occurs associated with the biotite, as porphyroblasts and in the matrix. Chlorite occurs as alteration products of biotite and is concentrated mostly along biotite cleavage planes and microshear planes.

The phyllites are finely laminated silver-grey rocks that contain muscovite, some plagioclase (albite), quartz, chlorite, sericite, + epidote, + calcite and opaque minerals. Accessory phases include apatite, tourmaline and zircon. The lamination is defined by the alternation of M- (chlorite) and QF- (quartz rich) domains, and this imparts sheen to the

rocks. The lamination planes have a silver grey lustre due to the development of sericite.

4.3.3 Metaconglomerate

4.3.3.1 Megascopic Description

The metaconglomerates show considerable variation in texture and composition. They form useful marker horizons consisting of rounded and subrounded pebbles of quartz, quartzite, granite and gneiss which are elongated (Plates 3.3 and 3.5). The metaconglomerate is seen to be poorly sorted with abundant granitic detritus. It consists of dark grey to purple fragments which are mostly rounded and deformed fragments of quartzite and schist set largely in an ill-sorted ferruginous schistose matrix.

Deformed boulders of migmatitic-gneisses up to 60 cm and rounded fragments of vein-quartz, orthoquartzite, pelitic materials and granite have been found in a schistose matrix. The granitic clasts consist of quartz, microcline, biotite with the quartz exhibiting strained extinction.

4.3.4 Metavolcanic rocks

4.3.4.1 Megascopic Description

The metavolcanics are represented by acid and intermediate rocks (Plate 3.7) which are interbedded with the metasediments at Makoda (UD115, 117) and Ganji (UD110). The volcanic rocks

are probably flows or sills intercalated, folded and altered with the metasediments, although there is no evidence of igneous activity elsewhere in the region.

4.3.4.2 Microscopic Description

Thin section studies reveal the existence of cloudy and highly altered feldspar phenocrysts in a pale groundmass consisting of muscovite, hornblende, plagioclase, chlorite, biotite, quartz, sericite and opaque minerals. Plagioclase (albite) is dominant over perthitic K-feldspar. Plagioclase phenocrysts make up between 22-41 % of the rock and have been saussuritized. Despite the alteration, it has retained subhedral to euhedral forms.

Quartz constitutes over 24-36% of the rock and occurs as phenocryst and in the groundmass. The quartz phenocrysts average 0.8 mm X 2 mm in size and some are strained and recrystallised. The fine grained groundmass consists essentially of quartz and plagioclase, disseminated biotite flakes (5-9%), chlorite (7%), hornblende, (<6%), and muscovite (2-6%). Very minor amounts of opaque minerals are present.

No primary igneous textures were observed during petrographic studies. They are now represented by metamorphic textures in the metavolcanics, which are probably derived from a porphyritic micro-tonalite.

4.3.5 Ferruginous quartzite

4.3.5.1 Megascopic Description

The ferruginous quartzite (FQZ) is thinly banded black to dark brownish fine-grained rock (Plate 3.8). It is composed of alternating and regular haematite rich and less iron-rich bands. The thickness of the bands range from 0.5-8 mm with euhedral grains of haematite, magnetite and quartz often developed in fractures.

The Kazaure exposure occurs as a dark grey FQZ composed of quartz, muscovite and porphyroblastic garnet (Plate 2.10). In transmitted light, the garnet appears as a dark grey to brown coloured mineral, locally showing some cataclastic textures. Other minerals include minor amounts of pyrite, and chlorite, and accessory amounts of opaques. Work in the area has revealed the existence of extensive zones in the phyllites caused by locally disseminated minor amounts of sulphides (chalcopyrite and pyrites) which give a rusty appearance to the rocks in the area. Results of microprobe analyses of garnet and amphibole from the pods of iron formation of Kazaure area are shown in Table 6.9 and discussed in Section 6.3.

4.3.5.2 Microscopic Description

Microscopic study of thin sections of the FQZ (including polished sections) revealed the existence of fine laminae of

dark coloured haematite rich layers (28%), separated by light coloured layers containing about 68% of irregular aggregates of mainly stable polygonal quartz and subordinate amounts of haematite. Minor constituents in both layers (up to 4%) are biotite, and accessory chlorite, ilmenite, apatite, magnetite and pyrite.

4.4 FAULT ROCKS

4.4.1 Microscopic description of the Fault rocks

Many of the fault rocks contain sheet silicates showing evidence of strain, induration and silicification. Foliation is well developed by the parallel alignment of the sheet silicates. Thin section studies have revealed that the competent grains and phenocrysts were cataclastically deformed, while the matrix was affected by ductile deformation (Plate 4.2).

The sheared granite gneisses are composed of quartz, biotite, muscovite, and plagioclase (oligoclase) and alkali feldspar (microcline), with zircon, epidote, opaque minerals and rutile the most common accessories (Table 4.2, Fig 4.1). In thin sections of the sheared gneisses, cataclastic textures are common as shown by bent plagioclase twin lamellae, broken grains of micas, feldspar and polycrystalline quartz with undulose extinction (Plate 4.3).

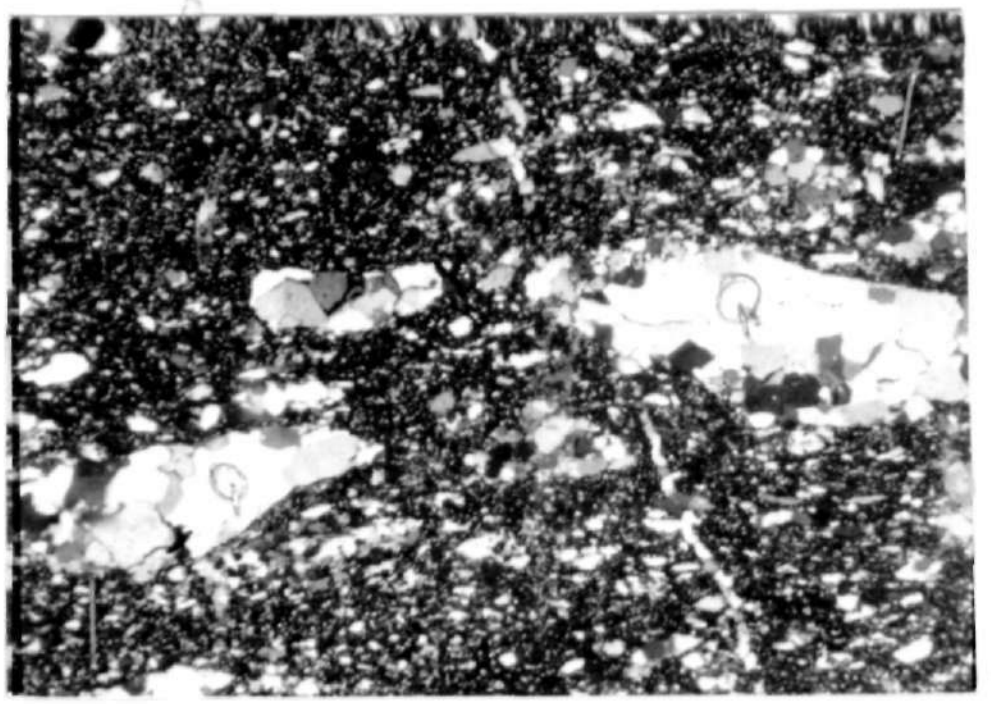


Plate 4.2. Photomicrograph of cataclastic texture in a quarztitic fault breccia. Note the recyrstallized quartz porphyroclasts (Q). Sample UD247.

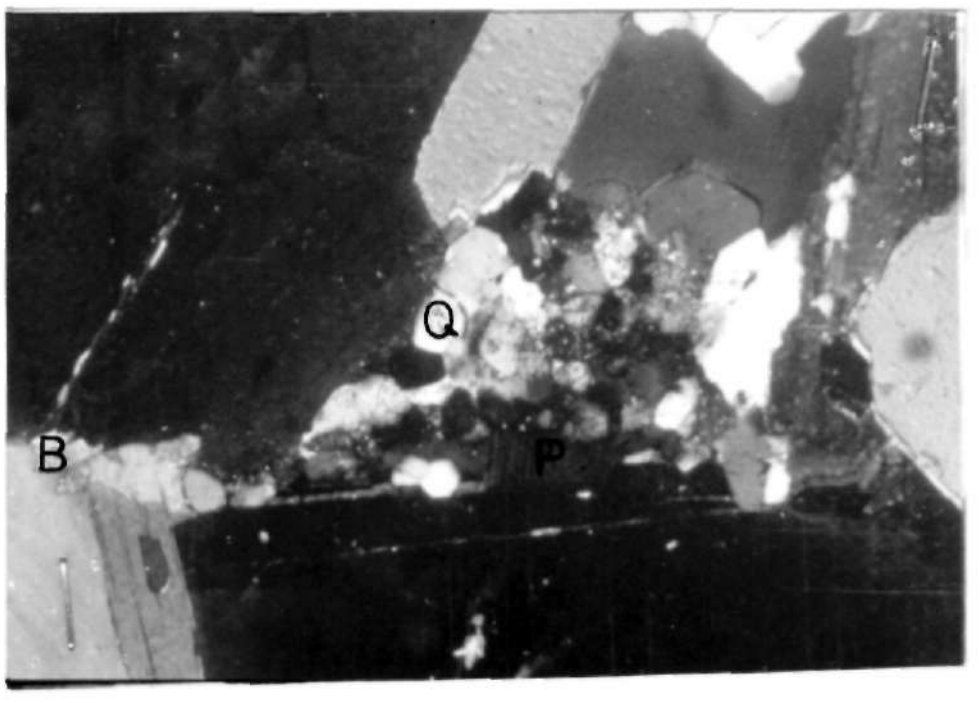


Plate 4.3 Photomicrograph of cataclastic texture showing strained and broken grains of quartz (Q) and plagioclase (P) in a thin section of the sheared gneiss (UD228).

Table 4.2 - Modal (volume percent) Analyses of Sheared Gneisses from the Kazaure area.

Rock Type	Sheared Granite Gneiss				
Sample No.	UD228	UD230	UD231	UD235	UD235
Quartz	36.0	34	39.0	30	31
Plagioclase	33.0	24	27.0	29	37
Potassic feldspar	25.0	18	30.0	24	28
Biotite	3.0	2	1.5	9	1
Muscovite	2.5	1	0.5	4	2
Opaque minerals	1.5	1	2.0	4	1

Locations of Samples (Map 2):

UD228: About 2 km SW of Tsanyawa.

UD230: An outcrop 1 km SE of Yan Awaki.

UD231: From 3 km SE of Yan Awaki along River Gari tributary.

UD234: From within Harbau.

UD235: river Gari, Gari Water works.

The fault breccia is a cataclastic quartzite composed of angular fragments of recrystallisation quartz embedded in a dense to very fine grained matrix of quartz and uncertain minerals. Pink quartz porphyroclasts in the fault breccia are broken into fragments (Plate 4.3), some of which are separated by very fine grained quartz. However, the quartzite breccia with quartz-haematite veining contains quartz (about 80%), sericite (12%), chlorite (3%) and large muscovite flakes (5%).

In thin section, the mylonitic rocks are seen to have complex textures, with some recrystallised quartz forming large and elongated porphyroclasts (Plate 4.3). The mylonitic foliation is defined by flattened and elongated feldspars and the growth of green biotite.

4.5 GRANITE

4.5.1 Megascopic Description

With the exception of the hornblende variety, all the granitic rocks in the map area are compositionally similar as they contain the same essential mineral assemblage of plagioclase, microcline and biotite. When weathered, the granites and aplite dykes mainly contain quartz with subordinate amounts of kaolinised plagioclase, microcline, haematite and muscovite.

4.5.1.1 Medium-grained Granite

The medium-grained granite is grey in colour and contains megacospically visible biotite, muscovite and scattered quartz and feldspar phenocrysts. It is slightly foliated which is due to localised planar arrangement of biotite. The foliation is similar to that of the porphyritic phase but is slightly more intense.

4.5.1.2 Granodiorite

The granodioritic rock unit is limited to the Karaftayi area where it occurs in a ridge form with a width of about 25 m trending N-S. The rock has a medium grained granular texture and is composed of quartz, mica and feldspar, with plagioclase constituting about 48% of the rock.

4.5.1.3 Porphyritic Granite

The porphyritic granite ranges from medium to coarse grained and is commonly massive to weakly foliated (Plate 3.10). The weak foliation is due to a weak planar orientation of the phenocrysts, and is commonly observed on weathered surfaces. The rock is characterised by large microcline phenocrysts in a fine to medium grained matrix. The phenocrysts of the rock are mainly pinkish (in some places whitish), subhedral and rectangular in shape, with average grain size of 4 X 1 cm.

4.5.1.4 Hornblende Granite

This coarse grained rock closely resembles the porphyritic granite in texture with the hornblende even visible in hand specimen. The hornblende constitutes about 8% of the rock by volume, with microcline, quartz, plagioclase and accessories accounting for the rest.

4.5.1.5 Aplite and pegmatite

There are documented occurrences of aplite, pegmatite and quartz veins. The aplites are pale pink to dark grey in colour, and have a true granitic composition as indicated by the average estimated modal proportions of K-feldspar (47%), quartz (28%), plagioclase (16%) and biotite (7%). This has been plotted in the QAP diagram of Fig. 4.1.

The pegmatites are pinkish in colour and coarse grained and occur as parallel sided intrusions with sharp margins. They are generally not more than 80 cm wide X 2.5 m length, with most containing euhedral to subhedral crystals of microcline, biotite, plagioclase and clear to smoky quartz. Some of the quartz veins are massive with clear and well formed quartz crystals. At Dusten Dan Bakoshi, the vein contains some semi-precious stones like tourmaline and amethyst quartz which are locally mined.

4.5.2 Microscopic Description

4.5.2.1 Medium-grained granite

In thin sections of the medium-grained granite (Plate 4.4), plagioclase is often sericitised, and its content is slightly higher than the average content of K-feldspar. The plagioclase occurs as anhedral to subhedral phenocrysts with albite and carlsbad twinning. It is present in amounts that range from 18 to 28%. The composition of the plagioclase as determined by extinction angles measured on the universal-stage ranges from albite to oligoclase (An_0 to An_{16}).

K-feldspar in the form of orthoclase, microcline and microperthite usually occurs as anhedral to subhedral grains (about 0.5 mm X 1 mm size) that constitute between 42% to 52% of the rock. It also forms intergrowth with plagioclase, and is usually identified by its microcline cross-hatched twinning and relatively unaltered appearance. Quartz constitutes 20% to 28% of the rock and typically forms a mortar texture formed by subgraining. Aspects of this texture include the occurrence of *strained phenocrysts surrounded by strain-free subgrains*.

Strongly pleochroic brown biotite occurs as small flakes, while hornblende occurs as small subhedral grains (sometimes subhedral). Biotite is typically intergrown with hornblende in large aggregates. Accessories are muscovite, allanite, sphene,

469974

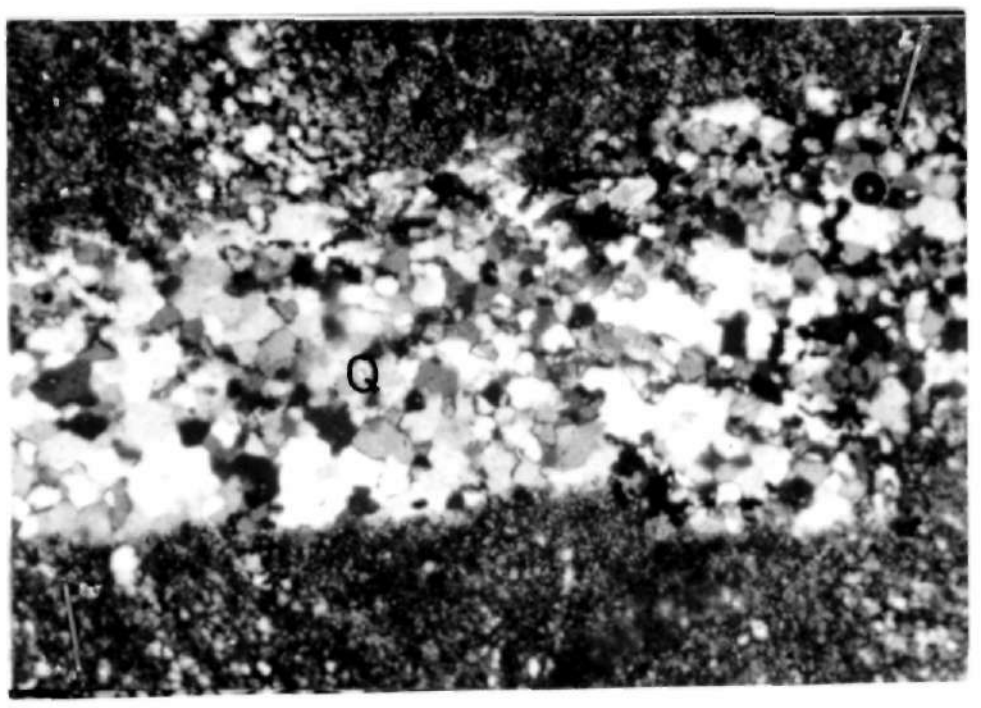


Plate 4.4 Photomicrograph of medium grained granite showing sericitized large grains of quartz (Q), plagioclase (P) and earlier formed biotite (B) extensively retrogressed to chlorite (C), Dansure (UD63). Magnification =X22. Cross polars.

clinozoisite, zircon, apatite and opaque minerals. Alteration products include epidote, chlorite sericite, and carbonate.

4.4.2.2 Granodiorite

In thin section the granodiorite has most of the plagioclase present having composition of An_0-An_{16} composition indicating that the plagioclases are mainly albite and oligoclase. The lamellae exhibits well defined twinning according to the albite law. Microcline occurs as a colourless mineral with low relief and cross-hatched twinning. It occurs as microperthite intergrowth with plagioclase. The microcline constitutes about 14% of the rock by volume, while quartz makes up about 28% of the rock. It has a low relief and do not show undulose extinction.

Biotite has a brownish colour with some being chloritised into bluish green chlorite. Such a replacement is almost complete in some crystals. The biotite makes up about 8% of the rock by volume. In this rock, two major accessory minerals were identified under the thin section. These are magnetite and apatite.

4.4.2.3 Porphyritic granite

In thin section, the porphyritic granite is mainly composed of K-feldspar (30%) and subordinate amounts of albite-oligoclase

(sodic) plagioclase (33%) and quartz. These account for 96% of the rock, the rest is mainly biotite or muscovite. Accessories include zircon, sphene and opaque minerals.

The dominant K-feldspar is microcline microperthite which forms subhedral phenocrysts, 2 to 6 mm long, or occupies an interstitial position in finer grained parts of the rock. The perthitic feldspar is composed of about 90% K-feldspar, while the plagioclase appears to be sodic oligoclase (An_{16}) in composition. It occurs in fine to medium-grained subhedral to euhedral tabular crystals. Some of these tabular crystals occur as inclusions within the K-feldspar. Some of the tabular crystals of the plagioclase show effects of strain. Quartz occurs as subhedral to anhedral crystals and as myrmekitic intergrowths with plagioclase.

Biotite typically forms subhedral to anhedral flakes scattered evenly throughout the rock. The biotite is altered to chlorite in some samples. Muscovite may occur as a thin rim on the biotite or as crystals intergrown with biotite and is subordinate to the biotite. The accessory minerals (zircon, opaque minerals and some sphene) are commonly associated with the biotite.

4.4.2.4 Hornblende granite

In thin section, the hornblende is a strongly pleochroic yellow-brown to dark green prismatic mineral that contains inclusions of quartz and plagioclase. Some of the hornblende crystals have altered to epidote, chlorite and aligned biotite flakes. The hornblende appears under plane polarised light as a greenish mineral and is pleochroic in shades of green. It has a subhedral form with two directions of cleavage intersecting each other at $124^0/56^0$. Biotite crystals are brownish, pleochroic from light green to brownish colours, and constitute about 4% of the rock by volume.

The K-feldspar is a microcline-microperthite and it occurs as subhedral grains, and makes up about 43% of the rock mineral content. The plagioclase is dominantly albite with some grains exhibiting albite twinning, and forms about 22% of the rock by proportion. Quartz occurs as strained and colourless medium sized grains that constitute about 24% of the mineral content. Among the accessories, zircon is always present while apatite, epidote, rutile and opaque minerals are less common. The zircon commonly occurs as inclusion within biotite.

4.6 THE DAURA YOUNGER GRANITE COMPLEX

4.6.1 Megascopic Description

Lithologically, the Daura Younger Granite Complex consists of rhyolite, syenite and biotite granite (Plates 3.11 and 3.12). The rhyolite consists of two different varieties: a porphyritic variety and an arfvedsonite and aegirine-augite bearing rhyolite. The syenite consists of a fine to medium grained variety and a coarse-grained variety. The biotite granite is classified into a porphyritic microgranite, a medium grained biotite granite and a coarse grained biotite granite.

4.6.1.1 Rhyolite

The porphyritic rhyolite consists of quartz, plagioclase, mica, substantial amounts of alkali feldspar, and sometimes hedenbergitic pyroxenes. The phenocrsyts of quartz ranged upto about 1 mm, with those of albite and K-feldspar having the same size, but with larger grains (about 4 mm across).

The arfvedsonite bearing rhyolite consists of arfvedsonite, aegirine and aegirine-augite, with the alkali amphibole imparting a peralkaline character to it. This rhyolite has a distinctive grey colour and fine laminations composed of alternating white feldspar-quartz bands, black arfvedsonite aegirine grains and greenish aegirine-augite crystals in the groundmass.

.6.1.2 Syenite

A zone of fine to medium grained syenite occurs within the chilled margin of the quartz syenite intrusion. This is enriched in quartz and has a peralkaline character with alkali amphibole and aegirine-augite. The next inner zone consists of coarse-grained, quartz-poor and non-peralkaline hornblende syenite which forms the central part of the intrusion.

4.6.1.3 Biotite granite

Hand specimen identification of a porphyritic microgranite, medium grained biotite granite and coarse grained biotite granite show these as distinctive rocks even when generally composed of alkali feldspars, some percentage of mafic minerals and quartz grains.

The porphyritic microgranite is pale grey in colour and consists of quartz, arfvedsonite, pink microcline feldspars and minor phenocrysts of biotite which are upto 3 mm long. The biotite and the perthitic microcline grains (upto 15 mm long) constitute the phenocrysts of the rock. The medium and coarse grained biotite granites are light brown in colour and consist of feldspars, quartz and biotite.

4.6.2 Microscopic Description

4.6.2.1 Rhyolite

The estimated percentage of the different minerals by volume in the rhyolite is: plagioclase (7%) and K-feldspar (44%), quartz (31%), arfvedsonite and aegirine-augite (20%), and others (3%). The arfvedsonite occurs in prismatic forms, exhibiting strong pleochroism from bluish green to brown and in close association to the aegirine. The aegirine crystals are also prismatic, and pleochroic from faint green to brownish green. The aegirine-augite form rims around the aegirine, but separate crystals with colourless-light green colour were also observed.

4.6.2.2 Syenite

The syenite contains a lower proportion of quartz and plagioclase than the granites, as perthitic textures are not well developed, although orthoclase feldspar occur as discrete crystals forming the dominant mineral. Accessory minerals include apatite, fluorite, magnetite and ilmenite.

4.6.2.3 Biotite granite

The groundmass of the porphyritic biotite granite is microgranitic in composition and constitutes about 62% by volume of the rock (UD503). The phenocyrsts constitute about

38% of the rock and are randomly distributed in the coarser microgranitic groundmass. The groundmass consists of quartz (32%), minor amounts of biotite (8%), nonperthitic microcline (15%), and albitic plagioclase (8%) which occurs as discrete crystals and perthitic intergrowths. Accessories include zircon and flourite.

The feldspars in the medium and coarse grained biotite granite are rich in albite (An_3) and microcline, with the albite occurring at the centre, and the microcline at the periphery. Other minerals found include pale green mica (muscovite), brown biotite and poikilitic fluorite, with columbite, opaque iron oxides and zircon forming the accessories.

CHAPTER FIVE:

STRUCTURAL GEOLOGY

5.1 INTRODUCTION

The planar and linear structures resulting from both ductile and brittle deformation events in the map area have been identified, described and classified in this section. The structural investigations covered megascopic, mesoscopic as well as microscopic structures. The geological mapping was carried out on structures discernible on outcrops and hand specimens, as well as on microstructures observed in thin sections of some of the rock samples. These include folds, foliations, lineations, joints and slickenside.

The above structural features were observed on scattered outcrops of the metasediments, basement gneisses and migmatites. The gneisses were mostly accompanied by migmatites, and migmatized gneisses, hence the style of deformation and the structures in these two lithologies are described together. In addition, the mesostuctural investigation in all of the migmatite-gneiss areas are presented separately from those structural observations made in the metasedimentary areas. Most of the detailed small scale structural analysis in the area were made on the younger metasediments.

5.2 METHOD OF ACCUMULATION AND ANALYSIS OF STRUCTURAL DATA

A remote sensing interpretation of air-photos, Landsat and SLAR images (Fig. 5.1) was first used to obtain a synoptic view of the structural elements and relationships in the area of study. The main interest was directed towards the identification of major structures (Fig. 5.2). This has simplified and aided the recognition of mesoscopic (small or minor) structures, following the arguments of Wilson (1961), who proposed that the geometry and orientation of major structures can be determined by the study of minor structures, and vice versa.

The amounts of good and continuous exposures are generally limited and mainly confined to river valleys and the top of quartzites ridges. For this reason, the younger metasedimentary area in and around Kazaure town was first studied in detail because of its relatively good exposures. An aerial photo enlarged to a scale of 1:12,500 was used as a base map for this detailed field mapping.

The lithological and structural data from this small area were identified, measured and plotted as a structural map of this locality (Fig 5.3). The experience gained during this exercise was used to map structures in the remaining metasedimentary areas. Qualitative estimate of strain was also undertaken in order to further understand the synopsis of the deformation(s)

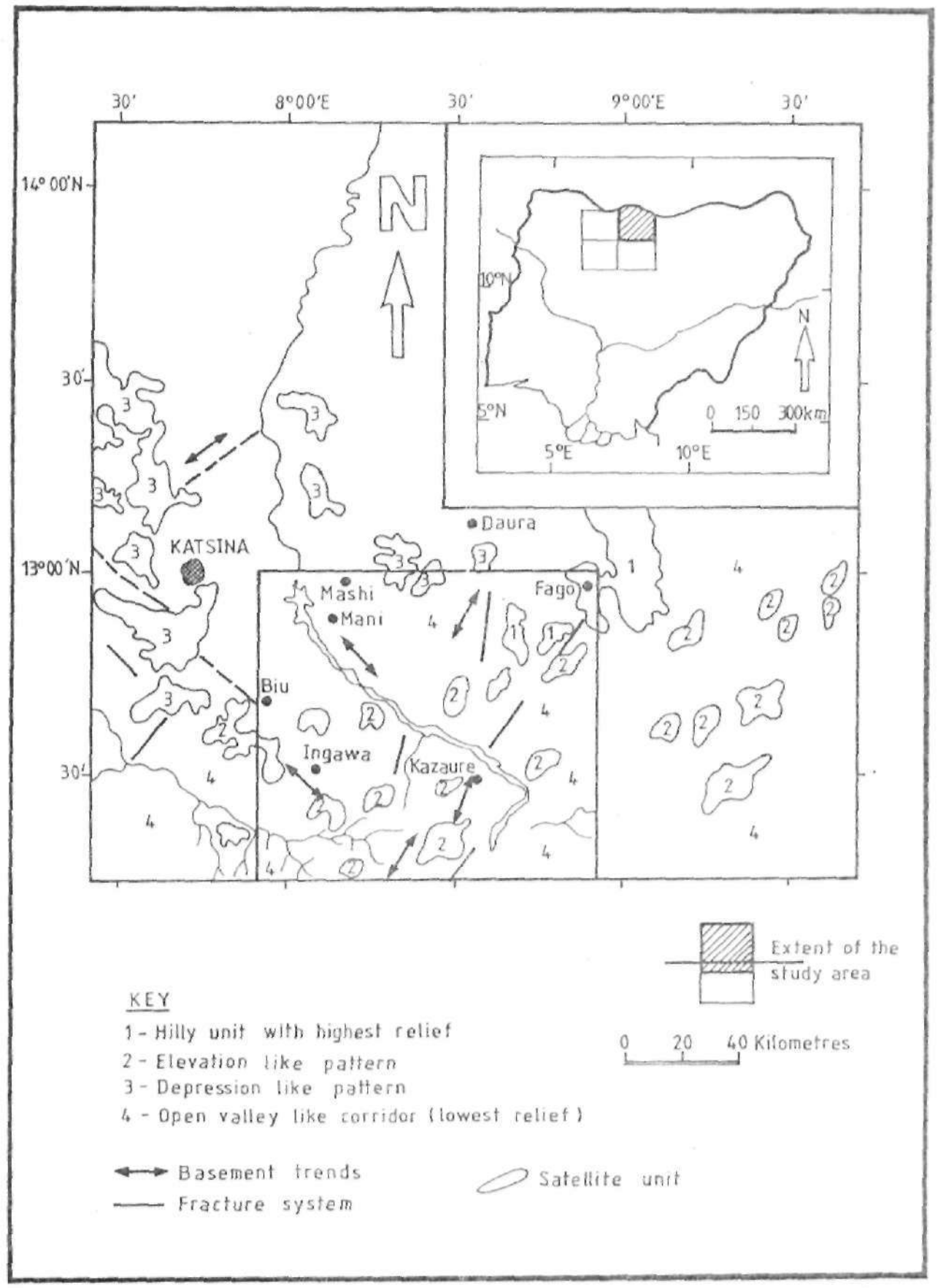


Fig. 5.1. An interpretation of satellite image of central Nigeria (7°40'N), Kazaure and the surrounding areas. Modified from Abubakar (1988).

Source: Landsat MSS Band 5 Image, 1:500 000 (ERTS)
(Total image outline shown inset)

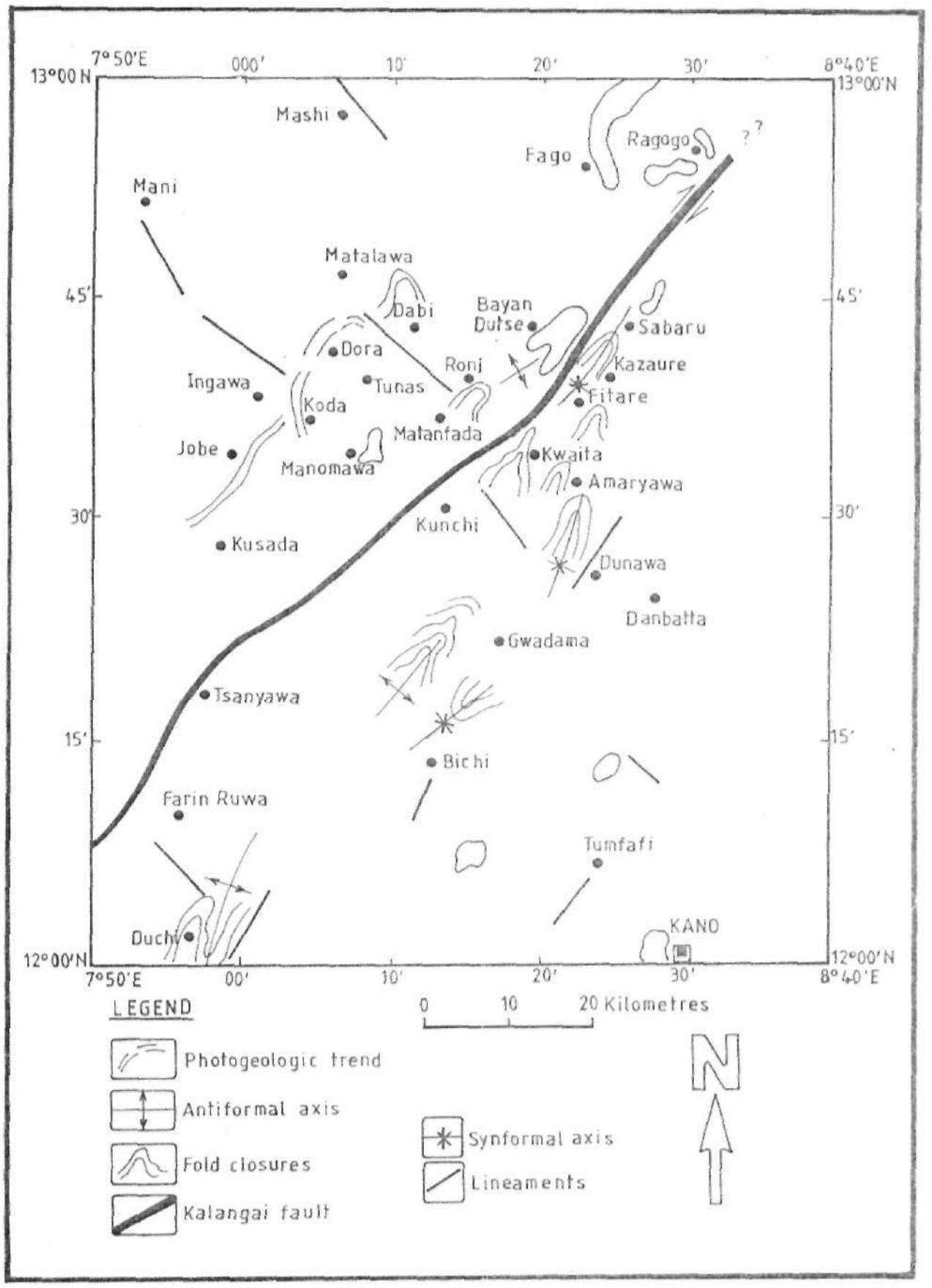


Fig. 5.2. Map showing location of major structures in the Kazaure region and adjacent areas.

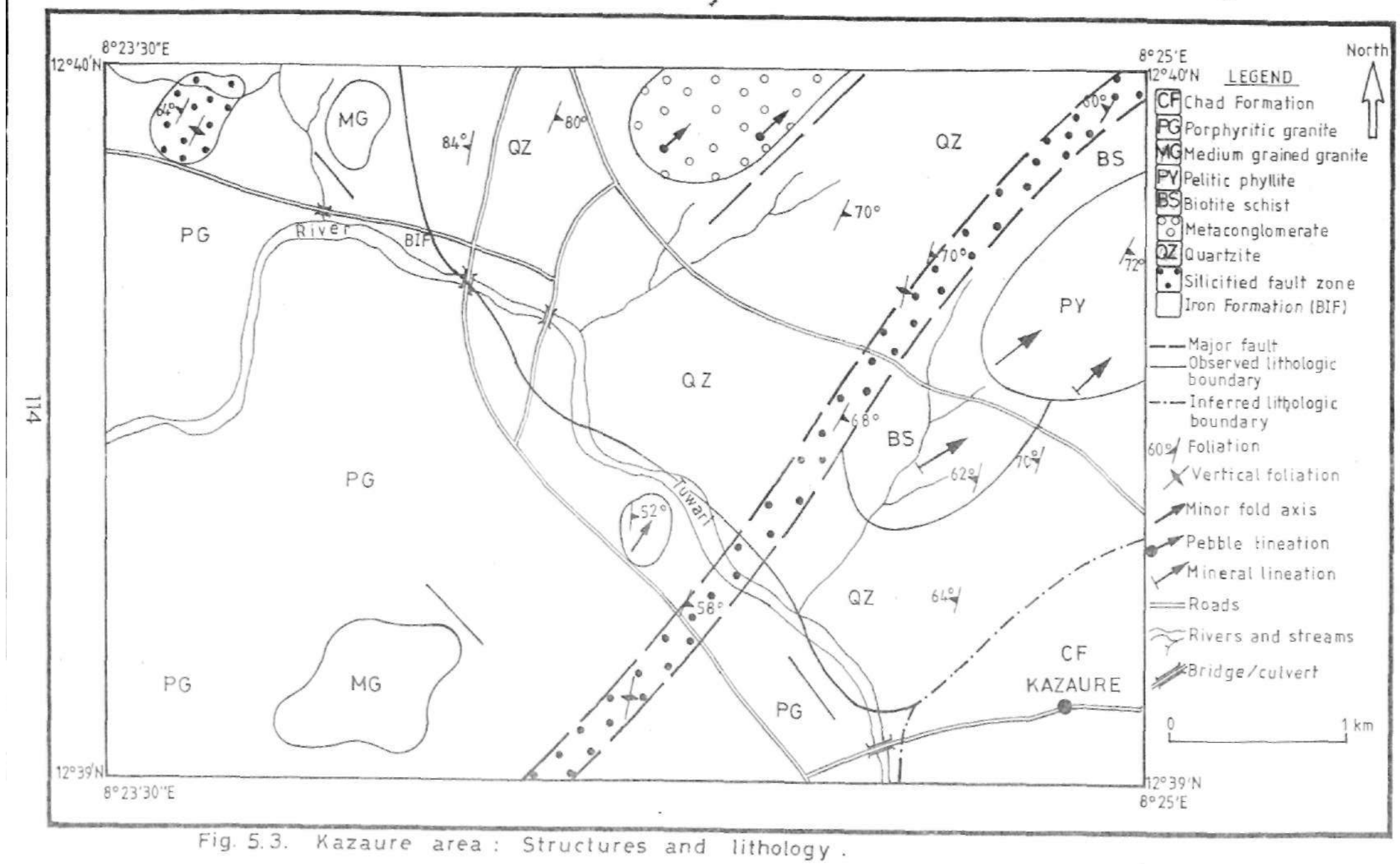


Fig. 5.3. Kazaure area : Structures and lithology .

in the study area. However, only by studying and correlating structures in the migmatitic-gneisses and the younger metasediments, was the sequence of deformational events completely analysed.

5.3 DESCRIPTION OF MEGASCOPIC STRUCTURES

5.3.1 Introduction

This section describes the major structures that resulted from both brittle and ductile deformation in the area. The Kazaure Belt (KZB) has an overall NE linear trend. As earlier mentioned, the surrounding rocks within the study area also include rocks of the northernmost portion of the Malumfashi belt which has a general N-S trend (Figs. 1.1 and 1.2). These defined the general geologic and structural trends in the area, with the brittle structures post-dating the ductile structures.

The major structures in the region (Fig. 5.2), are mainly revealed by air photos as folded migmatites, quartzites, conglomerates, and air-photo linear features (lineaments). Lithological boundaries among the above rock types are commonly steep and parallel in nature. The relationship between the major and minor structures is discussed in section 5.4.

5.3.2 Major Folds

The granitic areas are structurally simple, while the migmatite-gneiss and metasediments are complexely deformed. The migmatite-gneiss unit and the quartzite-mica schist association form persistent ridges which form topographic highs. They define the megascopic structures in the area. The distribution and attitude of such rocks were plotted as stereographic projections of S-poles and lineations (Fig 5.4).

Throughout the map area, a distinct tectonic event has produced two tight NE trending synformal and antiformal structures, with amplitudes in the range of hundreds of metres to 15 kms. These are illustrated in Fig. 5.2, and Maps 1 and 2. These structures are complementary to each other, and follow the NE trend of the Kazaure belt.

The antiform and synform are very clearly revealed in the cliffs of the hills behind the Kazaure Local Education Authority (L.E.A) Offices (Fig. 5.2). The synformal and antiformal structures have a moderate to steep plunge, as revealed by the axial trace of their outcrop patterns and stereoplots of their attitudes (Figs. 5.2 and 5.4).

The antiform has its eastern side terminating against a fault (Section 5.2.3). The conglomerate, quartzite, quartzite-mica schist association are preserved in the tight synform which

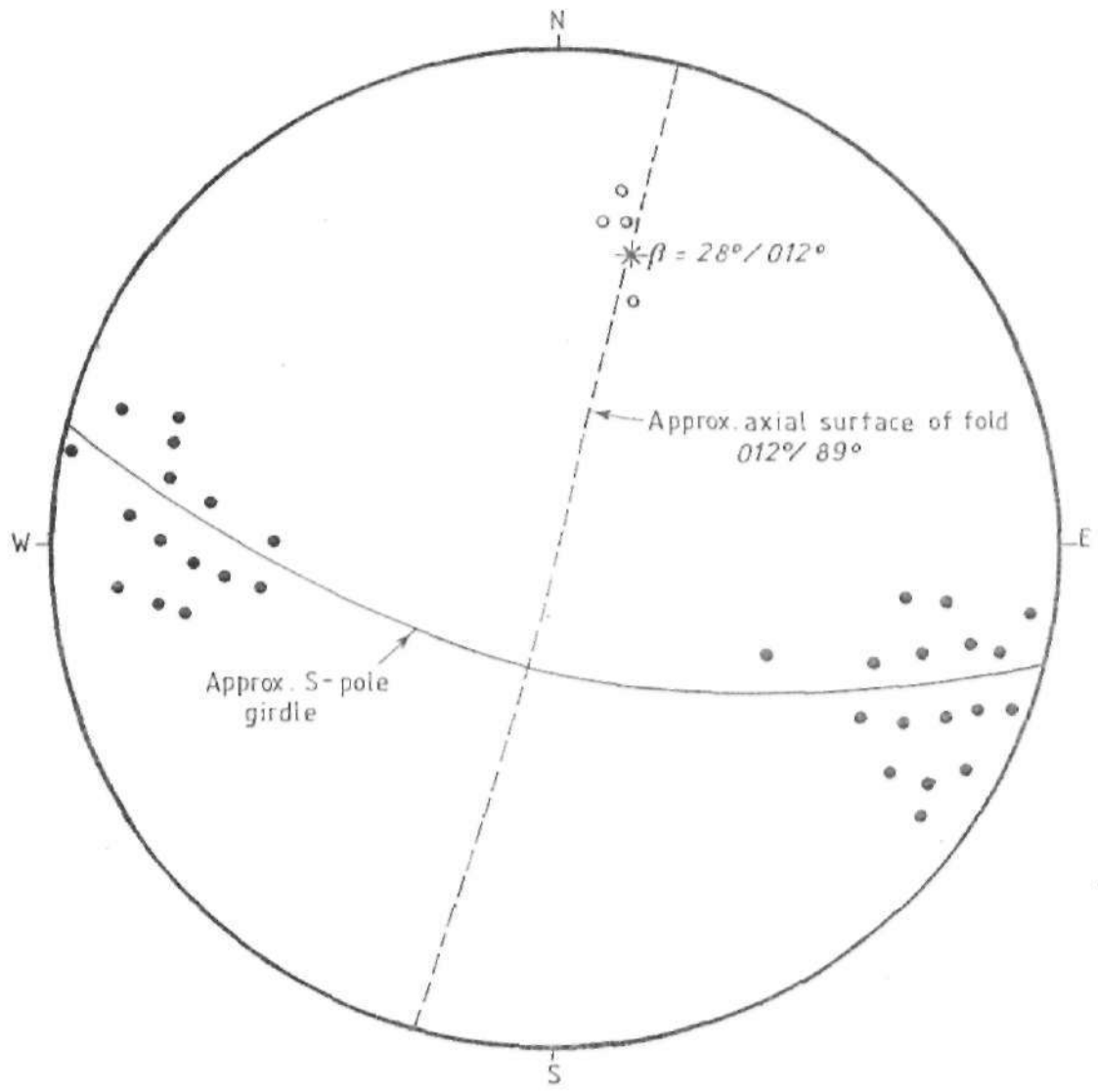


Fig.5.4. Lower hemisphere equal area projection of poles to foliation of Kazaure major antiform and minor F_2 fold axes.

occurs immediately east of the antiform. In the northeast near Sabaru, a small quartzite lens also occurs with its outcrop pattern suggesting an antiform (Fig. 5.2). At one other place, about 5 kms north of Roni and east of Bayan Dutse, the area is characterised by a general steep NE trending attitudes of isoclinally folded quartzite horizons.

In the extreme southeastern part, Amaryawa-Kwaita area, the quartzites define symmetrical isoclinal fold structures with axial traces about NNE (Fig. 5.2). In the central south eastern portions of the area, there are local fold closures which outline tight to isoclinal synformal and antiformal fold patterns with NE- trending axial surfaces (Fig. 5.2). The plunging attitude of the folds was inferred from the distribution of the quartzites and schists in the area (see phi-plot of fold axes, Fig. 5.4). It plunges shallowly towards the NE due to the cylindrical nature of the folds.

In the western half of the study area, the most prominent feature is the occurrence of isoclinal structures with NNE axial trends. The folding in the western area is more obvious from the rather shallow southeast plunge of linear structures (mineral lineation and small-scale fold axes, section 5.3). One of this structure is a fairly large antiformal structure at Manomawa, with an upright NNE- trending axial trace and wavelengths in the range of 60 - 100 m.

Two large folds, an antiform and a synform were mapped in the Dan Bakoshi area, occupying the Dutsin Dan Bakoshi hills. The folds here are very tightly compressed and have the same orientation of axes and axial surfaces. The grain elongation in this area is also NNE but swings to N-S in some places. All the major structures in the NW of the study area appear to have been controlled by the later emplacement of granites which form inselbergs and N-S trending ridges in the areas (Fig. 5.2).

A line of these granitic outcrops could be traced from Jobe village (the southern edge of Map 1) for a distance of about 20 kms, where it ends with the Dora stock. Another line of such granitic outcrops has defined a large NE trending structure directly northwest of Koda-Tunas-Dabi axis (Fig. 5.2). The crests of these structures formed central ridges mainly composed of granitoids.

The diapiric uprise of granitoids appear to have modified the shape of some folds in the area. A typical example is the large scale arcuation of some pre-existing tectonic planes about a ENE trending axes at Roni (Fig. 5.2).

6.3.3 Lineaments/Fractures

The topography of the Kazaure region and its environs is also influenced by zones of dislocation (shears). Throughout the

area there are numerous fractures and faults forming valleys and elongated lakes. The lineaments in the central metasedimentary areas represent foliation trends, while in other areas, they are related both to foliation and joints. They are generally poorly exposed with only weathering and erosional features defining their present ground positions.

Two main conjugate pairs of linear elements/fracture systems, visible on air photos and LANDSAT imagery are documented in the area (Maps 1 and 2, and Figs. 3.1, 5.1 and 5.2). These cut all the rocks of the area including the granites. The most prominent lineaments/fractures are best observed in Mashi, Kwaita, Fitare, Dunawa, Farin Ruwa and Bichi (Fig. 5.2) and represent dextral sets that strike NNE and NE. This is in agreement with the dominant NNE regional trend of the rocks in the area. The lineament near Fitare has subvertical planes with NNE trend, while the one around Farin Ruwa trends NE with no indications of strike-slip movements.

Other lineaments in the area include the inferred NW- trending ones which are generally poorly exposed and represented, but the continuity of their zone is shown by the trends of rivers and streams. One of this is the NW sinistral fault observed traversing the area. It cuts the terrain just 5 Km east of Tunas town. The length of Lake Dandi and its tributary which flows SE just south of Roni, also marks a sinistral fault with

a NW trend. There are also strong NW-SE fractures locally developed around Kazaure, Kuka, Dan Bakoshi and Kunchi (UD456), which show up well on air-photographs.

Trends of all linear features more than 2 kms long in the study area have been plotted on a rose diagram (Fig. 5.5), where three main peaks were identified. The trends of the peaks are NNE, NE and NW, and are well developed. The first and second peaks consist of NE to NNE trending fractures which are generally parallel to the alignment of the metasedimentary belts. The third peak formed the second fracture system with a NW trend but is not as prominent as the former one.

These lineaments/faults were interpreted as conjugate transcurrent system because their slip vectors are approximately horizontal. They are some of the tectonic elements due to differential stress system operating in the area, and are labelled Z_1 and Z_2, respectively (Fig. 5.5). The lineaments appear to be of the same age.

5.3.3.1 The Kalangai Fault System (KFS)

A prominent fault which roughly stretches through the middle of the Kazaure region, can be traced for over a length of at least 85 km with an average width of 0.3 km. Particular attention was given to the detailed investigation of this major lineament which bound the western side of the Kazaure

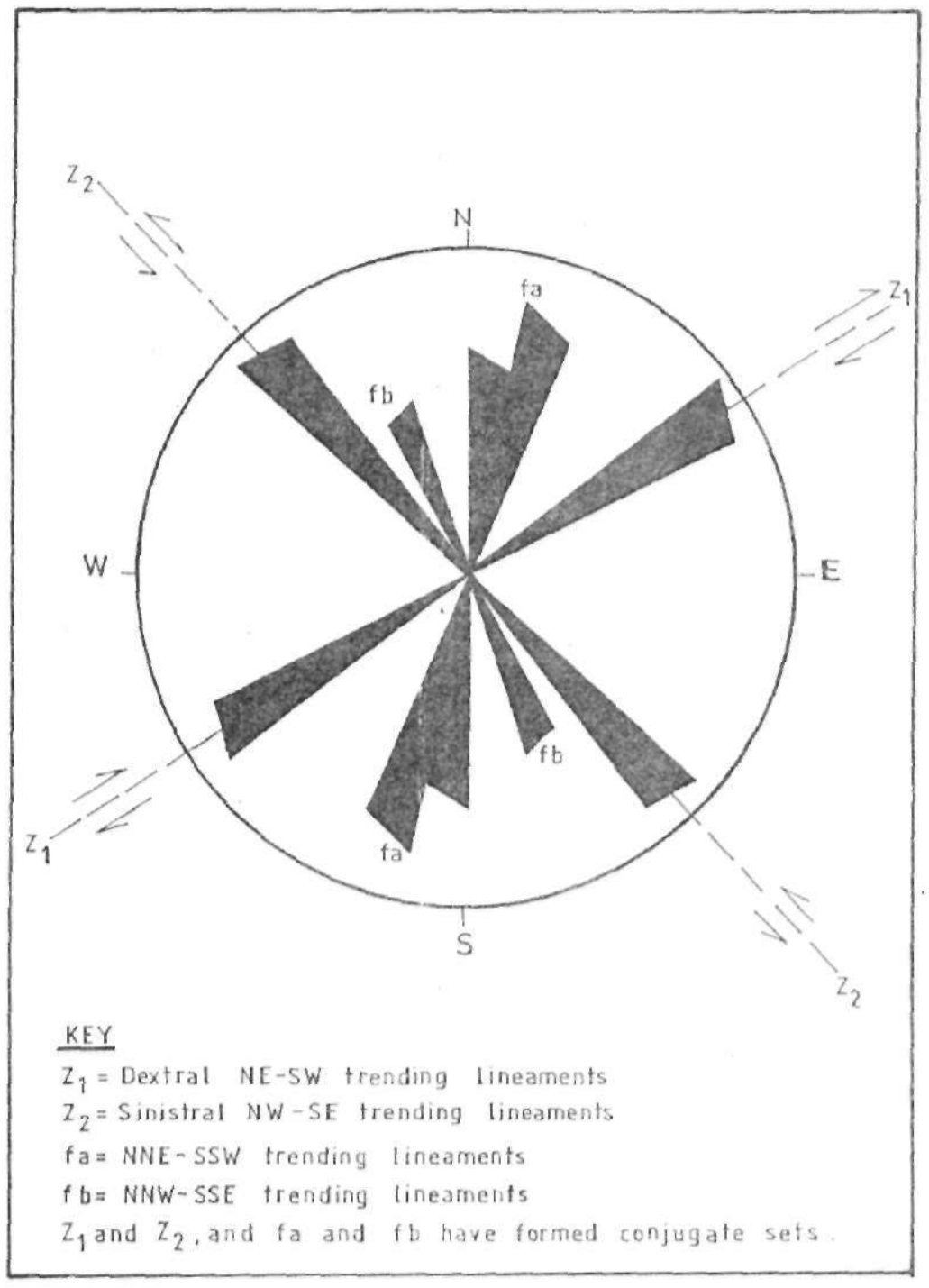


Fig. 5.5. Rose diagram of lineaments/fractures more than 2km long in the mapped area.

antiform (Fig. 5.2). West of Kazaure, the KFS forms the eastern boundary of the metaconglomerate, with moderate dip similar to that of the metaconglomerates and documented displacement of about 2.5 km. This displacement across the trend of the KFS is however not definitely of the magnitude of that of the Malumfashi area, where it has a dextral displacement of about 5 km to the NNE. Thus it appears as if the KFS in the Kazaure Belt has an "en 'echelon" pattern.

The KFS is dominated by a weak linear fabric (e.g slickensides) which records predominantly dextral movement with no subordinate normal component. The dextral displacement has been demonstrated in the field, where it displaced the axial trace of a NW-SE fold by up to 2.5 km around Kwaita and Fitare areas (Fig. 5.2). Dextral displacements over minor associated faults are also observed. However, in many other places no actual displacement (both vertical and horizontal) can be demonstrated due to the absence of suitable markers. The study of the relationships between the KFS and the rocks it has affected on a regional scale has already been given in section 3.6.

5.4 DESCRIPTION OF MESOSCOPIC STRUCTURES

5.4.1 Introduction

The minor ductile structures in the map area are described in this section. Even in the fairly well exposed areas, exposures

are too poor to enable the form of most minor folds to be traced along the rock outcrops. Only few of them where seen with complete forms, hence descriptions of most of the folds are incomplete. Some of the folds were deduced from opposing dips, as sufficient field measurements were made to assist in the structural analysis. However, the minor brittle structures documented in the study area are described in this section as joints.

5.4.2 MESOSTRUCTURES IN THE BASEMENT GNEISSES AND MIGMATITES

5.4.2.1 *Foliations in Migmatite-gneiss*

The migmatite-gneiss forms complex structures that are mainly reflected as N to NNE- trending stromatic and nebulitic fabrics. The stromatic structure forms a complex pattern in which ptygmatitic structure, flow structure and microfolds are common with pinch and swell structures defined by veins and dykes of pegmatitic materials (Plates 3.1 and 3.2). It occurs parallel to a pre-existing thin gneissic banding defined by a planar parallel arrangement of platy minerals like biotite and chlorite, at the northeast bank of River Karaduwa (Map 2). In some outcrops, the stromatic structure consists of large (1-3 cm) quartz-feldspar bands that fill spaces between boudins of granite gneiss, exhibiting a lit-par-lit injection pattern (Plate 5.1).

The nebulitic structure is characterised by the difficulty in differentiating the palaeosome from the neosome. Relics of the former neosome is marked by faint foliation planes which are concordant with the biotite fabric of the palaeosome. The agmatitic structure is the less common structure in the map area. It consists of bands of palaeosome in a neosome matrix of fine-grained granites, and is of localised occurrence especially along fault zones.

One of the migmatitic layering has a general N-S trend and consists of an alternate arrangement of mineralogical bands of palaeosome (biotite rich) and neosome (feldspar rich). In some places e.g Rorau (Map 1), NNE- striking cleavages occur as a gneissic foliation which dip very steeply at about 70^0 W. This is superimposed on a weak expression of gneissosity planes with N-S strikes, especially in the biotite gneiss (Plate 5.1).

The gneissosity planes are characterized by alternating layers of different mineral constituents in different proportions. The weak N-S oriented gneissic banding is a gneissosity plane defined by the planar parallel orientation of platy minerals like biotite, muscovite, and chlorite. The stereographic projections of S-poles (phi-diagram) for the migmatitic-gneiss area show a well developed S-pole girdle (Fig. 5.6).



Plate 5.1 Photograph of migmatite-gneiss exhibiting weak N-S oriented gneissic banding which is a gneissosity plane defined by the planar parallel orientation of platy minerals like biotite, muscovite, and chlorite. Note also the isoclinally folded ptygmatitic layers with a general N-S trends in the lower right-hand corner. Location: Tsaure (UD201).

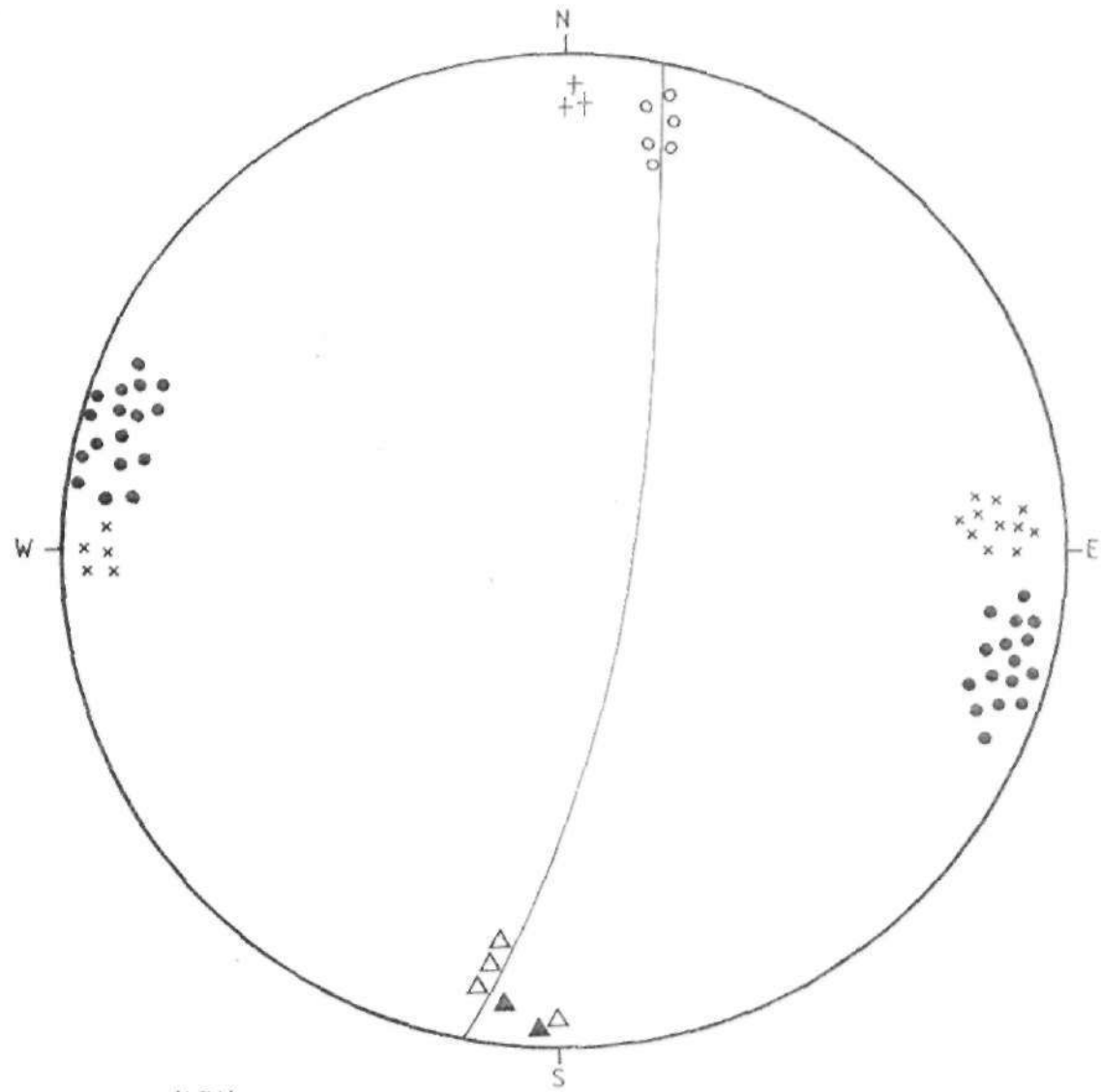


Fig. 5.6. Lower hemisphere equal area projection of poles to foliations and lineations in migmatite-gneiss areas.

5.4.2.2 Folds in migmatite and gneisses

Fold structures in the migmatites and gneisses are complex and ptygmatitic in nature, with variable trends and styles. The most complete and best preserved exposures containing these folds were found in and around Kekaji village (Map 2). These are tight folds with fold axes trending in N-S or NNE-SSW direction (Plates 3.1 and 3.2). In the gneisses, some of the folds are recumbent and are defined by tight to isoclinally folded ptygmatitic layers with a general N-S trends. The N-trending axes of these folds plunge gently at about 28^0.

In addition, isoclinal folds of foliation and quartz veins that trend NNE in the gneisses were observed (Plate 5.1, above), and their axes together with a linear arrangement of gneissosity planes, have defined a lineation. The axial planes of these types of folds are mainly developed in the migmatites to the southwest of Maraku (towards the Malumfashi belt). These were observed dipping steeply westwards. Fold axes of the folded ptygmatitic structures in the migmatites have a similar and general NNE orientation with fold axes in the gneisses.

5.4.2.3 Lineations in migmatites and gneisses

Granite gneisses are lineated rocks, with the lineation defined by a linear elongation of light felsic (feldspars) and dark mafic minerals (biotite, chlorite). Other linear

structures include fold axes of small mesoscopic folds, axes of boudinage and crenulation in the migmatites (Plate 3.2).

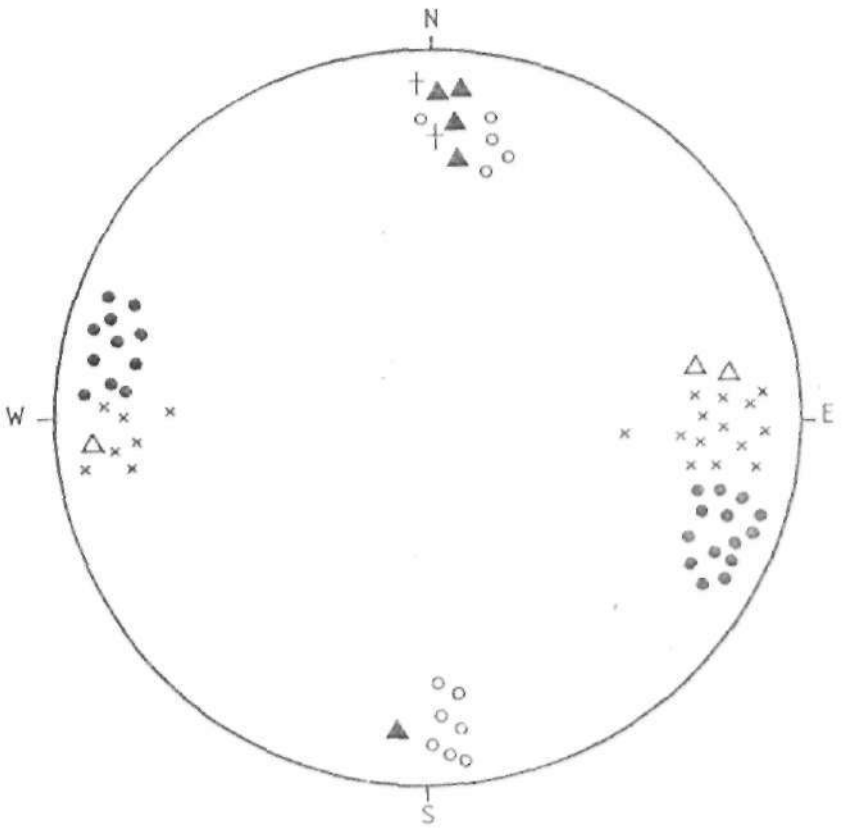
Some of the lineations have a major N-S direction, with some deformed by later generation folds. The NNE- trending fold axes in the granite gneiss and migmatites were also observed rotating N-S oriented foliation planes. Mineral lineation in the migmatite-gneiss plunges gently to the north and consists of aligned biotite and feldspar grains. In the granite gneisses, it is also defined by parallelism of long pegmatite veins that formed rods parallel to the NNE- trending fold axis.

5.4.3 MESOSTRUCTURES IN THE YOUNGER METASEDIMENTS

5.4.3.1 Kazaure area: In and around Kazaure Town.

a). Lithology in the Kazaure area

The Kazaure subarea underlie the northeastern portion of the mapped area and largely consists of four main rock types (Chapter 2 and Fig. 5.3). Most of the initial detail structural work was centered in this area as it contains the most complete and preserved superposed folds. The poles to the schistosity planes in this area were plotted on a stereonet (Fig. 5.7).



× = S_1 Foliations (23) ● = S_2 Foliations (48)
△ = L_1 Lineations (6) ▲ = L_2 Lineations (10)
+ = F_1 Fold axes (2) ○ = F_2 Fold axes (6)

Fig. 5.7. Lower hemisphere equal area projection of lineations and poles to foliation in the Kazaure area.

b). Foliations in the Kazaure area

The Kazaure subarea shows a more variable orientation of planar structures than the remaining metasedimentary areas. Foliations oriented N-S to NNE with dips ranging from sub-horizontal to steeply dipping are observed throughout this subarea. The N- striking foliations mainly occur as schistosity planes in the metasediments. In the massive quartzites, they are represented by closely spaced fracture cleavages.

In the pelitic schists and finer clastics however, the N-S cleavage locally occurs as an axial planar slaty schistosity that was overgrown by biotite. Its dip vary from 10^0 - 40^0 in the E or W direction. A quartz-muscovite schistosity with N-S trend in pelitic rocks is generally crenulated and transposed parallel to the NNE- striking cleavage.

In pelitic and finer psammites, the NNE oriented cleavage is a penetrative axial planar slaty cleavage at zones containing upright isoclinal folds whose axes are in the same direction. It is defined by the planar arrangement of biotite flakes, feldspars, quartz and locally by muscovite. The NNE- striking foliation is the main regional cleavage and has developed dipping almost vertically to the west (Plate 3.6). There is a poor development of foliation in the conglomerates.

Intrusions of syn to post-tectonic granites have affected the orientation of structures in this subarea. The effect of the intrusion is more apparent as the granite contact is approached. In such places, trends of structures like schistosities are rotated into a general ENE- orientation from their previous N-S/NNE-SSW strikes (Plate 5.2).

c). Folds in Kazaure subarea

Minor folds with N-S and NNE- trending axes are present. Their forms depend on the type of rock that is folded, but they generally ranged from flow type tight folds in the quartzites to crenulation folds in the pelitic schists. The N-S trending folds are more obvious in the southeast of the area where the quartzites and quartz veins define isoclinal folds with hinges preserved in areas of favourable exposures. At locality UD59, there is a N-S tight to isoclinal fold, with axial planes strike of 030^0 and limbs dipping shallowly to the east at an angle of about 20^0 W. The fold is generally small, with wavelengths of 12 - 105 cm, and gentle plunge. It has thickened noses and limbs and is largely obliterated by later deformations (Plate 5.3).

NNE- trending fold axial traces to the east of the area are also found refolding N-S oriented folds, especially along tributaries of rivers. On the side valley of River Tuwari behind L.E.A. Offices, folds with steeply plunging axes have

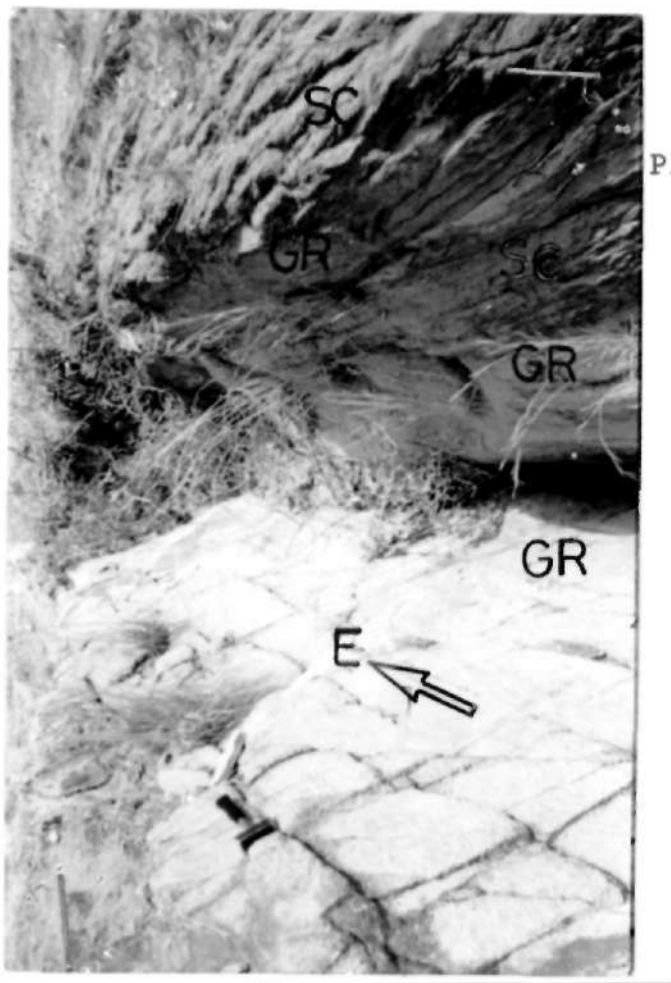


Plate 5.2 Photograph of medium grained granite intruding mica schist in the Kazaure area (UD59). Note re-orientation of pre-existing N-S structures into an ENE trend and the characteristic joint pattern. Hammer is lying directly on an E-W trending joint.

GR = GRANITE
SC = SCHIST
E = EAST



Plate 5.3. N-S oriented mesoscopic folds in micaceous quartzites, largely obliterated by later deformations. Note the contorted and domal form of the small interference structure due to the NNE-SSW refolding effect. Location: Dutsin Kiye (UD48).

been superimposed onto tight folds with an original N-S strike of the axial surfaces. These NNE- trending folds which in this area, are also documented in the form of tight to isoclinal cylindrical folds in the schists, are several centimetres across (Plate 5.4). They are always concordant with structures from the quartzites, suggesting they were formed during the same event.

The NNE- trending minor folds in the schists are mainly developed in the more siliceous layers. Their axial planes lie at NNE-NE and are the dominant types of folds in this area, in addition to their association with the most penetrative foliation. The NNE (less than 30^0 from the north) trending fold axes have steep plunges ranging from 74^0 - 90^0. The abrupt changes in the strike of the steeply dipping and NNE- trending foliation, as at Rorau, best illustrate the NNE oriented fold structures.

d). Lineations in the Kazaure Subarea

Lineations in the Kazaure subarea are defined by quartz rodding and striation marks which trend in a general NNE direction. It is marked in the quartzites where
the quartz grains are elongated parallel to the N-S directed fold axes with varying plunge values especially around Kazaure (Fig. 5.1). Also observed is a penetrative mineral or quartz rodding elongation lineation, which is a weaker subhorizontal



Plate 5.4 Photograph of tight to isoclinal NNE- trending non-cylindrical fold in a quartz schist. Note the foliation trending parallel to the axial trend of the fold as outlined, and also the lineation (L), and pebbles and cobbles of the schist occurring as floats. Location: Kazaure (UD59).

stretching fabric in X - direction (Plate 5.4). It has gentle plunge values (10-30^0) to the south and north on NNE trending foliation surfaces. This is mainly observed in the quartzites.

In the metaconglomerate, a gently plunging clast elongation lineation is defined by the orientation of the long axes of deformed conglomerate and quartzite clasts. Elongated direction of K-feldspars in some of the porphyritic granite has also defined a lineation. The mica-schists have a distinct lineation caused by microfolding of the N-S schistosity planes. This is an ab- lineation, as it is parallel to axes of NNE- trending microfolds (Plate 3.6).

A dominant mineral lineation is also occasionally developed in the fault rocks. It is defined by prominent striation marks (coated with micaceous minerals), which indicate strike-slip movements. They are relatively steep (40-70^0), but in the west around Ladan village, they flatten out to about 10-24^0.

6.4.3.2 Other Metasedimentary areas

The other subareas of detailed mapping and analysis of mesostructural patterns cover the metasediments in the central, western and southwest portions of the study area (Maps 1 and 2, and Fig. 3.1).

b). Foliations in other areas

Planar structures are very common in the metasedimentary subareas and they range from slaty to phyllitic fabrics in pelites to a poorly developed wide-spaced fracture cleavage in the quartzites. Orientations of various planar structures in the other metasedimentary areas are similar to that of the Kazaure subarea. N-S striking planar fabrics are localised and the only confirmed evidence for their existence is the occurrence of refolded cleavages and early and minor small-scale isoclinal folds. They did not influence later structures.

In pelitic and finer clastics, the N-S striking foliation is an axial planar slaty cleavage, while in the coarse clastics it occurs as a subhorizontal schistosity planes. It is also locally observed in the metapelites refolded into a NNE zonal crenulation cleavage defined by planar arrangement of platy and prismatic minerals. Sometimes it is represented by thin layers of different mineral proportions in the metapelites.

A cleavage which has developed with a strike of NNE and steep westerly dip can also be observed in many places. It is an axial planar slaty cleavage in pelitic and finer psammites, while in the quartzites and quartz schists, it occurs as a spaced crenulation fabric defined by the planar arrangement of

biotite flakes and quartz, and locally chlorite. This type of cleavage is still co-axial with fold axes that trend NNE, although bent in some places. The mean orientation of these cleavages is 010/70^{0}NE.

At some localities the NNE- striking foliation is superimposed on a pre-existing foliation with N-S strike, but in most places this foliation has largely been obliterated or transposed (Plate 5.5). On outcrop scale remnants of the N-S oriented foliation is generally associated with few minor and larger folds. At two localities (UD123 and UD125) a $_{N\text{-}S}$ slaty cleavage is replaced by a crenulation cleavage with NNE strikes in the form of microlithons (1 to 2 cm apart). This overprinting relationship is very common, so are NNE- striking fracture cleavages (Plate 5.5). The strong NNE-SSW foliations are axial planar to isoclinal folds especially in pelitic units where they are penetrative. They have affected earlier formed phyllosilicates by kinking and fracturing them.

In some parts of the areas underlain by granite (UD60), displacement due to the intrusion of the granite has affected the original orientations of schistosities and axial surfaces of small-scale folds. This has resulted in the rotation of some pre-existing tectonic planes about a ENE- trending axes (Plate 5.2).

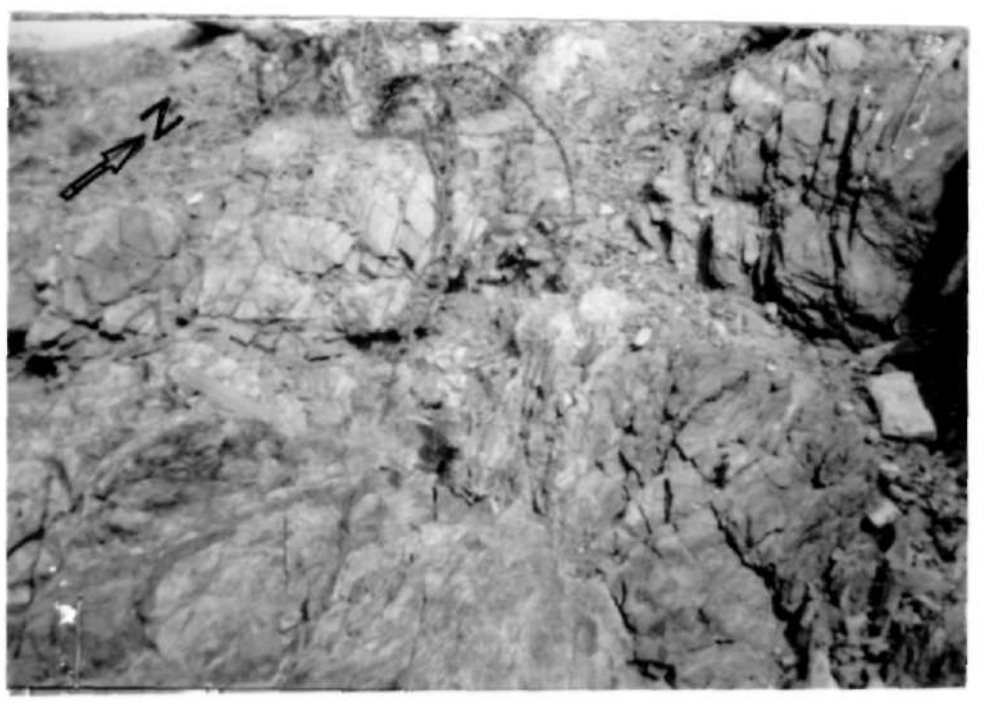


Plate 5.5: Photograph of quartz biotite schist showing intersection between the N-S/NNE- striking foliations. This was observed defining groovy shapes whose long axes are parallel to a lineation on the NNE-trending fabric (under biro). Location: Kan Dawa (Map 2).

Stereographic beta-plots of poles to foliation are generally arranged about more or less horizontal NNE- trending axis which is generally parallel to axial planes in this direction (Fig. 5.8). The phi-diagram shows a well-developed S-pole girdle, the few points lying off the girdle are probably a reflection of non-cylindrical form of folding.

c). **Folds in other areas**

The N-S structures are only preserved in the competent quartzites and were masked in the phyllites by the NNE-SSW deformation. There is evidence for the existence of two small-scale isoclinal folds with N-S trending axes in a micaceous quartzite ridge north of River Gari. They are defined by quartz veins and the main lithologic unit (quartzite), with hinges preserved in areas of favourable exposures.

The axial plane foliations of these folds have been refolded by upright folds, whose NNE- trending axes plunged towards the NE at an angle of 8^0-12^0. The distorted folds are mostly tight and overturned noncylindrical structures with rootless hinge zones. They have N-S orientation and are symmetrical with wavelengths up to one metre long in the two places.

The irregular and upright NNE fold structure is non-cylindrical. It has deformed and obliterated most of the N-S oriented structures, like folds, schistosities and microquartz

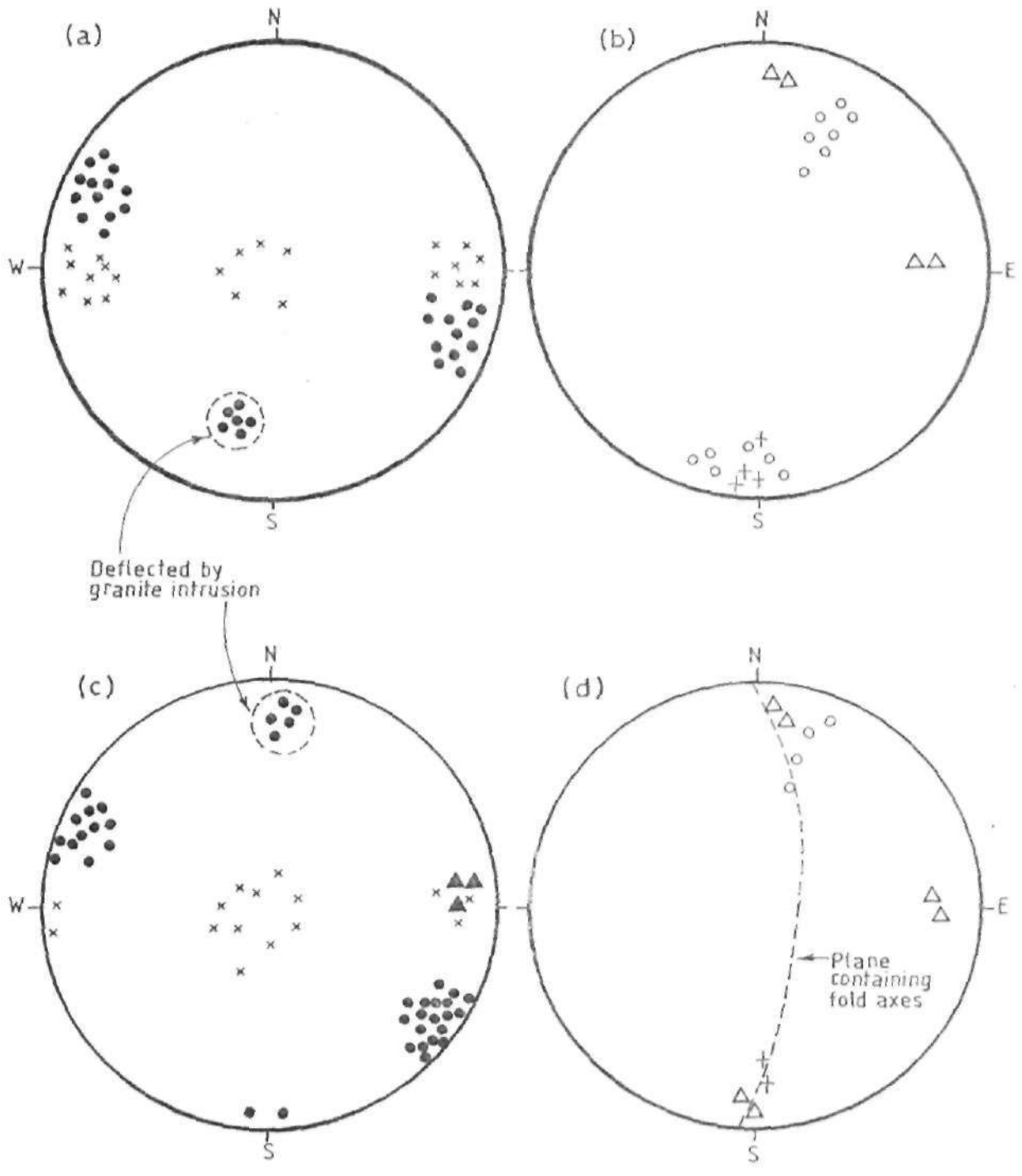


Fig. 5.8. Lower hemisphere equal area projection of lineations and poles to foliations in other metasedimentary areas. (a) and (b) Kazaure schist belt area fabric data. (c) and (d) Malumfashi schist belt area fabric data.

veinlets. The N-S trending folds now occur restricted to the limb portion of mesoscopic NNE- trending folds, as relics tight to isoclinal small-scale folds with moderately plunging axes.

The spatial distribution of foliations and quartz veins (Plate 3.7) has defined well developed tight to isoclinal folds with NNE trends. These folds have been intersected by prominent west-dipping axial surfaces which plunge N or S. The axial surfaces are penetrative and steeply dipping to upright with NNE trends at less than 20^0 from the approximate linear N-S trend of the Kazaure belt. They have a mean attitude of $353^0/80^0W$, with moderate north or south plunges.

The quartzites clearly illustrate the upright folds and kink bands in many parts of the metasedimentary subareas. They commonly occur as tight to isoclinal folds of schistosity, forming minor as well as mesoscopic fold structures. They generally have NNE- trending fold axes with steeply SE dipping to upright axial surfaces and large amplitude. The small-scale upright folds have their wavelengths greater than their amplitudes. The wavelengths vary from 5 cm to 25 cm and amplitudes from 3-10 cm. The plunge of the mean fold axis is $40^0/012^0$.

South of the Watari River (UD439) a chevron (macro fold) with NE-SW (044^0 - 224^0) trending axis and moderate plunge (50^0) was also observed defined by quartzo-feldspathic veins. The axial trace of this fold can be mapped throughout most of the area trending in a general NE- direction and dipping steeply to the west (Fig. 5.2). Its wavelength vary from 30 to 50 cm, amplitudes 20 to 40 cm with an interlimb angle of 40^0.

d). Lineations in other areas

Boudinage, pinch and swell structures and roddings are usually common, especially in quartz and pegmatite veins (Plates 3.3, 3.8 and 5.1). They are best developed in the road cut along Kazaure-Kwaita road (Map 1), and in the River Thomas at Kuka (Map 2). The relatively competent quartzitic rocks interbedded with the schists are also intensely boudinaged but not as intricately deformed as the surrounding schists. The development of boudins is however mainly limited to the competent quartzites.

Some of the linear structures are defined by stretched quartz rods in quartzites which are generally N-S plunging and subhorizontally oriented. The mineral lineation also occur rotated from their original orientation. It shows a radical change from shallow plunging in some places to subvertical plunging in other places. This change in orientation is also

more likely to be as a result of the effect of NNE- trending folds in such places.

The curving trend of the quartzitic rocks forming the Amaryawa-Waire ridges (UD425) could be due to a curving fold axis of moderate plunge. The plunge of the fold-axes is moderate to the east of north, though local variations are common in the form of both vertical undulations and lateral swings. This probably resulted from the superimposition of gentle undulations due to intrusions.

Associated penetrative mineral lineation is the dominant regional linear fabric, and is more common in the metasediments where it forms a subhorizontal stretching fabric in X-direction. The lineations occur as pinch and swell structures with variable plunge values to the N and S. The boudinaged structures are defined by the quartz veins and ferruginous quartzites lying parallel to the regionally developed NNE- trending cleavage. The boudins plunge parallel to the axes of the upright folds as well as NNE- striking foliations and are therefore regarded as sub-horizontal extension lineations.

A prominent rodding lineation is also developed in siliceous units where quartz is stretched into rods. This lineation commonly trends NNE and is co-axial with folds of all scales

related to the NNE- striking structures. The mineral lineations in the quartzites have higher plunge angles, and are characterised by a general N plunge.

There is also slickensides fault surfaces that are potential local indicators of the sense of displacement along lineaments. The ones observed are coated with micaceous minerals commonly displaying prominent striation marks, indicating strike-slip movements. It should be noted that, although the fault movement is only observed in the horizontal structural direction, the fault could have originated through both dip-slip and strike-slip movements.

The mica-schists have in addition to schistosity a distinct lineation caused by microfolding of the schistosity plane. It plunges 80^0 towards 020^0 in the mica schist. This is a b-lineation because it is parallel to larger folds which are parallel to these microfolds. It is defined by aggregates of light minerals and linear orientation of dark minerals. In some outcrops, intersection between the N-S/NNE-SSW foliations was observed defining groovy shapes whose long axes are parallel to a lineation on the NNE- trending fabric (Plate 5.5).

6.4.4 Joints

Lineaments not identified on aerial photographs are assumed to be narrow in width and short in length. These are mapped and discussed as joints. All the rocks in the study area are jointed, with the jointing almost always vertical or steeply inclined. It is more common in areas underlain by more competent and harder rocks where it controlled the drainage and topography (Plate 5.2). Joint analyses were undertaken and all the measured joint planes in the area were plotted on a rose diagram (Fig. 5.9). This has led to the recognition of at least two main joint sets in the whole area.

The first and well-defined joint direction is approximately NNE striking, mostly containing pegmatite and quartz veins. It is oriented parallel to the main statistical fold axis in the area (Section 5.9), and therefore appears to be a `bc' set. In most cases, the `bc' set trends at about 010^0 to 020^0 parallel to the NNE- trending fold axes, that is almost parallel to the lineations in the area. This suggests the distribution of the `bc' set is controlled by these folds.

The many joints oriented normal to lineations (cross joints) formed the second main set, and can be interpreted as (`ac' set). It trends at 078^0 to 092^0 and dips very steeply to the west (Its pole is at about $N60^0E$). Longitudinal joints are also prominent in the granites and could have formed during

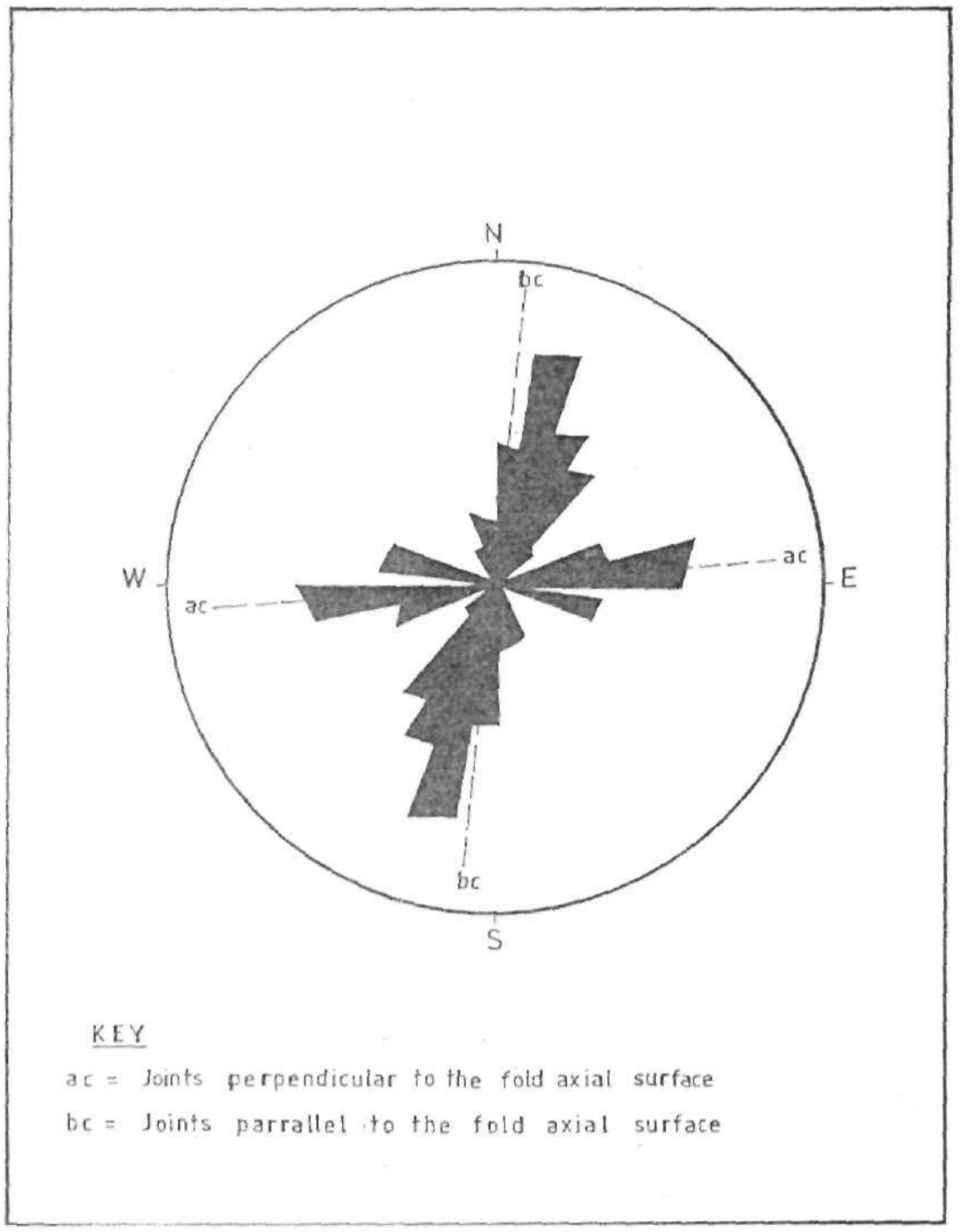


Fig. 5.9. Rose diagram for the strikes of joints measured in the study area.

granite consolidation or could be load release joints. There is also a vertical N113^{0}E joint orientation that may be an oblique joint near the faults. A nearly flat joint set was also documented on a number of granite outcrops.

5.5 DESCRIPTION OF MICROSCOPIC STRUCTURES

The field data derived from interpretation of many of the structural features recognised by observation of airphotos and outcrops, were complemented with microscopic structural studies of thin sections and detailed tectono-metamorphic observations (section 4.4). This has provided useful information with regard to the structural elements diagnostic of the different deformational styles in the different areas.

The microscopic fabric consists of flattened quartz grains and parallel aligned white micas and chlorite flakes. In most thin sections, the N-S and NNE- striking foliations have similar trends, consistent with field data (e.g Plates 4.1). The prominent foliations are the steeply inclined cleavages which strike NNE and are mainly parallel to sub-parallel mineralogical layering of phyllosilicate minerals.

In pelitic units the foliations are penetrative, except where biotite porphyroblasts are preserved microscopically as quartz-inclusion trails. Foliation is poorly developed in the

conglomerates, it is only evident in thin sections where it is defined by alignments and segregation of flattened minerals.

5.6. SUPERIMPOSITION OF STRUCTURES

Field observations and thin section studies (sections 3.1 and 4.4) have revealed the occurrence of a tectonic planar internal fabric superimposed on an earlier layering of probable similar origin. This implies the planar fabrics in the area developed during more than one deformation episode. In most cases, most of the ductile structures mentioned (e.g lineations) are found deformed by a fold, and the style of folding, the difference in orientations in both planar and linear structures, and overprinting relationships have allowed for the classification of the structures.

The symbols used for the structural descriptions are: D for deformation event, F for folds, S for foliations, and L for lineations, respectively. Relative ages of events are designated by subscript numbers, starting with the oldest. As such all the ductile structures have either been classified into an earlier D_1 structure or a later D_2 structure.

The first recognised planar fabric in the migmatite-gneisses and the associated metasediments is designated S_1. It originated during the earliest phase of deformation (D_1), and is an axial plane foliation with a general N-S trend. The D_1

deformation is followed by the second deformation episode (D_2) which produce structures with a general NNE- orientation. In the present work, most of the structures observed seem to follow this general framework.

The D_1 event has not been very significant and early N-S trending F_1 small-scale folds are poorly developed in the metasediments. They are only found where the D_2 deformation has been less intense. On the bank of River Tuwari a recumbent N-S fold is deformed by an upright tight to isoclinal NNE-striking fold to produce a type 2 interference pattern (Ramsay, 1967; Plate 5.3).

5.7 CLASSIFICATION OF THE MAJOR STRUCTURES

The small-scale structures in the different subareas are congruent with the large-scale structures in the study area. Therefore a relative chronology of all the documented large scale structures was established using information on the small-scale structures. All the major geologic structures in the study area have almost similar orientations throughout the area. Therefore, their deformational histories are likely to be the same.

On a regional scale, the S_1 and S_2 foliations are both widespread, conspicuous and easily distinguish from one another, because the S_2 which resulted from the re-alignment

of S_1, now has an angle of about 24^0 between them. The distribution and regional trends of most of the major structures could best be described as D_1/D_2 interference patterns mainly controlled by superimposed folding (Fig. 6.2).

5.7.1 Major D_1 Structures

The minor N-S trending relict F_1 folds are geometrically related to some of the large folds. The presence of early F_1 large fold structures was inferred from air photos and Landsat imagery. Two of these occur with N-S trends and recumbent axial plane dips, which vary to steeply plunging in the west. One of this fold is the major structure near Dabi (Map 1).

The other early D_1 large structure is defined by the quartzite ridge at Dan Bakoshi, in the adjacent Malumfashi belt. This has been demonstrated in the field, where the profile similarity between F_1 minor folds and an antiform in the eastern side of the Kalangai Fault System (KFS), suggests the Danbakoshi antiform to be an F_1 structure.

5.7.2 Major D_2 Structures

D_2 structures resembling those described from polydeformed areas occur with some zones intensely folded along NNE axes. The major folds with NNE axial trends include: the Kazaure synform and antiform, the Amaryawa structures, and the antiformal fold east of Manomawa village. The Dutsin Dan

Bakoshi structure (to the west) and the augen structure that occurs in a quartzite lens near Sabaru are probably due to F_2 cylindrical folding, superimposed on an earlier F_1 fold. This was confirmed from the undulating nature of fold axes which dip to N or S, due to the superimposed F_2 folding episode.

The structural pattern in the Western area around Jobe-Koda-Dara-Dabi-Tunas Axis can probably best be explained as formed by two fold phases, F_1 and F_2 (Fig. 5.2). The rest of the major structures (especially those that look like a dome) are localized around plutons and could be products of forceful emplacement of the magma.

5.8 STRAIN ANALYSIS (Kinematic indicator)

The bulk stress that has affected the rocks in the study area has imposed a bulk strain whose quantitative analysis was not undertaken because of lack of abundant suitable materials like deformed conglomerate clasts (e.g Flinn, 1962). Qualitative estimates of strain were however undertaken, based on conspicuous tectonic features which include fold tightness, lineations and cleavage developments.

The deformation events in the area have resulted in the formation of different types of cleavages and lineations. According to Hobbs et al., (1976), crenulation and slaty cleavages are known to develop perpendicular to the direction

of greatest shortening of the rocks in which the cleavages are formed. This observation was used to qualitatively define strains across the whole area.

There are local and narrow zones of high finite strain, probably related to the brittle-cataclastic deformation in the fracture zones (Section 5.2.8). In a given locality, the strain ellipsoid can be qualitatively defined by taking planar structures (axial surfaces, cleavages etc) to define the XY-plane and linear structures (lineations and fold axes) to define X. X is the major axis and is nearly horizontal, Z is minor axis of regional strain ellipsoid, intermediate axis Y is vertical (X>Y>Z). The plane of flattening (XY) is nearly vertical and trends N-S.

Oriented deformed pelitic clast samples were taken for analyses. One of this (Fig. 5.10) indicates a weaker subhorizontal stretching fabric in X-direction, with the almost vertical XY flattening plane striking nearly NNE.

Similarly, in another oriented conglomerate quartzite clast, the finite strain has a strong N-S subhorizontal X axis which defined the linear elements. The deformational strain was roughly estimated on these oriented samples of the clasts. The original shape of the quartzite clast is circular, while the original shape of the schistose clast has a ratio of 4:1.

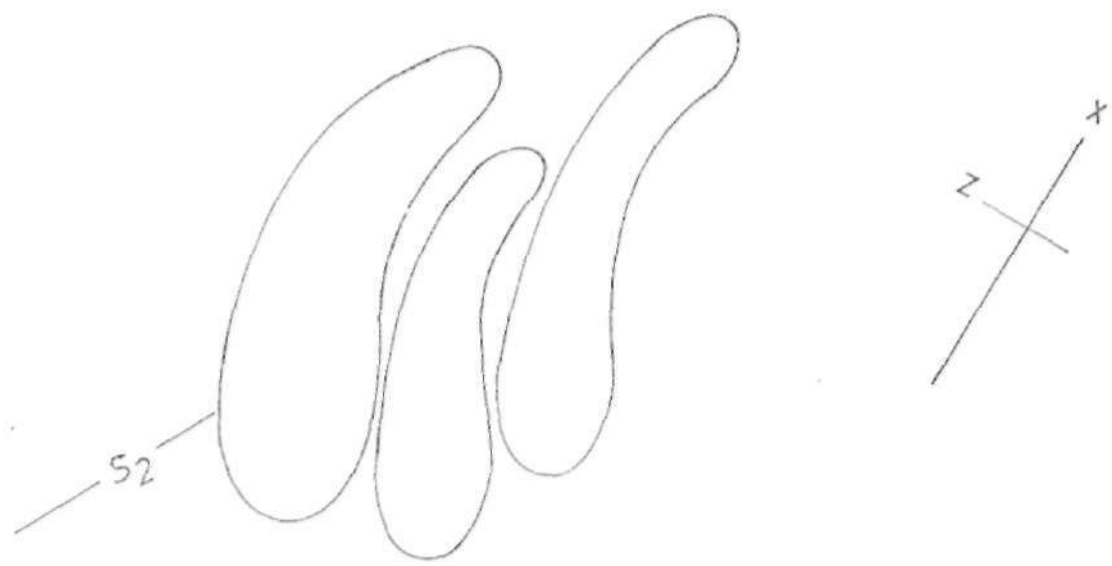


Fig. 5.10. Sketch of an ellipsoidal structure of deformed pelitic clasts exposing XZ surface. Maximum extension (x) is along (parallel to) the plane of the exposed surface. Finite-strain XZ ratios are about 5. Finite-strain ratios in the XY plane are about 2.2.
LOCATION: Exposure in River Tuwari, two kilometres N.W. of Kazaure (UD 59).

Measurements of axial ratio from the flattening field of the strain ellipsoid as defined by the pelitic clast is in the order of 22:8:1 (x:y:z), while the finite strain in the quartzitic clast is in the order of 7:2:1.The Kinematic analysis indicates the strain is due to a prevailing E-W stress which resulted in an E-W directed shortening. The qualitative observations also revealed that the pelites have undergone higher strain.

5.9 STRUCTURAL SYNTHESIS

5.9.1 Ductile Structures

The structural relationships in a metamorphic terrane is usually complex, especially when dealing with different rock types. Simple deformation in such a terrain usually produces structures with various styles but with similar orientations. The structural analysis in this study has revealed that most of the outcrops have structures that provide evidence for the polyphase deformational character of the rocks in the area. The migmatite-gneisses and quartzites are not as deformed as the pelites. This should primarily be due to their lithologic differences. However, there is a strong similarity between the structural pattern from the Kazaure area to that of other metasedimentary areas in this study.

The rocks in the area studied have been deformed by at least two intense phases of ductile deformation (D_1 and D_2, Fig. 5.11), with the first deformational episode D_1, the less

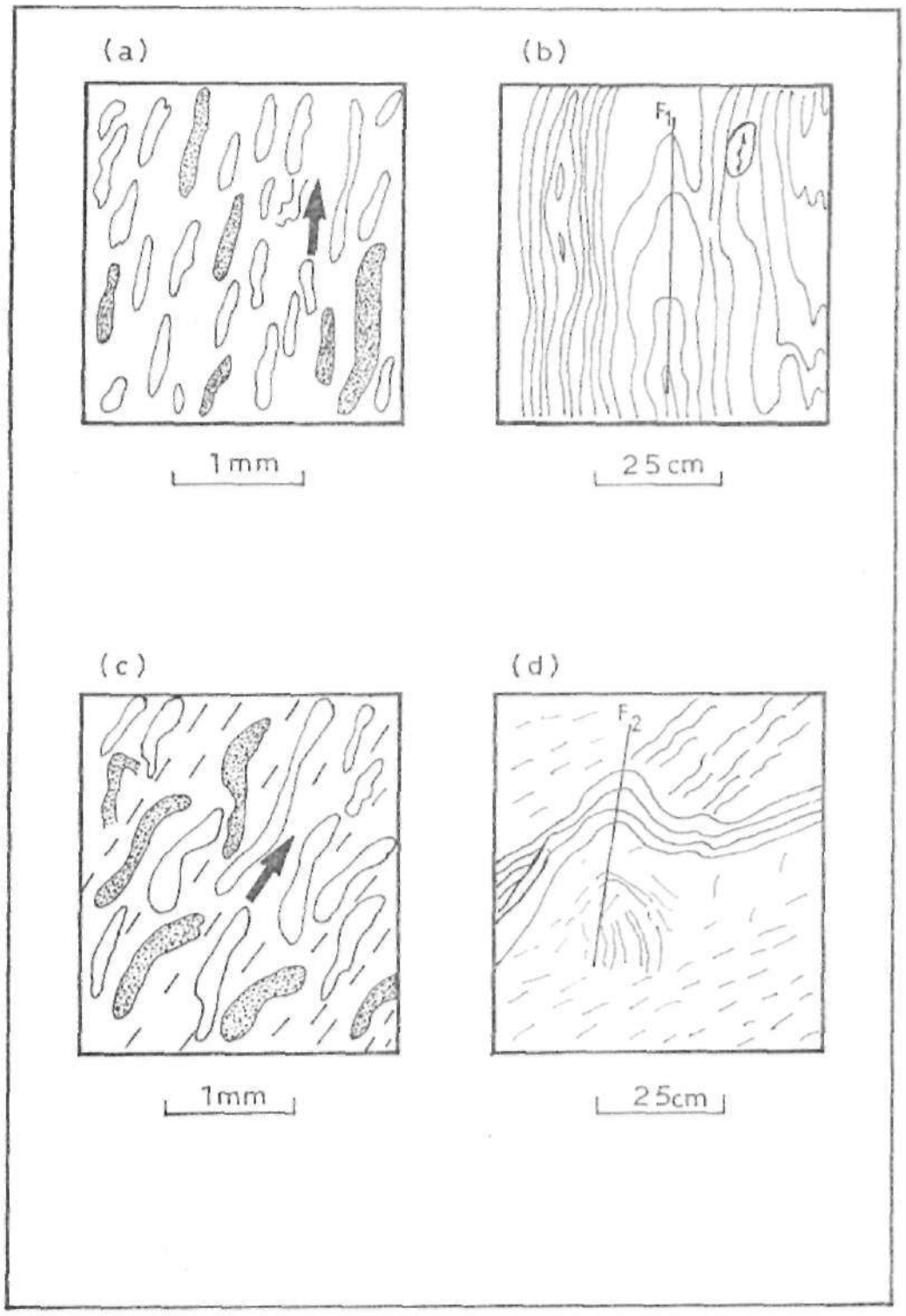


Fig. 5.11. Sketch diagrams drawn from the field and thin-sections showing fabric relations in quartz-muscovite-schist at Kazaure (UD 49). A = S_1 cleavage; B = tight to isoclinal F_1 folds; C and D = S_2 cleavages and F_2 folds.

intense of the two. The D1 event gave rise to recumbent and isoclinal N-S trending F_1 folds, while the later event (D_2) resulted in the formation of upright NNE- trending F_2 folds (Fig. 5.12).

The D_1 deformation produced a N-S trending tectonic planar internal fabric, S_1, and is thought to be the older. Indications of the occurrence of the S_1 slaty cleavage were indirectly confirmed from observation of an S_2 crenulation cleavage. Folds of the earliest recognised deformational phase (F_1) now occur as relict flat-lying folds with thickened noses and limbs.

A feature of the D_2 event is the steeply dipping to upright NNE- trending F_2 folds it produced. These are tight to isoclinal in the fine-grained clastic rocks and more open in the coarse clastic types. The F_2 folds are cylindrical and shallowly plunging, with variable wavelengths. The D_2 event has refolded F_1 folds and the earlier tectonic fabric (S_1 segregation layering) to produce the F_2 folds, which are more prominent than the F_1 folds. They have obliterated or transposed S_1 banding in many places. Over much of the area, the F_2 folds are found to be mainly of mesoscopic scale and generally have subrounded hinge zones and tight forms. Their sense of vergence depends on their position in the megascopic fold structures.

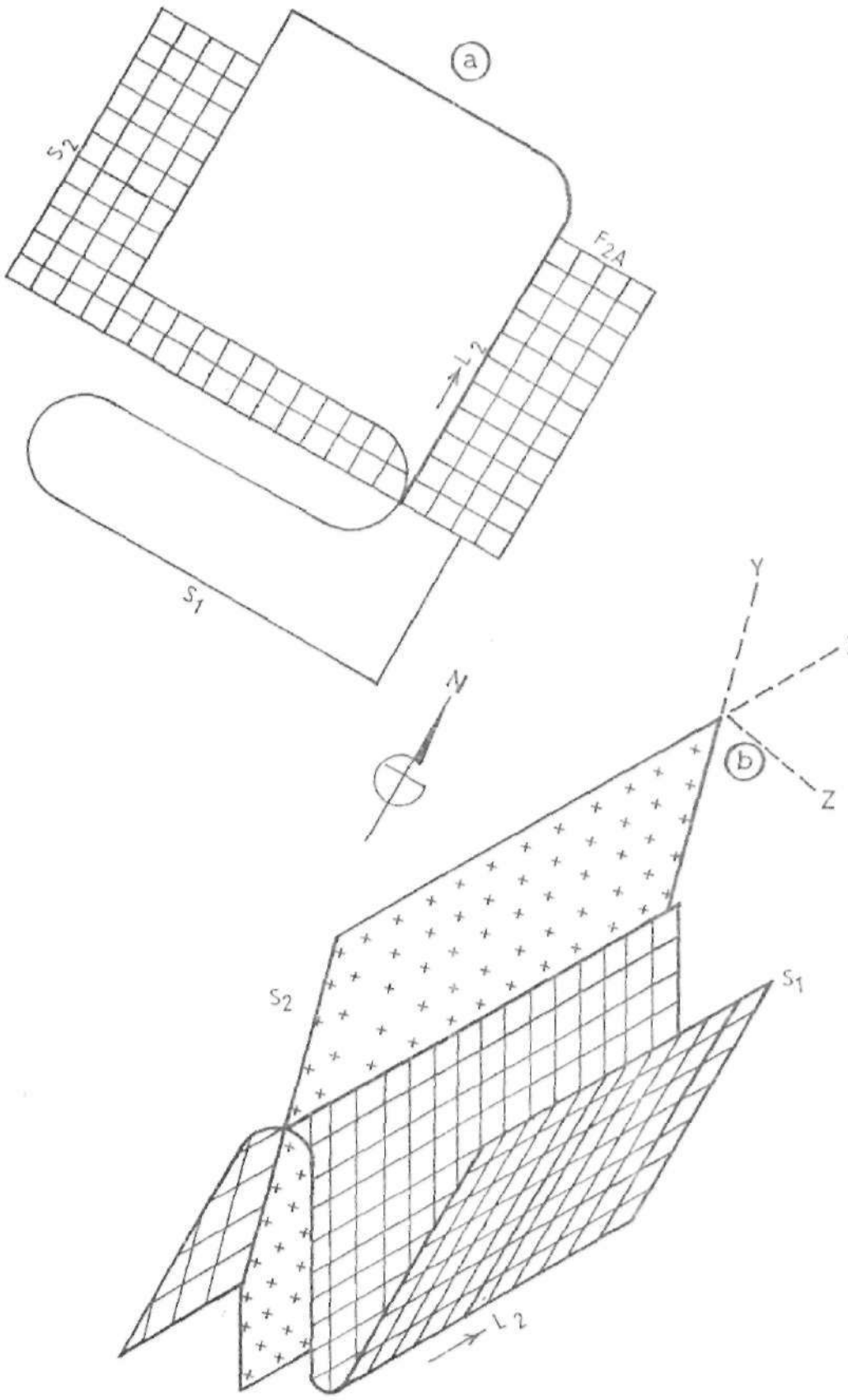
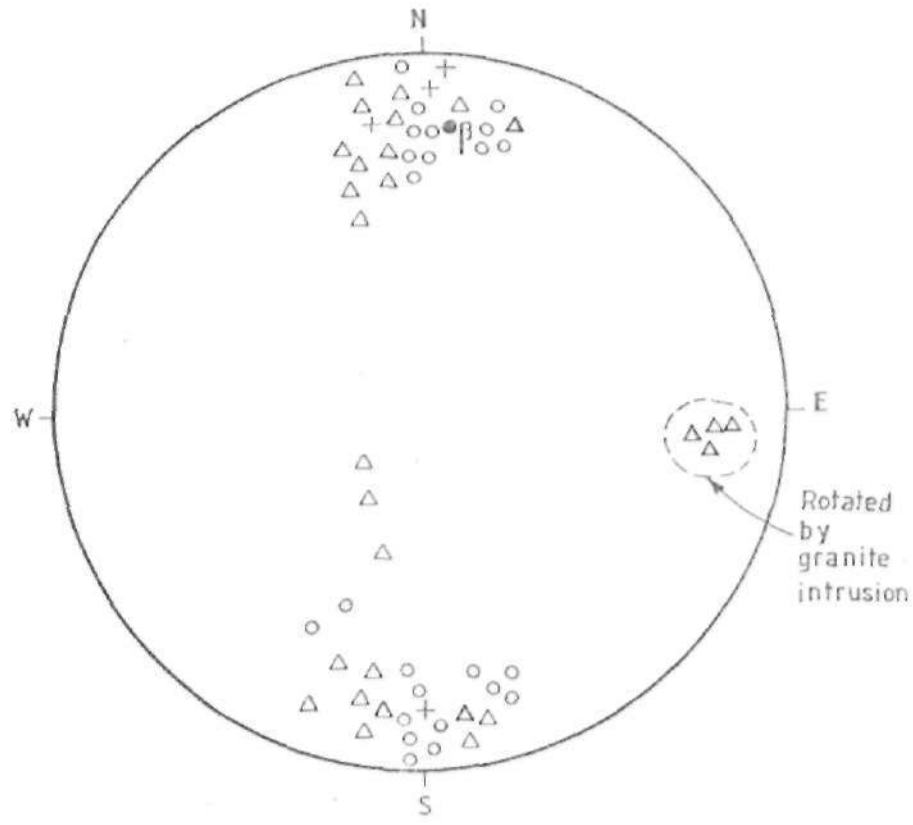


Fig. 5.12. Schematic block diagrams showing the major style of folding. (a) N-S recumbent F_1 phase of folding (b) NNE-SSW upright F_2 phase of folding.

Both small- and large-scale F_2 fold axial surfaces are penetrative and dip steeply to the east or west, with fold axes plunging moderately to the north or south. The S_2 fabrics are clearly of tectonic origin because they are sometimes axial planar in areas of high strain F_2 folds. They are the most prominent and widespread planar fabrics in the area. In the massive quartzites it manifests as an S_2 spaced crenulation cleavage, as well as a pressure solution cleavage.

Correlation of structures in the migmatite-gneisses and the younger metasediments, has also revealed that structures described from the metasediments are coaxial and coplanar with structures in the migmatite-gneisses. This suggests the two lithologies were affected by the same deformation events. During the D_1 and D_2 events the supracrustal sediments were regionally deformed and the basement migmatite-gneisses reactivated.

Measurements of planar and linear minor structures have been compiled and plotted. The stereographic plot of the trends of the linear structures (Figs. 5.13), reveal that the F_1 and F_2 fold axes are separated by an angle of 20^0. The main statistical fold axis (Φ) plunges steeply to the north, but there is also a subsidiary statistical fold axis (Φi) with gentle northwesterly plunge, whose direction is defined by the strike of vertical and steeply dipping beds in a number of



KEY

- •β = Regional fold axes
- △ = L_2 Lineations (68)
- o = F_2 Fold axes (25)
- △ = L_1 Lineations (42)
- + = F_1 Fold axes (12)

Fig. 5.13. Lower hemisphere equal area projection of poles to linear minor structures and regional fold axes.

exposures. These two statistical directions are the result of the re-folding of an earlier N-S trending F_1 fold. The stereographic plots of poles to foliation in the whole area is shown in Fig. 5.14.

The interference pattern produced in the area is dominantly the mushroom type (Fig. 5.11). This resulted in the formation of antiforms and synforms, and F_1 and F_2 fold axes and planes that are not at high angle and are not co-axial. Most of the F_2 folds have varying plunge values and styles, and resemble Class 1C folds of Ramsay (1967). They were formed when the rocks are in a plastic state probably during metamorphism and/or migmatisation.

5.9.2 Brittle Structures

Brittle deformation events recorded in the study area include localized displacement of pre-existing structures around plutons due to forceful magmatic emplacement. Others include a major Pan-African crustal consolidation that produced major shear zones which generally trend NW-SE and NE-SW. Many shear zones contain fault rocks that have cataclastic or protomylonitic textures which indicate their response to brittle deformation (Ajibade and Mbonu, 1982; Higgins, 1971; Sibson, 1967 and Mower, 1986). This is a function of their physical properties, which in turn is determined by the crustal depth at which the rock(s) occur within the shear zone.

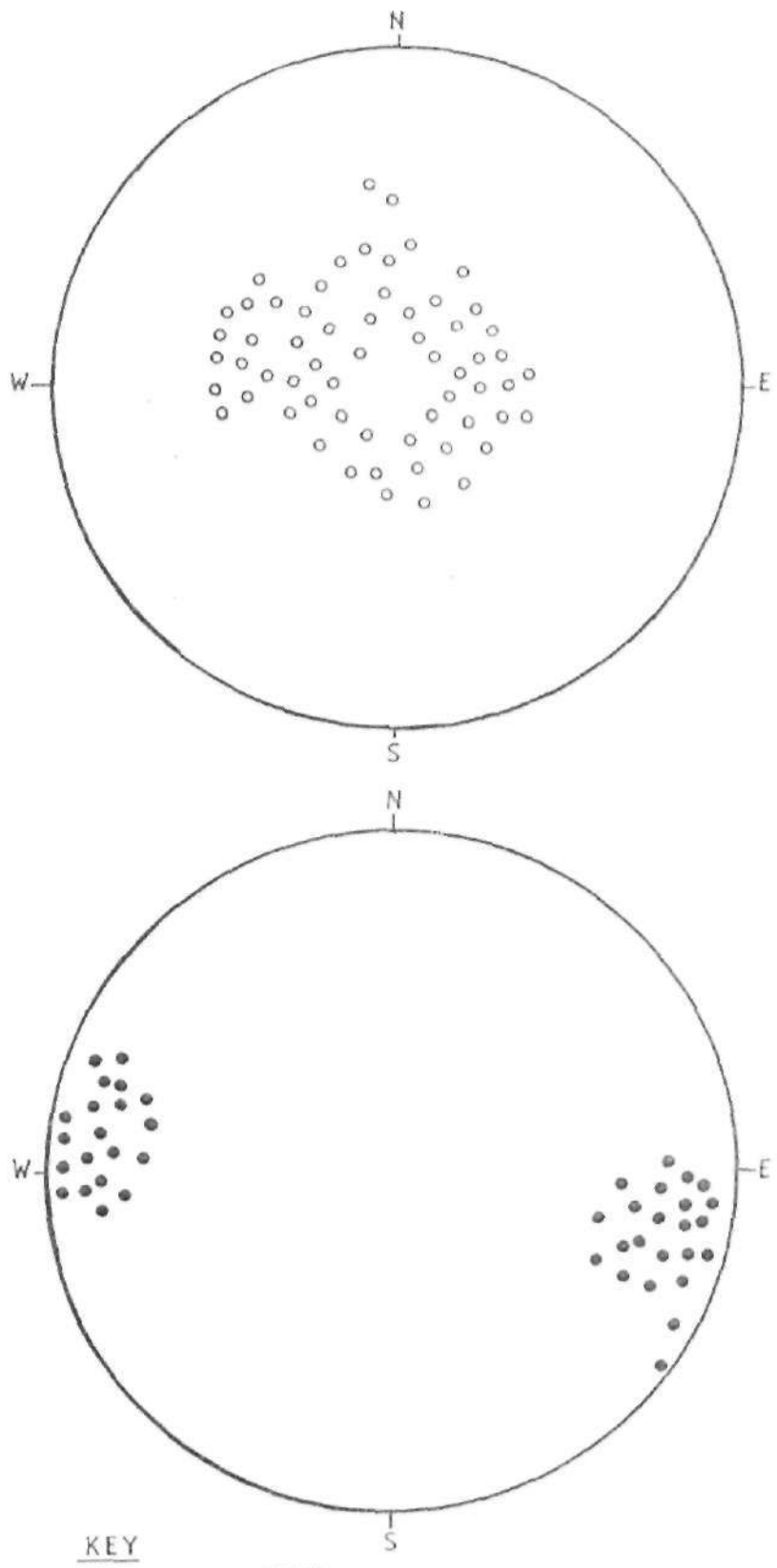


Fig. 5.14. Lower hemisphere equal area projection of compiled planar structures. (a) Poles to S_1 foliations showing dome-like structure. (b) Poles to S_2 foliations.

According to Sibson (1977; 1989), shear zones could be subdivided into three parts which include:

i). the seismogenic zone (upper 10 km) where brittle deformation (gouge-breccia) dominates.

ii) the transitional zone (10 - 15 km) with cataclasite.

iii) the third zone occurs at deeper levels where mylonites developed.

The most prominent lineament in the study area, Kalangai Fault System (KFS), is marked by fault breccia, cataclasite and mylonitic rocks (Section 3.6).

5.9.3 Summary of Structural events

As revealed by the similarities in structural styles and symmetry pattern, the documented structures conform to a pattern of recumbent D_1 folds locally refolded by D_2 and affected by granite intrusion and heterogeneous strain related to faulting. The two phases of folding could just be a result of one orogenic episode, with the differences in tectonic styles due to locally varying Pressure-Temperature conditions during the orogeny.

The migmatite-gneiss-feldspathic quartzite basement had probably been deformed before the deposition and earliest deformation event in the metasediments. The records of pre-D_1 deformation and metamorphism in the basement rocks (if any),

are very heavily obliterated and re-oriented by subsequent deformations. Primary sedimentary structures in the area were only observed in the ferruginous quartzites.

The relationship between S_1 and the original bedding and/or cleavage (S_0) is not very clear. However, the S_1 cleavage is observed trending parallel to lithological and compositional boundaries (Plates 5.1), and is presumed to also be parallel to S_0. The foliation being parallel to the lithological boundary also explains the isoclinal folding in the area. L_1 lineations trend N-S with plunge values that vary from nearly horizontal to almost vertical.

D_1 structures are rare, where present their initial orientations cannot be determined with any certainty due to heavy overprinting and obliteration by subsequent events. However, foliations with ENE trends have also been documented, especially near granite contacts. In the absence of field or petrographic evidence for superimposed structures in such places, the ENE trends are interpreted to be the result of re-orientation of earlier fabrics by the granite intrusion.

The said intrusions could have rotated the original orientations of early schistosities and fold axial surfaces from their previous N-S/NNE-SSW trends into ENE trends, in the area mapped by McCurry (1971; 1976). It is pertinent to note

that McCurry (1971) has also made similar deductions in NW of Sheet 78 where she interpreted ENE- foliation trends in migmatites to be due to deflection by late emplacement of adjacent granite bodies.

The D_1 event may have only involved flexural shear with considerable flattening processes during the formation of F_1 folds. Only S-pole girdle is apparent on the phi-diagram for the area because of the cylindrical nature of the folding. The well developed axial plane cleavages and cylindrical nature of most of the F_2 folds suggest simple flexural shear mechanisms superimposed on the folded rocks during the D_2 folding.

The F_1 and F_2 foldings are responsible for the linear NNE to N regional strikes in the study area. They could represent regional strains due to complex fold interference patterns. This relationship is common in poly-deformed Precambrian terranes (Turner and Weiss, 1963; Hobbs, et al., 1976; Shackleton, 1976). The recognition of two phases of deformation in the Kazaure Belt constitutes a significant departure from the generally accepted idea of gentle folding of the belt (Turner and Webb, 1974; Grant, 1978).

The presence of early flat-lying structures in the Kazaure belt and part of the Malumfashi belt not mapped by McCurry (1971; 1976) has provided evidence to support McCurry's

contention that early flat-lying fabrics probably occur in areas adjacent to the Malumfashi belt. The present study has revealed no evidence for a major tectonic distinction between the Kazaure belt and the presently mapped northernmost portion of the Malumfashi belt and its southern portion studied by McCurry (1971; 1973; 1976).

The overall tectono-metamorphic similarities established for the Kazaure and Malumfashi belt in the present study is reflected in the virtually similar structural and metamorphic events in the two areas. In view of their close proximity, the belts may have been the same basin before the Pan-African plutonism (notwithstanding the intervening rocks).

CHAPTER SIX:

GEOCHEMISTRY AND GEOCHRONOLOGY

6.1 INTRODUCTION

Different workers (like Chikhaoui et al., 1980; Bertrand et al., 1984; Ekwueme, 1985) have undertaken in each case a systematic approach while studying polydeformed and polymetamorphosed terrains. Such studies involved structural and geochronological analyses, as well as geochemical analysis for the major, trace and rare earth elements (REE) of rocks in the terrains. These are in turn used as guides in interpreting the ancient tectonic environments of such terrains. Such a systematic approach is hereby employed in the study of the Kazaure Schist Belt.

Twelve specimens of the metasediments, five of the metavolcanics and Eighteen specimens of the granite, were prepared for whole-rock geochemical analyses. All of the metasediments and granites specimens were analysed for major and trace elements, while the metavolcanic specimens were only analysed for major elements. In addition, the six samples of the mica schists have been analyzed for ten rare earth elements (REE).

The whole-rock geochemical data from the thirty five representative rock samples above were used to classify them in terms of origin and geotectonic setting. The geochemical characterisation also involved documenting the differences in their bulk compositions, as well as speculating the nature of the protolith of the metamorphic rocks, where possible. The geochronological analysis was carried out on five whole-rock samples of granitoids intruding the Kazaure belt near Kazaure at the Dam Area, where the rocks are exposed at quarries (Maps 1 and 2).

6.2 GEOCHEMISTRY OF METASEDIMENTS

Six representative specimens each of the quartzites and mica schist were also analysed and the major and trace elements characterised. Geochemical discrimination between the mica schists and the quartzites is easily achieved, in spite of the uncertainities inherent in their field relationships.

6.2.1 Major Elements

The quartzites contain the highest values of SiO_2 and lowest values of TiO_2, Al_2O_3, total iron and MgO, with the exception of the two ferruginous quartzite samples (Tables 6.1 and 6.2). A systematic decreasing trend of total iron with decrease of total alkalis is noticeable as you move from the mica schist to the quartzites. An exception is in the total iron contents (48.59 and 44.53 weight %) in the two ferruginous quartzite

Table 6.1- Chemical (weight percent) and trace element (parts per million) composition of the Mica Schist from the Kazaure Schist Belt area.

Sample No.	UD10	UD36	UD48	UD57	UD59	UD60
Laboratory No.	DA20	DA21	DA22	DA23	DA24	DA25
CHEMICAL COMPOSITION (weight percent)						
SiO_2	71.00	69.20	64.20	67.04	62.07	65.85
TiO_2	1.08	1.34	1.22	0.80	1.07	0.92
Al_2O_3	11.42	13.59	18.98	16.07	17.05	15.48
$(Fe_2O_3)T$	7.50	5.49	6.59	4.53	6.49	4.89
MnO	0.06	0.16	0.17	0.18	0.33	0.07
MgO	1.92	2.38	1.30	2.37	2.83	3.30
CaO	1.07	1.09	1.09	2.09	1.83	2.73
Na_2O	2.72	1.69	1.57	2.02	1.69	2.57
K_2O	2.86	3.40	2.89	2.72	3.81	2.89
P_2O_5	0.22	0.20	0.26	0.23	0.26	0.27
LOI	1.16	1.44	1.59	2.16	1.69	0.79
Total	100.01	99.98	98.86	100.21	99.92	99.76
TRACE ELEMENT COMPOSITION (ppm)						
Nb	121	109	74	89	53	119
Zr	205	218	212	115	138	129
Y	15	11	14	25	24	26
Sr	221	234	288	258	238	277
U	22	44	54	78	62	89
Rb	256	230	271	196	189	111
Th	116	115	108	126	128	127
Pb	12	14	22	27	22	26
Ga	24	29	28	102	106	111

$(Fe_2O_3)T$ = total FeO + Fe_2O_3.

Description of Samples (Maps 1 and 2):

UD10: Quartz mica schist from Makadi forest reserve.
UD36: Quartz mica shist, from W of Gora.
UD48: Mica schist intercalated with quartzite, Dutsin Kiye forest reserve, about 5 km NE of Kazaure.
UD57: Mica schist outcrops, slightly weathered, Unqwan Kaya.
UD59: Mica schist from SE of Kazaure. Intruded by granite in the west and intercalated with schistose quartzites in the SE.
UD60: Quartz mica schist from about 6 km W of Saye.

Table 6.2- Chemical (weight percent)and trace element (parts per million) composition of the Quartzite from the Kazaure Schist Belt area.

Sample No.	UD26	UD40	UD72	UD81	UD62	UD65
Laboratory No.	DA26	DA27	DA28	DA29	DA30	DA31
CHEMICAL COMPOSITION (weight percent)						
SiO_2	89.44	81.99	41.20	44.04	84.90	86.85
TiO_2	0.08	0.34	0.22	0.26	0.07	0.29
Al_2O_3	4.42	9.50	5.98	6.07	8.05	6.26
$(Fe_2O_3)T$	1.50	1.49	48.59	44.53	0.49	0.99
MnO	0.16	0.06	0.07	0.18	0.33	0.27
MgO	0.39	1.58	0.30	0.37	1.33	0.48
CaO	0.27	0.69	0.20	0.32	0.83	0.73
Na_2O	0.72	1.20	0.57	0.62	0.69	0.79
K_2O	2.42	2.10	2.19	2.22	2.31	2.49
P_2O_5	0.02	0.06	0.06	0.23	0.26	0.07
LOI	0.16	0.46	0.59	1.16	0.69	0.79
Total	99.58	99.41	99.97	100.00	99.95	99.91
TRACE ELEMENT COMPOSITION (ppm)						
Nb	11	9	4	9	5	11
Zr	105	108	112	115	118	119
Y	15	11	14	21	24	26
Sr	132	147	206	198	138	135
U	22	44	56	18	22	39
Rb	56	30	71	76	89	91
Th	116	115	108	116	118	120
Pb	12	14	11	17	22	20
Ga	24	29	28	32	36	31

$(Fe_2O_3)T$ = total FeO + Fe_2O_3.

Description of Samples (Maps 1 and 2):

UD26: Massive quartzite, SE of Amaryawa.
UD40: Schistose quartzite ridge alon the road to Wawanrafi.
UD72: Ferruginous quartzite ridge, 2 km NW of Kunchi.
UD81: Ferruginous quartzite, 2 km SE of Matanfad.
UD62: Medium grained quartzite 4 km north of Bichi.
UD65: Massive quartzite ridge, 3 km E of Malikawan Sarari.

KASHIM IBR

samples. The mica schist samples are lowest in SiO_2 but have the highest CaO content of all the metasediments. Compared with the quartzite, the mica schist samples have higher Al_2O_3, K_2O, and Na_2O. However, all the analysed metasediments of the KSB area are rich in alumina and their potash content is in excess of that of soda. Further more, MgO is in excess of CaO in these metasediments, possibly indicating the carbonate-free nature of their parent rock (e.g Ekwueme and Onyeagocha, 1986).

6.2.2 Trace Elements

As for the trace elements, apart from the mica schist samples which have the highest Strontium contents among the metasediments, there is a general decrease in Sr with increasing SiO_2. Rubidium, Zirconium and Lead increase to a maximum at the composition of the mica schists, then decrease in a fairly regular fashion to the fine to medium grained and massive quartzite varieties.

All other trace elements [Ybtrium, Niobium, and Uranium] decrease fairly regularly/or have virtually identical values. Sample UD 52 has the lowest contents of Pb (11 ppm) and Nb (4 ppm) in the quartzites, but has the highest U (56 ppm) content. It is noteworthy that there is an enhancement of the U content in the metasediments relative to its 0 ppm value in the granitoids (Tables 6.4, 6.5 and 6.6).

In addition to the field and petrographic evidence as to the nature of the metasediments, geochemical criteria will also be considered. Several workers have used discrimination diagrams based on few elements or computed parameters to indicate the protolith of rocks. For example, on an ACF diagram (Fig. 6.1), all the metasediments specimens plot in the metamorphic rocks fields of shale-greywacke (Miyashiro, 1973). In addition, the SiO_2 and TiO_2 composition of the quartzite and mica schist specimens were plotted in TiO_2-SiO_2 discrimination diagram after Tarney (1977). In this diagram, (Fig. 6.2), a clear sedimentary origin was also deduced for the metasediments.

Pettijohn (1957) noted that there is abundance of alumina and potash is generally in excess of soda in an average composition of shale. These features are indicated in the KSB metasediments and as such this is a further evidence the rocks falls within the range of analysed shales (e.g Middleton, 1960; Butler, 1965).

Electron microprobe analyses of garnet from the ferruginous quartzite occurrence at Kazaure was also undertaken (Table 6.3). The garnet was found to have end-member composition of spesssartine (Mn rich), pyrope (Mg rich) and almandine (Deer et al., 1966). A Ca rich (andradite) garnet was also identified. The high Fe^{3+} in the andradite probably explain the strong magnetic nature of some of the samples.



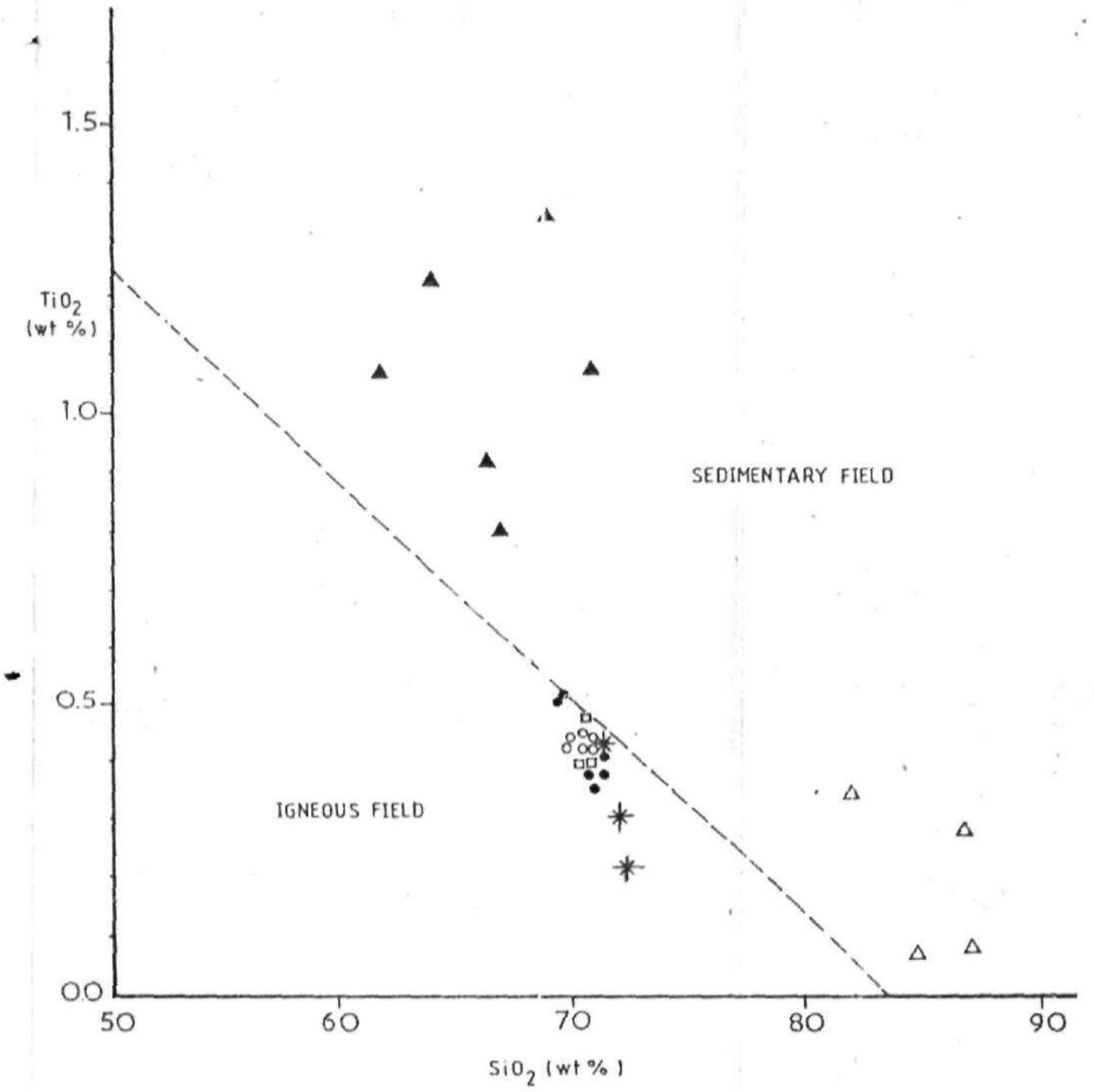


Fig.6.2. TiO_2 versus SiO_2 discrimination diagram (after Tarney, 1977). Dashed line separates sedimentary from igneous rocks.

Symbols

- ● Medium grained granite
- ○ Porphyritic granite
- △ Quartzites
- □ Granodiorite
- ✳ Hornblende granite
- △ Mica schist

Table 6.3- Chemical composition (weight percent)of Garnet from the BIF at Kazaure.

Mineral Type	Andradite	Spessartine	Pyrope	Andradite
Sample No.	UD240	UD240	UD240	UD240
Laboratory No.	DA19	DA19	DA19	DA19
SiO_2	35.52	36.10	43.03	38.15
TiO	-	0.19	0.47	0.15
Al_2O_3	0.00	21.39	20.37	0.00
Fe_2O_3	29.19	-	-	26.23
FeO	-	1.76	8.35	-
MnO	0.32	40.00	0.00	0.31
MgO	0.52	0.47	21.06	0.45
CaO	34.46	0.08	4.80	33.76
Cr_2O_3	0.00	0.00	1.93	0.94
Total	100.00	100.00	100.00	100.00

Description of Sample (Map 1)

UD240: Garnet from within a farmland 1 km off Kazaure-Roni road, near a laterite quarry.

6.2.2.1 Rare Earth Elements (REE)

a) Background

Ten rare earth elements (REE) abundances in three Kazaure mica schists whole rock specimens were determined using the inductively coupled plasma atomic emission spectrometry (ICP-AES, see Appendix A). This was also done in the McGill University Geochemical Laboratory. The REE distribution in these Kazaure mica schists are given in Table 6.4.

All the REE abundances were normalized after Taylor and McLennan (1995), and then plotted in Fig. 6.3. The REE in the schists were studied in order to understand the protolith rock type and the character of the source area (e.g Ekwueme, 1994b).

b) Deductions from the REE distribution pattern

All the samples have REE concentrations that are slightly enriched with respect to chondritic abundances (about 1-30 X). Their chondrite-normalized plotted distribution patterns are smooth curves of decreasing relative abundances towards the heavy lanthanides (Fig. 6.3). A specific aspect best illustrated is the high La_N/Sm_N and low Gd_N/Lu_N ratios of the mica schists, ranging from 2.57 to 2.80, and from 1.20 to 127, respectively. This indicates the predominance of light REE over heavy ones in the Kazaure mica schists.

Table 6.4 - Rare earth element (REE) contents in mica schists from the Kazaure belt

Sample No.	UD10	UD36	UD59	UD60
Laboratory No.	DA20	DA21	DA24	DA25
	RARE EARTH ELEMENT COMPOSITION (ppm)			
La	18.37	24.21	29.43	17.45
Ce	45.15	49.20	53.31	43.91
Nd	23.24	25.44	26.83	22.81
Sm	4.31	5.13	6.34	4.32
Eu	0.93	0.99	1.06	0.89
Gd	3.96	4.59	4.14	3.74
Dy	4.23	4.56	4.67	3.93
Er	2.39	2.63	3.04	2.23
Yb	1.57	1.67	1.82	1.52
Lu	0.37	0.43	0.41	0.36
TOTAL REE (Σ)	104.5	123.0	126.9	108.8?
	CHONDRITE- NORMALISED			
La	55.5	73.1	88.9	52.7
Ce	51.9	56.6	61.3	50.5
Nd	37.0	40.4	42.6	35.1
Sm	21.6	25.7	31.7	21.6
Eu	11.8	12.6	13.5	11.4
*Gd	14.5	16.6	15.1	13.7
Dy	12.6	13.6	13.9	11.7
Er	10.4	11.5	13.3	9.7
Yb	7.0	7.5	8.2	6.8
Lu	11.2	13.0	12.4	11.0
Σ	234.0	276.0	296.8	227.6
La_N/Sm_N	2.57	2.84	2.80	2.44
Gd_N/Lu_N	1.27	1.27	1.20	1.25
Eu^*	17.00	20.00	23.00	17.00
Eu/Eu^*	0.69	0.63	0.59	0.67

N = Chondrite normalized concentrations.

Eu^* = Eu concentration obtained by a straight line interpolation between the concentrations of Sm and Gd.

Average chondrite values were taken from Haskin et al. (1968).

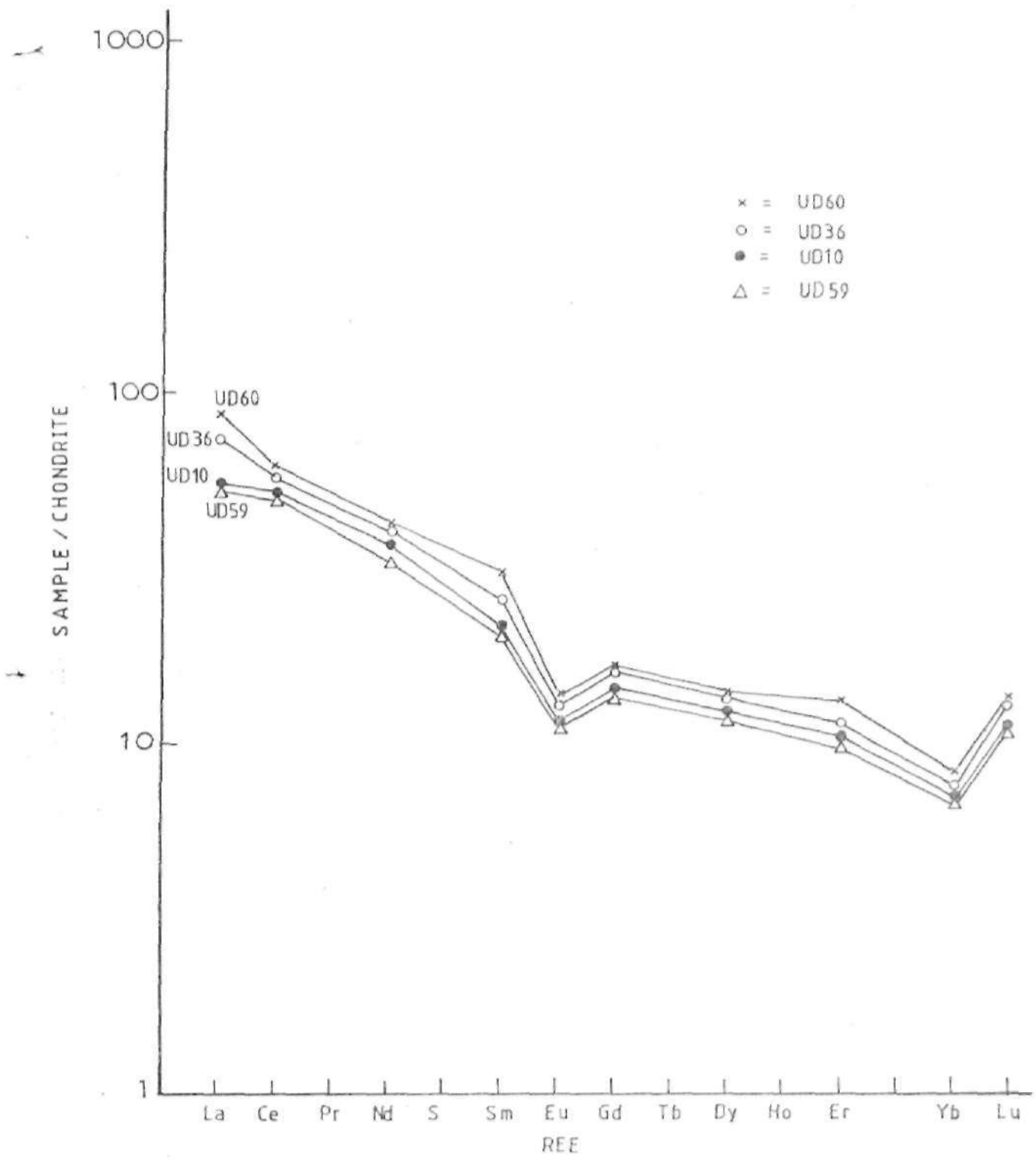


Fig. 6.3. Chondrite-normalized REE distribution patterns in four Kazaure mica schist samples.

In other words, the curves have a steep to moderate REE trend showing strong relative depletion of the heavy REE (HREE) relative to light REE (LREE). All the Kazaure specimens have small negative Eu anomalies (Eu/Eu^{*} values of 0.69, 0.63, 0.59 and 0.67 respectively), indicating Eu depletion in the younger metasediments.

The curves of normalized REE contents themselves are similar to that of post-Archaean shales known from throughout the world (Haskin et al., 1966; Martin and Meyneck, 1979; Taylor and McLennan, 1985). All post-Archaean clastic sedimentary rocks (of shale composition) have a negative Eu anomaly (with $Eu/Eu^{*} = 0.66$), which is the average composition of the Upper Crust (Taylor and McLennan, 1985).

By comparison, Taylor and McLennan (1985) believed a lack of an Eu-anomaly ($Eu/Eu^{*} = 1.0$) or the presence of local positive Eu-anomaly indicate Archaean sedimentary rocks. Nance and Taylor (1977) on the other hand, attributed the negative Eu-anomaly in the post-Archaean clastic sedimentary rocks to detrital sources, during/throughout the formation of Eu depleted feldspar granites, after its formation by chemical fractionation.

The near equivalence of the REE pattern in both the Kazaure phyllites and post-Archaean sedimentary rocks is important for

understanding the genesis of the Kazaure phyllites. The comparable Eu/Eu^{*} values between the mica schists and that of the upper crust, suggests the rocks were derived from similar source area with typical clay sediments. On the basis of the above REE geochemical parameter, one can also conclude that the younger metasediments are metamorphosed shale-greywacke sequence derived from the upper crust where acid magmatic rocks are dominant (Martin and Meyneck, 1979).

6.3 GEOCHEMISTRY OF METAVOLCANICS

Whole-rock geochemical analyses of major elements in the metavolcanics are presented in Table 6.5. They have a composition that lies within and around dacite-rhyolite (Fig. 6.4). The rhyolites form both the high-silica (>75% SiO_2) and a low-silica (71-75% SiO_2) group. The high-silica group contains lower contents of all oxides except SiO_2. It seems that the high silica rhyolite is leached of mobile oxides and therefore enriched in SiO_2 relative to the low silica rhyolite which has a `normal' rhyolite composition. TiO_2 values tend to confirm this, as it is a relatively immobile oxide.

The approximately high contents of K_2O (mean 4.9%) as compared to that of Na_2O (mean 3.3%), suggest the possibility of hydrothermal alteration processes in all the samples (Irvine and Baragar, 1971). Fe_2O_3 (total) vary randomly in both the low and high silica rhyolite.

Table 6.5- Chemical composition (weight percent) of the Metavolcanic rocks.

Rock type:	High-silica rhyolite			Low-silica rhyolite	
Sample No.	UD110	UD113	UD115	UD117	UD119
Laboratory No.	DA32	DA33	DA34	DA35	DA36
	CHEMICAL COMPOSITION (weight percent)				
SiO_2	76.64	74.11	75.45	71.24	69.84
Al_2O_3	12.60	13.64	13.23	14.12	14.16
$(Fe_2O_3)T$	2.42	2.26	2.13	2.60	2.54
MgO	0.12	0.15	0.12	0.46	0.56
CaO	0.09	0.12	0.10	0.32	1.11
Na_2O	3.03	3.78	3.58	3.91	3.99
K_2O	4.18	4.61	4.38	5.28	5.66
TiO_2	0.37	0.38	0.39	0.40	0.40
P_2O_5	0.05	0.02	0.05	0.13	0.20
MnO	0.10	0.08	0.12	0.37	0.41
LOI	0.24	0.28	0.26	0.43	1.05
Total	99.84	99.43	99.65	99.26	99.92

$(Fe_2O_3)T$ = total FeO + Fe_2O_3.

Description of Samples:

UD110: Outcrops SE of Ganji.
UD113: West of Dunawa.
UD115: From within Makoda.
UD117: NE of Makoda.

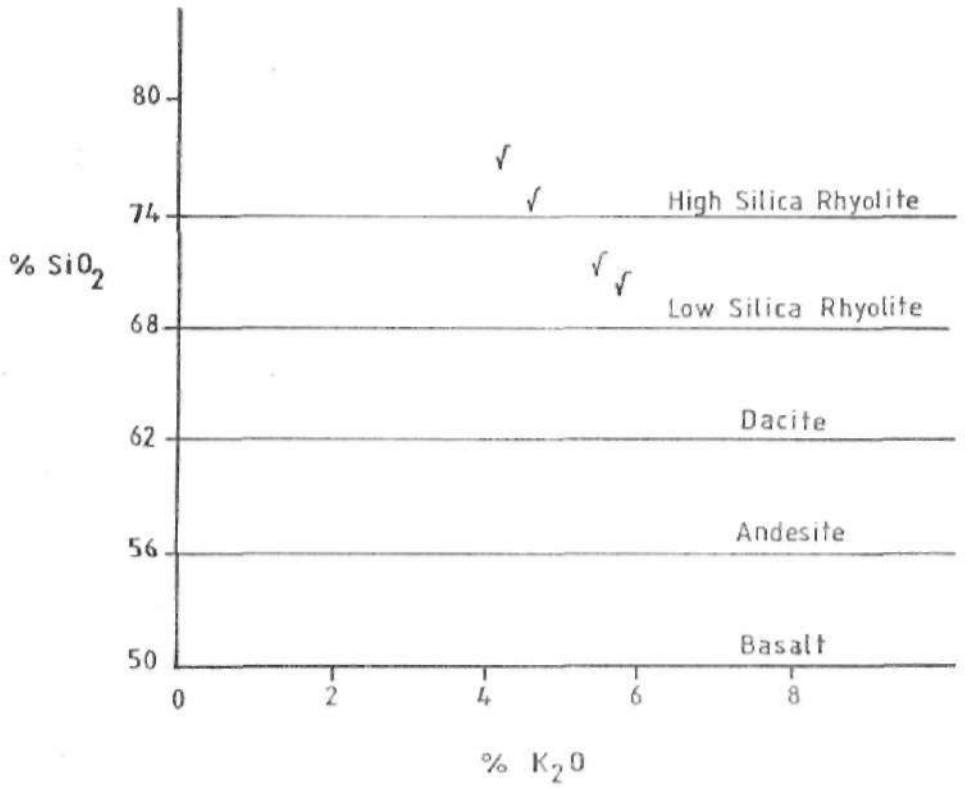


Fig.6.4. $SiO_2 - K_2O$ diagram of Kazaure metavolcanics (Classification after Taylor, 1969).

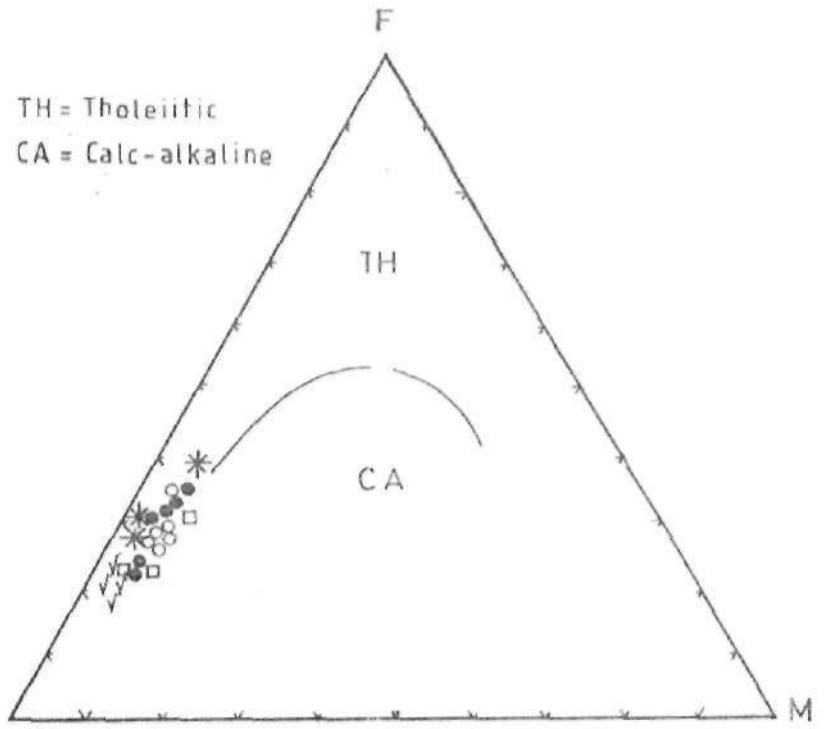
However, P_2O_5 and MnO in all the analysed metavolcanic samples lie in the range of 0.02 to 0.41. Furthermore, the metavolcanics follow a calc-alkaline trend on an AFM diagram (Fig. 6.5). Data for the major elements in the four analysed metavolcanics samples fall within the range reported by other workers (McCurry and Wright, 1977).

6.4 GEOCHEMISTRY OF THE GRANITES

6.4.1 Major Elements

The major element data and CIPW norms from the Kazaure granitoids are presented in Tables 6.6, 6.7 and 6.8. The CIPW norms were calculated from the geochemical data obtained on the granitoids. Their normative felsic compositions were plotted on the conventional Q-Or-Ab projection (Tuttle and Bowen, 1958). This has revealed the geochemical range of the granitic rocks, as well as their broad classification.

The granites show a slightly small range of variations in their SiO_2 content (69.76-72.03 weight-percent), with high alkali-oxide content ($Na_2O + K_2O > 7$ weight-percent), high Na_2O content >3.2 weight-percert, low CaO and MgO with subordinate Fe_2O_3 (total). The very low ratio of MgO to ($FeO + Fe_2O_3$) in the bulk composition of the granites (0.09-0.30) suggests that the rocks are enriched in iron.



A = Na_2O + K_2O ; F = Total Fe as Fe_2O_3 ; M = MgO

√ Metavolcanics

Fig. 6.5. AFM diagram showing compositional variation of the granitic and metavolcanics rocks. Boundary between tholeiitic and calc-alkaline fields after Irvine and Baragar (1971). Symbols as in fig. 6.2.

Table 6.6- Major chemical (weight percent) and normative composition of the porphyritic Granite.

Sample No.	UD39	UD60	UD66	UD67	UD68	UD69
Laboratory No.	DA01	DA02	DA03	DA04	DA05	DA06
CHEMICAL COMPOSITION (weight percent)						
SiO_2	71.04	70.18	70.02	70.88	70.85	71.13
TiO_2	0.44	0.44	0.42	0.44	0.43	0.45
Al_2O_3	14.62	14.49	14.77	14.52	14.31	14.42
$(Fe_2O_3)T$	3.56	3.66	3.21	3.31	3.31	3.49
MnO	0.06	0.06	0.05	0.05	0.05	0.07
MgO	0.47	0.49	0.44	0.46	0.46	0.43
CaO	1.79	1.80	1.80	1.78	1.76	1.71
Na_2O	3.22	3.22	3.28	3.20	3.23	3.24
K_2O	5.02	5.03	5.19	5.08	5.18	5.13
LOI	0.38	0.38	0.40	0.39	0.39	0.39
P_2O_5	0.12	0.13	0.12	0.11	0.11	0.16
Total	100.72	99.88	99.70	100.22	100.08	100.60
NORMATIVE COMPOSITION						
ap	0.27	0.29	0.27	0.24	0.24	0.36
il	0.13	0.13	0.11	0.11	0.11	0.15
or	30.05	30.07	31.01	30.36	30.86	30.72
ab	27.60	27.58	28.07	27.39	27.56	27.79
an	8.20	8.18	8.24	8.21	8.08	7.54
hy	0.78	0.81	0.73	0.76	0.76	0.71
q	29.31	28.85	27.24	29.00	28.36	29.30
hm	3.62	3.71	3.26	3.36	3.35	3.53
ru	0.38	0.38	0.37	0.39	0.38	0.38
q + ab + or	95.16	94.68	94.56	94.96	94.86	95.35

$(Fe_2O_3)T$ = total FeO + Fe_2O_3.

Description of Samples (Maps 1 and 2):

UD 39: Porphyritic granite, from a rock quarry, Kazaure Dam area.
UD 60: Porphyritic Granite, 5 km SW of Ladan (near fault).
UD 66: Porphyritic granite, south of Malikawan Sarari.
UD 67: Porphyritic granite in a dome shaped outcrop surronded by the tributaries of River Kunchi.
UD 68: Porphyritic granite, 3 km north of Ladan.
UD 69: Coarse grained porphyritic granite, from a whaleback 1.5 km SW of Ladan.

Table 6.7- Major chemical (weight percent) and normative composition of the fine to medium grained Granite.

Sample No.	UD54	UD55	UD62	UD63	UD64	UD65
Laboratory No.	DA07	DA08	DA09	DA10	DA11	DA12
CHEMICAL COMPOSITION (weight percent)						
SiO_2	71.50	69.98	69.81	71.41	71.37	71.07
TiO_2	0.41	0.50	0.51	0.38	0.23	0.35
Al_2O_3	14.36	14.79	14.71	14.33	14.13	14.25
$(Fe_2O_3)T$	2.48	2.76	2.83	2.52	3.01	2.48
MnO	0.14	0.07	0.25	0.03	0.35	0.09
MgO	0.37	0.47	0.52	0.45	0.43	0.49
CaO	2.34	2.71	2.70	2.61	2.36	2.73
Na_2O	3.71	3.25	3.23	3.41	3.43	3.37
K_2O	4.40	4.93	4.88	4.32	4.17	4.71
LOI	0.22	0.38	0.36	0.34	0.32	0.32
P_2O_5	0.09	0.07	0.20	0.15	0.21	0.18
Total	100.01	99.91	100.00	99.95	100.01	100.04
NORMATIVE COMPOSITION						
ap	0.20	0.16	0.37	0.31	0.47	0.40
il	0.31	0.07	0.06	0.76	0.45	0.20
or	26.41	29.58	28.95	25.61	25.23	28.19
ab	31.89	27.93	27.80	29.31	29.72	28.89
an	6.16	8.15	8.85	7.39	5.50	7.50
di	0.00	0.00	0.00	0.00	0.00	0.00
hy	0.62	0.28	0.65	0.55	0.72	0.81
q	30.42	28.51	28.26	33.63	33.32	29.93
mt	3.55	3.83	3.32	2.32	3.78	3.45
ru	0.26	0.51	0.39	0.38	0.00	0.25
tn	0.00	0.00	0.00	0.00	0.00	1.38
wo	0.00	0.00	0.00	0.12	0.00	0.20
q + ab + an + or	94.88	94.17	92.86	95.94	93.77	94.51

$(Fe_2O_3)T$ = total FeO + Fe_2O_3.

Description of Samples (Maps 1 and 2):

UD54: Fine-grained granite, SW of Dara.
UD55: Coarse-medium grained Granite, from SE of Matalawa.
UD62: Fine-grained granite, north of Tinki.
UD63: Medium-grained granite, along stream south of Dansure.
UD64: Weakly foliated granite, east of Chiromawa.
UD65: Fine-medium grained granite, north of Gontai.

Table 6.8-Major chemical (weight percent) and normative composition of the hornblende granite and granodiorite.

Sample No.	UD129	UD137	UD139	UD221	UD224	UD227
Laboratory No.	DA13	DA14	DA15	DA16	DA17	DA18
CHEMICAL COMPOSITION (weight percent)						
SiO_2	72.50	71.32	72.23	70.86	70.67	70.59
TiO_2	0.22	0.42	0.35	0.41	0.43	0.49
Al_2O_3	14.16	14.20	14.21	14.03	14.13	14.15
$(Fe_2O_3)T$	2.72	2.60	2.71	2.02	2.41	2.48
MnO	0.11	0.13	0.15	0.23	0.35	0.37
MgO	0.27	0.37	0.46	0.67	0.73	0.69
CaO	2.53	2.51	2.72	2.41	2.56	2.59
Na_2O	3.51	3.70	3.43	3.41	4.07	3.53
K_2O	3.60	3.33	3.18	4.02	4.07	4.01
LOI	0.52	0.38	0.41	0.44	0.46	0.52
P_2O_5	0.19	0.21	0.17	0.48	0.51	0.58
Total	100.33	100.17	100.22	100.58	100.09	100.00
NORMATIVE COMPOSITION						
ap	0.31	0.31	0.27	1.06	1.24	1.24
il	0.46	0.76	0.33	0.25	1.06	0.91
or	20.04	19.48	19.39	23.72	23.95	23.94
ab	29.90	31.21	31.95	27.80	29.90	30.42
an	11.76	11.62	7.96	11.09	8.90	9.46
di	0.35	0.45	0.00	0.64	0.90	0.85
hy	0.35	0.45	0.77	0.93	0.90	0.85
q	33.02	32.21	35.68	28.49	29.68	29.17
mt	3.55	3.20	3.26	3.03	2.55	2.32
ru	0.26	0.31	0.39	0.38	0.00	0.22
tn	0.00	0.00	0.00	0.00	0.00	0.00
wo	0.00	0.00	0.00	0.00	0.00	0.00
q + ab + an + or	94.72	94.52	94.98	91.10	92.43	92.99

$(Fe_2O_3)T$ = total FeO + Fe_2O_3.

Description of Samples (Maps 1 and 2):

UD129: Hornblende granite, 3 km N of Birkin.
UD137: Coarse-medium grained hornblende granite, W of Birkin.
UD139: Coarse-grained hornblende granite, south of Kunchi.
UD220: Massive and porphyritic granodiorite within southern edge of Ladan.
UD224: Weakly foliated granodiorite NW of Dan Ashitari.
UD227: Fine-medium grained granodiorite S of Takwurdawa.

All the granitic samples plot in the granodiorite and granite fields (Fig. 6.6). Normative diopside appears in only one of the analysed granite sample (UD410), with a value of 0.64. Alteration processes might be responsible for the observed range of K_2O contents (from 3.18 to 5.19 weight-percent) in all the granite samples. The granites contain between 7.60 and 8.47 weight-percent $Na_2O + K_2O$, but this percentage in the hornblende granite is between 6.61 and 6.90. The difference could be ascribed to the higher alkali feldspar content of the porphyritic granites compared to the higher plagioclase content of the hornblende granite.

The granitoids mainly cluster in the granodiorite field with only one sample in the adamellite field (Fig. 6.7). On an AFM diagram (Fig. 6.5), the Kazaure granite follow a calc-alkaline trend which is similar to typical calc-alkaline trends shown by other Pan-African granitic rocks in northwestern Nigeria (e.g Fitches et al., 1985). However, on an alumina saturation diagram (Fig 6.8), the $Al_2O_3/(CaO + Na_2O + K_2O)$ molar ratios (A/CNK, Shand Index) does not exceed 1.6, indicating the slightly peraluminous tendencies of the studied granitoid rocks.

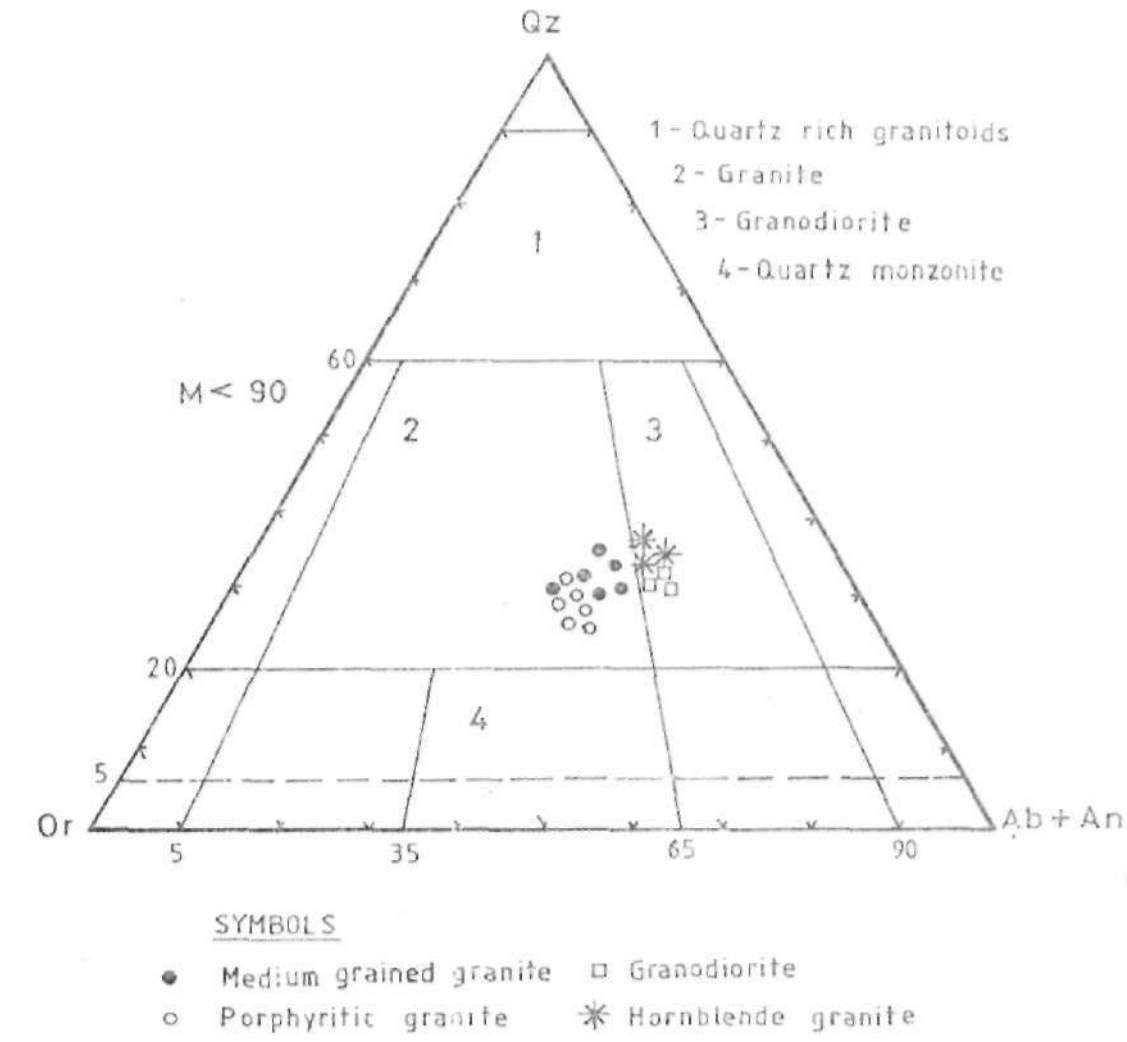


Fig. 6.6. The field of the Kazaure granitoids in a CIPW normative Qz-Or-Ab+An triangular diagram. The composition fields are named as in the QAP triangle of Streickeisen (1976).

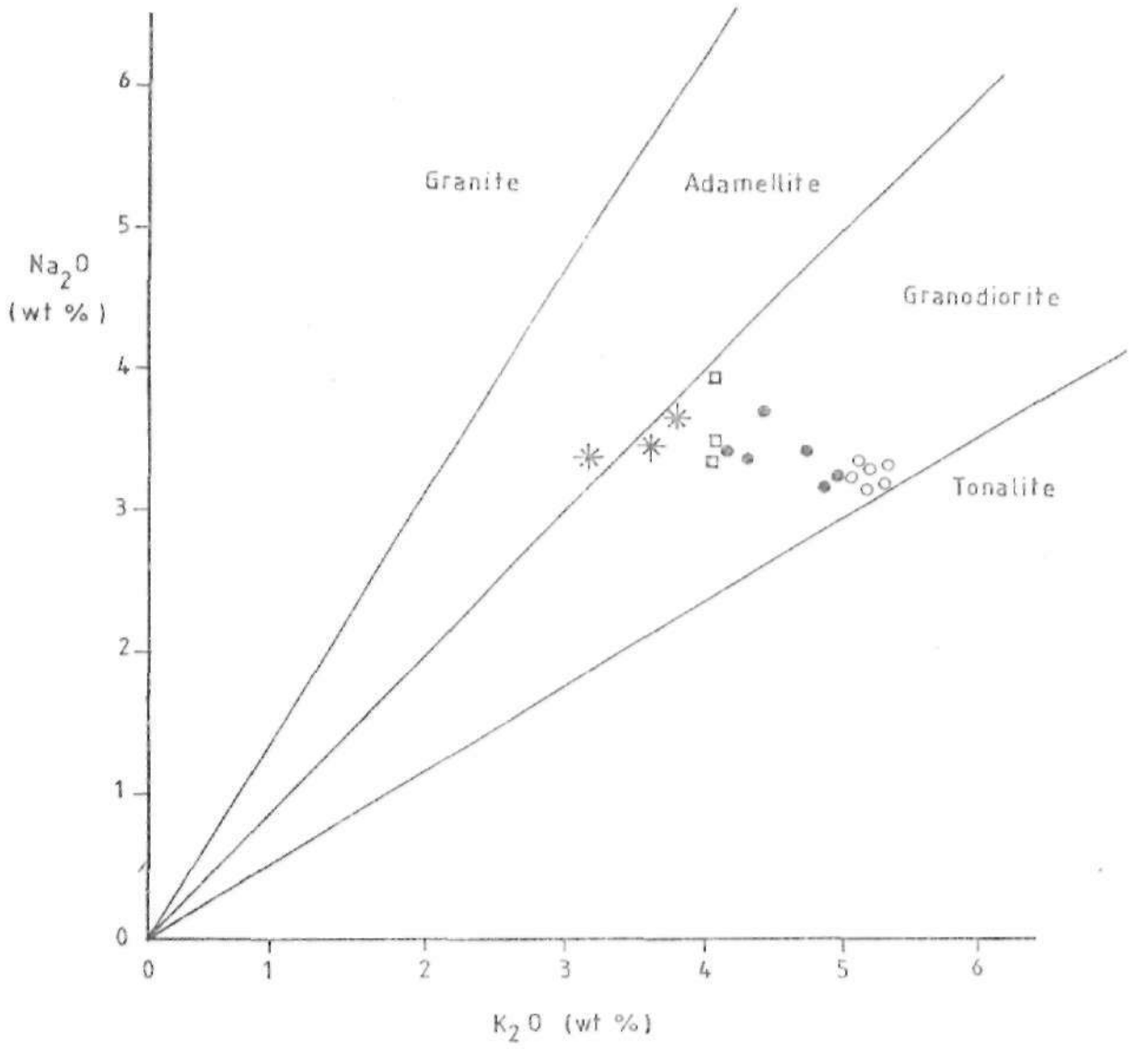
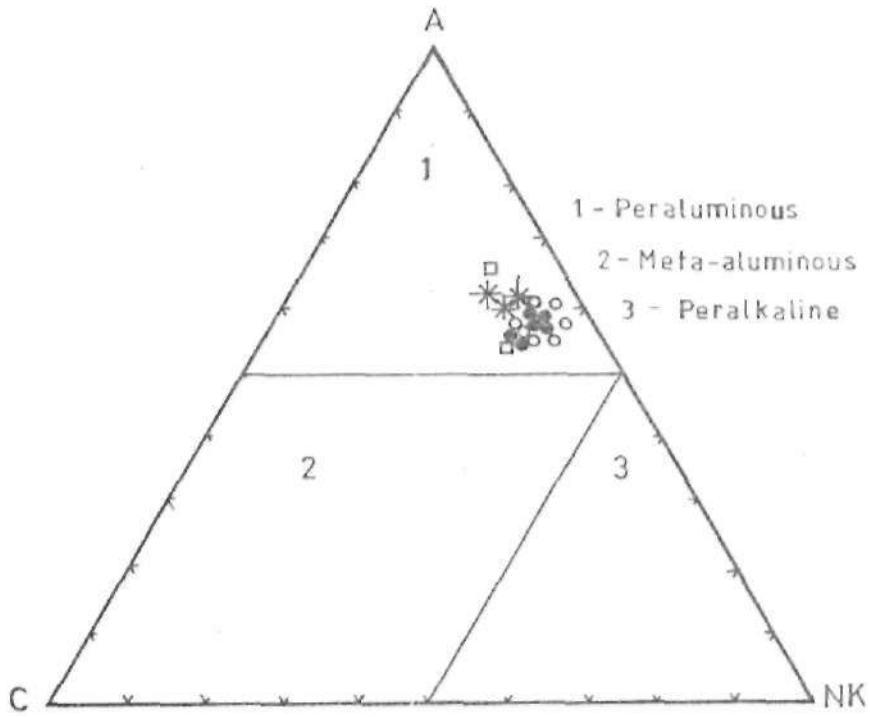


Fig 6.7. Chemical classification of Kazaure plutonic rocks based on alkali contents (after Harpum, 1963). Symbols as in Fig. 6.2



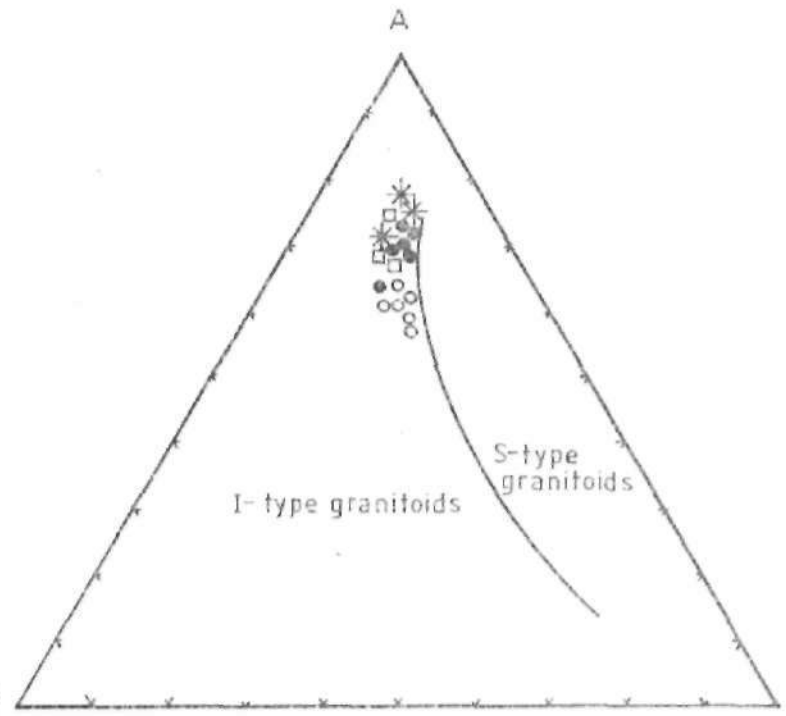
$A = Al_2O_3$; $C = CaO$; $NK = Na_2O + K_2O$

Fig. 6.8. An A/CNK (Shand Index) diagram showing the Peraluminous nature of the granitoids. Classification is based on Shand (1927). Symbols as in fig. 6.2.

Calc-alkaline orogenic granitoids have been geochemically classified into I-type and S-type granitoids. These granitoids are regarded as products of partial melting of crustal materials, either of igneous (I) origin or (S) sedimentary origin. For this, the Shand Index may also help to differentiate between granitoids derived from S-type and I-type sources (Chappell and White, 1974). It is a crude indicator of the S-type component involved in the generation of anatectic granite melts.

A Shand index of < 2 suggests the granitoids to be I-type. The Kazaure granitoids also plot in the field of I-type on an ACF classification diagram (Fig. 6.9) according to Hine et al., (1978). Similarly, Tarney (1977) presented a SiO_2 versus TiO_2 discrimination diagram in which the compositional fields of sedimentary and igneous rocks are outlined (Fig. 6.2). In this diagram, a clear igneous origin is inferred for the granitoids.

The CIPW normative compositions have shown that two samples of the granite, UD210 and UD213, are slightly calcic and are characterised by the appearance of normative wollastonite. In addition, the UD213 specimen has normative titanium (1.38 weight-percent) in its composition. The absence of normative corundum in all the granitic specimens is an indicator of their igneous parentage (Blacburn, 1974). This also suggests



$A = (Al_2O_3 + Na_2O - K_2O)$; $C = CaO$; $F = FeO + MgO$

Fig 6.9. An ACF diagram showing the I-type character of the Kazaure granitoids. Classification is according to Hine et.al. (1978). Symbols as in fig.6.2.

the absence of significant contamination of the magma by host crustal rocks.

Regional considerations and geochemistry of the granitic rocks in the study area (e.g their high Na_2O content >3.2 weight-percent and low Shand index of < 1.6), all appear to indicate their closely related nature to I-type granitoids. By comparison, the S-type have low content of Na_2O, a high Shand Index > 2.0, and a very strong peraluminous character suggesting heavy contamination by crustal rocks, among others.

6.4.2 Trace Elements

All the granitic samples show a consistent variation of trace element contents (Tables 6.9, 6.10 and 6.11), and some of these could be used in tectonic discrimination diagrams. These are elaborated below.

There is a similarity in the average Zirconium content of 179 ppm for all the granitic specimens when compared with an average of 180 ppm for granitic rocks (Taylor and McLennan, 1985). Niobium values range from 22-29 ppm indicating a distinctive "Arc/or syn-collisional fields" signature (Pearce and Gale 1977). The silica saturated granites were therefore probably formed through syn-collisional processes related to subduction related magmatism.

Table 6.9 - Trace element (parts per million)

chemical composition of the porphyritic Granite.

Sample No.	UD39	UD60	UD66	UD67	UD68	UD69
Laboratory No.	DA01	DA02	DA03	DA04	DA05	DA06
TRACE ELEMENT COMPOSITION (ppm)						
Nb	24	24	22	24	23	24
Zr	203	206	198	185	198	185
Y	51	51	47	55	48	47
Sr	138	140	159	133	133	145
U	0	0	0	0	0	0
Rb	197	329	110	263	166	212
Th	26	25	18	16	18	17
Pb	23	22	22	22	23	24
Ga	20	21	21	20	20	21

Table 6.10- Trace element chemical composition (parts per million) of the fine to medium grained granite.

Sample No.	UD54	UD55	UD62	UD63	UD64	UD65
Laboratory No.	DA07	DA08	DA09	DA10	DA11	DA12
TRACE ELEMENT COMPOSITION (ppm)						
Nb	29	22	29	28	25	27
Zr	135	182	180	139	158	193
Y	48	44	40	47	53	50
Sr	138	142	136	138	138	142
U	0	0	0	0	0	0
Rb	261	262	251	195	262	261
Th	26	14	24	22	37	26
Pb	19	20	19	30	25	19
Ga	20	19	20	19	18	19

Table 6.11- Trace element chemical composition (parts per million) of the hornblende granite and granodiorite.

Sample No.	UD129	UD137	UD139	UD221	UD224	UD227
Laboratory No.	DA13	DA14	DA15	DA16	DA17	DA18
TRACE ELEMENT COMPOSITION (ppm)						
Nb	29	25	28	24	24	26
Zr	155	182	178	159	158	193
Y	42	40	39	47	53	50
Sr	136	137	135	138	140	142
U	0	0	0	0	0	0
Rb	252	208	215	195	183	221
Th	26	24	22	42	47	36
Pb	22	22	24	32	28	29
Ga	21	18	21	19	18	19

The high contents of Strontium (Sr > 133 ppm) and Rubidium (Rb> 85 ppm) indicates that the magma source must have been rich in Sr and Rb. It also indicates the likely crustal origin of the magma and the less efficient removal of these elements by mafic and salic phenocrysts. The syn-collisional nature of Kazaure granitoids was further confirmed on a rubidium-silica diagram (Fig. 6.10), which gives the tectonic classification of granitic rocks after Pearce et al., (1984).

The Kazaure granites have a slight increase in the average concentration of Yttrium (Y > 48 ppm) when compared with an average of 40 ppm Y for granites (Taylor, 1965). This might be due to the differentiation of the granitic melt.

6.5 GEOCHRONOLOGY OF KAZAURE GRANITES

6.5.1 Analytical methods

Absolute ages of the granitic rocks in the Kazaure area were not previously determined, although certain geological arguments suggest that the rocks are of Pan-African age (e.g Ajibade et al., 1997a). In the present work, the age of the granite was determined in the Isotope Laboratory of Universite' de Montreal' using the whole-rock Rb-Sr instrumentation which they share with McGill University. The analytical techniques used are as outlined in Appendix A7. The five reported samples are taken from separate porphyritic granite bodies which formed part of the Kazaure pluton, the

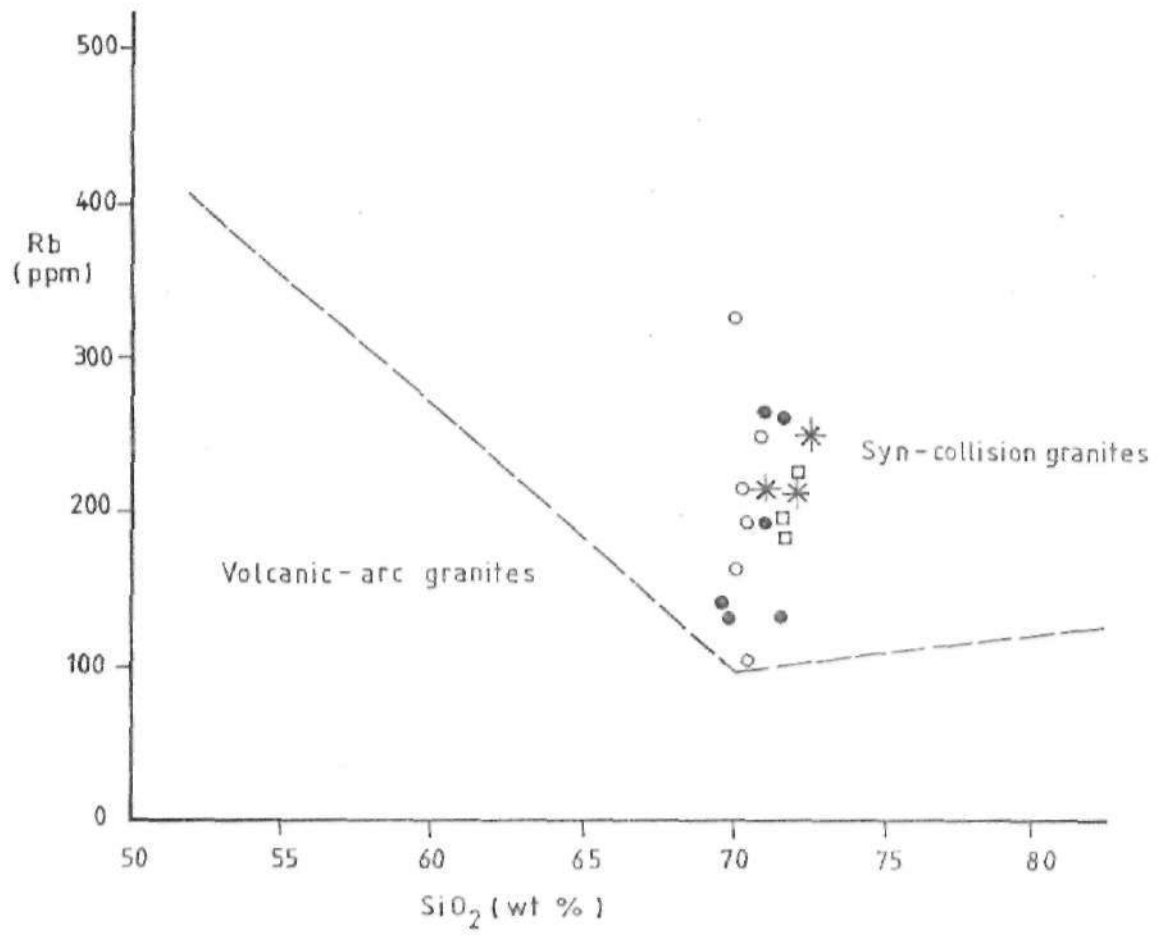


Fig. 6.10. $Rb - SiO_2$ discrimination diagram used for the tectonic classification of granitic rocks. Diagram is after Pearce et.al.,(1984). The broken line separates Syn-collision granites from Volcanic-arc granites. Symbols as in Fig.6.2.

locations of which are indicated in Maps 1 and 2, and Tables 6.12 and 6.13.

The analysed samples are slightly deformed and the porphyrocrysts are faintly aligned parallel to the regional trend in the Kazaure belt (NNE- trend of structures). It also contains some xenolith trails aligned in this direction. The type of fabric described from available field evidence also indicates that the porphyritic granite is slightly lineated.

Regression line (slope and intercept) for the whole rock isochron was calculated with computer programmes according to the least squares methods of York (1969) and Williamson (1968). The initial $^{87}Sr/^{86}Sr$ ratios were normalized for $^{86}Sr/^{88}Sr = 0.1194$ by on-line computers. Goodness of fit of the regression line was tested by the value MSWD = SUMS/(n-2) as described by Brooks et al. (1972). Scatter in the data in excess of analytical uncertainty is usually indicated by >2.5. The age was calculated using $^{87}Rb = 1.42 \times 10^{-11}$ a-1p (1.42×10^{-5} per Ma), the constant recommended by the IUGS Subcommission (Steiger and Jager, 1977).

6.5.2 Isotope Results and Computations

The isotopic analyses of five whole rock samples are given in Tables 6.12 and 6.13, and on conventional isochron diagram in Fig. 6.11. Analytical errors of $\pm$ 2.0% and $\pm$ 0.01% were

Table 6.12 Geochronometric Samples' Description, Locality and Co-ordinates.

Sample No.	Description	Locality	Coordinates
UD39,DA01	Porphyritic granite	Kazaure Dam area	12°39'N, 8°22'E
UD60,DA02	Porphyritic granite	Inselberg SSW of Ladan Area	12°31'N, 8°11'E
UD66,DA03	Porphyritic granite	North of Kunchi Rock Quarry	12°34'N, 8°13'E
UD68,DA05	Weakly foliated Porphyritic granite	Rock Quarry about 3 km N of Ladan area	12°32'N, 8°10'E
UD69,DA06	Porphyritic grained granite	1.5 km SSE of Ladan area	12°34'N, 8°13'E

Table 6.13 Rb-Sr analytical data of Whole-rock Determinations from Granites in the Kazaure Schist belt region.

Sample No.	Sr (ppm)	Rb (ppm)	Rb/Sr (ppm)	$^{87}Rb/^{86}Sr$ (± 1.5%)	$^{\#87}Sr/^{86}Sr$ (± 0.0020)
UD 39,DA01	138	197	1.43	4.1545	0.74431
UD 60,DA02	140	329	2.35	6.8539	0.76452
UD 66,DA03	159	110	0.63	1.8539	0.72553
UD 68,DA05	133	166	1.25	3.6537	0.74328
UD 69,DA06	145	212	1.46	4.3529	0.74563

Rb-Sr: Quoted errors at 2@ level, Sr ratios reproducible to 0.05%.

#=$^{87}Sr/^{86}Sr$ atomic ratio normalized to $^{86}Sr/^{88}$ Sr of 0.1194

ppm = Mg/g.

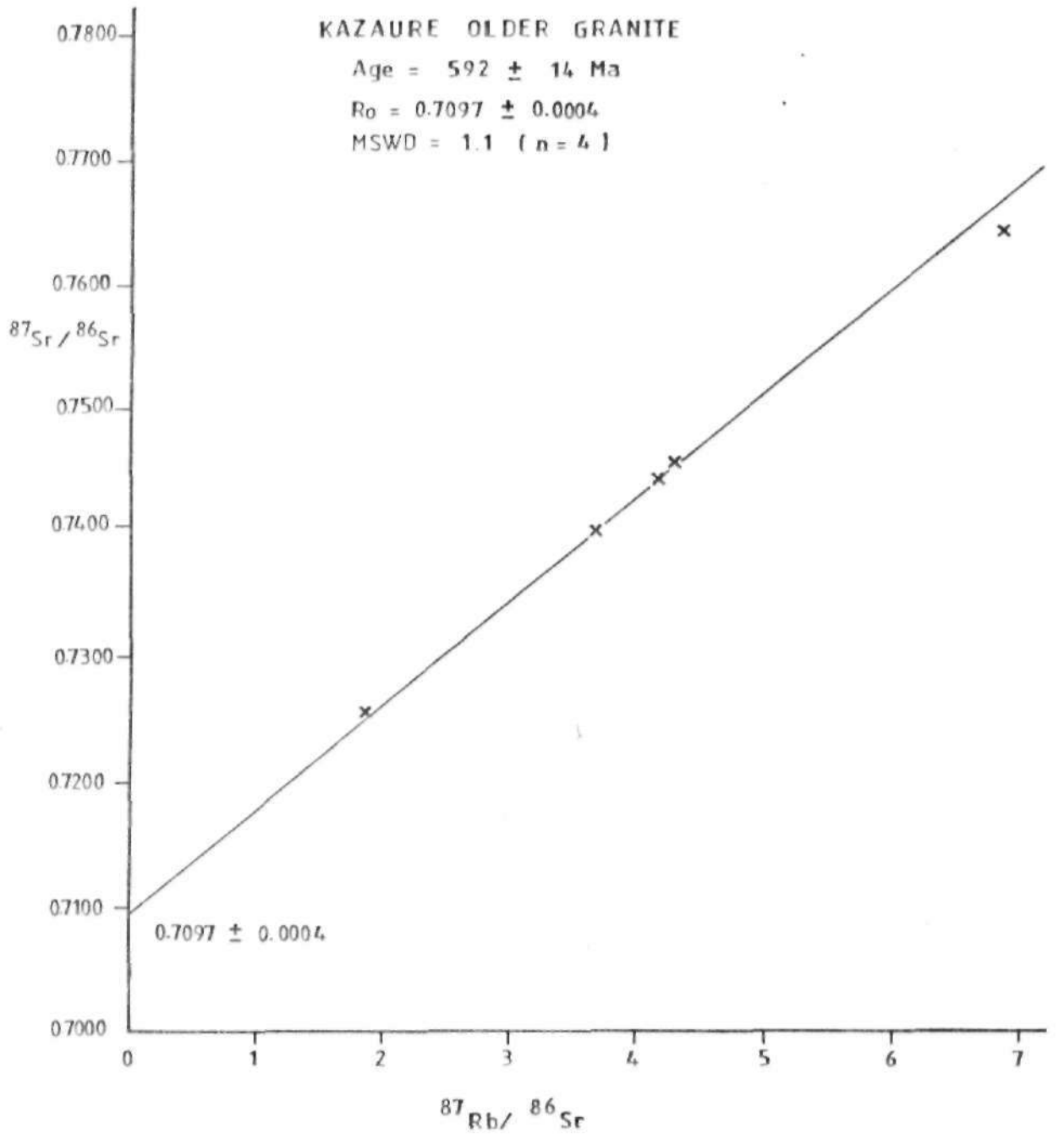


Fig. 6.11. Rb - Sr isochron diagram for the whole rock samples from the Kazaure belt Older Granites.

Ro stands for isotopic ratio of initial Sr; MSWD represents "Mean Squares of Weighted Deviates"; and n is the number of points forming the isochron.

assigned for the $^{87}Rb/^{86}Sr$ and $^{87}Sr/^{86}Sr$, respectively. Errors quoted in the results are 2 sigma of the means. Isotopic data are often difficult to analyse because of a number of problemsusually encountered. Some of these problems have been outlined in the Appendix. The age was determined by comparing the radiogenic ^{87}Sr generated in the rock with the amount of radioactive parental ^{87}Rb present in the rock.

The isochron was calculated for 4 samples, excluding sample UD60 (DA02) as it appears slightly weathered in thin section, with evidence of chloritization of biotites. This, together with its occurrence near the Kalangai Fault System (KFS) may have caused the loss of radiogenic ^{87}Sr. Consequently, the sample was omitted in the calculation of the best fit line (isochron), as it deviates from the line by more than four times the analytical uncertainty. Its inclusion will certainly have some effect on the age and initial ($^{87}Sr/^{86}Sr$, Ro) estimates.

The regression equation Y = 0.7097 + 0.008407 X, has produced a least-squares line through the granite samples (MSWD = 1.2) which corresponds to an initial ($^{87}Sr/^{86}Sr$, Ro) of 0.7097 + 0.0004, and t (the time of establishment of this isotopic composition) of 592 + 14 Ma (Fig. 5.11). Ro is the isotopic ratio of the initial Sr and it is given by the intercept of the regression line. It is also the $^{87}Sr/^{86}Sr$ ratio of the Sr common to all minerals in the rock.

The MSWD of 1.2 is just slightly more than 1, and this means the residual variance is less than experimental variance. For four regressed points, a limiting MSWD = 3.07 value is given in the F-distribution table of Brooks et al. (1972). Therefore the Rb-Sr regression age of 592 + 14 Ma. based on four points, with lower MSWD value of 1.2 and errors of 1.5% percent at the 95 percent confidence limits in this work, is fairly satisfactory. Therefore none of the calculation models of McIntyre et al., (1966) was used.

6.5.3 Interpretations

It has been possible to obtain an isochron on the porphyritic granite that was emplaced into the Kazaure younger metasediments during metamorphism and tectonism. The developed foliation in the granite is a tectonic feature corresonding to the regional Pan-African deformation/metamorphism as recorded in other areas. The age of 592 + 14 Ma could therefore represents the time of fabric formation in the porphyritic granite.

The isotopic data has revealed the Kazaure granites to be similar to many of the NW Nigeria Older Granites. The high initial $^{87}Sr/^{86}Sr$ ratio for the Kazaure pluton (Ro = 0.7097 + 0.0004) can be interpreted as indicating a crustal origin.

All the radioactive ages obtained from the Older Granites in northern Nigeria range from 794 to 505 Ma. The studied Zaria

and Malumfashi syntectonic granite plutons and the Kano hornblende granite, appear to be most relevant for comparison with the Kazaure granites. For the Zaria Granite, Ogezi (1977) cited 794 + 73 Ma as the age of its emplacement and deformation. However, according to Ogezi (1977), the Pan-African metamorphism/deformation recorded at Malumfashi had affected the Rb-Sr systematics of the gneisses there. He obtained an errorchron age of 615 + 30 Ma, which he interpreted as due to a metamorphic event. For the Kano hornblende granite, Snelling (1964) reported an emplacement K-Ar age of 780 + 40 Ma.

The syn-tectonic Kazaure pluton is one of the youngest dated members of the Pan-African granite cycle in NW Nigeria. It defines a 4-point, whole-rock Rb-Sr, errorchron corresponding to an age of 592 + 14 Ma with an initial ratio of 0.7097 + 0.0004. The present geochronological study on the Kazaure granites has provided further evidence for Older Granites emplacement during the Pan-African Orogeny.

The ages obtained from the above granitoids show that syn-tectonic granite emplacement reached its peak around 600 Ma ago. The significance of this statement has earlier been highlighted by Harper, et al., (1973), who suggested that the Pan-African event took place between the time span circa 700 Ma to circa 600 Ma. And indications are that Rb-Sr whole-rock systems are sometimes affected by metamorphism.

Therefore caution should be exercised in interpreting Rb-Sr data in terms of intrusion, metamorphism and deformation. This is because many of the isotope data are imprecise in nature, and frequently have large quoted errors. This explains the difficulty in comparing and inter-relating the isotopic data from these places, all of which broadly occur in the same area, northern Nigeria.

6.6 AGE OF THE KAZAURE SCHIST BELT

The true original deposition, deformation and metamorphic age of the younger metasediments is not known. This is especially so as there is no evidence of contact metamorphic minerals in the metasediments. In addition, the absolute ages of the younger metasediments and basement rocks at the Kazaure belt area are unknown. Therefore, for accurate interpretation and modelling of the evolution of the KZSB and its adjacent areas, the previous geochronological works undertaken on the basement rocks of NW Nigeria are referred. This will provide a framework for the conceptual interpretation of a Rb-Sr isotopic age data now available from the Kazaure Belt area.

As well as demonstrating the time of formation of the Older Granite, the isotopic data has placed a lower limit on the age of the Kazaure belt. This is so as the younger metasediments must clearly be older than 592 + 14 Ma, the age of the granite that intrudes them. In addition, the REE data from the schist

has constrained the age of the metasediments to be post-Archaean (Section 6.2.2).

The Maru phyllites (Holt et al., 1978), the Gusau migmatite (Ogezi, 1977), were all assigned Kibaran (pre-Pan-African) ages. However, Ogezi (1977) obtained scattered ages between 3,100 and 600 Ma on the Malumfashi migmatites. These migmatites truncate and separate the Kazaure belt from others (Fig 3.1). The emplacement age of the Kazaure granite (592 + 14 Ma) suggests a Neoproterozoic (Kibaran/Pan-African) tectono-metamorphic event in the Kazaure Belt.

Possibly the orogeny preceding the Pan-African (the Kibaran) probably marks the upper limit of the initiation of the Kazaure Schist Belt. The Pan-African tectonism, metamorphism and plutonism which took place around 700 and 600 Ma ago could be the first time of metamorphism and subsequent folding of the KZSB. This suggestion is supported by interpretation of the geologic relations in the Malumfashi and Anka Belts which have been interpreted as Pan-African.

The Younger supracrustal rocks in the Kazaure area are also associated with Younger Granite intrusions. However, this is not the first time these Younger Granites are studied, as an isotopic age of about 160 Ma has since been established for the Nigerian Younger granites (Jacobson et al., 1963).

CHAPTER SEVEN:

DEFORMATION HISTORY AND METAMORPHISM

7.1 INTRODUCTION

Regional metamorphism in the study area has affected both the younger metasediments and the migmatite and gneisses. The poorly exposed nature of the rocks, which is a function of the high degree of weathering in the area has prevented detailed metamorphic studies. This makes it difficult to identify any metamorphic zones and isograds in the study area (e.g Ekwueme and Onyeagocha, 1985a). Although it is most likely that the sequence as in Barrovian type is not applicable to the study area. In addition, no pressure and temperature conditions that existed during or after the deformations and metamorphism, were calculated (e.g Ekwueme and Onyeagocha, 1990). The metamorphic temperature was however estimated using biotite.

The microscopic textures of the deformed rocks were studied with focus on the criteria suggested for recognizing time relationships between tectonic and metamorphic events (e.g Vernon, 1968; 1976; Norton, 1975 and Ekwueme, 1993). These include:

(i) Cross-cutting relationships between schistosity and porphyroblasts.

(ii) Deflection of fabrics (for example, kink bands) around porphyroblasts,

(iii) Sigmoidally arranged inclusions in prograde porphyroblasts.

(iv) Undeformed trains of inclusions in porphyroblasts which indicate static growth.

(v) Porphyroblasts that include S surfaces or fold hinges.

(vi) Deformed porphyroblasts.

7.2 MINERAL PARAGENESES

The metamorphic mineral assemblages associated with the penetrative deformation rock fabrics have been mentioned in previous sections. They include biotite, muscovite, quartz, garnet, hornblende, chlorite, and plagioclase feldspar Table 7.1).

7.2.1 Gneisses and Migmatites

Common mineral assemblages in the gneisses are as follows:
oligoclase + microcline + quartz + biotite
+ muscovite + hornblende + garnet + epidote

The garnet occurs as porphyroblasts, while the muscovite crystallized as small flakes. However, the biotite, quartz, hornblende and chlorite occur as tiny crystals. Hornblende is commonly replaced by aligned biotite flakes.

Table 7.1 Mineral Paragenesis in the rocks of Kazaure Schist Belt

MINERAL/ROCKS	GNEISSES	MIGMATITES: NEOSOMES	MIGMATITES: PALAOESOMES	PHYLLITES
SERICITE	-	-	-	/
CHLORITE	-	-	-	/
OLIGOCLASE	/	/	/	/
MICROCLINE	/	/	/	-
QUARTZ	/	/	/	-
BIOTITE	/	/	/	-
MUSCOVITE	/	/	/	-
HORNBLENDE	/	-	/	-
GARNET	/	-	-	-
EPIDOTE	/	-	/	-
CALCITE	-	-	-	/

B.

MINERAL/ROCKS	BIOTITE SCHISTS	MUSCOVITE SCHISTS	QUARTZ-BIOTITE SCHISTS	SCHISTOSE QUARTZITE
SERICITE	-	-	-	-
CHLORITE	-	-	-	/
OLIGOCLASE	/	/	/	-
MICROCLINE	-	-	/	-
QUARTZ	/	/	/	/
BIOTITE	/	-	/	/
MUSCOVITE	-	/	-	-
HORNBLENDE	-	-	-	-
GARNET	-	-	-	-
EPIDOTE	-	-	-	-
CALCITE	-	-	-	-

SYMBOLS: / (TICK) = PRESENT - (DASHED) = ABSENT

In the migmatite, the following mineral associations were observed in the respective fabrics of the rocks:

Neosomes: quartz + K-feldspar + oligoclase (An26) + biotite + muscovite + microcline.

Palaeosomes: quartz + K-feldspar + andesine (An34) + biotite + green hornblende + muscovite + epidote + microcline.

The poor twinning and lack of zoning of plagioclase porphyroblasts indicate metamorphic recrystallization (Smith, 1974).

7.2.2 Metasediments

The common mineral associations of each lithologic type within the younger metasediments is listed below:

Phyllites	:sericite + chlorite + quartz + albite + calcite.
Biotite schists	:quartz + green biotite + oligoclase +
Muscovite schists	:quartz + muscovite + albite + chlorite
Quartz-biotite schists	:quartz + brown biotite + chlorite + oligoclase.
Quartzite	:quartz (-muscovite, biotite, chlorite).

Green biotite occurs as small flakes together with chlorite and muscovite laths which could be primary in origin (Plate

7.1 and Table 7.1). Plagioclase occurs as a porphyroblast, while the few muscovite flakes present are replaced by K-feldspar (Plate 7.2). The muscovite grains here occur pseudomorphing microcline crystals during an intermediate pressure type metamorphism.

7.3 METAMORPHIC GRADE

The anorthite content of plagioclases can be use to characterise metamorphic grade of rocks, as those with low anorthite content (albite) suggests low grade, while that with intermediate anorthite content (oligoclase) suggests a medium grade. However, it should be pointed out that in the presence of epidote, the anorthite content in a stable assemblage consisting of plagioclase + hornblende + quartz, is usually higher than in its absence (Winkler, 1979).

The mineral assemblages in the Kazaure rocks are compared with those of universally established assemblages (Miyashiro, 1973; Winkler, 1979) in order to identify the metamorphic grade and/or facies classification in the area. According to Winkler (1967; 1979), the equilibrium mineral paragenesis of oligoclase (An_{24-26}) + quartz + green hornblende + brown biotite + almandine garnet in the migmatite-gneiss (Table 7.1) is stable under high grade (upper amphibolite facies) conditions of metamorphism. He also interpreted the equilibrium mineral association of albite + green biotite +

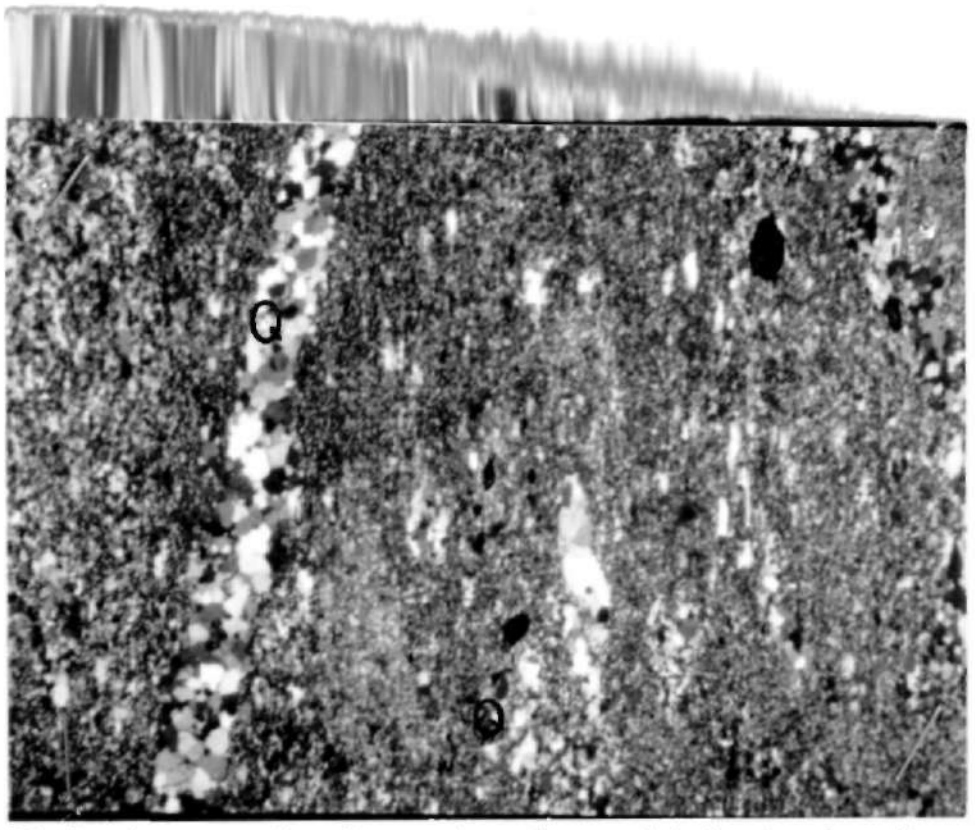


Plate 7.1 Photomicrograph of quartz mica schist showing S_1 schistosity parallel to the recrystallised quartz vein (Q) formed during M_1 metamorphism defined by fine-grained biotite, muscovite, chlorite and larger quartz grains. Sample UD36, Gora.

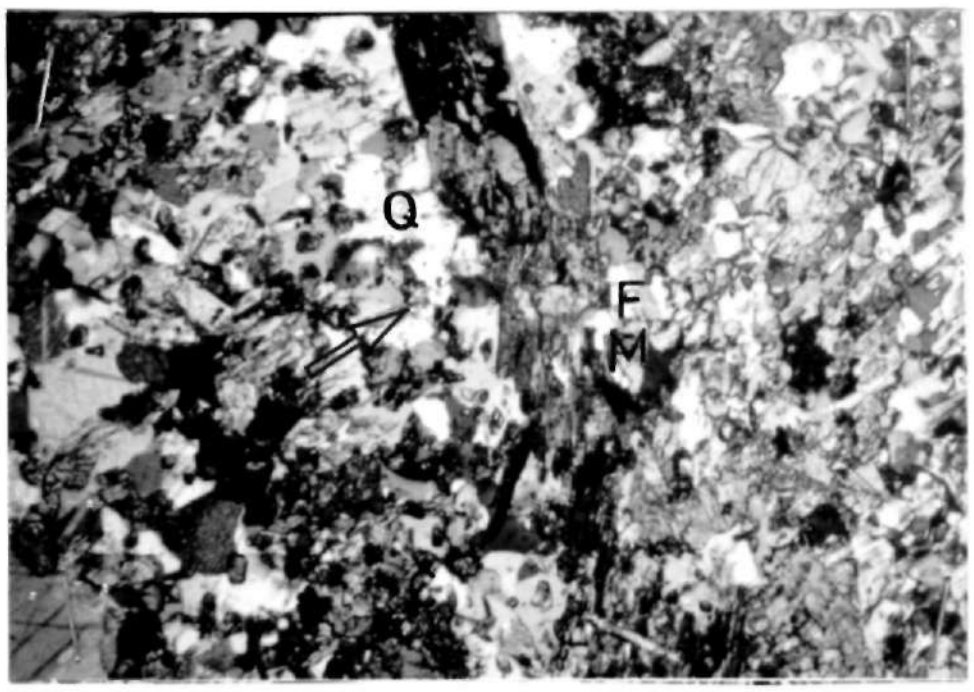


Plate 7.2 Photomicrograph of S_2 cleavage in metapelites marked by the preferred growth (arrow) of quartz (Q) and mica (M), which is altered to chlorite (C) in some places. Note the K-feldspar (F) replacing the muscovite. This preferred orientations formed during the M_2 Metamorphism. Sample UD10, Makadi.

muscovite + chlorite + quartz as suggesting low grade (lower greenschist facies).

The mineral parageneses (Table 7.1) suggest a bimodal distribution of hydrous metamorphic facies similar to the medium pressure metamorphic conditions of Barrovian-type regional metamorphism (Miyashiro, 1973; Winkler, 1967; 1979). They are the latest equilibrated assemblages that occur by simultaneous increase in temperature and pressure in both the migmatite-gneiss and the younger metasediments.

Retrogressed assemblages in the gneisses include albite + sericite + muscovite + epidote + chlorite and calcite derived from the feldspars. These indicate a retrogression of the high amphibolite facies to the medium grade greenschist facies. Accessory minerals associated with the retrogression effects include rutile, magnetite and haematite.

The temperature condition during metamorphism was estimated using biotite, following the arguments of Baker (1990). According to Baker (1990), the stable occurrence of biotite associated with muscovite in an assemblage indicates an upper greenschist facies conditions in the metamorphic temperature range of 425-450^{0}C. He also pointed out that the absence of biotite in a mineral assemblage suggests a lower greenschist metamorphic temperature of 300-425^{0}C.

The documented occurrence of amphibolite facies of metamorphism suggests that the metamorphic temperature in the study area has possibly exceeded these ranges, as the lower stability limit of the amphibolite facies is 540 ± 20^{0}C at 2kb PH_2O (Winkler, 1967). The metamorphic temperature could even have been close to the melting point of granite. This becomes significant in the formation of granite and granitic leucosomes in the migmatite-gneisses, possibly at higher grades.

7.4 RELATIONSHIP OF THE METAMORPHIC EVENTS TO THE DEFORMATION EPISODES (Tectono-metamorphic events)

7.4.1 First Metamorphic Event (M_1)

The earliest progressive metamorphism recognised in the area (M_1) reached medium grade (amphibolite facies) condition of metamorphism. The M1 event also produced an S_1 schistosity parallel to the fold axial planes in the pelites. In the pelites, the schistosity is defined by fine-grained green biotite, muscovite, chlorite and larger quartz grains (Plate 7.1).

7.4.2 The Second Metamorphic Event (M_2)

The second progressive metamorphic event (M_2) is correlated in time with the second phase of deformation (D_2). It is the main metamorphic event in the area. The M_2 metamorphism is in the low grade (greenschist facies) and was syn to late tectonic

with the contemporaneous D_2 ductile deformation that affected S_1 schistosity (Plate 7.3).

The M_2 metamorphic event also caused the preferential growth of S_2 penetrative schistosity which is marked by preferred orientations of quartz, chlorite and mica, particularly biotite. The S_2 fabrics are the main metamorphic structure of the pelites and semi-pelites. In some specimens, the major period of porphyroblasts development followed the D2 event, particularly the growth of abundant second generation biotite expressed as trails in all of the mica schists in the area (Plate 7.4).

7.4.3 The Retrograde Metamorphism (X)

In the `X' metamorphic event, the D_1 and D_2 deformations ceased, resulting in static low grade metamorphism in which unoriented mineral growth was possible. The static metamorphism is accompanied by cataclastic movements, plagioclase retrogressed to sericite and muscovite, biotite, and chlorite porphyroblasts.

Quartz crystals with undulose extinction, deformation bands, polygonisation and recrystallisation effects, are probably due to cataclastic deformation and a stage of metamorphism confined to narrow shear zones (Plates 4.17 and 4.18). The X static event attained greenschist facies (albite + biotite +

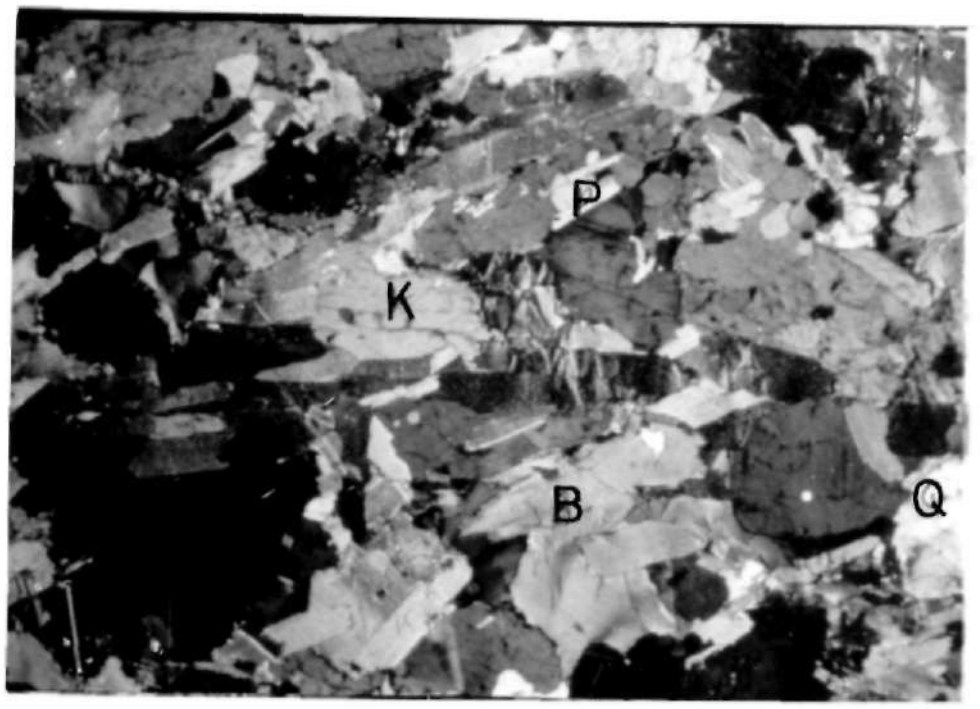


Plate 7.3 Photomicrograph of a biotite gneiss showing M_2 metamorphic fabric which is contemporaneous with the D_2 ductile deformation event that rotated porphyroblasts and affected S_1 schistosity. Note the larger grains of quartz (Q), biotite (B), K-feldspar (K) and Plagioclase (P). Sample UD190, from NW of Tsanyawa.



Plate 7.4 Photomicrograph of mica schist showing trains of biotite crystals (arrow) which formed during the major period of biotite porpyroblasts (B) growth. Sample UD57, from Ungwan Kaya.

muscovite + quartz). However, earlier formed synkinematic biotite is extensively retrogressed to chlorite. The late chlorite and muscovite porphyroblasts were also observed growing across the main stage folded S_2 fabric of biotite, quartz and feldspar. The muscovite do not exhibit undulatory extinction. The retrograde minerals do not show any preferred alignment in all of the lithologies in the area, hence the difficulty in recognising D_1 and D_2 foliations.

The retrograde effects could be due to the superimposition of a lower grade metamorphism on any D_1 or D_2 mineralogy and texture. Retrogressive rims of minerals reflect the lower temperatures and pressures.

7.4.4 Summary of Metamorphic events

The basement rocks of the study area have been deformed under regional metamorphic conditions of upper greenschist to lower amphibolite facies, and the metamorphic series of the area were due to low pressure type polymetamorphism. The metamorphic mineral assemblages show evidence of being either syn-D_1, and syn or post-D_2 related to recrystallisation together with some plastic style of folding.

The metamorphic events are ascribed to the D1 and D2 deformation events, and two periods of progressive metamorphic events and a retrograde metamorphism have been documented. The

first metamorphic event (M_1) is synchronous with D_1. It developed a high grade (amphibolite facies) metamorphic assemblages. M_2 is the main regional metamorphic event in the Kazaure area, and is related to the D_2 deformation event. It bears a low pressure greenschist facies metamorphic assemblage. This is followed by the post D_1 and D_2 retrograde metamorphism (X), which locally occurs mainly in lineaments with low grade (greenschist facies) assemblages. Apart from garnet, no any higher grade diagnostic index minerals are known in the project area. The upper amphibolite facies represents the highest grade attained in the area.

CHAPTER EIGHT:

GEOTECTONIC EVOLUTION OF THE KAZAURE SCHIST BELT

8.1 INTRODUCTION

In the preceding chapters conclusions have been reached regarding the lithology, structures, metamorphism, geochemistry and geochronology of the Kazaure Schist Belt. A number of such geological observations in the KZSB region have important regional implications in the NW Nigeria metamorphic terrain. Therefore, for accurate interpretation and modelling of the overall regional geotectonic evolution of the KZSB, the results obtained in the present work are compared with those earlier deduced on the other NW Nigeria Schist Belts.

This has now allowed the formulation of a geotectonic model that shows how the geologic and structural framework of the the Kazaure Belt and its adjacent areas has evolved (Section 8.5). An attempt has also been made in this chapter to contribute to the evolutionary framework of the entire NW Nigerian Schist belt province.

8.2 ORIGIN OF THE KAZAURE ROCKS

Deformational and metamorphic activities have affected the rocks of the study area. Table 8.1 gives the chronological

Table 8.1 The chronological order of events in Kazaure region.

a. Classification of the rocks in the project area

Classification	Geological History	Rock types
Sedimentary rocks	Youngest cover rocks	Chad & Gundumi Formations
Daura Igneous Complex rocks (Mesozoic)	Extrusive and intrusive activities leading to Younger Granite formation	Syenite Rhyolites, Biotite granite
Intrusive Suite (Pan-African)	Granite intrusion, faulting, fracturing, high level magmatic activities.	Older Granites, Quartz and Pegmatite veins
Younger metasediments (Pan-African)	Geosynclinal deposition, orogenesis, deformation and metamorphism.	Schist, BIF, Quartzites, Metavolcanics, Metaconglome-rates and Metasandstones
Basement suite (Pan-African/ Kibaran?)	Orogenesis, deformation, metamorphism, migmatisation and reactivation of pre-existing rocks	Migmatite-Cycle?, Gneiss.
Crystalline Basement (Eburnian or Liberian)	Possible early formation of migmatite-gneiss complex	Gneiss, migmatites and Older metasediments.

b. Sequence of structural events

Classification	Structural Imprint	Types of structures
Late-tectonic	Brittle deformation that forms fractures	Joints, sinistral and dextral faults.
Second deformation event (D_2)	Ductile deformation producing second generation structures	F_2, S_2 and L_2 folds, cleavages, lineations.
First deformation event (D_1)	Ductile deformation producing first generation structures	F_1, S_1 and L_1 folds, cleavages, lineations.

order of events in the Kazaure Schist Belt and its surrounding regions including part of the Malumfashi belt. The migmatite-gneiss basement complex seems to be the oldest rock unit and is considered to be derived from a pre-existing sedimentary series (paragenesis), possibly Archaean, through several tectono-metamorphic episodes (Ekwueme and Kroner, 1994).

The Younger Metasediments lie on the migmatite-gneiss basement (Fig. 8.1), and subsequent compressional tectonics led to at least two episodes of deformation (Section 6.9.3). The intense deformations and isoclinal foldings along N-S and NNE-SSW axes were accompanied by regional metamorphism and extensive migmatisation of the basement. The fault rocks along the KFS were certainly derived from pre-existing rocks.

8.2.1 Origin of the migmatite-gneiss Basement

In Nigeria, the migmatite-gneiss complex and granite gneisses are considered to have formed during the period of Older Granite intrusion, as well as other periods of Plutonic activities like Eburnean (Cooray, 1974; Rahaman, 1976a; 1976b). There is a link between the formation of migmatites and deformation (Robin, 1979). Some of the structural relations within the stromatic, nebulitic and agmatitic migmatites seem to support this contention, as they were produced during a period of migmatization correlated with the emplacement of the Pan-African Older Granites (Turner 1971; McCurry, 1971; 1976).

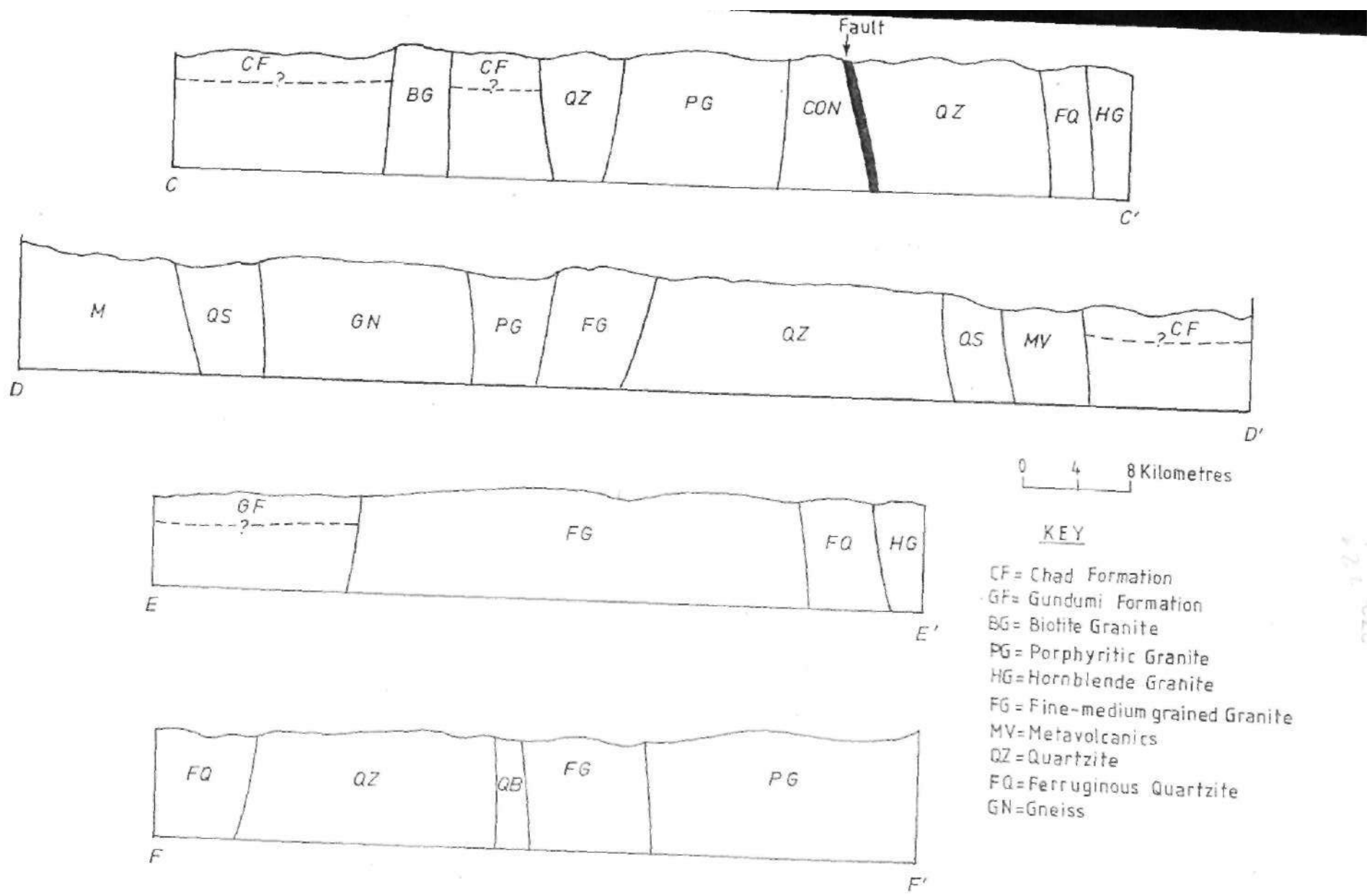


Fig. 8.1. Cross-sections through the project area. Lines of cross-sections are as in maps 1 and 2.

The migmatite-gneiss and quartzo-feldspathic veins could have been produced by high grade metamorphism of pre-existing granites through transitional processess of granitisation and gneissification, that results in the formation of homogenous migmatite (gneiss) after losing its banding through mixing the leucosome and paleosome.

The P-T condition of metamorphism and the composition of the original rocks are some of the factors controlling the formation of migmatites, especially in gneiss regions (Mehnert, 1971; Winkler, 1976). They generally develope in metamorphic terrains formed during regional metamorphism. The development of the stromatic migmatites is as a result of metamorphic segregation, external metasomatism and anatexis of an originally banded rock (Gupta and Johannes, 1982). Brecciation and injection of magma could have led to the formation of the agmatitic migmatite (Mehnert, 1968; Chinner, 1978). Pegmatitic and aplitic injections along zones of brittle fractures and fold axial planes in these rocks are very common. They were observed on several outcrops.

8.2.2 The origin and palaeo-environment of deposition of the Younger Metasediments and metavolcanics

The reconstruction of the palaeo-environment of deposition for the younger metasedimentary rocks is difficult, as there is no direct evidence of the precise nature of the bedrock directly under the metasediments within the Kazaure palaeobasin.

However, few speculative statements on the protoliths and palaeo-environment types can be made based on the evaluation of the characteristics of the different lithologic types.

Although most of the original sedimentary structures have been destroyed, one can still argue for a sedimentary origin for the metasediments, more especially as twelve (12) samples of the metasediments and five (5) of the metavolcanics were analysed for major and trace elements (Section 5.3). The geochemicl studies (e.g REE characterisation on six (6) of the mica schist samples) have revealed that the Kazaure metasediments are metamorphosed shale-greywacke sequence.

Petrographic studies have shown the metasediments are quartz-rich and contain abundant plagioclase and biotite, with small amount of muscovite. The quartzites are detrital and their protoliths were most likely quartzwackes approaching fine-grained quartz arenites in some places (Pettijohn et al., 1973).

The conglomerates and arenaceous sediments were rapidly deposited in a much higher energy ancient environment than the pelites. A possible environment of deposition was a shallow basinal continental or littoral environment (e.g. shelf or deltaic environment). This probably allowed the deposition of the coarse clastic sediments as basin margin alluvial fans, clastic wedges and prograde deltaic sequence (Pettijohn,

1957). However, the conglomerates were probably debris flow deposited through slumping.

The metapelites represent a sequence of poorly bedded mudstones and shales. Fine-grained laminated metapelites and the ferruginous quartzites (BIF) indicate quiet and shallow water environment, as the oxide facies iron formation is characteristically found in the shallow parts of a depositional environment (Lepp and Godich, 1984). The interbedded nature of occurrence between the fine and coarse clastics (especially schistose quartzites) suggests that at least part of the metapelites were deposited together with the coarse clastics, during a local quiet water conditions. The metavolcanics are interlayered with the metasediments, and may represent an igneous rock, probably microtonalite.

The genesis of the BIF has not been investigated. However Mucke et al., (1996) have proposed a model to explain the genesis of the Nigerian BIF. According to this model, a regional metamorphism (of low amphibolite facies) is responsible for the formation of both the metasediments and the iron-formation, and that the protoliths include mud-like sediments derived from volcanic exhalations. This is in-line with James (1992), who presumed amorphous iron-rich silicate gels to be the protolith of silicate BIFs.

James (1954) classified all B.I.F's into four end members, based on depositional facies concept. These are: the oxide, silicate, carbonate and sulphide facies. Only the oxide facies iron formation predominates in the Kazaure region, while the others, especially the sulphide facies iron formation, are not common. The documented iron formation near Kazaure town is interpreted as a metamorphic equivalent of the sulphide facies deposited under anoxic conditions in the study area. The BIF is chert-bearing and has a high silica-iron ratio (except in the sulphide facies).

The oxide in the BIF is formed at a relatively high Eh (at shallow marine environment, but the sulphide is formed at strongly negative Eh environment (deep euxinic condition). It is considered to be related to volcanic exhalative activity. Spessartine garnet is more abundant in the BIF probably because of the higher Mn content of the FQZ. Based on the above it is suggested that the Kazaure belt evolved in an ensialic restricted basin which has survived erosion on older basement crust (Fig. 8.1, above).

8.2.3 Origin and Tectonic environment of Older Granite Emplacement

Physical relations (e.g sharp contacts) show clearly that the granites in the study area were emplaced as liquid melts, and that the fine-medium grained varieties are older than the porphyritic variety. In addition, it is probable that the N-S

structural grain in the Kazaure area has influenced the emplacement of the granitic melt.

Field relations, petrographic studies, geochemical data (Section 5.2) and isotopic studies (Section 5.5) have revealed the granites to be broadly similar to the ones obtained for the NW Nigeria Older Granites. The geochemistry of the Older Granite rocks in the study area, all appear to indicate their calc-alkaline nature and I-type characteristics similar to magmas generated from igneous source materials in subduction and continent-continent collision zones. Geologic criteria suggest a late Precambrian emplacement which has been confirmed by Rb-Sr radiometric age determination which gave an isochron age of 592 $\pm$ 14 Ma.

8.3 CORRELATION WITH OTHER NW NIGERIA SCHIST BELTS

Although attempts have earlier been made at correlating the schist belts of NW Nigeria (e.g Ajibade, 1980; Egbuniwe, 1982; Turner, 1983), these are restricted in nature. Therefore the KZSB rocks are now correlated with those of other northwestern Nigeria schist belts on both lithological, evolutionary and structural grounds.

8.3.1 Comparison of the Younger Metasediments

The lithologies in the map area consist of low grade metapelites, quartz schist, quartzites, conglomerates, acid and intermediate volcanic rocks, as well as rare iron

formation. These have similarities with lithologies in other NW Nigeria schist belts (Figs. 1.1 and 2.1).

The Malumfashi, Maru, Anka, Birnin Gwari and Zuru belts contain coarse clastic sequences and acid-intermediate volcanic rocks, as at Kazaure and the northernmost portion of the Malumfashi belt. The above belts are composed of pelites and clastic metasediments including thick layers of quartzites and conglomerates. There is no lithological contrast between the northern and southern portions of the Malumfashi belt.

There is no mafic or ultramafic rock in the Kazaure-Malumfashi area. It lacks the mafic volcanic rocks that characterize Anka, Maru and many other belts. Ophiolite sequences and subduction related accretionary rock have not been observed in the KZSB. And the typical sediments found in the belt, suggest a shallow palaeobasin of deposition with limited width.

The Banded Iron Formation (B.I.F) occurring in the study area is similar to Precambrian iron formations described elsewhere in the NW Nigeria schist belts (Wright and McCurry, 1970; Turner, 1983 and Adekoya, 1993). These occurrences of BIF include the silicate facies of Malumfashi Schist Belt (Tudun Kudu and Unguwan Mallam Ayuba), and that of the Maru Schist Belt (Maraba hill, Bingi, and Ruwan Dorawa). BIF's have also been reported from: Birnin Gwari, Kushaka, Muro and

Igarra-Kabba-Lokoja schist belts. However there is no BIF in Anka, nor in Zuru and Ife-Ilesha belts.

Mineral paragenesis in the Kazaure and Malumfashi Belts suggests a bimodal distribution of metamorphic facies from lower greenschist to middle amphibolite facies in the area. This appear to be similar to those of adjacent areas of NW Nigeria (McCurry, 1970, 1976; Ajibade, 1980; Egbuniwe, 1982; Ekwueme, 1983; and Annor and Coker, 1994). It is one of the lowest in the whole of NW Nigeria. In addition, it is characteristic of upper levels of the earth crust. This further supports ideas that the Kazaure metasediments are a sedimentary cover upon a pre-existing basement (Section 8.5).

8.3.2 Comparison of the ductile structures

The rocks in the study area have undergone a minimum of two major ductile deformational events and this resulted in two recognisable phases of deformation, D_1 and D_2. The earlier clearly recognisable event is the D_1 deformation which affects the migmatite-gneiss basement and early banding (S_0) in the cover rocks of the Younger Metasediments. This led to the development of L_1S_1 fabric which resulted in the folding of S_0 fabrics into tight to isoclinal relics F_1 folds with N-S hinges and S_1 axial trace. These have been largely over-printed, obscurred and/or obliterated by subsequent structures.

Subsequently the migmatite-gneiss-older metasediments basement and the Younger Metasediments were congruently deformed one more time during the D_2 event. The second deformation event led to the formation of L_2S_2 fabrics as a result of the folding of S_1 into isoclinal NNE-SSW trending upright folds.

The comparison of structural events in the study area with those of some NW Nigeria schist belts has indicated similar structural trends. The pattern of deformation in the Kazaure belt can be fitted reasonably well into the regional deformation history established for the schist belts in the NW Nigeria region (Table 8.2). There are similarities of the dominant deformations in all the belts, with the exception of the minor D_3 and D_4 events. These minor events were not documented in the Kazaure area.

The Kazaure belt has flat-lying N-S trending early D_1 structures which are also present in the Maru, Birnin Gwari, Kushaka and Zuru belts, and also in the northernmost portion of the Malumfashi belts. However, there is a major difference in orientation between the ENE- trending early flatlying structures in the southern Malumfashi belt (McCurry, 1971; 1976), as against the present documented N-S trends of similar early structures in the Kazaure Belt and northern part of the Malumfashi Belt.

Table 8.2: Deformation history established for the schist belts in NW Nigeria.

Belt/ Source of information → ---------- Deformation event ↓	Kazaure Belt (This work).	Malumfa-shi Belt (McCurry, 1973).	Anka Belt (Holt, 1982).	SW of Zuru Belt (Danbatta, 1991)	Kushaka Belt (Grant, 1978).	Birnin Gwari (Ajibade, 1980)	Maru Belt (Egbuniwe, 1982)
D4				?	Rare and relict minor folds. Local development of strain-slip Cleavage.	Steeply dipping folds and kinks. Axial planes strike N-S/E-W.	Steeply dipping kinks with E-W strike.
D3				Open folds with smooth profiles and steep NNE-SSW axial planes dip	Open folds with NNE-SSW axial planes. Axes plunge north and south.	Open folds with NE-SW axial planes dip and rounded or angular crests	Open to tight chevron folds and tight to isoclinal folds.
D2	Upright isoclinal folds with NNE-SSW axial planes. Cleavages developed	Tight to isoclinal D_L folds with N-S axial planes strike. Cleavages developed	Steeply dipping, E-W striking bands.	Tight to isoclinal folds with moderate plunging axes. N-S cleavages developed.	Tight to isoclinal disharmonic folds with steep axes. Axial planes strike N-S.	Co-planar with D1. Open to isoclinal large scale folds of S1 schistosity. Axial planes Strike NE-SW.	Open to isoclinal folds. Steeply sipping N-S striking cleavage.
D1	Relict recumbent isoclinal folds with N-S trending axial planes. Mostly oblitera-ted.	Early ENE-WSW foliation related to D_E folds. Largely oblitera-ted.	Open to isoclinal upright folds with NNE-SSW axial planes and Axes.	Rare and obliterated minor folds with shallowly dipping E-W to ENE-WSW trends. S1 axial plane cleavage.	Rare minor folds with E-W axial planes.	Folding of cover rocks on NE-SW trending axial planes. Cataclastic deformation of basement/ cover contact Cleavage well developed.	Relicts flatlying folds with N-S axes and S1 cleavage. Folds oblitera-ted by transpos-ition.

232

This could be because D_1 structures are not very well documented in the belts due to their heavy overprinting and obliteration by subsequent events. Hence, there is no simple correlation between the orientation of the early structures in these two belts and the other schist belts. However, the main difference between the structural deductions in the present work and that of McCurry's (1976), could also have been due to the intrusion of granitoids (Section 6.9.3).

All the belts were deformed by a regional and contemporaneous D_2 event which produced upright NNE-SSW folds and axial planar cleavages. The D_2 is the last major deformation and metamorphic event in each of the schist belts.

8.3.3 Comparison of brittle structures

Brittle-cataclastic deformations related to jointing and strike-slip faulting are evident in the study area, as well as in other NW Nigeria schist belts. Two major regional fault systems trending in a general NE-SW direction have been established in Nigeria (Fig. 8.2). These are the Anka Fault System (AFS) and the Kalangai Fault System (KFS), both of which are mainly dextral wrench faults with locally developed conjugate sinistral faults (Wright, 1976; Holt et al., 1978; Ball, 1980, Oluyide, 1988).

The AFS is considered to be a deep strike-slip lineament and a possible Pan-African crustal suture (Wright, 1976; McCurry

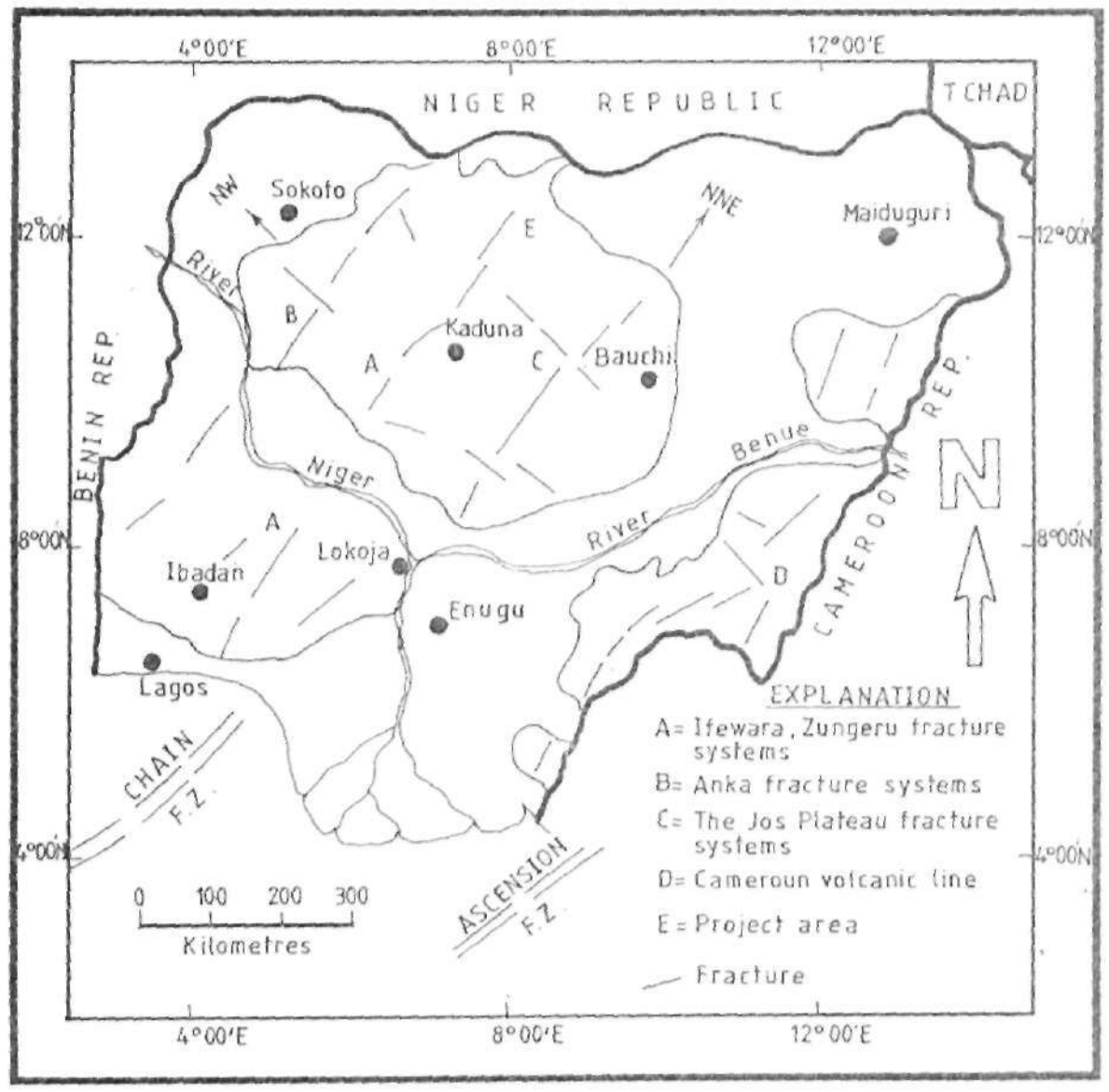


Fig. 8.2. Major fracture and lineament trends in the Nigerian Basement Complex. (Simplified and adapted from Wright, 1976 and Oluyide, 1988).

and Wright, 1977; Ajibade and Wright, 1988). Significant dextral displacements are known within the AFS and many ultramafic/mafic and felsic rocks lie within or very close to it. Danbatta (1991) also described the Yelwa Fault Zone (YFZ), which traverses the Zuru Belt as a subsidiary of the AFS. He was able to map the occurrence of amphibolites which have been mylonitised along the YFZ, especially west of Iri village.

Truswell and Cope (1963) were the first to map and name a NE-SW trending dextral wrench fault, the Kalangai Fault System (KFS), which traverses the Kushaka Schist Belt on Sheet 31. The KFS is 80 km long and has a maximum displacement of 12 km,and the rocks along it have been silicified. Wright (1976) was the first to suggest that the KFS may have been an ancient fault zone reactivated several times in NW Nigeria.

This major wrench fault zone traverses the whole of NW Nigeria and is continuous into the Zaria region, where it dextrally displaced rocks of the Malumfashi belt, ranging from a maximum of 13 Km in the south to 5 km in the Zaria region (McCurry, 1970; Akinyede, 1981). According to McCurry (1970), the KFS has a total length of over 300 km.

Verhejein and Ajakaiye (1977) had also correlated the distinct negative gravity anomaly running from Daura to Malumfashi (through Kazaure), to the metasediments in the area. According

to them, the negative gravity contours show strong northeasterly and to a lesser degree, northwesterly trends. These trends appear to be related to the KFS which displaced the Malumfashi belt.

The present work has shown that this lineament passes through the Kazaure-Malumfashi area in a general NE-SW to NNE-SSW direction. The KFS is longer than formerly shown and extends into and beyond the Kazaure belt area. In addition, the Kalangai Fault System (KFS) was named the Zungeru Fracture System by Oluyide (1988), who traced it northwards to the Niger Republic, and south-westwards, to the Ifewara Fault of Wright (1976), as illustrated in Fig. 8.2. The north-eastward extension of the dextral KFS into the neighbouring southern Niger Republic, provides a further indication of the regional setting of this line of continuity (Section 8.4).

In a regional sense, the NE-SW trending dextral faults have complementary NW-SE trending sinistral ones (Ball, 1980). Workers in the Nigerian basement have mapped a number of such sinistral transcurrent fault zones with NW-SE trends (McCurry, 1976; Rahaman et al., 1983; Oluyide, 1988 and Ike, 1988). The faults in NW Nigeria have variously been interpreted as evidence for fault bounded ensialic basins of deposition of the schist belts (Chukwu-Ike, 1977; 1978) or as evidence for

a major suture where small oceans closed (Rahaman, 1988b; Ogezi, 1977; Ajibade and Wright, 1989).

McCurry (1976) suggested that the pattern of these fracture systems was probably established during the Pan-African orogeny. Similarly, Ajibade and Wright (1989) observed that the dextral sense of shearing along the two main NNE-trending fracture systems in NW Nigeria is consistent with the movement pattern required by a Pan-African crustal shortening. Ball (1980) also considered this fault to be the result of a horizontal maximum stress axis `õ 1' oriented E-W.

The faults are considered as first order dextral and sinistral faults in response to a primary E-W stress, reactivated towards the end of the Pan-African orogeny. The continental collision at the margin of the rigid West African Craton has been linked to this E-W compression.

8.4 CORRELATION WITH DAMAGARAN, HOGGAR AND ADRAR DE FORAS REGIONS

The Nigerian basement (including the KZSB region) has many common features with northern Damagaran and the central zone that comprises Central Hoggar and Eastern Adrar Des Iforas region (Section 2.6). These regions formed the northern sector of the Pan-African mobile belt at the eastern margin of the West African craton (Black and Guirod, 1970). The major

tectonic episodes as well as formation of orogenic granites in both areas are ascribed to the Pan-African event. This appears to explain the occurrence of similar tectono-metamorphic imprints in the two areas.

Turner and Webb (1974) were among the first to correlate the rocks of the Kazaure Schist Belt with similar rocks in the Damagaran region of Southern Niger. They also traced the dextral Kalangai fault system as a silicified zone near Maibara that extends northeastward into the Basement of Damagaran. This is supported by Black (1980) who suggested the continuity between the structures and lithologic formations in the Nigerian-Benin terrain and that of Niger region.

In particular, Ball (1980) proposed that the Nigerian, Mali and Hoggar transcurrent faults and fractures are a part of a major strike-slip conjugate fault system reactivated during the Pan-African. Similarly, Katz (1981) describes the NE- and SE- trending fracture systems of Africa and South America, as representing a conjugate set developed as a result of primary dextral simple shear along zone of continental dimensions. The few NW-SE faults are mainly sinistral second order strike slip faults (Ramsay, 1967; Park, 1983). The present interpretation appears to conform with observations from the whole of the Nigerian basement and the Adrar Des Iforas - Hoggar region, all of which lie in the internal region of the Pan-African belt of West Africa.

8.5 MODEL FOR THE EVOLUTION OF THE KAZAURE SCHIST BELT IN THE CONTEXT OF NW NIGERIA

8.5.1 Preamble

The Lithospheric extension model (McKenzie, 1978; Jarvis and McKenzie, 1980) was used to explain the formation of rifts in West Africa (Burke, 1976; Falvey and Middleton, 1981; Middleton, 1984; Fairhead and Okereke, 1990). Some other models on the evolution of sedimentary basins and rifts include: the Lithospheric uplift model (Girdler et al., 1969; Bott, 1981) and the Wedge subsidence model (Bott, 1976).

Of these models, the Lithospheric extension model best conforms to the geophysical and geological evidence for the possible evolution of the Archaen and lower Proterozoic Rocas Verdes belt in South Chile (Tarney et al., 1976). They proposed back-arc extension, basin formation and sedimentation, followed by closure of the basin and syn-orogenic plutonism, to explain the evolution of the Rocas Verdes granite-greenstone belt (Fig. 8.3).

The Rocas Verdes belt marginal basin model was modified and used to explain the evolution of the Anka and Maru belts by Egbuniwe (1982) and Holt (1982), because of the similarities between greenstone belts and schist belts (Section 1.3.2). The same models (Figs. 2.2 and 2.3) and others on the evolution of the NW Nigeria schist belts have now been invoked to explain the evolution of the KZSB (Figs. 8.4, 8.6 and 8.7).

8.5.2 Origin of the Kazaure Palaeo-basin

Parts of the present West African craton and the Benin-Nigeria shield are assumed to have formed a large stable shield in pre-Pan-African times. This stable block underwent doming, extension and continental rifting at the present West African cratonic margin, probably related to crustal tension and thinning in the underlying basement caused by mantle upwelling. This led to lithospheric stretching (McKenzie, 1978), resulting in brittle fracture in the upper thinned continental crust and ductile flow in the lower, as well as a thinned continental crust and plume-related tectonics in Nigeria.

The resultant rifting and crustal extension led to the formation of rifts (Fig. 8.4), troughs, graben- and horst-complexes and basins, which acted as elongate basins of deposition for the protoliths of the schist belts in Nigeria. (e.g Kroner 1984). One of these acted as an elongate basin of deposition for the protoliths of the Kazaure Schist Belt. The fractures (e.g Kalangai Fault System) provided vents along which volcanic materials were poured into the Kazaure basin. This probably include Fe-Mn rich sediments derived from volcanic exhalations which are the protoliths of the Banded Iron Formation (BIF).

The sediments were deposited in the basin with the coarseness of the basin fill decreasing from west to east, such that

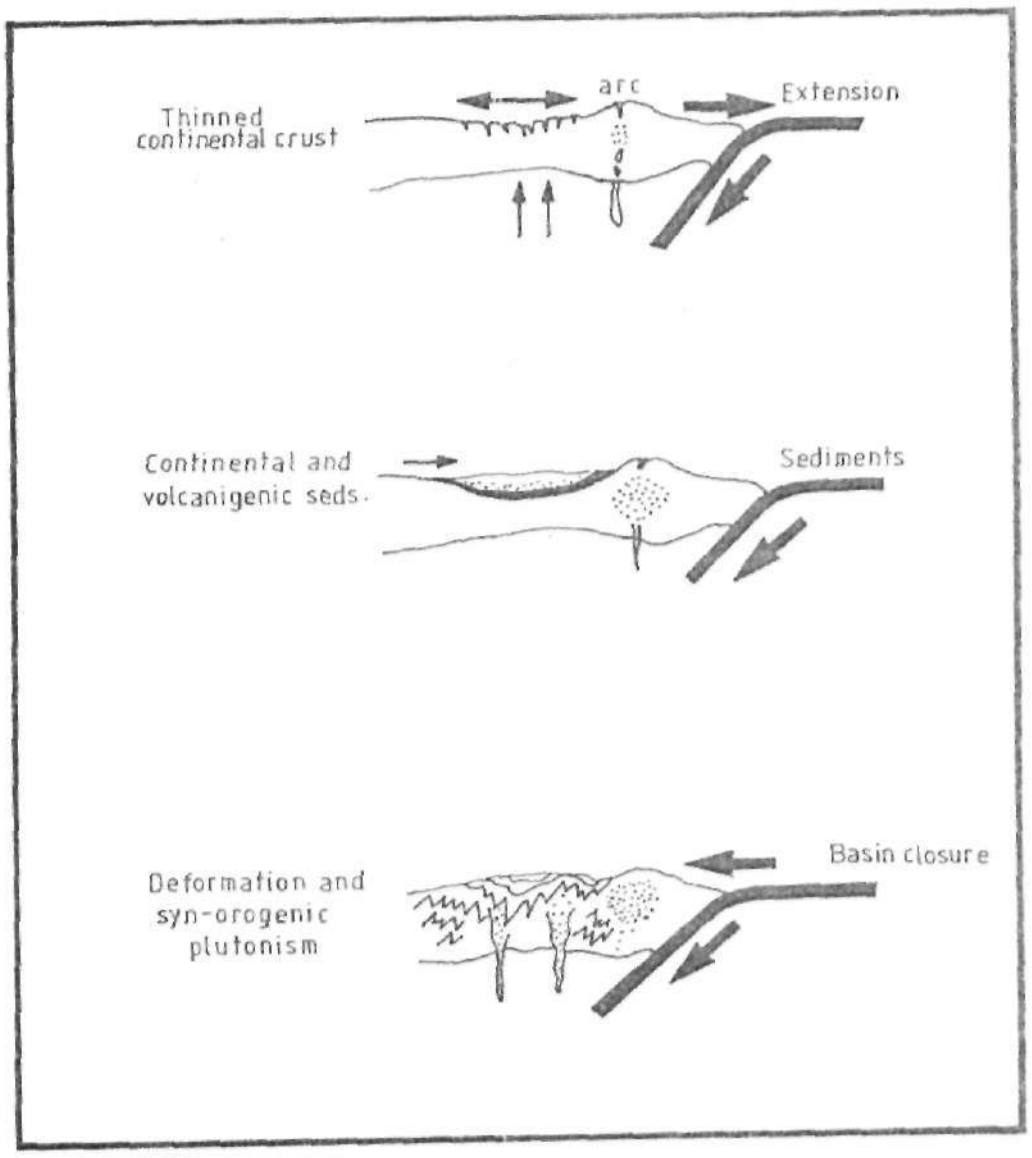


Fig. 8.3. Development of a greenstone type margin basin by back-arc extension (Modified from Tarney et.al., 1976).

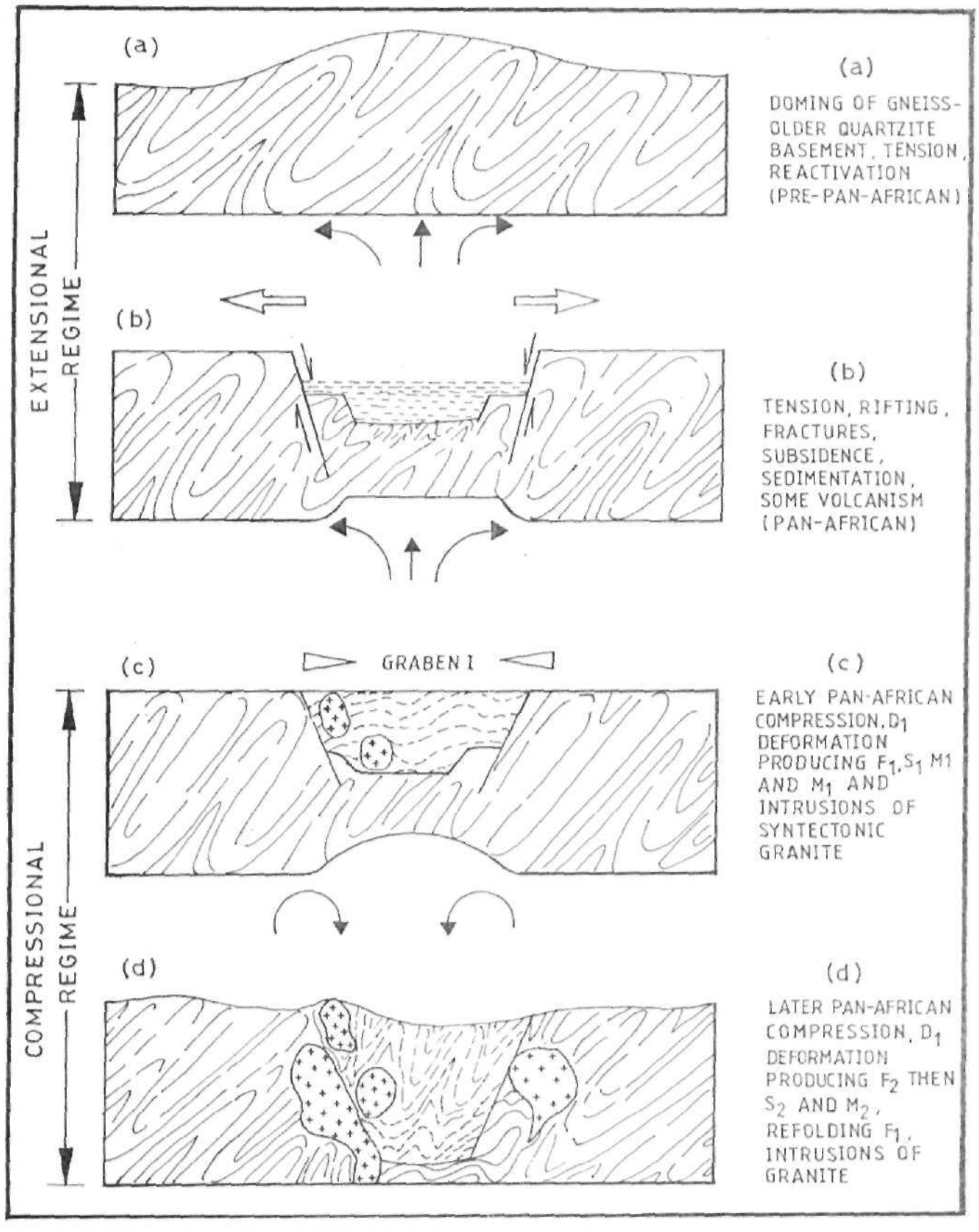


Fig. 8.4 Diagrams showing hypothetical evolution of the Kazaure Schist Belt.

conglomerates pass into sandstones and shales. There are vertical movements during the stretching phase due to isostatic compensation of the thinned low density crust and weight of sediments accumulating in the basin. This led to sedimentation which is accompanied by intermittent subsidence on the rather unstable Kazaure palaeo-basin.

8.5.3 Compression of the Kazaure Palaeo-basin

Subsequent closure of the Kazaure basin led to D_1 deformation and the reactivation of faults. At this time the flat-lying Kazaure supracrustals were first heteregenously deformed and metamorphosed, while the migmatite-gneiss basement was reactivated by the D_1 event.

D_1 induced a tectonic layering, S_1 foliation, accompanied by a medium grade (amphibolite facies) regional metamorphism, M_1. The D_1 deformation also formed very rare early layer-parallel isoclinal folding along the N-S axis. These folds are overturned to the west and with flat-lying fold axes (F_1) oriented N-S, because of the prevailing E-W compressive stress.

Another episode of the compression coupled with the prevalent temperature conditions led to the formation of the second deformational event (D_2). This produced steeply dipping to upright NNE- trending F_2 folds, with penetrative and steeply

dipping axial surfaces (S_2). The S_2 were accompanied by a low grade (greenschist) M_2 regional metamorphism. These later F_2 folds have deformed and refolded the earlier (F_1) in some places, and is responsible for the complex NNE- structural grain of the Kazaure schist belt.

Melts were generated from the partial melting of the lower crust and upper mantle. The "Older Granite" melts rose into already existing or developing large scale folds in the Younger Metasediments. The display of weak foliation indicates that these plutonic rocks were emplaced early in the period of D_2 regional deformations.

8.5.4 Late tectonic effects

Late tectonic effects include epeirogenic uplift, reactivation of fracture and fault zones, and intrusion of aplites, quartz and pegmatite veins and dykes. The M_1 and M_2 were later followed by a period of static metamorphism (X), when there were no major disturbances. The X metamorphism mainly accompanied the deformation episode that resulted in the formation of brittle structures, as described earlier. The widespread occurrence of secondary albite, muscovite and chlorite associated with the new penetrative D_2 structures suggests the localised retrogression of the M_1 to low grade greenschist facies.

Field evidence reveals that emplacement of most of the pegmatitic and quartz veins resulted from the development of fractures when the basement rocks were uplifted epeirogenically. The Kalangai Fault System (KFS) is believed to have formed silicified zones that bounded the western side of the area during this time. It also characterised the E-W compressional stress field.

8.5.5 Timing of Basin formation and Closure

The main features of the above model include crustal extension and thinning and the development of the Kazaure palaeo-basin. These are considered to be related to subduction at the West African cratonic margin during the early stages of the Pan-African orogeny (Section 2.3.3). During this event a marginal basin environment (Hynes, 1987) developed in the Nigerian-Benin shield, due to plume-related tectonics that led to Back-arc extension (Fig. 8.5). The back-arc extension was sufficient for the formation of the Kazaure basin and emplacement of volcanic rocks.

The Buem ocean started closing after 800 Ma ago (Black et al., 1979). If this is the case, it is most likely that the initial rifting and initiation of the Nigerian palaeo-basins belts which is associated with this Pan-African closure, took place after 800 Ma ago. The initiation of the said palaeo-basins

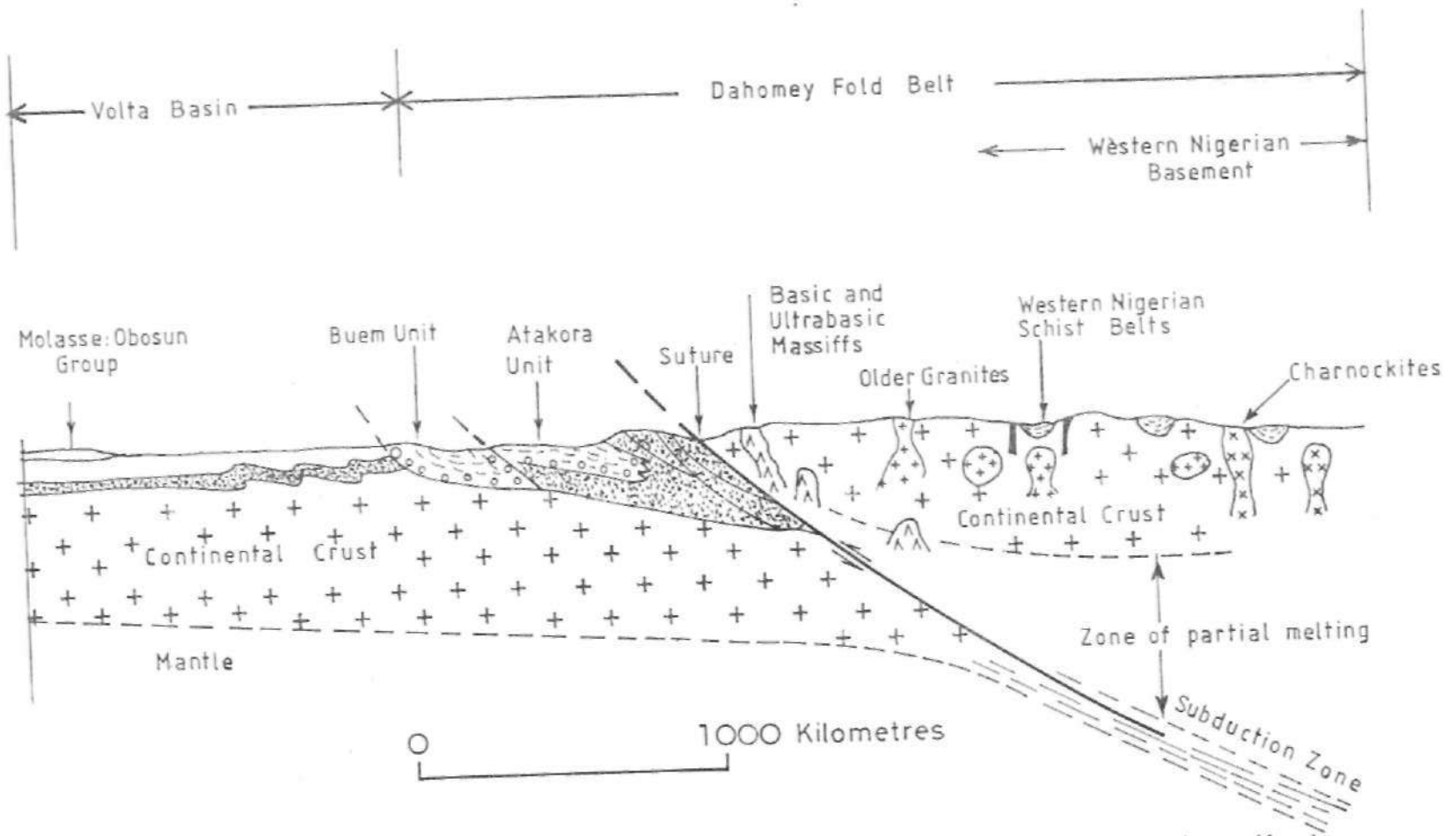


Fig. 8.5. Schematic section across the West African margin showing the effects of the Pan-African event in basement of Western Nigeria. (Modified from Burke and Dewey, 1973; Troumpette, 1979).

could have also been related to the rifting that took place around 800 Ma ago in the Hoggar (Bertrand and Caby, 1978).

An episode of Pan-African compression (Section 2.2.3), related to E-W crustal shortening due to plate tectonic processes led to horizontal shortening and the first deformational event (D_1) in the schist belts. Continuation of the compression episode led to the formation of the second deformational event (D_2) and the intrusion of Older Granite plutons.

This event was the last movement due to continental collision and is also marked by NE-SW trending dextral shear zones (Turner, 1983; Utke, 1987). These strike-slip planes could have been the developing fracture zone under extensional regime, which are now modified (e.g Kroner, 1984).

8.5.6 Remarks on the Evolution of the whole NW Nigeria Schist Belts

There seems to be some geographical correlation between the NW Nigeria schist belts as you move from north to south (Figs. 1.1 and 2.1). Starting from east to west: the Kazaure Belt seems to be the northern projection of the Malumfashi Belt; the Wonaka belt seems to link with the Kushaka Belt; the Maru Belt seems to link southwards with the Birnin Gwari Belt; the Anka Belt is similar to the Zuru Belt (Grant, 1978; Turner, 1983).

The new proposed model in this study considers the evolution of the Nigerian schist belts in the context of Pan-African deformations, under extensional and compressional regimes. West of the Anka area, back-arc extension was sufficient for the formation of a small basin (probably the Sado/Maikwonanga ocean?) and the emplacement of volcanic rocks (Ogezi, 1977; Holt, 1982). The Pan-African orogeny is the first time of deformation, metamorphism and early plutonism in these supracrustals. It is also the time for subsequent folding, metamorphism and stabilisation of the schist belts. The Pan-African compression also indicates the closure of one or more marginal basins in the NW Nigerian basement.

The Pan-African event could be contemporaneous with the closure of the small ocean at the Zuru microcontinental margin. The presumed palaeosuture is at the NW Nigerian basement where there is sequence of mylonite, basic/ultrabasic Sado and Maikwonga igneous assemblages related to the Anka Fault Zone (Ajibade and Wright, 1989). Plate tectonic processes were responsible for juxtaposing the Anka with the Zuru Belt. This explains the marked difference in structures on either side of the Zuru suture. The NW Nigeria schist belts thus evolved through both ensialic and ensimatic processes (Figs. 8.6 and 8.7).

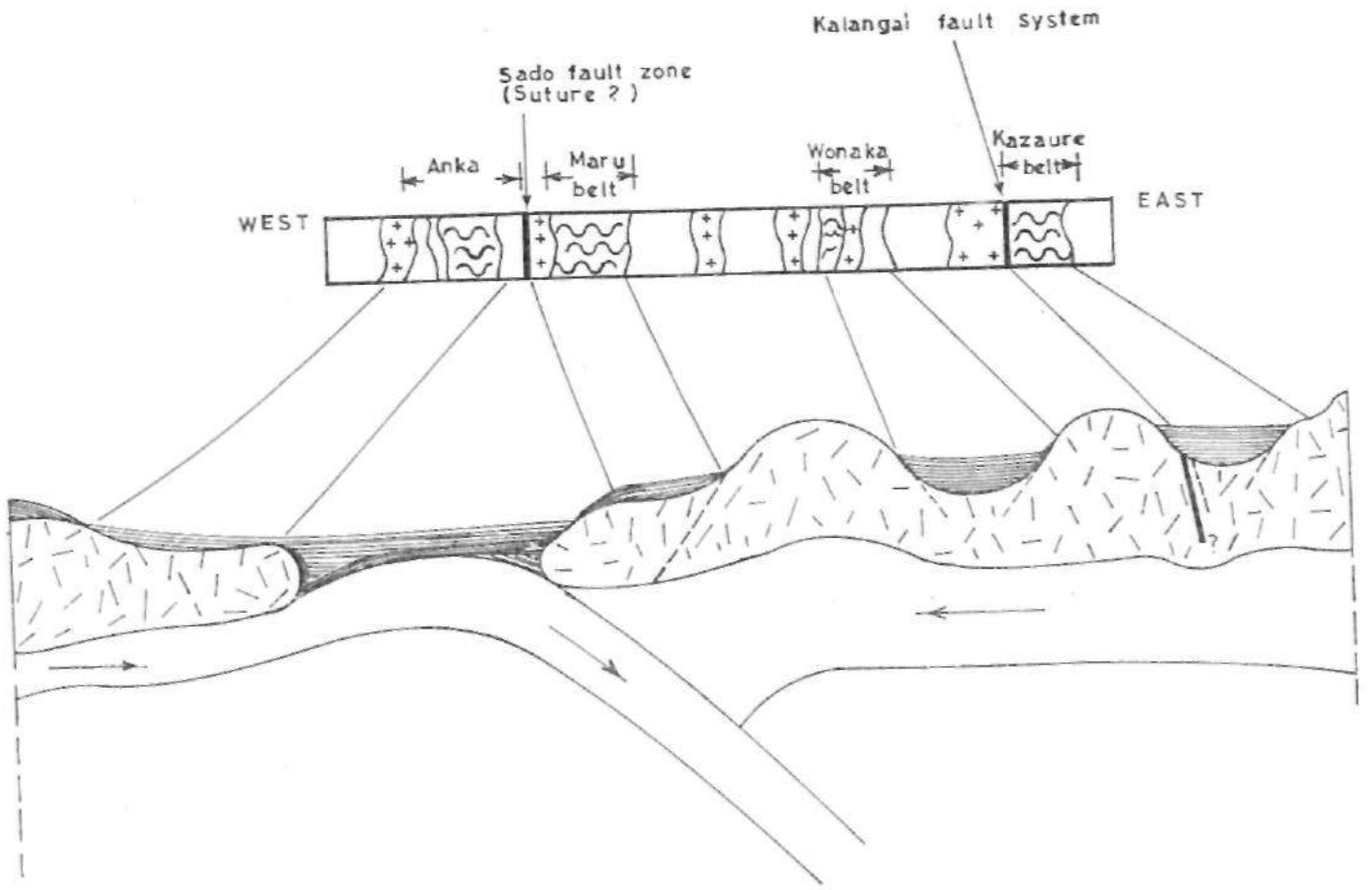


Fig. 8.6. Diagrams showing hypothetical evolution of Anka, Maru, Wonaka and Kazaure schist belts. The line of section is along 12°30'N. Diagrams are not to scale.

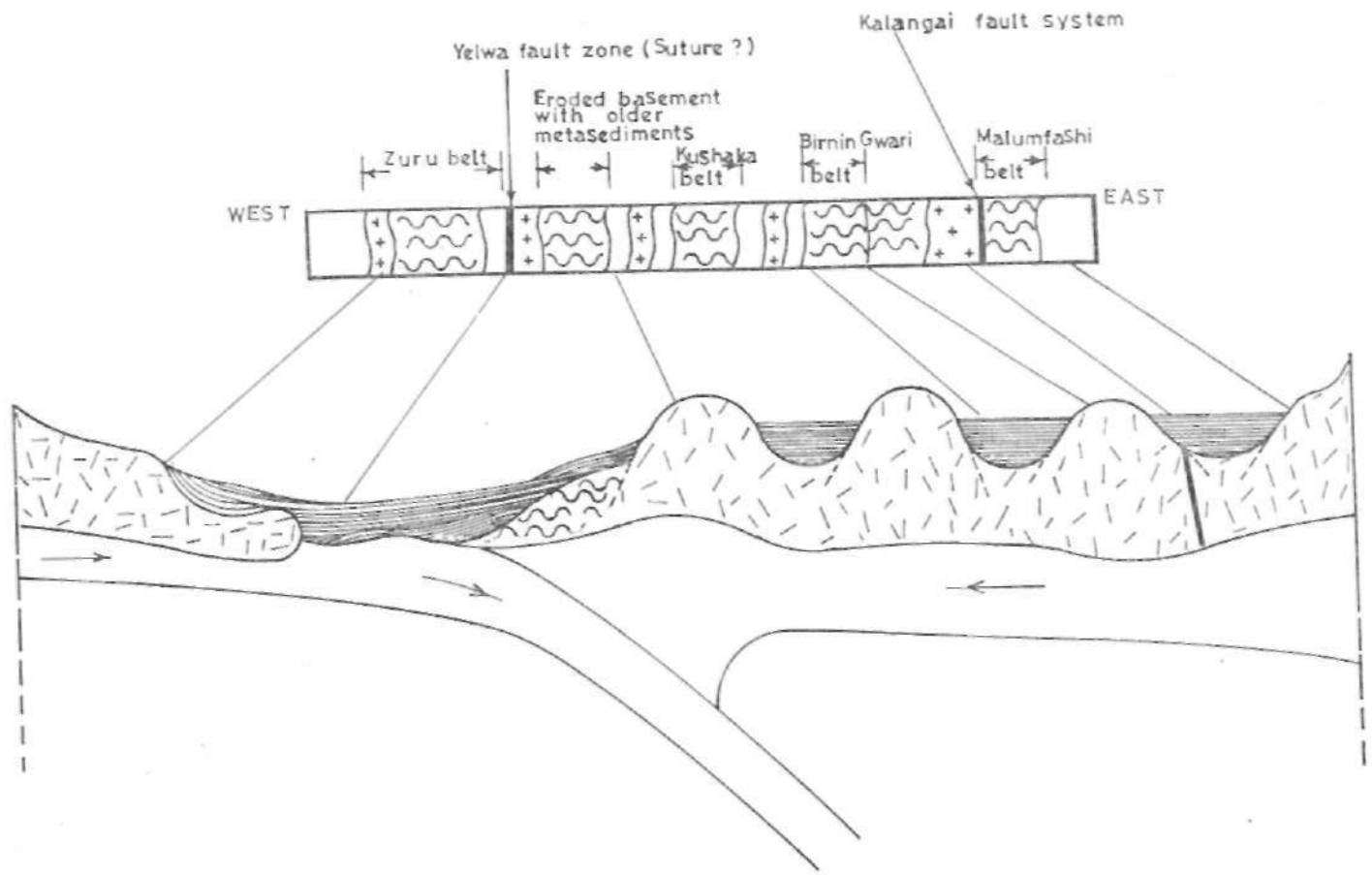


Fig. 8.7. Diagrams showing hypothetical evolution of Zuru, Kushaka, Birnin Gwari and Malumfashi belts. The line of section is along 11°05'N. Diagrams are not to scale.

Some of the various features that support the presumed Zuru palaeosuture include the great width of the Pan-African belt, the spread of ages within the Pan-African (750-450 Ma) and relics of Archaean to Eburnean ages, recumbent structures (Hubbard, 1975) and the contrasted volcano-sedimentary characteristic of the different supra-crustal belts i.e the NW Nigeria schist belts.

A previous model of evolution suggested a westward dipping Benioff zone in NW Nigeria (e.g Wright, 1979 and Fig. 2.2). However, following Burke and Dewey (1972), Grant (1973) and Trompette (1979), the probable suture at the Zuru terrain (Ajibade and Wright, 1989) is interpreted as an eastward dipping subduction related zone (Figs. 8.6 and 8.7).
The same Pan-African event also caused syn to post-tectonic plutonism for the second time in the belts, as is suggested by the presence of Older Granite plutons with Pan-African ages. Generation of igneous rocks at some distances from the sites of subduction are usually related to partial melting of the upper mantle and reactivation of older crustal structures during plate tectonic event.

The I-type chemistry of the Older Granites intruding/ separating the NW Nigeria schist belts, suggests their

comparison to magmas generated in subduction and continent-continent collision zones. As such, most earlier workers attributed the Older Granites to the subduction zone that emerged at the margin of the West African craton 250 to 350 Km to the west of the Nigerian Pan-African province.

However, the distance from the West African craton margin (site of the Pan-African subduction event) to the nearest Nigeria schist belt area is large (200-250 km), while the distance suggested by the marginal basin model of Tarney et al. (1976) is 50-100 km. To accept the model, it has to therefore be assumed that the Zuru palaeo suture has also contributed to the generation of igneous rocks not far from the site of subduction.

The present proposed geotectonic model of evolution of the schist belts is mostly in agreement with previous models of evolution of NW Nigeria belts. It is also in aggrement with that of Olade and Elueze (1979), who suggested a marginal basin model for the origin of the Pan-African schist belts.

The model explains the contrasting lithologies between some of the belts by proposing that some of the belts were developed in separate basins, as was suggested by some earlier workers

(Truswell and Cope, 1963; Grant, 1978 and Turner, 1983). For the Kazaure Belt, the model is consistent with the present

interpretation that rocks of this belt were deposited and deformed in an ensialic sedimentary trough (Section 8.4.7).

The new model only differs from previous ones in suggesting an additional probable suture as also responsible for the generation of the Older Granite plutons, in an attempt to explain the apparent discrepancy due to the distance of the belts from the sites of subduction.

8.6 CONCLUSION

The present study provides convincing evidence of similarity in structures, lithologies, and metamorphism between the Kazaure Schist Belt and other NW Nigeria schist belts. The mapping has allowed for the extension of the areal extent of the KZSB belt and for extending the area underlain by basement complex rocks to as far east as 80^0 40' in the Kazaure belt area. The presence of basement inliers between the adjacent Kazaure and Malumfashi belts, is also quite significant.

The Kazaure Schist Belt evolved through ensialic processes. The protoliths of the metasediments forming the KZSB must have been deposited in a predominantly shelf or deltaic

environment to allow deposition of coarse clastic sediments. The proposed geotectonic model of evolution of the KZSB is in agreement with that for some neighbouring belts whose

evolution was ascribed to ensialic processes (e.g Chukwu-Ike, 1978; Ajibade, 1980; and Olabaniyi, 1997).

As already observed, there are significant similarities between rock-types, structural and metamorphic events in the Kazaure Schist Belt and the present studied northernmost portion of Malumfashi Schist Belt. The age of D_1 and D_2 deformations and metamorphisms in the Kazaure-Malumfashi Belts has been shown to be Pan-African on comparative grounds, while the granite plutonism during the same late Proterozoic times, are as a result of basement reactivation due to plate tectonics subduction processes. The migmatite-gneiss basement and the younger metasediments were deformed and metamorphosed together as a single unit during the two deformation events.

The major event of metamorphism correspond to medium temperature amphibolite facies, which probably formed the gneisess due to the same thermal event that caused 2migmatisation. In summary, the early stage of the Pan-African is the probable time of initiation and first metamorphism under medium temperature amphibolite facies, and the middle-late Pan-African orogeny as the time for subsequent folding,

low grade (greenschist facies) metamorphism and stabilisation of the Kazaure Schist Belt. The intrusive and extrusive rhyolites of Daura and their related younger granites and syenites were emplaced much later during the Mesozoic era (Turner and Webb, 1974).

Apart from the exposed ridges defining the KZSB, other ridges may exist buried beneath the intervening superficial sand and clay deposits of the Chad formation. This suggestion was earlier made by Fitches et al. (1985) and Ajibade et al. (1987a) who have shown that each belt was not initially confined to its present map limits.

The structures in the Kazaure Schist Belt and those from the Malumfashi Schist Belt follow a similar structural framework outlined by two isoclinal foldings, one recumbent the later upright. In the context of the disposition and evolution of the schist belt of NW Nigeria, the present work considered the Kazaure Schist Belt and the Malumfashi Schist Belt to be a pair of belts of similar lithologies and evolution.

8.7 RECOMMENDATIONS FOR FUTURE WORK

There are usually more than one hypothesis on the evolution of polymetamorphic areas like the Nigerian basement. Therefore, proposing an acceptable tectonic model for the geotectonic, geochemical and geochronological evolution of the Nigerian

KASH

schist belts and their overall position in the regional evolution of the West African region, provides an area of future research.

To successfully do this, more geochemical, petrological and geochronological data are needed in order to further constrain the evolution of the Nigerian basement, especially in the northwest where it outcrops most.

REFERENCES

Abubakar, S.M., 1988: Determination of Physical relationships between aeolian deposits, relief and vegetation using satellite image and airphotographs in SE Katsina. *Unpublished B.Sc. Thesis, Dept. of Geography, Bayero University Kano.*

Adekoya, J.A, 1993: Proterozoic Maru and Birnin Gwari banded iron formations northwestern Nigeria. *J. Min. Geol.* 29, pp. 63-76.

Aderotoye, S.F., 1977: The geology of the 1:100,000 Sheet 35 (Kazaure). *Geol. Surv. Nigeria* Unpubl. Rept. No. 1045.

Ajibade, A.C., 1971: The geology of the country around Zungeru, North Western State of Nigeria. Unpublished *M.Sc. Thesis, Univ. Ibadan,* pp. 12-23.

Ajibade, A.C., 1976: Provisional Classification and Correlation of the Schist Belts of northwestern Nigeria. *In. C.A Kogbe (Ed) Geology of Nigeria,* pp. 85-90, Elizabethan Publishing Co.

Ajibade, A.C., 1980: Geotectonic Evolution of the Zungeru Region, Nigeria. Unpublished *Ph.D. Thesis of University College of Wales, Aberystwyth,* pp. 286.

Ajibade, A.C., 1982: The origin of the Older Granites of Nigeria: Some evidence from the Zungeru region. *Nigeria Jour. Min. and Geol.*, 19, pp. 223-230.

Ajibade, A.C., Fitches, W.R and Wright, J.B., 1979: The Zungeru Mylonites, the identification of a Major tetonic unit in the NW Nigerian Basement. *Revue de Geol. Phys.*, 21[5], pp. 359- 363.

Ajibade, A.C. and W.C. Mbonu, 1982: On the Silicified Fault Zone in the Gneissic Complex of the Malumfashi Area, Nigeria. *Nigeria Jour. Min. and Geol.*, 19, pp. 223-230.

Ajibade, A.C., Woakes, M. and Rahaman, M.A., 1987a: Proterozoic crustal development in the Pan-African regime of Nigeria. *American Geoph. Union*, pp. 259-271.

Ajibade, A.C., Fitches, W.R. and Wright, J.B., 1987b: Basement Cover relationships in the Minna region of the Pan-African domain of Nigeria. *Current Res. In: Africa Earth Sciences*. Eds. G. Matheis and H. Schantelmeier.

Ajibade, A.C. and Wright, J.B., 1989: The Togo-Benin-Nigeria shield: Evidence of crustal aggregation in the Pan-African belt. *Tectonophysics, 165*; pp. 125-129.

Ajidahun, M., 1996: Geology of the Area around Amaryawa-Kwaita and their environs, Part of Sheet 35 (Kazaure). *Unpublished B.Sc. Thesis*, A.B.U. Zaria.

Akinyede, O.A., 1981: A geochemical stream sediment survey in Kafur-Malumfashi area, Kaduna State, Nigeria. Unpublished *M.Sc. Thesis. A.B.U. Zaria.*

Annor, A.E., 1995: U-Pb age for Kabba-Okene granodiorite gneiss: Implication for Nigeria's basement chronology. *Africa Geosci. Rev. 2*, pp. 101-105.

Annor, A.E. and Coker A.S., 1994: A Structural Appraisal of the cover and Basement Hypothesis for the Precambrian terrain of Birnin Gwari, Kushaka Area, NW Nigeria. (Abs.) 30th Conf. of *Nigerian Mining, and Geos. Soc.*, Jos, pp. 12.

Annor, A.E., Olobaniyi, S.B. and Mucke, A., 1998: Are the Nigerian Schist Belts of Neoproterozoic Age? 34th Annual Conf. of *Nigerian Mining, and Geos. Soc.* March 1998, Ife.

Baer, H.P, 1981: Structural evolution of Precambrian to lower Paleozoic fold belts in West Africa (Ghana) and their continuation in NE brazil. In: *UNESCO Bulletin D'information Newsletter*, pp. 4-5.

Bafor, B.E., 1982: The Zungeru metavolcanics of north-western Nigeria: their geochemistry and tectonic setting. *J. Min. Geol. 18*, pp. 42-52.

Bafor, B.E., 1988: Some geochemical considerations in the evolution of the Nigerian basement in the Egbe area of southwestern Nigeria. In: *Precambrian Geology of Nigeria. Geol Surv. of Nigeria*, pp. 277-288.

Barber, W., 1965: Pressure water in the Chad formation of Bornu and Dikwa Emirates, NE Nigeria. *Geological survey of Nigeria Bulletin No. 35.*

Barker, A.J., 1990: Introduction to metamorphic textures and microstructures, *Blackie*, pp. 162.

Ball, E., 1980: An example of very consistent Brittle Deformation Over a wide intra continental Area: the late Pan African Fracture system of the Tuareg and Nigerian Shields. *Tectonophysics, 61 [4]*, pp. 363-379.

Bertin, E.P., 1975: Principles and practice of X-ray spectrometric analysis. *Plenum Press, New York*, pp. 1076.

Betrand, J.M.I. and Caby, R., 1978: Geodynamic Evolution of the Pan-African Orogenic Belt. A New Interpretation of the Hoggar Shield. *Geol. Rundsch. 67*, pp. 357 - 338.

Betrand, J.M., Dupuy, C., Dostal, J. and Davison, I. 1984: Geochemistry and geotectonic interpretation of granitoids from central Iforas (Mali, West Africa). *Prec. Res. 26*, pp. 265-283.

Blacburn, W.H., 1974: Origin of the cordierite-bearing gneisses of the Gananoque-Westport area, Ontario. *Annal. Soc. Geol. Belgique 97*, pp. 297-309.

Black, R., 1980: Precambrian of West Africa. *Episodes 4*, pp. 3-8.

Black, R. and Guirod, M., 1970: Late Proterozoic to Recent igneous activity in West Africa and its relationship to basement structure. In: T.N. Clifford and I.N. Gass (eds), *African Magmatism and Tectonics. Hafner. Darien. Conn.*, pp. 185-210.

Black, R., Caby, R., Monssine Pouchkin, A., Bayer, R., Bertrand, J.M., Bourllier, A.M., Fabre, J. and Lesquer, A., 1979: Evidence for Late Precambrian plate tectonics in W. Africa. *Nature, 278*, pp. 233-237.

Bott, M.H.P., 1976: Formation of sedimentary basin of Graben type by exension of the continental crust, *Tectonophysics, 36*, pp. 77-86.

Bott, M.H.P., 1981: Crustal doming and the mechanism of continental rifting. Tectonophysics, 73, pp. 1-8.

Brooks, C., Hart, S.R. and Wendt, I., 1972: Realistic use of two-error regression treatments applied to rubidium data. *Rev. Geophys. Space Phys., 10*, pp. 551-577.

Burke, K., 1976: Development of graben associated with the initial rupture of the Atlantic Ocean, *Tectonophysics 36*, pp. 93-112.

Burke, K.C. and Durotoye, B., 1970: The Quarternary in Nigeria: A review. *Bull. de Asequa No. 27/28.* pp. 70-98.

Burke, K.C. and Dewey, J.F., 1972: Orogeny in Africa. In Dessauvagie, T.F.J. and Whiteman, A.J. eds., *African Geology, Univ. Ibadan* 1970, pp. 583-608.

Butler, B.C.M., 1965: A chemical study of some rocks of the Moine series of Scotland. *Quart. J. Geol. Soc. London 121,* pp. 163-208.

Caby, R., Bertrand, J.M.L. and Black, R., 1981: Pan-African Ocean closure and continental collision in the Hoggar-Iforas segment, central Sahara. In: Kroner, A. (ed) Precambrian Plate Tectonics. *Elsevier, Amsterdam,* pp. 407-34.

Chappel, B.W. and White, A.J.R., 1974: Two contrasting granite types. *Pacific Geology, 8,* pp. 173-174.

Chikhaoui, M., Dupuy, C. and Dostal, J. 1980: Geochemistry and Petrogenesis of late Proterozoic volcanic rocks from north western Africa. *Contri. Min. Petrol. 73,* pp. 375-388.

Chinner, G. A., 1978: Metamorphic rocks, p.343-427. In Nockolds, S.R. Kust, K.W. O'B and Chinner, G. A. *Petrology for students, Cambridge University Press Center,* pp. 455.

Chukwu-Ike, I.M., 1977: Regional Photogeologic of the Tectonic Features of the Central Nigerian Basement Complex: A Satellite Imagery Based study. Unpublished *Ph.D. Thesis University of London.*

Chukwu-Ike, I.M., 1978: The regional tectonic setting of the Northwestern Nigeria Low-grade metasedimentary belt. *J. Min. and Geology, 15,* pp. 19-22.

Clifford, T.N., 1970: The Structural Framework of Africa, in Clifford, T.N. and Gass, I.G. (Eds)., *African magmatism and tectonics,* Oliver and Boyd, (Edinburg) pp. 1-26.

Cooray, P.G., 1974: Some aspects of the Precambrian of Nigeria: A review. *Journal Min. and Geology, 8(1),* pp. 17-43.

Dada, S.S., 1995: Crust forming Ages and Proterozoic crustal evolution: Reappraisal of current Interpretations. *Paper read at 31st Annual Conf. of Nigerian Mining, and Geos. Soc.* March 1995, Calabar.

Danbatta, U.A., 1986: Geology of Gital and the Photogeology of the Surrounding Parts of Dass-Tafawa Balewa areas, Bauchi State. Unpublished *B.Sc. Thesis, A.B.U. Zaria.*

Danbatta, U.A., 1991: Geologic Investigations of the SW portion of the Zuru Schist Belt, NW Nigeria. Unpublished *M.Sc. Thesis, A.B.U. Zaria.*

Danpullo, S.B., 1996: Geology of the Area around Kunchi and its their environs, Part of Sheet 35 (Kazaure). *Unpublished B.Sc. Thesis, A.B.U. Zaria.*

Dessauvagie, T.F.J., 1974: Geological Map of Nigeria, 1:1,000,000. *J. Min. Geol. 1975 (for 1972), 9(142),* pp.3-28.

Deer, W.A., Howie, R.A. and Zussman, J., 1966: An Introduction to Rock-forming Minerals. *Longman London,* pp. 528.

Dunstan, W.R., 1908: Report on the results of the Mineral Survey of Northern Nigeria, 1907-1908. *Colon Rep. Misc. Ser. No. 79.*

KASHIM IB...

Egbuniwe, I.G., 1982: Geotectonic Evolution of the Maru Belt, NW Nigeria Unpublished *Ph.D. Thesis, Univ. of Wales, Aberrystwyth.*

Egbuniwe, I.G., 1994: On the occurrence of silicified fault zone in Mainamaji Area, Bauchi State. *(Abs.) 30th Annual Conf. of Nigerian Mining, and Geos. Soc.* April 1994, Jos.

Ekwueme, B.N., 1983: Regional Metamorphism of Pelitic Rocks, South-East of Lokoja, Nigeria. *Nigeria Jour. Min. and Geol., 20,* pp. 71-77.

Ekwueme, B.N., 1985: Petrology, geochemistry and Rb-Sr geochronology of metamorphosed rocks of Uwet area, South eastern Nigeria. *Unpublished Ph.D. Thesis, Univ. of Nigeria.*

Ekwueme, B.N., 1987a: Structural orientations and Precambrian deformational episodes of Uwet area, Oban massif, SE Nigeria. *Prec., Res, 34,* pp. 269-289.

Ekwueme, B.N., 1987b: Kibaran orogeny in Africa - a re-evaluation. In: *Current Researches in African Earth Sciences* (ed. G. Matheis and H. Schandemeier) A.A. Balkema, Rotterdam, pp. 31-32.

Ekwueme, B.N., 1988: The Kibaran rocks of Nigeria, West Africa. *IGCP 255 Newsletter 1,* pp. 15-18.

Ekwueme, B.N., 1990a: On the Occurrence of crystalline (Basement Complex) Rocks in SW Ugep, Nigeria. *J. Min. Geol. 26,* pp. 65-74.

Ekwueme, B.N., 1990b: Rb-Sr ages and petrologic features of Precambrian rocks from the Oban massif, southeastern Nigeria. *Precambrian Research 47,* pp. 271 - 286.

Ekwueme, B.N., 1990c: The nature and distribution of Archaean in Nigeria. Extended *Abstract* 3rd International Archaean Symposium Perth, Australia. *Geoconferences W.A. Publication,* pp. 99-101.

Ekwueme, B.N., 1992: Rb-Sr age of Pan-African migmatites in the Oban massif SE Nigeria. *J. Afri. Earth Sci.* 15, pp. 65-72.

Ekwueme, B.N., 1993: *An Easy Approach to Metamorphic Petrology.* 1st Edition. Univ of Calabar Press, pp. 169.

Ekwueme, B.N., 1994a: *Elementary Crystallography and Mineralogy (including optics).* Univ. of Calabar Press Nigeria. pp. 290.

Ekwueme, B.N., 1994b: REE Abundances and distribution patterns of Lokoja Schists. (Abs.) *30th Annual Conf. of Nigerian Mining, and Geos. Soc.* March 1994, Calabar.

Ekwueme, B.N., 1995a: Pertogenesis of schists in southeast Lokoja, Central Nigeria. *Dec-Ford J. Pure & Appl. Sci.* Vol. 1, pp. 70 - 83.

Ekwueme, B.N. and Onyeagocha, A.C., 1982: The pre-Pan African features in northcentral Nigeria. *Nigerian Journal Min. Geol. 19 (2).* pp. 74-77.

Ekwueme, B.N. and Onyeagocha, A.C., 1985a: Metamorphic isograds of Uwet area, southeastern Nigeria. *J. Afr. Earth Sci. 3,* pp. 443-454.

Ekwueme, B.N. and Onyeagocha, A.C., 1985b: Petrology of intrusive rocks in the basement complex of Uwet area, Oban massif, southeastern Nigeria. *Nigerian Jour. Min. Geol. 22,* pp. 71-78.

Ekwueme, B.N. and Onyeagocha, A.C., 1986: Geochemistry of metasedimentary rocks of Uwet area, Oban massif, southern, in Nigeria. *Geol. Rdsh.* 75/2, pp. 411-420.

Ekwueme, B.N., Caen-Vachette, M. and Onyeagocha, A.C., 1987: Rb-Sr geochronology of metasedimentary schists and gneisses in Uwet area, Oban massif, southeastern Nigeria. *Nigerian Jour. Min. Geol.* 23, pp. 119-124.

Ekwueme, B.N., and Attoh, K., 1997: Greenstone belts of the West African shield. In: *Tectonic Evolution of Greenstone Belts*. M.J. De Wit and L.D. Ashwal (Eds.), Oxford Monograph on Geology and Geophysics, Clarendon Press, Oxford, pp. 517 - 528.

Ekwueme, B.N. and Onyeagocha, A.C., 1990: Temperature-Pressure distribution patterns in metamorphosed rocks of the Nigerian Basement Complex- a preliminary analysis. *J. Afr. Earth Sci* 11 No. 1/2, pp. 83 - 93.

Ekwueme, B.N. and Caen-Vachette, M., 1992: Kibaran charnockites in Oban massif, SE Nigeria. *IGCP 255 Newsletter/Bulletin 4,* pp. 67 - 71.

Ekwueme, B.N., and Kroner, A., 1994: The Nature of the Archaean Crust in Nigeria; a new discovery. *USGS circular 1107.*

Elueze, A.A., 1988: Geology of the Precambrian Schist belt in the Ilesha area, Southwestern Nigeria. In: *Precambrian Geology of Nigeria.* Geol. Surv. Nig. pp. 77-82.

Fairhead, J.D. and Okereke, C.S., 1990: A regional study of the West African rift system in Nigeria and Cameroon, In I.B. Ramberg and G. Quale (Es)., Continental and Regional Characteristics, *Tectonophysics, 143,* pp.141-159.

Falconer, J.D., 1911: *The Geology and Geography of northern Nigeria.* Macmillan, London.

Falvey, D.A. and Middleton, M.F., 1981: Passive continental Margins: evidence for a pre-break up, Deep crustal metamorphism, subsidence mechanism, *Oceanic, Acta., No. 59,* Colloque C3 Geology of Continental Margins, pp 103-114.

Fargher, M.N., 1961. The Precambrian geology of the *1:100,00 sheet 52 (Anka), Sokoto Province. Geol. Survey Nigeria (GSN)* Unpublish. Rept. No. 1324.

Fitches, W.R., 1970: Pan-African Orogeny in the coastal region of Ghana. *Nature, 226,* pp. 744-746.

Fitches, W.R., Ajibade, A.C., Egbuniwe, I.G., Holt, R.W., and Wright, J.B. 1985: Late Proterozoic Schist belts and Plutonism in NW Nigeria. *J. Geol. Soc. London, 142,* pp. 319-337.

Flinn, D. 1962: On folding during 3-D progressive deformation. *Q.J.G.S. Vol. 118.* pp. 385 - 433.

Garba, M.L., 1996: Geology of the Area around Amaryawa-Kwaita and their environs, Part of Sheet .Kazaure. Unpublished *B.Sc. Thesis, A.B.U. Zaria.*

Girdler, R.W., Searle R.C., and Sowerbutts, W.T.C. 1969. Evolution of rifting in Africa, *Nature, 224:* pp. 1178-1182.

Grant, N.K., 1968: Complete Late Pre-Cambrian to Early Palaezoic Orogenic cycle in Ghana, Togo and Dahomey. *Nature, 215,* pp. 609-610.

Grant, N.K., 1969: The Late Precambrian to Early Palaeozoic Pan-African orogeny in Ghana, Togo, Dahomey and Nigeria. *Geol. Soc. Amer. Bull., 80,* pp. 45-56.

Grant, N.K., 1970: Geochemistry of Precambrian basement rocks from Ibadan, Southwestern Nigeria, *Earth planet. Sci. let., 10,* pp. 29-33.

Grant, N.K., 1971: A compilation of radiometric ages from Nigeria: *Jour. Mining Geology, v.6,* pp. 37-54.

Grant, N.K., 1978: Structural distinction between a metasedimentary cover and an underlying Basement in the 600 Ma Old Pan-African domain of north western Nigeria. *Geol. Soc. Amer. Bull., 89,* pp. 50-58.

Grant, N.K., 1979: The Late Precambrian to early Palaezoic Pan-African Orogeny in Ghana, Togo, Dahomey and Nigeria. *Geol. Soc. Amer. Bull., 80,* pp. 45-46.

Grant, N.K., Hickman, M.H., Burkholder, F.R., and Powell, J.L., 1972. Kibaran metamorphic belt in the Pan-African domain of West Africa. *Nature (London) Phys. Sci. 238,* pp. 90-91.

Grim, R.E., (1968): *Clay Mineralogy.* New York, McGraw-Hill, 1968, 2nd Edition.

Gupta, E.C. and Johannes, R.Y., 1982. Petrogenesis of a stromatic migmatite (Nelaug, southern Norway). *J. Petrology (Oxford), 23,* pp. 548-567.

Harper, C. T., Sherrer, G., McCurry, P. and Wright, J.B., 1973: K-Ar retention ages from Pan-African of northern Nigeria. *Geol. Soc. Amer. Bull, 84,* pp. 919-926.

Harpum, J.R., 1963: Petrographic classification of granitic rocks by partial chemical analysis. *Tanganyika Geol Surv. Rep., 10,* pp. 80-85.

Haskin, L.A., Frey, F.A.and Wilderman, T.R., 1968: Relative and absolute terrestial abundances of the rare-earths. In *origin and distribution of the rare earths. L.H. Ahren (ed.), Pergamon Press.*

Haskin, L.A., Haskin, M.A., Frey, F.A., Collins, K.A., Keddy, C.R. and Haskin, N.A., 1966: Rare earths in sediments. *J. Geophys. Res.* (Richmond, Va), 71, pp. 6091-6105.

Higgins, M., 1971: Cataclastic Rocks. *Prof. Pap., U.S. Geol. Surv.*, 687, pp. 97.

Hine, H.K., Williams, I.S., Chappel, B.W. and White, A.J.R., 1978: Contrasts between I and S-type granitoids of the Kosciusko batholith. *Jour. Geol. Soc. Austr. 25*, pp. 219 - 234.

Hobbs, B.E., Means, W.D., and Williams, P.F., 1976: An outline of Structural Geology. *John Wiley and Sons Inc.*, New York, pp. 571.

Holt, R., 1982: Geotectonic evolution of the Anka belt in the Precambrian Basement Complex of NW Nigeria. Unpublished *Ph.D. Thesis. Open University, England.*

Holt, R., Egbuniwe, I.G., Fitches, W.R. and Wright, J.B. 1978: The relationship between low-grade metasedimentary belts, Calc-alkaline volcanism and the Pan-African Orogeny in NW Nigeria. *Geol. Rundsch, 67*, pp. 631-646.

Hubbard, F.H., 1968: The association Charnockite-Older Granite in southwestern Nigeriaa. *J. Min. Geol. 3*, pp. 25-33.

Hubbard, F.H., 1975: Precambrian Crustal development in western Nigeria: Indications from the Iwo region. *Bull. Soc. Amer.*, 86, pp. 548-554.

Hurley, P.M, 1966: Continental drift investigations: *M.I.T. 14th Ann. Progress Rept., (for* 1966).

Hynes, A. 1987: Back-arc spreading in the Proterozoic- a theoritical approach *Precam. Res. 36,* pp. 189 - 199.

Ibrahim, A., 1996: Geology of the Area around Sabaru Area and its environs, Part of Sheet 35 (Kazaure). Unpublished *B.Sc. Thesis, A.B.U. Zaria.*

Ike, E.C., 1988: Late Stage Geological phenomena in the Zaria Basement Granites. In: *Precambrian Geology of Nigeria*. Geol. Surv. Nigeria Publ.

Irvine, T.N. and Baragar, W.R.A., 1971: A guide to the chemical classification of the common volcanic rocks. *Can. J. Earth Sci., 8,* pp. 523-548.

Jacobson, R.R.E., Snelling, N.J. and Truswell, J.F., 1964: Age determinations in the Geology of Nigeria with special reference to the Older and Younger Granites. *Overseas Geol. Min. Resources, 9,* pp. 168-182.

James, H.L., 1954: Sedimentary facies formation, *Econ. Geol., 49,* pp. 235-293.

James, H.L., 1992: Precambrian iron formation; nature, origin and mineralogic evolution from sedimentation to metamorphism. *In: Developments in Sedimentology (Wolf, KK.H. and Chiligarian C.V. eds). 47,* pp. 543-589.

Jarret H.R., 1976: `A' Geography of West Africa. *Evans Brothers Ltd.* pp. 89-96.

Jarvis, G.T. and McKenzie, D.P., 1980: Sedimentary basin formation with finiteextensional rates: *Earth Planet. Sci. Lett. 48:* pp. 42-52.

Katz, M.B., 1981: A shear-mobile transform belt in the Precambrian Gondwanaland of Africa-South American. *Geol. Rdsch., 70(3),* pp. 1012-1019.

Kennedy, W.Q., 1964. The structural differentiation of Africa in the Pan-African thermotectonic episode. *Univ. Leeds, Res. Inst. Afr. Geol., 8th Annu. Rep.,* pp. 48-49.

Klein, C. and Beukes, N.J., 1993: Proterozoic iron-formations. In: Proterozoic crustal evolution *(Condie, K.C. ed.). Developments in Precambrian Geology, 10,* pp. 383-418.

Klemm, D., W. Schneider and B. Wagner, 1984: The Precambrian metavolcanic-sedimentary sequence east of Ife and Ilesha, S.W. Nigeria, A Nigerian greenstone belt? *Jl. Afr. Earth Sci., 2:2,* pp. 161-176.

Kogbe, C.A., 1977: Geology of the South Eastern (Sokoto) Sector of the Iullemmeden Basin. Bulletin of the Depat. Of geology, A.B.U. Zaria, Vol. 2. No. 1.

Kroner, A., 1981: Precambrian plate tectonics. *Elsevier, Amsterdam,* pp. 781.

Kroner, A., 1983: Proterozoic mobile belts compatible with the plate tectonic comcept. - In: Medaris L.G.,. Jr., Byers, C.W., Mickelson, D.M. and Shanks, W.C. (eds.) *Proterozoic geology. Geol. Soc. America Memoir 161,* pp. 59-74.

Kroner, A., 1984: Fold belts and plate tectonics in the Precambrian. Proceedings of the 27th International Geological Congress, *Precambrian Geology,* Vol. 5 pp. 247-280.

Lepp, H. and Godich, S.S., 1984: Origin of Precambrian iron formations. *Econ. Geol. 59,* pp. 1025-60.

Macleod, W., 1966: Kaolin deposits near Bichi Province and near Kankara. *Rep Geol Surv. Nig. No. 1442* (Unpublished).

Martin, J.M. and Meybeck, M., 1979: Elemental mass-balance of material carried by major world rivers. *Mar. Chem.*, 7.

Mbonu, W.C., 1974: Interim report on the geology of 1:100,000 Sheet 79 (Malumfashi, *GSN Unpublished report*.

McIntyre, G.A., Brooks, C., Compston, W. and Turek, A., 1966: The statistical assessment of Rb-Sr isochrons. *J. Geophys. Res. 71,* pp. 5459-5468.

McCurry, P., 1970: The Geology of Degree Sheet 21 (Zaria), Nigeria, Unpublished *M.Sc. Thesis. Ahmadu Bello University.*

McCurry, P., 1971: Pan-African Orogeny in N. Nigeria. *Geol. Soc. Amer. Bull. 82,* pp. 3251-3262.

McCurry, P., 1973: Geology of degree sheet 21, Zaria. Nigeria. *Overseas Geol. and Min. Resources, No. 45, H.M.S.O. London.*

McCurry, P., 1976: The Geology of the Precambrian to Lower Palaeozoic rocks of Northern Nigeria - a review. *In Geology of Nigeria.* Ed. C.A. Kogbe, pp. 15-39, Elizabethan Pub. C. Lagos.

McCurry, P., 1978: Geology of degree sheets 10 (Zuru), 20 (Chafe), and part of 9 (Katsina) Nigeria. *Overseas Geol. Min. Res., 53 H.M.S.O. London.*

McCurry, P. and Wright, J.B., 1971: On place and Time in Orogenic Granite Plutonism. *Geol. Soc. Amer. Bul. 82,* pp. 1713-1476.

McCurry, P. and Wright, J.B. 1977: Geochemistry of calc-alkaline volcanics in northwestern Nigeria, and a possible Pan-African suture zone. *Earth Planet. Sci. Letts.*, pp. 90-96.

McKenzie, D.P., 1978: Some remarks on the development of sedimentary basins: *Earth Planet. Sci. Lett., 40:* pp. 25-32.

Mehnert, K.R., 1968: Migmatites and the origin of granitic rocks. *Elsevier Scientific Publishing Co., Amsterdam,* pp. 396.

Mehnert, K.R., 1971: Migmatites and the origin of granitc rocks. *Developments in Petrology 1. 2nd ed.*, 450pp. Elsevier Scientific Publi. Co., Amsterdam.

Middleton, G.V., 1960: Chemical composition of sandstones. *Geol. Soc. Am. Bull. 71,* pp. 1011 - 1026.

Middleton, M.E., 1984: Formation of rifted continental margins: a discussion of mechanisms: First Break, *E.A.E.G., 2(4),* pp. 9-14.

Miyashiro, A., 1973: Metamorphism and metamorphic belts. pp. 440. *George Allen and Halsted Press, New York.*

Morton, A.S., 1967: Water Supply and Geology of the Crystalline basement of part of sheet 35 (Kazaure). Unpublished *Rep., Geol. Surv. Nigeria.*

Mower, C.K., 1986: What is a Mylonite? *Geoscience Canada, 13(1).*

Muecke, G.K, Price, C and Sarkar, P., 1979: Rare earth element geochemistry of regional metamorphic rocks. *Phys. Chem. Earth, 11,* pp. 449-464.

Muecke, A., Annor, A. and Neumann, U., 1996. The Algoma-type iron formation of the Nigerian metavolcano-sedimentary schist belts. *Mineral. Deposit, 28,* pp. 136-145.

Mullum, H.S., 1978: Structural distinction between a metasedimentary cover and an underlying basement in the 600 m.y Pan-African domain of NW Nigeria, W. Africa: Discussion. *Geol Soc. Am. Bull. 19,* pp. 988-984.

Nance, W.B. and Taylor, S.R., 1977: Rare earth element geochemistry of regional metamorphic rocks from Kalgoorlie, Australia. *Geochem. Cosmochim. Acta (London),* 41, pp. 225-231.

Norton, S.A., 1975: Chronology of Paleozoic Tectonic and Thermal Metamorphic Events in Ordovician, Cambrian, and Precambrian Rocks at the North End of the Berkshire Massif, Massachusetts. *U.S.A Geol. Surv. Prof. Paper 888-B,* pp. 145- 213.

Odoma, A., 1996: Geology of the Area around Kazaure Area and its environs, Part of Sheet 35 (Kazaure). Unpublished *B.Sc. Thesis, A.B.U. Zaria.*

Ogezi, A.E.O., 1977: Geochemistry and Geochronology of Basement Rocks from NW Nigeria. Unpublished *Ph.D. Thesis. University of Leeds, England.*

Ogezi, A.E.O., 1988: Geochemistry, age and tectonic significance of the Anka Formation, NW Nigeria: A molasse of the Pan-African Orogeny? *In: Precambrian Geology of Nigeria.* Geol. Surv. Nigeria Publ.

Olabaniyi, S.B., 1997: Geological and Geochemical Studies of the Basement rocks and associated Iron-Formation of Isanlu area in the Egbe-Isanlu Schist Belt, SW Nigeria. Unpublished *Ph.D. Thesis. University of Ilorin.*

Olade, M.A. and Elueze, A.A., 1979: Petrochemistry of the Ilesha amphibolites and Precambrian crustal evolution in the Pan-African domain of SW Nigeria. *Prec. Res. 8,* pp. 303-318.

Oluyide, P.O., 1988: Structural trends in the Nigerian Basement Complex: *J. Nigerian Mining, Geol. and Metall. Soc.*, 1, pp. 87-102.

Oversby, V.M., 1975: Lead isotopic studies of aplites from the Precambrian basement rocks near Ibadan, S.W. Nigeria. *Earth planet. Sci. Lett. 27,* pp. 177-80.

Oyawoye, M.O., 1964: The geology of the Nigerian basement Complex. *J. Nigerian Mining, Geol. and Metall. Soc., 1,* pp. 87-102.

Oyawoye, M.O., 1972: The basement complex of Nigeria. In Dessauvagie, T.F.J. and Whiteman, A.J. (Eds.) *African geology: Univ. Ibadan 1970,* pp. 66-102.

Park, R.G., 1983: *Foundation of Structural Geology,* Blackie, Glasgow and London, pp. 122.

Pankhurst, R.J. and O'nions, R.K., 1973: Determination of Rb/Sr and Sr87/Sr86 ratios of some standard rocks and evaluation of X-ray fluorescence spectrometry in Rb/Sr geochemistry. *Chem. Geol., 12,* pp. 127-136.

Pearce, J.A and Gale, N.H., 1977: Identification of ore deposition environments from trace-element geochemistry. Trans. Inst. Min. Matall.

Pearce, J.A., Harris, N.B.W and Tindle, A.G., 1984: Trace element discrimination diagrams for the tectonic interpretations of granitic rocks. *J. Petrol., 25* pp. 956-983.

Pettijohn, F.J., 1957: *Sedimentary rocks*. New York, Harper, pp. 718.

Pettijohn, F.J., Potter, P.E. and Siever, R., 1973: *Sand and sandstone*, pp. 581. New York: Springer Verlag.

Potts, P.J., 1987: *Handbook of Silicate rock analysis*, pp. 485. New York: Springer Verlag.

Rahaman, M.A., 1971: Classification of rocks in the Nigerian Precambrian Basement Complex. (Abs) at 5th Annual Conf. of *Nigerian Mining, Geol. and Metall. Soc.*, Kaduna.

Rahaman, M.A., 1973: The geology of the district around Iseyin, Western State, Nigeria. Unpublished *Ph.D. Thesis. University of Ibadan.*

Rahaman, M.A., 1976a: Review of the Basement geology of Southwestern Nigeria. In *Geology of Nigeria*, Ed. C.A. Kogbe, pp. 41-51. Elizabethan. Publ. Co. Lagos.

Rahaman, M.A., 1976b: Progressive Polyphase metamorphism in pelitic schists around Aiyetoro, Oyo State, Nigeria. *Journ. Mining and Geology, 13(2)*, pp. 33-44.

Rahaman, M.A., 1988a: Precambrian Geology of Nigeria. In Benin-Nigeria Geotraverse. *Int. Meeting on Proterozoic Geology and Tectonics of High Grade Terrains*, Nov. pp. 28-30.

Rahaman, M.A., 1988b: Recent advances in the study of Basement Complex of Nigeria. In *Precamb. Geol. of Nigeria*. Geol. Surv. Nigeria, pp. 11-44.

Rahaman, M.A., Emofureta, W.O and Caen Vachetta, M. 1983: The Potassic-granites of the Igbetti area: Further evidence of the Polycylic evolution of the Pan-African belt in Southwestern Nigeria, *Prec. Res. 22,* pp. 25-92.

Rahaman, M.A., Ajayi, T.R., Oshin, I.O. and Asubiojo, F.O.I., 1988. Trace element geochemistry and geotectonic setting of Ife-Ilesha schist belt. In *Precamb. Geol. of Nigeria. Publ. by Geol. Surv. Nigeria,* pp. 241-256.

Ramsay, J.G., 1967: *Folding and Fracturing of rocks.* New York, McGraw-Hill Boot Co.

Read, H.H. and Watson, J., 1975: *Early Stages of Earth History,* ELBS, London, pp. 221.

Robin, P., 1979: Theory of metamorphic segregtion and related processes. *Geochem. Cosmochim Acta (London), 43,* pp. 1587-1600.

Russ, W., 1957: The geology of parts of Niger, Zaria and Sokoto Provinces, with special references to the occurence of gold. *Bull. Geols. Surv. Nigeria.,* No.27.

Shackleton, R.M., 1976: Pan-African structures. *Phil, Trans. R. Soc. Lond. A. 280,* pp. 491-497.

Shand, S.J., 1927: *Eruptive Rocks.* T. Murby & Co., London, pp. 360.

Shibayan, Y., (1990): Field evidence for the Ophiolitic Nature of the serpentinites in the Proterozoic supracrustals of NW Nigeria. In: *Recent Data in African Earth Sciences,* Eds. Rocci, G. and M. Deschamps, pp. 123-128.

Sibson, R.H., 1977: Fault rocks and Fault Mechanisms, *J.Geol. Soc. Lond., 133(3),* pp. 191-214.

Sibson, R.H., 1989: Earthquake faulting as a structural process. *Jour. Struct. Geol.*, 11, pp. 1-14.

Smith, J.V., 1974: *Feldspar Minerals. I. Crystal Structure and Physical Properties*. Springer-Verlag, Heidelberg, pp. 627.

Snelling, N.J., 1964: Age determination unit. *Ann. Rep. Inst. geol. Sci.* 1963, pp. 30-40.

Steiger, R.H and Jager, E., 1977. Subcommission on geochronology: convention of the use of decay constants in geo- and cosmochronology. *Earth planet. Sci. Letters 36*, pp. 359-362.

Streickeisen, A., 1976: To each plutonic rock its proper name. *Earth-Science Review. 13*, pp 1-33.

Tarney, J., 1977: Petrology, mineralogy and geochemistry of the Falkland plateau basement rocks, Site 330, *Deep Sea Drilling Project. Init. Rep.* Deep Sea Drilling Project 36, pp. 893-921.

Tarney, J. Dalziel, J.W.D. and De Wit, M.J., 1976: Marginal basin `Rocas Verdes' complex from S. Chile: A model for Archaean greenstone belt formation: In: *Early History of the Earth* (Ed. Windley, B.F).

Taylor, S.R., 1965: The application of trace element data to problems of petrology. In: L. Ahrens, F. Press, S.K. Runcorn and C. Urey (eds.), *Physics and Chemistry of the earth, Vol. 6. Pergamon Press, Oxford*, pp. 133-214.

Taylor, S.R., 1969: Trace element chemistry of andesites and associated calc-alkaline rocks. *Oregon Dept. Geol. Min. Ind. Bull., 65*, pp. 43-63.

Taylor, S.R. and McLennan, S.M., 1985: The continental crust: its composition and evolution. *Blackwell Sc. Publ., Oxford*, pp. 379.

Tougarinov, A.I., Knorre, K.G., Shanin, L.L. and Prokofieva, L.N., 1968: The geochronology of some Precambrian rocks of southern West Africa. *Canadian Jour. Earth Sci., 5,* pp. 639-642.

Trompette, R., 1979: The Pan-African Dahomeyide fold belt: A collison orogeny? *10th Colloque de Geologie Africaine,* Montpellier, pp. 72-73.

Truswell, J.F. and Cope, R.N., 1963: The geology of parts of Niger and Zaria provinces, northern Nigeria. *Bull Geol. Surv. Nigeria, No. 29.*

Turner, D.C., 1971: The Precambrian and Lower Palaeozoic Basement of Nigeria. Unesco 1971. *Tectonics of Africa Earth Sciences 6,* pp. 255-258.

Turner, D.C., 1983: Upper Proterozoic Schist Belts in the Nigerian sector of the Pan-African province of West Africa. *Prec. Res. 21,* pp. 55-79.

Turner, D.C. and Webb, P.K., 1974: The Daura igneous complex, N. Nigeria, a link between the Younger Granite districts of Nigeria and S. Niger. *Jour. Geol. Soc. Lond., 130,* pp. 71-77.

Turner, F.J. and Weiss, L.E., 1963: *Structural analysis of metamorphic tectonites.* New York, McGrow-Hill Book Co. pp. 545.

Tuttle and Bowen, 1958: Origin of granite in the light of experimental studies in the system $NaAlSi_3O_8$ - $KAlSi_3O_8$.

Udoh, A. N., 1987: Remote Sensing interpretation of the Geology of parts of Kaduna, Nigeria, Kwara and Sokoto States, Nigeria. Unpublished *M.Sc Thesis, Ahmadu bello University.*

Utke, A.W., 1987: New aspects on the evolution of the Late Proterozoic crust in NW Nigeria. In: Mattheis, G. and Schandelmeier, H. (Eds). *Current Research in African Earth Sciences, Balkema,* Rotterdam.

Van Breeman, O., Pigeon, R.T. and Bowden, P., 1977: Age and Isotopic studies of some Pan-African granites from N. Central Nigeria. *Precam. Res., 4,* pp. 307-319.

Vaniman, D.T., 1976: The Godani granodiorite plutons. Nigeria, Petrology and Regional setting, *Ph.D. thesis Univ. California, Santa Cruz.*

Verheijein, P.J.T and Ajakaiye, D.E., 1977: Gravity Survey across the Quaternary-Basement areas of Kano-State. *Proceedings of the 13th Annual Conf. of the Nig. Min., Geol., and Metall. Soc., Held at AB.U. Zaria,* 29th March - 2nd April.

Vernon, R.H., 1968: Porphyroblast matrix microstructural relationships in deformed metamorphic rocks. *Geol. Runsch. Band 67, Heft. 1.*

Vernon, R.H., 1976: Metamorphic processes. *George Allen and Unwin, London.*

Walsh, J.N., Buckley, F. and Barker, J., 1981. The simultaneous determination of the rare-earth elements in rocks using Inductively Coupled Plasma source Spectrometry. *Chemical Geology, 33.*

Watkins, M, 1989: Instrumentation method for Rare Earth Element analysis: In Ahmedali, T. (Ed). Analysis in the Geological Sciences: Advances in Methodology (1989) pp. 71-90.

Wilson, G., 1961: The Tectonic significance of Small-Scale structures, and their importance to the geologist in the field. *Ann. Sc. Geologique de Belgique, 74,* pp. 423-548.

Williamson, J.H., 1968: Least squares fitting of a straight line. *Can. J. Phys., 46*, pp. 1845-1847.

Winkler, G.F., 1967: Petrogenesis of metamorphic rocks. 2nd Ed., pp. 237. *Springer-Verlag*, New York, Berlin, Heidelberg.

Winkler, G.F., 1979: *Petrogenesis of Metamorphic Rocks*. Springer-Verlag, Berlin, pp. 334.

Wright, E.P., 1971: Basement Complex. *Geol. Surv. Nigeria, Bull. 32(1)*, pp. 12-47.

Wright, J.B., 1976: Fracture systems in Nigeria and initiation of fracture zones in the South Atlantic. *Tectonophysics, 34, T43- T47.*

Wright, J.B., 1979: *Crustal Evolution in northwestern Nigeria* - a personal view. (Unpublished).

Wright, J.B., 1985: Mineral Resources of West Africa

Wright, J.B. and McCurry, P., 1970: A reappraisal of some aspects of Precambrian shield geology: Discusion. *Bull. geol. Soc Am. 81*, pp. 3491-3492.

Wright, J.B. and Ogezi, A.E.O., 1977: Serpentinites in the Basement of NW Nigeria. *Nigeria J. Min. Geol., 14;* pp. 34-37.

Wright, J.B., Hastings, D.A. Jones W.B. and Williams, H.R., 1985. *Geology and Mineral Resources of West Africa*. Allen and Unwin. London.

York, D., 1969. Least squares fitting of a straight line with correlated error. *E.P.S..L. 5*, pp. 320-324.

KASHIM IBRAHIM LIBRARY

APPENDIX A

ANALYTICAL METHODS

A1. Sampling

2-8 kg of the metasediments, metavolcanics and Older Granite samples were collected from different localities. The 2-5 kg specimens used for Rb-Sr mineral analyses were obtained from sites exhibiting fresh rocks, especially freshly blasted sites.

A2. Sample Preparation

35 representative whole-rock samples preparation was carried out by the author in the Geochemical laboratories of the Department of Earth and Planetary Sciences, McGill University. Specimens were initially washed, dried and split into smaller fragments using a hydraulic splitter. These fragments were then crushed and then reduced to powder in an agate barrel tema grinder for about 22 minutes. The powdered specimens were used for several chemical analyses (both dry and wet), as described below.

Sample preparation for REE determination involved mixing of 0.50g mica schist sample powders with lithium metaborate ($LiBO_2$) in a platinum crucible. These were fused at 1000^0C in an electric muffle furnace for 30 mins. The resulting bead was dissolved in 110ml dilute HCL. The REE were then eluted in an ion exchange column using 100 ml of 6 M HNO_3 containing 0.63g

of oxalic acid dihydrate. The elute was dried and redissolved in 5 ml of 10% HNO3 and analysed by ICP-MS following the methods of Walsh et al. (1981) and Watkins (1989).

Fused glass beads for X-ray fluorescence analysis (XRF) were prepared using 0.40g sample powders mixed with borax flux (mixture of prefused lithium tetraborate, lithium metaborate and LiF), and ignited for 20 mins at 1200^{0}C in graphite crucibles. Polishing and carbon coating of thin sections for isotopic analyses were carried out by Mr. Smith. About 8 gm of the rock powder, in each case, was used to prepare the pressed pellets. The rock powder was binded using `movial' as a binder, and later pressed under hydraulic pressure. The pellets were then dried at 110^{0}C for about 5 hours.

A3. Electron Microprobe Analysis

The analysis of some samples of the BIF was carried out on carbon-coated polished thin sections using JOEL 733 Superprobe and Microscan 5 Microprobe. The instrument was operated at an acceleration voltage of 15kv and 2-4 uA beam current, with a counting time of 100 sec. The microprobe chemical data was compared with values of mineral standards.

A4. Major element analysis by X-ray fluorescence analysis (XRF)

All major elements (wt.%) concentrations were analysed by X-ray fluorescence analysis (XRF) of fused beads prepared from ignited whole-rock samples. The X-ray fluorescence (XRF) analyses of the whole-rock samples were carried out under the supervision of Prof. A. Tariq in a new Phillips PW2400 X- ray Fluorescence Spectrometer System. The Spectrometer is automated, with data controlled by Phillips X40 Software package. The lower limits of detection for the major elements is 0.01% (10 ppm). Volatile constituents (H_2O- and loss on ignition, LOI) were determined by drying the sample at 110oC (H_2O) followed by roasting in a muffle furnace at 1000^{0}C (LOI).

A5. Trace element analysis by X-ray fluorescence Technique

All trace elements (ppm) were determined by using sequential X-ray Spectrometer (XRF) on pressed powder briquttes, by comparing the samples absorptions with those of artificial standards (Bertin, 1975). Trace elements determined in all samples were Nb, Zr, Y, Sr, U, Rb, Th, Pb, and Ga. The lower limits of detection for the trace elements is 2 ppm.

A6. Determination of Rare earth elements (REE)

Rare earth elements (REE) concentrations were determined using ICP-MS method through a standard cation-exchange separation technique. These techniques were employed in the REE analysis of the mica schist samples.

A7. Mass Spectrometry

The geochronological analytical procedures applied at Universite' de Mon'treal were employed in the determination of Rb and Sr concentration and isotope ratios. Rubidium consists of two isotopes, ^{87}Rb (27.2%) and ^{85}Rb (72.8%), with the first the only radioactive isotope that undergo beta (ß) decay to produce ^{87}Sr. Only 0.5 - 1.0% of the earth's strontium is radiogenic, and they should be differentiated from ordinary ^{87}Sr which is also found in the Sr.

The Sr isotope analysis involved the separation of Sr using standard cation-exchange following sample dissolution in HF-HNO3-HCL. Blanks were in order of 1 ng. Chemical preparations for the measurements were done by Dr. N. Norman. The Sr concentrations and compositions were measured in the Isotope Laboratory Lab using VG-Sector Mass spectrometer. The Mass spectrometer separates charged atoms and molecules on the basis of their masses as they moved in magnetic and/or electrical fields.

All computations and analytical procedures for the mass spectrometric analyses were controlled by automated online computer facilities. The $^{87}Sr/^{86}Sr$ ratios were determined to better than $\pm$ 0.01%, and this is the error used in the isochron calculation. All the ratios are normalised to $^{86}Sr/^{88}Sr$ = 0.1194.

The Rb/Sr ratios in whole rock powders were determined using X-ray fluorescence spectrometry by Prof. A. Tariq of McGill University, following Pankhurst and O'Nions (1973). Analytical errors of $\pm$ 2.0% (2σ) were assigned for the $^{87}Rb/^{86}Sr$. 2σ is equivalent to two standard deviations of 100 ratios for Sr.

APPENDIX B

B1. Fundamentals and Experimental Uncertainties of Radiogenic Isotope Analyses.

The Rb-Sr whole-rock dating method is mostly based on the accumulation of daughter atoms (^{87}Sr) produced by parent nucleides (^{87}Rb), through a beta decay. It involves analyzing splits from 2-10 kg of rock for total Rb and Sr, as well as for the strontium isotopic composition. The age is determined by comparing the radiogenic ^{87}Sr generated in the rock with the amount of radioactive parental ^{87}Rb present in the rock. As one can not measure the amount of ^{87}Sr present when the rock was formed, an assumption is made.

The assumption is that at the time of formation of the rocks the abundance of ^{87}Sr relative to one of the stable Sr isotopes (^{86}Sr by convention) was the same in all the samples. This assumption is verified if the analytical data, expressed on a plot of $^{87}Sr/^{86}Sr$ versus Rb/Sr, lie on a straight line. The isotopic composition of the initial strontium is shown at the intercept of the line with the vertical axis.

Ground water may have removed the daughter elements produced, and this is likely to be a source of error. Systematic errors also exist especially during geochronometric analysis. The combination of X-ray fluorescence analysis methods to determine the Rb:Sr ratio and mass spectrometry to determine

the $^{87}Sr:^{86}Sr$ mineral of a rock should minimize errors during the extraction and analysis of strontium.

B2. Statistical Isochron Calculation

The method of linear regression used throughout this work is described below. It follows the treatments of York (1966) and Williamson (1968), and no allowance have been made for error correlation. Brooks et al. (1972) have shown that, for most whole rock Rb-Sr data in which $^{87}Sr:^{86}Sr$ data is less than one, such a correlation is not significant.

The principle of least squares requires the minimizing of the sum of the weighted squares of the residuals, designated as S. The line which best fits such arrays is that for which the sum of the squares of the deviations for each datum point from the line is a minimum. The minimized value of S has an X^2 distribution with an average value of n-2, where n is the number of data points defining the line of slope. Two equations, $\Gamma Y = nb_0 + b_1\Gamma X$ and $\Gamma XY = b_0\Gamma X + b_1\Gamma X^2$, where n = number of samples, b_0 = intercept and b_1 = slope, are the ones usually employed.

However, McIntyre et al. (1966) introduced procedures to enhance errors to take into account geological scatter or error Rb-Sr dating. This is the scatter of data points about the best-fit line, that is scatter greater than that due to

experimental errors. A geological error is usually assumed when the MSWD (S/n-2) exceeded unity, and error enhancement procedure to give MSWD = 1, should be undertaken.

McIntyre et al., (1966) adopted three error enhancement procedures. These are McIntyre model II, McIntyre model III and McIntyre model IV. For example, Model II calculations procedure assumes that the geological variation of $^{87}Sr/^{86}Sr$ is proportional to (87Rb/86Sr)2 was used. This model is preferred if the whole rock isochron yield younger age (700 m.y), thus indicating slight redistribution of radiogenic ^{87}Sr. Higher ages are associated with lower Sr contents indicating a relative depletion of ^{86}Sr. Following McIntyre et al. (1966) the index S/(n-2) is conventionally known as 'the mean square of weighted deviates' or MSWD.

Brooks et al., (1972) also suggested that such error enhancement may not be necessary, especially for a small number of samples, and for circumstances in which the experimental errors are less well known. They published an F-variate table which gives a limiting MSWD value(above which excess scatter is clearly indicated) in terms of the number of samples regressed.

According to Brooks et al., (1972), 2.5 is a compromised value appropriate to a six-point regression and assumes that the

errors are very well established. The regression in this work is based on five points, which were fitted using the technique of McIntrye et al., (1996), with errors quoted at 95% confidence limit.

To determine the age of a rock that contains ^{87}Rb and ^{87}Sr, the amount of each in the rock is measured, so as to reconstitute the original amounts of the parent material (^{87}Rb). The exponential law of radioactive decay, $dN = -\lambda N dt$, (where N= number of radioactive nucleii present at a time t, and λ = decay constant which gives the probability of decay), together with the rate of production of the isotope are use in determining the age.

$$t\ (age) = \frac{\%^{87}Sr}{\%^{87}Rb} \times \frac{1}{\lambda} \quad \text{where } \lambda = 1.42 \times 10^{-11}\ yr^{-1}.$$

The standard error of the slope is usually translated to that of the age by a simple proportional calculation using $@t = (@b/b) \times t$.